Modelling and Simulation of Car Following Driving Behaviour

Joseph Appiah

Transport Research Institute

School of Engineering and the Built Environment

Edinburgh Napier University

A thesis submitted in partial fulfilment of the requirements of Edinburgh Napier University, for the award of

Doctor of Philosophy

January, 2018

ABSTRACT

Driver behaviour has become an important aspect of transport research and over the years a considerable number of car following models have been developed. However, many of these models do not accurately simulate actual driving behaviour due to a lack of suitable qualitative and quantitative data. Moreover, the inclusion of socioeconomic variables in the existing models to ascertain the effect on car following behaviour is lacking. This research underlines the need to further investigate driving behaviour and car following models and to develop techniques to provide a better understanding of driver-vehicle interactions during car following. It investigates data collection techniques and develop better techniques to enhance and improve the collection of microscopic driver behaviour and traffic flow data. This study developed a novel data collection technique which involved instrumenting a private vehicle with front and rear advanced radar sensors, both forward and rear facing video-audio recorders connected to GPS based time series speed and distance measurement devices, an in-vehicle computer logging vehicle speed and a CAN monitoring interface user program to provide real time monitoring and display of data. This system has been utilised to collect a more enhanced and reliable microscopic driver behaviour data in three consecutive vehicles movements which represents an improvement from previously used systems.

Three different versions of the GHR car following model were produced for: car following car, truck following car and car following truck. Further analysis of the GHR model showed that in the case of car following car, car drivers responses to the lead car are more obviously stronger than in the case of truck following a car. A distance-based car following model and distance-based two-leader car following model that predict the safe following distance of following vehicles were developed to provide a better understanding of driver behaviour. An extension of these models to include gender, corridor (road) type and vehicle occupancy showed evidence of statistical significance of these variables on driver behaviour. A bus following model that predicts the “following distance” also has been calibrated to describe the interactions between a bus and a car within urban-rural driving conditions. In addition, data analysis showed that drivers were inconsistent with their driving behaviour and that there was variability in driving behaviour across the drivers observed in keeping a safe or desired following distance.

This study provides a platform for a number of future research agendas including data collection techniques for collection of driver behaviour data; evaluation of different ITS technologies; impact assessment of ACC on driver safety and improvement of traffic microscopic simulation tools in order to strengthen their ability to simulate realistic transport problems for efficient and effective transportation systems.

DECLARATION

I hereby declare that this thesis and any material contained in this thesis has not been submitted for the award of any other degree or professional qualification in any university. I declare that this thesis and all work contained in this thesis is the result of my own independent work. To the best of my knowledge and belief, this thesis contains no material previously published or written by another person except where due acknowledge to others has been made.

Joseph Appiah

ACKNOWLEDGEMENTS

I would like to express my sincere and profound gratitude to my Director of Studies, Professor Wafaa Saleh for her invaluable advice, guidance, support and help during this work. I express my sincere appreciation to my second Supervisor Dr. Kathryn Stewart for her guidance and support during this work.

I would like to acknowledge and thank Dr. Callum Wilson for his advice and technical support. I would also like to thank Mr Ron Hunter for his invaluable technical support. My appreciation goes to Messrs Stephen Paterson, Dave Baxter, James Gordon and the electronics technical team of Edinburgh Napier University for various support during the course of my PhD. My thanks also extend to the staff of Transport Research Institute and the administrative staff of SEBE at the School Office.

I am grateful to Mr Peter Schmok and Mr Roland Liebske of Continental Engineering Services GmbH, Germany, Mr Michael Maidhof and the support team of PEAK-Syetem Technik GmbH, Germany and Ms Katie Harland, Ms Luci Norwell and the support team of Racelogic Ltd, UK for their various technical advice, help and support. I am also grateful to Mr. Malcolm Calvert of SYSTRA (formerly SIAS), Edinburgh.

I would like to express my appreciation to all who volunteered their precious time to help with this study during the experiment and contributed in diverse ways to make this work a success. I say a big thank you to all. I thank all my colleagues at Edinburgh Napier University who provided inspirational support during the time I spend with them at the research office. I appreciate and thank Mr. George Ofori Appiah for his support. I thank Mr. George Tetteh Wayo Tekpetey (father-in-law) for his encouragement.

Without the support and sacrifices of my family, this study would not have been successfully completed. I am very much grateful to my wife, Eugenia Larko Appiah for her prayers, advice, support and encouragement to make this study completion a success. I thank my mother, Sarah Boateng and daughter, Georgina Amankwah Appiah for their prayers and support. I thank Joseph Kyei Appiah, Daniel Appiah, Felix Appiah, Eduard Appiah, Kwame Poku, Diana Appiah, Yaa Ampong, Afia Hemaa and all my family members for their prayers and support. I am grateful to my sister, the Late Dora Appiah (Agyeiwaa) and my father, the Late Joseph Evans Appiah, who has been my inspiration.

Finally, my deepest appreciation goes to God, The Almighty Father, for graciously looking after me and my family and given me the strength to complete this study.

DEDICATION

This thesis is dedicated to the most beautiful and most strong women in my life.

My Dear Beautiful Wife

Eugenia Larko Appiah

And

My Precious Mother

Sarah Boateng

(Alias: Awonkor)

TABLE OF CONTENT

LIST OF APPENDICES

LIST OF FIGURES

LIST OF TABLES

CHAPTER 1 INTRODUCTION

1.1 Background

Since early investigations on traffic flow, especially in the mid-thirties, where actual traffic flows (vehicles per hour) and individual observed vehicles speeds were measured (Greenshields, 1935) through to the fifties where the relationship between traffic flow and traffic density was developed (Greenberg, 1959), there have been numerous studies on traffic flow dynamics to address the traffic flow problems that have gained much attention with significant interest for many years (Bando et al., 1995). Over the past several years, vehicle ownerships and vehicle journeys have increased and continue to increase resulting in increases in the traffic flows in and around most cities causing congestion.

In congested cities, however, prolonged traffic queues and frequent travel delays during rush hour periods adversely affect driver behaviour, which has become an important factor for the evaluation of road safety and network capacity analysis. Hoogendoorn and Ossen (2006) suggested that drivers who spend long times driving in congested traffic streams, at some stage, lose the incentive of driving and this adversely affect their driving behaviours following the vehicle directly ahead. Attempts by researchers to provide better understanding of the behaviour of drivers in traffic streams have resulted in numerous mathematical equations being proposed to describe driver-vehicle interactions in both congested and free flow traffic streams.

Most of these mathematical models attempt to predict the driver behaviour of vehicles following one another within traffic streams. One such model is the car following model, which is based on the follow-the-leader concept. Car following models describe the interactions between two successive vehicles travelling in the same direction in a single lane of traffic stream without passing or overtaking involved. There are different rules that govern how individual drivers follow the vehicles directly ahead and these rules are established based on experimental observations and theoretical considerations of the traffic flows (Zhang and Kim, 2002). Ever since research on car following models started over half a century ago, several models have been proposed based on different assumptions, methods and the application of different data sets. The earlier known models developed in the mid-fifties such as the well-known non-linear GHR (Gazis-Herman-Rothery) model (Gazis et al., 1961), and linear models (e.g., Helly, 1959) used the drivers' acceleration predictions to describe drivers behaviour in car following. Other models that

predict the safety distance or collision avoidance (e.g., Kometani and Sasaki, 1959) of following vehicles including the Gipps (1981) model were developed later (see Bevrani and Chung, 2011). Over time, more models were proposed that include psychophysical models, fuzzy logic-based models and optimal velocity models (OVM) (see Brackstone and McDonald, 1999). During the past several years, a considerable number of car following models have been proposed that tend to mimic realistic driving behaviour in car following situations.

Car following models form the basis of microscopic traffic simulation tools, which have become an important tool for transportation planning, traffic design, traffic management and the evaluation of intelligent transportation systems (ITS) within existing road infrastructure. It also forms the basis of operational outlining of in-vehicle control systems such as advanced vehicle control and safety systems (AVCSS) that are being introduced in modern vehicles as aids for driver safety, which seek to simulate real driver behaviour while eliminating any potential danger that may occur to vehicle drivers (Zhao and Gao 2005; Mehmood et al., 2003). The complexity of these models in recent years has become more apparent due to the complexity in the driving behaviour as technology advances. The increase in the complexity of car following models has not necessarily improved the performances of these models, however, few of these models have definite improvements over the existing simple models in describing driver behaviour in a car following situation (Brockfeld et al., 2004; Hoogendoorn and Ossen, 2006).

Moreover, there has been an increase in research involving multiple leader vehicle following models, which have gained the attention of many researchers in recent years. This has led to a number of multiple leader car following models that have been proposed as extensions of existing car following models (Bexelius, 1968; Lenz et al., 1999; Zhou and Li, 2012; Farhi et al., 2012). These days, the availability of microscopic traffic or driver behaviour data and the ability to calibrate car following models with a more realistic miscrocopic driver behaviour data have raised further interest in driving behaviour research in the literature (Kesting and Treiber, 2008).

To improve driver-vehicle interactions and driver behaviour models, different methods of data collection techniques have been used to collect the driver behaviour data. Some of the most commonly used techniques of traffic data collection by researchers and transport engineers includes the use of aerial photography involving helicopter to capture and observe traffic flow (Treiterer and Myers, 1974; Hoogendoorn et al., 2003), the use

of inductive loop detectors both at the road surface or underneath the surface of the road (Ayres et. al., 2001) and the use of video recordings either mounted high on tall buildings overlooking the roads (Halkias and Colyar 2006) or instrumented vehicles (Chandler et al., 1958; McDonald et al., 1999; Kim, 2005) to collect traffic flow and driver behaviour data. All these data collection techniques are not without limitations, however, these techniques have helped in the collection of traffic data that may have been impossible to collect in the past due to the advancement in data collection technology. All these methods enable transport engineers and researchers to calibrate and validate car following models, in order to improve their performance in an attempt to replicate the actual driver-vehicle interactions and provide better understanding of how the driver-vehicle interactions affect traffic flows.

This research seeks to enhance the collection of microscopic driver behaviour data and in doing so, calibrate and validate existing car following models and recommend appropriate model calibration parameters. More attention has been given to drivers' acceleration behaviour car following models by researchers but little or no attention have been given to drivers' safe or desired following distance behaviour models in recent years. This research seeks to investigate drivers' safe following distance behaviour and proposes new car following models that best describe drivers' safe following distance behaviour in car following situations.

1.2 Car Following Models: State of the Art and Research Questions

Driver behaviour models have been used for various traffic and transportation management systems including planning, design, safety impact studies, operations of network facilities and capacity analysis. The effective managements of transportation systems are mostly aimed to minimise congestion, reduce long queues, reduce travel delays, enable effective use of the network, remove potential hazards for road users, increase economic activities and ensure driving experience becomes less stressful for all motorist including all road users. Driver behaviour has become an important aspect in ensuring proper and efficient management of the transportation system. Driver behaviour studies especially car following behaviour have become important in recent years which enable better understanding of driving behaviour and driver-vehicle interactions for the improvement of road safety and better management of the traffic systems and networks.

Car following models have become complex since the first model was proposed several years ago due to the complexity associated with driver behaviour and technological advancement, which comes with more sophisticated computer programs and faster computer processing abilities. Research in the area of car following has been given much attention in the literature recently. This has led to the development of many car following models based on different assumptions with each attempting to describe the driver behaviour at different traffic conditions. Attempts by other researchers to calibrate most of the car following models with improved microscopic traffic data have resulted in different calibration parameters of the same model being proposed. For instance, the well-known GHR car following model has many versions in the available literature as a result of calibration of the model with different data sets by researchers.

The continuous urge by researchers to improve on car following models performance in predicting realistic driver behaviour in real world scenarios has led to different data collection techniques being adapted for different studies. Data collection techniques have been improving with the use of more advanced technology in data collection systems for car following studies. In spite of the improvements in car following models and data collection techniques over the years, there are, however, more studies that needs to be done in these areas as the dynamics of traffic flows keep changing and drivers' behaviour becoming more complex as well as more advanced technologies being introduced into the networks. Therefore, this current research seeks to use the available technology to enhance the collection of microscopic traffic data in all traffic flow conditions. Using the available data, this research looks to improve the performance of one of the existing car following models and to assess driver behaviour of the model in respect to driver-vehicle interactions in car following situations which have not been given the needed attention in the available literature.

Even though many car following models have been proposed as mentioned earlier, what this research seeks to accomplish is to add to the existing models in the literature with new models that address the aspects of driver behaviour car following models that have not been given much attention in recent years. Again, there are other special following behaviours such as bus following behaviour that impact on other traffic that have not been given the needed attention which this research seeks to investigate. This research framework is design to basically answer the primary research questions with respect to driving behaviour within urban and rural traffic conditions including highway driving situations.

Therefore the following research questions have been identified.

1. Can the available vehicle monitoring devices be used to improve the understanding of driving behaviour and data collection techniques related to the car following models?

2. Can we improve the existing car following models formulations using the newly collected data?

3. What is the impact of further parameters such as gender, vehicle occupancy, corridor type and other parameters on the accuracy of existing car following models?

1.3 Aim and Objectives

The main aim of this research is to investigate driving behaviour and car following models and techniques as well as enhancing the collection of microscopic traffic flow and driver behaviour data. In order to achieve the research aim, a number of objectives have been formulated and include:

1. Carry out a review of literature on car following models, data collection techniques and analytical approach.

2. Identify the case study and the study area including selection of traffic corridors for this research.

3. Instrument a private vehicle with advanced measuring and video-audio camera recording devices to enhance microscopic traffic flow and driver behaviour data collection.

4. Collect driver behaviour data and carry out data extraction, management and data preparation for driver behaviour analysis.

5. Analyse the data and model car following including bus following, as well as calibrate and validate existing car following models. Conclude and recommend for further research.

1.4 Application or Beneficiary of this Study

There are lots of benefits this current study offers to wider research communities and transport engineers as well as to policy makers. Some of the benefits or possible applications of this research are discussed in this section. The acquisition of reliable, accurate and quality traffic data is fundamental to every research and for effective traffic planning, design and management of road networks. The traffic flow and driver behaviour data collection methods have seen much improvement in recent years which has enabled real time sufficient microscopic traffic data to be collected. In most cases, additional software are required to process the large data sets or databases, which might not be readily available. This would result in some difficulties in handling some aspects of the data and, therefore, making some existing traffic database quality uncertain. Moreover, lots of traffic databases contain traffic flow and driver behaviour data sets that were obtained over limited scope of coverage area that makes it impossible to observe driving behaviour over the entire road or network for proper evaluation of that behaviour over long periods. Notwithstanding the usefulness of many data collection techniques, more improvement is still required to enhance the collection of accurate, reliable and quality traffic flow and driver behaviour data with the latest advanced technology.

The benefit of this research, therefore, is that the data collection technique developed can be used to create more accurate, reliable, quality and sufficient microscopic driver behaviour and traffic flow data that will involve several vehicles both downstream and upstream for the entire road or network. Especially, three consecutive vehicles movements database can be created for an entire corridor or network for future studies. Another beneficiary of this technique is the possibility of measurement of traffic flow in the opposing lane of traffic, for example, using moving observer method to measure traffic flow. Driver behaviour data can also be monitored and assessed in the opposing lane of traffic. There are other possible applications of this data collection technique in studies such as lane changing driving behaviour on highways and gap acceptance behaviour.

Considerable numbers of microscopic traffic simulation tools are available for modelling complex traffic situations to provide better understanding of different transportation scenarios for efficient and effective traffic planning, traffic design, traffic management and for road safety improvement schemes. The simulation tools provide the platform for appropriate development, testing and evaluation of ITS. These microscopic simulation

tools use car following processes as their basic models that mostly uses the drivers' acceleration or speed to simulate drivers' behaviour. Most of these simulation tools do not consider the responses of one or two vehicles directly ahead of the following vehicles in simulating the driver behaviour. Moreover, other socioeconomic factors are not considered as the basic principles of the underlying car following models of which these simulation tools rely on in their simulation processes. Majority of these simulation tools also have parameters that are inbuilt, but when calibrated for specific local traffic conditions most of the time they do not necessarily replicate the specific local conditions that should be represented. Most of these simulation tools are calibrated with non-realistic driver behaviour data that does not represent actual driving behaviour. Some of the drawbacks associated with these tools often hinder their accurate representation of the localised traffic conditions that the simulation tools are built to replicate.

Therefore the results of this research can be used to improve the calibration of these microscopic simulation tools with real time microscopic driver behaviour data for accurate and efficient simulation outputs that could represent specific local conditions. The realistic driver behaviour data to calibrate these simulation tools will strengthen their ability to replicate realistic transport problems on the simulation platform to enhance transportation research for efficient traffic planning and management. Moreover, with the application of the car following models developed in this research, the simulation tools could accurately predict the inter-vehicle distances and the time gaps (i.e. time headway) separations between vehicles within traffic streams that could be used to evaluate network capacities and driver safety impact studies as well as effective management of the network. Since most of these models use drivers' acceleration or velocity behaviour, application of this research car following models will improve the simulation tools and provide the platform for collision avoidance research in preventing rear end collision and ultimately enhance drivers' safety.

Extensive use of car following model applications in the area of vehicle design and human factor evaluation in advanced driver assistance systems (ADAS) such as adaptive cruise control (ACC), which can regulate vehicles speed to adapt to the traffic environment during vehicle following process in traffic streams have been reported in the literature. These intelligent systems, especially the in-vehicle systems, are mostly calibrated and programmed using laboratory based vehicle simulation test results to mimic actual driver behaviour during operation. The end results of the control systems operation might not necessarily replicate actual driver behaviour which the technology is built to operate.

Since driver behaviour continues to evolve, improvement of ITS systems such as ACC with better performing and realistic car following models and continuous updating or calibration with real time series data will improve driver safety and minimised errors in such systems.

Therefore, the application of the car following models developed in this research will be useful for the evaluation of different ITS technologies and assess the impact of ADAS or ACC on safety and traffic flow dynamics. Moreover, the microscopic driver behaviour data collection techniques developed in this research can be used to collect data from different subjects that can then be used to calibrate the in-vehicle control systems such as ACC to improve the operations and performances of these systems to accurately mimic actual driver behaviour compared to the laboratory based simulated test data used for calibration. Another possible application of this research is the application of the self-drive (i.e. autonomous) vehicle development and the application of self-drive vehicle convoy movements to improve vehicle convoy safety. Using the system developed in this research, in-car devices can be integrated together to provide further information for drivers to improve driving experience and enhance driver-vehicle interactions for driver safety.

1.5 Structure of the Thesis

The research thesis report is structured in eleven chapters and a description of each chapter is given as follows. Chapter 1 presents the introduction of this research. It discusses the research background and the research questions, aim and objectives as well as the application or beneficiary of this research. A critical review of literature on car following models, driver behaviour data collection techniques and analytical approach is discussed in Chapter 2. Chapter 3 presents the methodology of this research. It discusses the case study and selection of the study traffic corridors, the instrumentation of test vehicle and the data collection of this research.

Chapter 4 discusses the data cleaning and preparation analysis. It also discusses the general statistics of the research data collected. Chapter 5 presents the general analysis of the research data collected. Chapter 6 discusses the analysis of the GHR car following model calibration and validation. The chapter also discusses the driver-vehicle interactions in car following scenarios. The distance-based car following model formulation that includes the formulation of car following model, two-leader car

following model and the bus following model are discussed in Chapter 7. Distance-based car following models calibration and validation are presented in Chapter 8. The two-leader car following model results and analysis are discussed in Chapter 9. Bus following model and analysis that includes the analysis of bus following behaviour and bus following model results are discussed in Chapter 10. Finally, Chapter 11 presents the discussions and conclusions of this research.

CHAPTER 2 LITERATURE REVIEW

2.1 Introduction

Chapter 2 discussed the research background, research questions, research aim and objectives. In this chapter, the review of the literature relevant to this research is discussed. Research on driver behaviour and car following models dates back in the early fifties and continues to the present date. The data collection techniques used in transport research have been improving over the years since the beginning of traffic flow studies in the late fifties. In this chapter, the literature on the previous work carried out on car following models and the data collection techniques used in collecting traffic and driver behaviour data is reviewed and gaps in the literature identified.

In this chapter, the review of literature on previous work is discussed under three main sections. The first section discusses the previous work done on car following models. The second section discusses the literature on data collection techniques used in the collection of driver behaviour data and, the third and final section discusses the literature on analytical approach used in transport research data analysis. This chapter concludes with a summary of the reviewed literature discussed in each section.

2.2 Car-Following Models

Research on car-following driver behaviour models has been studied over half a century ago. Research in traffic engineering and vehicle safety has, in recent years; develop into one of the important subject in the area of car-following models (Brackstone and McDonald, 1999). There are about a hundred different models that exist, which tends to mimic the behaviour of real traffic stream for a selected sets of driver behaviour parameters, and yet no primary modelling principles has been definitely established (Orosz et al., 2011).

The motivation to develop a reliable car-following model originates from the necessity to evaluate the impacts on the traffic flow regarding any plan changes to the road network. In car-following, it is important to assess what the impact of the potential changes to the driving surroundings will have on the flow of traffic when predicting the reactions of a following vehicle travelling in a traffic stream to the behaviour of the vehicle immediately in front (Gipps, 1981). Gipps recognised that all the different models that have been

proposed to explain this behaviour have different strengths and weaknesses. Car-following models often described in traffic stream as the process of interactions between two successive vehicles travelling on the same single lane on a particular road network. Ranney (1999) asserts that car-following is characterized by the headway i.e. distance or time between vehicles and the extent to which the vehicle following traces the speed variations of the vehicle directly in front.

A car following model is assessed based on the essential factors that affect the driver behaviour in the network. These factors that impact on the car-following driver behaviour, quite a number of them have been established by several transport researchers. These factors had been grouped into two main categories: individual differences factors and situational factors (i.e. involving both environmental and individual). Factors like driving skills, vehicle performance characteristics, vehicle size, risk-taking behaviour as well as age and gender are classified as the individual differences factors. Those factors that are classified as the situational factors includes road and weather conditions, speed and spacing information of the following and lead vehicles, time of day and also time of week. Factors classified as situational individual factors include situations such as hurry and distraction, impairment as a result of alcohol, drugs, stress, and fatigue, trip purpose and length of drive (Ranney, 1999; Panwai and Dia, 2005; Mehmood and Easa, 2010).

2.2.1 Fundamental Equations of Dynamics of Traffic Flow

The most common theories that attempt to describe the traffic flow are derived from statistical study of the flow. It is established from studies that traffic flow increase with increasing vehicular density until a maximum is reached, the flow also decreases to zero when the density is increased further (Greenberg, 1959). A statistical approach was adapted by Lighthill and Whitham (1955) who treated the traffic flow as a compressible fluid flow to develop a general flow theory describing the flow-density relation. Greenberg (1959) developed a relationship between the traffic flow and the density of traffic in studying the analysis of traffic flow. He treated the traffic flow as a continuous fluid that describes the steady state relationship between the flow q and the flow density k and/or between the streams velocity u (Edie, 1961). The equation of motion suggested by Greenberg is given by:

$$\frac{du}{dt} = - \left(\frac{c^2}{k}\right)\frac{\partial k}{\partial x} \tag{2-1}$$

The final equation of traffic velocity (fluid velocity) is given by:

$$u = c\ In\ \left(\frac{k_j}{k}\right) \tag{2-2}$$

and that of the flow q in terms of the density is given by:

$$q = ku = ck\ In\left(\frac{k_j}{k}\right) \tag{2-3}$$

where c is the parameter that is determined from the fluid state of the fluid, t is the time, x is the distance along the road and k_j is the jam density that occurs when traffic stops.

These equations by Greenberg primarily depends on two parameters namely the traffic jam characteristics and the velocity of the stream resulted from the maximum flow. Greenshields (1935) was the first to conduct an empirical study of traffic flow (capacity) where actual traffic flows were measured (vehicles per hour) and observed individual vehicles in the stream. He collected the data by using photographic method of 11800 groups of 100 individual vehicles. However, Greenberg (1959) argued that the data set used by Greenshields in 1935 study was limited. Improving the data sets, Greenberg instead used data he collected from the Lincoln Tunnel using a Simplex Productograph machine to calibrate the equations he derived. Using the data obtained in the experiment, Greenberg obtained the value of c = 17.2 miles/hour (Greenberg, 1959).

Gazis et al. (1959) argues that even though there is a satisfactory understanding between the Greenberg's theory and his experimental results obtained but there has been no explanation given for the assumptions he made for the dynamic fluid motion equation on which the flow theory was based. They pointed out that it is truly complex to ascertain why there should be any connection existing between this proposed equation and the vehicles' actual dynamic laws of motion. Despite the Greenberg's experimental results he obtained which was based on particular assumptions, Gazis et al. (1959) argues that these assumptions of which led to the traffic velocity formula cannot be construed as justification for his assumptions because these assumptions are not related to the assumptions used in the case of follow-the-leader theory.

A new steady-state flow equation of follow-the-leader theory was derived by Gazis et al. (1959) based on the assumption that the sensitivity is not constant but is considered to be inversely proportional to the distance of separation, which was not considered in previous flow theories so as to maintain the linearity of equations of motion. The Gazis et al. (1959)

equation is given by $q = ku = ck\ In\left(\frac{y}{y_j}\right)$, where y is the separation distance, and using the relation y = k^{-1} yield the same as Greenberg's equations of motion but with different assumptions. Gazis et al. (1959) plotted a least squared fit to the data analysed by Greenberg for the variable and constant sensitivity cases of their model. They found that in the variable sensitivity situation, the values of c = 17.2 miles/hour and k_j = 228 cars/mile were the same as what Greenberg obtained in his experiment. They pointed out that the constant sensitivity theory did not fit better than the theory of variable sensitivity to the experimental data.

Edie (1961) assert that there was a valid link between the Greenberg's equation and the study done by Gazis et al. (1959) on vehicular traffic flow. Edie pointed out that this is true when investigating a situation where one vehicle follows another vehicle closely enough for the speed of the following vehicle to be affected by the speed changes of the leading vehicle. Greenberg's equation as argued by Edie made no effort to connect the equation to the observable characteristics of a vehicular traffic stream; although the equation did show good agreement with empirical data when it was applied. The Gazis et al. (1959) formulation can therefore be considered as a stimulus-response equation (Edie, 1961).

2.2.2 Types of Car-Following Models

Car-following models have been categorised in different groups and the most common classifications are: Gazis-Herman-Rothery (GHR) model, linear models, safety distance or collision-avoidance (CA) models, psychophysical models, fuzzy logic-based models and optimal velocity model (OVM) (Brackstone and McDonald, 1999; Ranjitkar et al., 2005; Chang and Chong, 2005; Panwai and Dia, 2005; Li and Sun, 2012).

2.2.2.1 The Gazis-Herman-Rothery (GHR) Model

The basic general formulation of car-following models which often referred to as the follow-the-leader models that express the notion that individual driver of a vehicle in a traffic stream response to a given stimulus (Gazis et al., 1961), that was established in the late fifties, is given by:

$$\text{Response (t)} = \text{Sensitivity (t)} \times \text{Stimulus (t)} \qquad (2\text{-}4)$$

The response was assumed to be the acceleration (or deceleration) of the following vehicle since a driver in reality has a direct control through the control pedals. The stimulus assumed to be a function of the number of vehicles' positions and their time derivatives, generally expressed as the relative speed between the two vehicles. The sensitivity was considered to be a proportionality factor and taken as constant initially and later expressed as inversely proportional to separation distance between the two vehicles.

The stimulus-response model developed by Chandler et al. (1958) describes the movement of a vehicle following another vehicle ahead in a single lane of traffic stream. The model is expressed as:

$$a_n(t-\tau) = \alpha[v_n(t-\tau) - v_{n-1}(t-\tau)] \tag{2-5}$$

where a_n is the acceleration of the *nth* vehicle at the end of the reaction time $(t-\tau)$, v_n is the speed of the nth vehicle, v_{n-1} is the speed of the *(n-1)* vehicle, τ is the time lag or reaction time of response to the stimulus, *t* is the time and α is sensitivity constant.

Kometani and Sasaki (1958) conducted a comparable analysis to the Chandler et al. (1958) study. They proposed that the speed of the following vehicle only depends on the distance between the leading and the following vehicles. Their finding which was independently obtained agreed with the Chandler et al. fundamental car-following theory. The above equation was developed on the idea that the sensitivity is always constant. This limitation, however, was addressed by Gazis et al. (1959) by including the space (distance) headway between the two vehicles in the sensitivity term. They developed a new model which is formulated as follows:

$$a_n(t-\tau) = \alpha \frac{v_n(t-\tau) - v_{n-1}(t-\tau)}{x_n(t-\tau) - x_{n-1}(t-\tau)} \tag{2-6}$$

where $(x_n - x_{n-1})$ is the spacing at the end of the reaction time $(t-\tau)$.

Edie (1961) argued that the model developed by Gazis et al. (1959) (eqn. 2-6) provided no explanation for the traffic flow at low density. He pointed out that at extremely low density traffic, the follow-the-leader theory would not be applicable since at that situation there will be no vehicle interactions. In addressing this limitation, Edie made changes to the sensitivity term by introducing the speed of the following vehicle. Edie's sensitivity term was considered proportional to the speed of the following vehicle and inversely

proportional to the square of the headway between the two vehicles. Edie's model is given by:

$$a_n(t-\tau) = \alpha \frac{v_n(t-\tau)}{[x_n(t-\tau) - x_{n-1}(t-\tau)]^2}[v_n(t-\tau) - v_{n-1}(t-\tau)] \quad (2\text{-}7)$$

At low densities this model proved to perform better than equation (2-6) developed by Gazis et al. (1959). Edie suggested that the traffic flow could be described by two different flow relationships: one representing congested and the other representing non-congested traffic flow. The above model can be integrated to yield the Greenberg's speed-density relationship (eqn. 2-2) as shown by Edie (1961). It is essential for a non-linear car-following model to describe and ascertain, at least the fact that the steady-state relationship between average headway and average speed is nonlinear model as was pointed out by Gazis et al. (1959). Newell (1961) argues that not much has been done to investigate the capabilities of nonlinear models. In studying the nonlinear effects in car-following dynamics and without using the sensitivity-stimulus equation (Gazis et al., 1961) as the basis, Newell (1961) proposed a new relationship between the speed and headway in car-following. He made the assumption that the speed v_n of the nth vehicle at time *t*, is some nonlinear function of the headway at time $(t-\tau)$. Newell model is given by:

$$V_n(t) = G_n[x_n(t-\tau) - x_{n-1}(t-\tau)] \quad (2\text{-}8)$$

where G_n is express as a function of the parameters associated with the nth vehicle and whose form determines the specification of the model above. The model can be integrated to obtain different macroscopic speed-flow-density relationship. No evidence suggested that Newell attempted to obtain a quantitative result to validate the model he proposed.

Gazis et al. (1961) addressing the limitations of equation (2-6) (Gazis et al., 1959) developed a new nonlinear car-following model which has become the most well-known car-following model since the late fifties. They introduced a new calibration parameters *m* and *l* in the model in which the sensitivity, namely the gain factor, was considered proportional to the speed of the following vehicle raised to the power *m*, and inversely proportional to the relative distance (i.e. space headway) raised to the power *l*. The Gazis-Herman-Rothery (GHR) model, also known as General Motors (GM) model (i.e. developed at the General Motors Corporation Research Centre in Detroit) is formulated as follows:

$$a_n(t) = cv_n^m(t)\frac{\Delta v(t-\tau)}{\Delta x^l(t-\tau)} \quad (2\text{-}9)$$

where Δx is the relative distance between the vehicle following nth and the vehicle immediately in front, $(n-1)$, $\Delta\, v$ is the relative speed of the following vehicle nth and the vehicle immediately in front $(n-1)$ and c, m, l are calibration parameters. It is worth noting that Greenshields (1935) macroscopic flow-speed relationship can be derived from the GHR model when the calibration parameters *m* and *l* are set to 0 and 2 respectively. It is worth mentioning that this equation when integrated can result about any kind of flow versus concentration equation one may desire (Gazis, 2002).

Chandler et al. (1958) was the first to calibrate the GHR model in an experiment using vehicles linked with wires to study the reactions of eight male (employees from General Motors) as test drivers (age between 24 – 34 years) to a more realistic speed profile of a lead vehicle. The leading driver randomly changes his driving speeds within the range of 10 mph to 80 mph and allowed to include many braking actions, with each subjects driving for about 20 to 30 minutes on a test track. Two conclusions emanated from this investigation from the data obtained, with the assumption that both the relative speed Δv and the distance headway Δx terms were linear. In the first instance, it was revealed that the distance headway Δx had little influence to the following formulation and therefore could be excluded in the formulation, resulting in the GHR model with $l = m = 0$, having the value of $r^2 > 0.8$.

In the second instance, the sensitivity i.e. scaling constant showed a high variation between the drivers that took part in the test (with value in the range of 0.17 to 0.74 seconds) as well as the reaction time τ in range of 1.0 seconds to 2.2 seconds. In order to calibrate the new model, Herman and Potts (1959) conducted successions of empirical study on real roads in three selected tunnels in New York. They used eleven participants each driving through the tunnels for about 4 to 16 runs at an average of 4 minutes per participant. The relative distance was varying between 15 metres to 50 metres. The results of the experiment resulted in $m = 0$, $l = 1$ for the model (with r^2 values in the range of 0.8 to 0.98). The new reaction time τ (average) of 1.2 seconds and the constant parameter produced $c = 19.8$ ft/s. Edie (1961) produced calibration parameters of $m = l = 1$ using his approach of the nonlinear model. Gazis et al. (1961) produce the value of *m* in the range of 0 to 2 (i.e. $m = 0 – 2$) and *l* value in the range of 1 – 2 (i.e. $l = 1 – 2$) when they

analysed 18 data sets combination for their new model. May and Keller (1967) obtained m = 1 and l = 3 when they performed experiment using new sets of data.

Heyes and Ashworth (1972) using the data from the Mersey tunnel in England produced a new model with m = -0.8, l = 1.2. Hoefs (1972) in calibrating the GHR model found a new sets of model parameters for vehicles accelerating and decelerating with or without braking. The vehicles accelerating were found to have model parameters m = 1.5, l = 0.9. For vehicles decelerating without braking and with braking, the model parameters were m = 0.2, l = 0.9 and m = 0.6 and l = 3.2 respectively. Treiterer and Myers (1974) used a KA 62A aerial camera mounted in a Bell 47 J2 helicopter and aerial photographs taken at an interval of 1.0 seconds above the urban freeway, Interstate 71 in the City of Columbus, Ohio to monitor the trajectories of a number of vehicles. The trajectories of about 70 vehicles covering a distance of 3.3 miles with a total time interval of 238 seconds were observed and analysed for the study. They extracted the vehicles positions from the film footage from which the vehicle trajectories were derived and separately analysed the data into acceleration and deceleration phases. The study obtained the optimal calibration parameters with m = 0.2, l = 1.6 and m = 0.7 and l = 2.5 for acceleration and deceleration respectively.

In Paris in 1988, an instrumented vehicle was used to gather traffic data on car following in a variety of traffic situations by Aron. Using the traffic data which was collected at a typical speed of 7 metres/second and a separation distance of 14 metres, Aron (1988) separated the responses into 3 stages: acceleration, deceleration and steady-state driving. In all, sixty minutes of data was collected for the study. Aron (1988) found in the study that the scaling constant c = 2.46, m = 0.14 and l = 0.18; c = 2.45, m = 0.655 and l = 0.676; and c = 2.67, m = 0.26 and l = 0.5 for acceleration, deceleration and steady-state driving respectively. Later, another study was conducted by Ozaki (1993) using 2000 vehicles data obtained from a video recorder mounted on the 32nd floor of an office building overlooking the motorway. This gave a view of 160 metres stretch of the motorway, a total of 90 minutes of data was extracted for the study. He found the optimum combination parameters to be c = 1.1, m = -0.2, l = 0.2 and c = 1.1, m = 0.9, l = 1 for acceleration and deceleration respectively. With this short range of view as pointed out by Brackstone and McDonald (1999) it can only be possible to extract less than 10 seconds of time series data for each passing vehicle.

Since the first calibration of the GHR model, several researchers have carried out experiments in order to try and describe the correct sets of calibration parameters *m* and *l*. For instance, Bevrani et al. (2012) evaluated the GHR model and the capabilities in modelling the driver behaviour for safety purposes. The authors extracted 251 vehicles trajectories out of 3,000 vehicles of 15 minutes data within a range of 640 metres from the Next Generation Simulation data (NGSIM) in USA. The authors found the calibration parameters for acceleration and deceleration phases to be $m = 0.2$, $l = 0.1$ and $m = 0.7$, $l = 1.2$ respectively, and in the driving phase the value of $c = 1.1$ was obtained which was the same as Ozaki (1993) value of $c = 1.1$. Table 2-1 shows a summary of the calibration parameters of the GHR model reviewed in this study.

It is evident that there have not been generalised model parameters since the model was first proposed in the late fifties and early sixties. It is also evident that different data sets produced different values of calibration parameters; hence there is the need for further investigation to be done with real time series data to produce a new acceptable model parameters based on local traffic conditions.

Table 2-1: Summary of optimal values calibration parameters *m*, *l* and *c* reviewed in literature (see Brackstone and McDonald, 1999)

Models Reviewed	Models Calibration Parameters		
	m	*l*	*c*
Chandler et al. (1958)	0	0	0.17 - 0.74
Herman and Potts (1959)	0	1	19.8 ft/s
Edie (1961)	1	1	-
Gazis et al. (1961)	0 - 2	1 - 2	-
May and Keller (1967)	1	3	-
Heyes and Ashworth (1972)	-0.8	1.2	-
Hoefs (1972)	1.5/0.6**	0.91/3.2**	-
Treiterer and Myers (1974)	0.2/0.7*	1.6/2.5*	-
Aron (1988)	0.14/0.66*	0.18/0.68*	2.46/2.45*
Ozaki (1993)	-0.2/0.9*	0.2/1*	1.1/1.1*
Bevrani et al. (2012)	0.2/0.7*	0.1/1.2*	1.1

* Deceleration. ** Deceleration with braking

2.2.2.2 The Linear (Helly) Model

The model first proposed by Chandler et al. (1958) at the early stages of the GHR model development was considered as a simple linear car-following model. The linear model proposed by Helly (1959) included some additional terms for the variations of the

acceleration in relation to whether the lead vehicle and the second vehicle ahead were braking. The assumption of the model is that the rate of acceleration of the vehicle following depends primarily on the reaction-time of the driver, the desired distance followed, the vehicle following speed, the relative spacing and speed between the vehicle following and the vehicle leading. The formulation is given by:

$$a_n(t) = C_1 \Delta v(t-\tau) + C_2[\Delta x(t-\tau) - D_n(t)] \quad (2\text{-}10)$$

$$D_n(t) = \alpha + \beta v(t-\tau) + \gamma a_n(t-\tau) \quad (2\text{-}11)$$

where $a_n(t)$ is the acceleration of vehicle *n* at time *t*, Δv is the relative speed of the following vehicle *n* and the vehicle immediately in front (n-1), Δx is the relative distance between the following vehicle *n* and the vehicle immediately in front (n-1), $D_n(t)$ is the desired following distance at time *t*, v is the speed of vehicle *n*, τ is the reaction time of driver and α, β, γ, C_1, C_2 are the calibration parameters.

In order to calibrate the model, Helly used data collected by 14 subject drivers in an experiment. The results produced good least squared fit parameters for nearly all the subjects with the reaction time τ in the range of 0.5 – 2.2 seconds (average of 0.75 seconds) and the parameter C_1 in the range of 0.17 – 1.3 (average of 0.5). In order to estimate the parameter C_2 value, Helly set the relative speed and the relative distance equal and opposite which produced no acceleration, namely free driving, when a vehicle notices a motionless object along its path. The final value of C_2 was averaged 0.125. The final model of Helly is given by:

$$a_n(t) = 0.5\Delta v(t-0.5) + 0.125[\Delta x(t-0.5) - D_n(t)] \quad (2\text{-}12)$$

$$D_n(t) = 20 + v(t-0.5) \quad (2\text{-}13)$$

In an attempt to calibrate the Helly model, Hanken and Rockwell (1967) and Rockwell et al. (1968) performed an empirical study on free roads and on a congested urban freeway. On the free roads all the subject drivers encountered similar acceleration sequence of the leading vehicle while during the congested urban freeway experiment, the subject drivers were opened to the real traffic flow variations. The authors used a wire-linked vehicle and run the test 3 times for each subject in a 10 minutes period and sampling at every 0.5 seconds intervals. The speed for each subject was at the range of 20 – 60 mph with the headway of between 40 feet and 250 feet. This experiment produced a new model that

was considered to be highly linear in nature. The model was found in later simulations to perform well in acceleration pattern but was found to produce higher headways than those observed. The model was formulated as follows:

$$a_n(t+\tau) = 0.058\Delta x + 0.125\Delta v - 0.048v_{n-1} - 6.24 \quad (2\text{-}14)$$

Different experiments have been carried out to attempt to calibrate the Helly model by other researches using different data sets (Bekey et al., 1977; Aron, 1988; Xing, 1995)

2.2.2.3 The Safety Distance or Collision Avoidance (CA) Model

Kometani and Sasaki (1959) developed the first collision avoidance (CA) car-following model. The collision avoidance model determines the safe following distance necessary to prevent a collision in case the driver of the vehicle in front reacts unexpectedly. The model is expressed as:

$$\Delta x(t-\tau) = \alpha v_{n-1}^2(t-\tau) + \beta_1 v_n^2(t) + \beta v_n(t) + b_0 \quad (2\text{-}15)$$

where $\Delta x(t-\tau)$ is the safe following distance (m) for the vehicle following at time $(t-\tau)$ (seconds (s)), v_{n-1} is the speed (km/h) of the vehicle in front at time $(t-\tau)$, v_n is the speed (km/h) of the vehicle following, and α, β, β_1 are calibration parameters.

Gipps (1981) recognised that the above model and all other proposed existing models in literature describing the behaviour of one vehicle attempting to follow the other in front have different strengths and weakness. Based on the assumption that individual driver sets limits to their desired braking and acceleration rates for response of the following vehicle, a new model was proposed by Gipps (1981) to address some of the weakness of the existing models. Gipps considered two constraints in the development of the new model that relates to the following vehicle; the first constraint was that the following vehicle driver's required speed should not be exceeded and as the engine torque increases the vehicle's free acceleration should initially increase with the speed and then decreases to bring the vehicle to a stop as it reaches the required speed. The second constraint Gipps considered was the braking constraint. Gipps asserts that if the lead vehicle start braking as hard as required of the driver at time t, the vehicle will come to a stop at a point. The vehicle travelling directly behind the lead vehicle will not respond until at time *t* plus the

reaction time and subsequently will come to a stop before reaching the lead vehicle. Gipps model is formulated as follows:

$$v_n(t+\tau) \leq b_n\tau + \sqrt{b_n^2\tau^2 - b_n\left\{2[y_{n-1}(t) - s_{n-1} - y_n(t)] - v_n(t)\tau - \frac{[v_{n-1}(t)]^2}{b^*}\right\}}$$

(2-16)

where $v_n(t+\tau)$ is the speed of the following vehicle at end of the reaction time ($t+\tau$), b_n is the following vehicle deceleration rate, τ is the reaction time, $y_{n-1}(t)$ is the position of the leading vehicle at time *t*; s_{n-1} is the length of vehicle $n-1$ which includes the stationary stoppage allowance, $y_n(t)$ is the position of the following vehicle at time *t*, $v_n(t)$ is the speed of the following vehicle at time *t*, $v_{n-1}(t)$ is the leading vehicle speed at time *t* and b^* is the perceived (by the following driver) deceleration of the leading vehicle.

Three main factors primarily control the corporate behaviour of the flow of traffic (Gipps, 1981) and these factors include: the desired vehicle speed (*v*) distribution, the reaction time (τ) and finally the ratio of the mean braking rate to the mean braking rate of the driver's estimates (i/d). At the same time the distributions of vehicle's acceleration, braking and effective length control each vehicle's driving behaviour. Gipps (1981) performed a series of simulation using realistic values for the proposed model and found that the model performed well during simulation when the reaction time is the same as the interval between successive recalculations (Seddon, 1972) of vehicle speed and position.

The Gipps model and other existing models assumed that when the leading vehicle gradually comes to a stop, the following vehicle will also come to a stop at a certain time behind the leading vehicle to avoid a collision. This might not be the case in certain situations where the following driver does not necessarily stop but attempt to pass the vehicle stopping when there is a weak discipline of lane-based driving. A new model was proposed by Gunay (2007) that takes into account the weak discipline of lane-based driving in car-following. The proposed model by Gunay is based on the uneasiness in driving induced by lateral friction between vehicles in a traffic stream. For the relationship between the following and lead vehicles, he assumed that the following vehicle's movement can be expressed as a function of the off-centre effects of its

leader(s). It is assumed that speed of a vehicle is affected by the travel path width. Gunay (2007) new model is formulated as follows:

$$v_n(t+\tau) \leq b_n\tau + \sqrt{(b_n\tau)^2 - 2b_n\left\{ v_n(t)\frac{\tau}{2} + \frac{MES^2}{2b_n} + \frac{v_{n-1}^2}{2b_{n-1}} + y_n(t) - y_{n-1}(t) + s_{n-1}\right\}} \quad (2\text{-}17)$$

where MES is the maximum escape route. The model shows the maximum speed that the following vehicle should not exceed at the end of the reaction time so as to maintain the desired safe following distance. And for the following vehicle to perform the desired manoeuvre, the formulation is given by:

$$v_n(t+\tau) \leq 2\frac{y_{n-1}(rest) - y_n(t) - \frac{v_n}{2}\tau - \frac{t_{veer}}{2}MES - d_{body}}{t_{veer}+\tau} \quad (2\text{-}18)$$

Where t_{veer} is the time during the veering manoeuvre and d_{body} is the distance the vehicle body pass. In order to do a safe manoeuvre the speed of the following vehicle should not exceed equation (2-18) at the end of the reaction time (Gunay, 2007).

Gunay found that by applying a car-following stopping-distance method and simulating the model, the following vehicle speed was influenced by the wideness of the travel route. Gunay shown that in an exceptional circumstance when the maximum escape speed (MES) is set to zero, the model produced equal outcome as the basic car-following model did for the standard car following situation, for example Gipps model. Gunay reported that the validation can only be achieved by the simulation of traffic stream in conjunction with all other elements (namely, lane changing manoeuvres) or different traffic compositions in order to obtain the results including speed, density and traffic flow characteristics. But no evidence of empirical data was reported in the relevant literature that was used to validate the model by Gunay (2007).

2.2.2.4 Psychophysical Models

A flow theory was proposed by Michaels (1963) that formed the basis of psychophysical models. Michaels suggested the idea that drivers would at first be able to tell when they are coming close to a vehicle ahead of them in a traffic stream, mainly as a result of the gradual changes in the size of the vehicle ahead by observing the relative speed by means of the changes on the visual angle subtended by the vehicle in-front. Michaels proposed

a threshold within which a driver will react to the vehicle in front when this threshold is reached. The threshold presented by Michaels is widely known in academic literature and is given as $d/d(t)(\sim \Delta v/\Delta x^2) = \sim 6 \times 10^{-4}$. When this threshold is exceeded, and as long as the threshold is not re-exceeded, drivers will decide to decelerate up until the point where they can no longer observe any relative speed to the vehicle in front, the drivers' performances will then depend on whether they can observe any variations in the vehicles spacing as they travel along.

Brackstone and McDonald (1999) mentioned that the action point, namely the spacing based threshold, is mainly important when relative speeds, at close headways, is likely to be lower than the threshold. Hence, for noticeable variations, the Δx must vary by just noticeable distance (JND), as in relation to Weber's Law and to be precise, the variation in the visual angle need to be by a set percentage, usually 10%. This set percentage depends on the front vehicle's width and the space between the driver's eyes and the front vehicle's rear bumper. The front vehicle's visual angel can be estimated as a $\tan(W/D_p)$, where W is the width of the front vehicle in metres and D_p is the preferred following distance (Van Winsum, 1999). At the angle at which the driver of the vehicle begins to see that the front vehicle is getting closer than the preferred headways is expressed as $(1+g) * a\ tan(W/D_p)$, where g is the Weber fraction of JND in visual angle of 0.1 or 10%. At a certain distance the driver will choose to decelerate and this is given by (Van Winsum, 1999):

$$D_d = W/\left(tan\left((1+g) * a\ tan(W/D_p)\right)\right) \quad (2\text{-}19)$$

where D_d is the distance at which the vehicle decelerates.

For an opening condition, the threshold is approximately 12%, which as a driver constantly draws closer to and slow down to move back away from the vehicle ahead, it will result in a slow drifting apart between the vehicles. The psychophysical or action point (AP) models were developed on the basis of this assumption that an action will be performed by a driver when a threshold of his perception-reaction is reached (Van Winsum, 1999). Interestingly, Brackstone and McDonald (1999) mentioned that there has not been a definite conclusion as to the validity of the existing psychophysical models proposed in literature, even though the entire system would seem to simulate an acceptable behaviour, however, less success have been achieved in calibrating individual

elements and thresholds. The basic assumptions on which the psychophysical models are based on are considered the most coherent and best describe most of the characteristics of day to day driving behaviour, however, as pointed out by Brackstone and McDonald (1999) little research work has been done since the sixties on the theories involved in these models with the aim of contributing to the compilation of a coherent driver behaviour model. The psychophysical models are now in use in MISSION model and incorporated in PARAMIC-CM (Parallel Microsimulation – Congestion Management), (for further review see Brackstone and McDonald, 1999).

2.2.2.5 The Fuzzy Logic-Based Models

The use of the first fuzzy logic method was by Kikuchi and Chakroborty (1992), which they tried to 'fuzzify' the GHR model by assigning values to the parameters in the GHR equation as inputs and as a natural language base set. The fuzzy logic models (rule base) tries to describe the reaction of the following vehicle to the variations of the relative speed and distance to the vehicle in front in relation to the driver's own free speed and the desired safe distance. Every variable in the fuzzy model usually consists of many different overlapping 'fuzzy sets' as input parameters (Wu et al., 2000), where each describes exactly how effectively a variable fits the description of the term. For instance, the term 'too close' can be assigned a fuzzy sets variable that could be used to describe and quantify the meaning of the term.

This can further be explained as, for example, a distance separation of not more than 0.5 seconds can certainly be 'too close' and hence assigned the value of 1 as the degree of truth or membership, whereas a distance separation of 2 seconds can be considered not close and hence assigned the value of 0 as the degree of truth, and with the values in between them are assumed to show the degrees of truth and possess different i.e. fractional degrees of membership. After these sets of driving rules are defined, the sets can now be assigned through logic operators to the corresponding fuzzy output sets, for example, IF the vehicle following is 'close' AND still 'closing' THEN 'brake', and with the real procedures being evaluated from the sets of the model outputs and calculated as the summation of all the possible outcomes of the model (Brackstone and McDonald, 1999).

In the fuzzy-logic models, for example, when determining the decision a vehicle's driver will make, a set of driving rules based on common sense through experiment and

experience will have to be developed and assigned a fuzzy sets. It is worth mentioning that there is no evidence in literature that suggest that Kikuchi and Chakroborty (1992) validated their model with field data.

2.2.2.6 Optimal Velocity Model (OVM)

Bando et al. (1995) was the first to propose a new dynamical model that incorporates the optimal (legal) velocity, which is also a function of the headway. Bando et al. argued that two main types of concept on regulations govern car-following. The first concept was based on the notion that individual driver must keep a safe following distance that is considered to legal from its leader, which depends on the velocity difference between the two successive vehicles. The second concept assumes that the individual driver has the safe (legal) velocity determined by the following distance from the vehicle in front. Bando et al. (1995) proposed a new model based on the second concept that incorporates the optimal velocity into the model. The sensitivity was taken as constant and the stimulus was taken as a function of the following distance. The model also known as the Optimal Velocity (OV) is formulated as follows:

$$a_n(t+\tau) = \alpha\big(V\big(x_{n+1}(t) - x_n(t)\big) - v_n(t)\big) \tag{2-20}$$

$$V(\Delta x_n(t)) = 0.5 v_{max}[\tanh(\Delta x_n(t) - h_c) + \tanh(h_c)] \tag{2-21}$$

Where a_n is the acceleration at the time $(t+\tau)$, V is the optimal velocity express as function of the headway i.e. $(V(\Delta x))$, $x_n(t)$ is the position of the *n*th vehicle at time *t*, $v_n(t)$ is velocity of the *n*th vehicle and α is constant sensitivity of the driver, v_{max} is the maximal speed of the *n*th vehicle, h_c is the safe distance (headway), $\tanh(\cdot)$ is the hyperbolic tangent function (Bando et al., 1995).

It is worth noting that comparative studies on car following models including models reviewed in Section 2.2.2 have been carried out by other researchers (Ossen and Hoogendoorn, 2005; Ranjitkar et al., 2005; Chang and Chong, 2005; Panwai and Dia, 2005; Bevrani et al., 2012: Appiah et al., 2015). However, it is beyond the scope of this study to carry out comparative review and analysis of the existing car following models. These models reviewed and several other car following models have been successfully implemented in different applications such as traffic microsimulation models (Papageorgiou and Maimaris, 2012; Higgs et al., 2011). For instance, the Gipps (1981)

model have been implemented in AIMSUN (Olstam and Tapani, 2004), the action point or psychophysical model employed in VISSIM (Wiedemann, 1994) and PARAMICS (Fritzsche, 1994; Brockfeld et al., 2003) and the car-following model used in MITSIM (Olstam and Tapani, 2004) is drawn from the GHR model (Yang and Koutsopoulos, 1996).

2.2.3 Two-Leader Car Following Model

Bexelius (1968) proposed a new car-following model by extending the basic car-following model (Chandler et al., 1958) on the assumption that every individual driver response to many of the preceding vehicles. The final model incorporates the critical and optimum speed, the maximum flow and the vehicle spacing. Bando et al. (1995) optimal velocity model was extended by Lenz et al. (1999) by including multi-vehicle interactions in the model and revealed that the response to several vehicles in front of the following vehicle contributes to the stabilization of the dynamical behaviour. Zhou and Li (2012) also extended the basic optimal velocity car-following model proposed by Bando et al. (1995) by including the vehicle immediately preceding the lead vehicle.

Farhi et al. (2012) extended the piecewise-linear car following model proposed by Bando et al. (1995) to multi-anticipative piecewise-linear car-following model where it is assumed that drivers control their speed by considering the positions and the speed of vehicles ahead. Extending the existing car following models to multiple-leader models does not necessarily make these models accurate in describing the driving behaviour of following vehicles in a multiple leader car following scenario. Evidence suggests that these models were developed with studies that were based on non-scientific arguments (Hoogendoorn and Ossen, 2006), but on the assumption that drivers response to multiple vehicles ahead downstream and as such might not effectively replicate real world situation.

Hoogendoorn and Ossen (2006) used empirical data to analyse the two-car following model proposed by Bexelius (1968) taking into account the second vehicle ahead of the leading vehicle. The data were collected using a helicopter mounted with video recording equipment on a section of the three-lane motorway in the city of Rotterdam, Netherlands. In a previous study by Ossen and Hoogendoorn (2005), a safe headway limit based on the length of the following distance at which to include vehicles data involved in the

experiment was set. They set a maximum mean gross distance headway threshold value at 70 metres based on a formula (i.e. eqn. 2-22) to calculate a safe headway on the assumption that the vehicles all having nearly the same braking distances. Emphasising more on how the safe headway distance threshold value was set, they used, as an example, a vehicle travelling at 25 metres per second (m/s) with an assumed length of 4.7 metres and a reserved distance of 1 metres and assumed reaction time between 1 and 2 seconds to calculate the vehicle's minimum safe headway distance. They obtained a minimum safe headway value of 30.5 metres to 55.5 metres and to ensure all the vehicles influenced by the leading vehicles to be analysed, they set the experimental mean distance headway threshold at 70 metres. The safe distance headway (SDH) calculation formula used by Ossen and Hoogendoorn (2005) is expressed as:

$$\text{SDH} = \text{overall reaction time} * v(t) + l_{sf} \qquad (2\text{-}22)$$

Where $v(t)$ is the speed of the following vehicle and l_{sf} represent the vehicle length plus the reserve safety distance at rest. Hoogendoorn and Ossen (2006) found, on average, that the following driver's sensitivity to the second leader was higher than the sensitivity of the vehicle immediately in front, which was estimated to be half of the first leader's sensitivity value. This, they suggested that drivers pay attention not only to the vehicle in front of them but also the second vehicle immediately ahead. Hoogendoorn and Ossen (2006) noticed from the estimation results that the sum of the sensitivities with regard to the two-leader model was almost equal to sensitivity with regard to the one-leader model. They also found that the multiple vehicle interactions they incorporated were seen to have a stabilizing effect on the dynamics behaviour of the flow of traffic (see also Lenz et al., 1999).

Mehmood and Easa (2010) proposed a new model that take into account the changes in the drivers' perception-reaction time and the influence on the following vehicle by both the vehicle at the back and front, the driver's age and gender in a car-following scenario. Sample data of 80 following vehicles were obtained from the Next Generation Simulation (NGSIM) database in USA without motorcycles and trucks data. The authors restricted the time headway for the two vehicles to below 3 seconds. Mehmood and Easa found that in the deceleration scenarios, the rate of change of speed for braking was higher than that of the non-braking and that the vehicle behind only contributed in the acceleration scenario by approaching with a higher speed. Mehmood and Easa pointed out that the vehicle in front reactions has a prominent impact on the actions of the driver of the vehicle

following. They found out that females and older drivers travel with a lesser speed than male and younger drivers respectively (Mehmood and Easa, 2010). It was mentioned that calibration parameters may possibly differ from other types of roadways. It is worth noting that the age and gender were assumed based on the statistical distribution of the sample taken from the NGSIM for the validation.

2.2.4 Reaction Times

The reaction time often referred to as time delays (e.g. Orosz et al., 2011) or interpreted as update time (Kesting and Treiber, 2008b) has been studied by several researchers in the past several years. It is considered an important factor in human driving behaviour (Gunay, 2007; Kesting and Treiber, 2008) contributing to the instabilities in the flow of traffic and, subsequently, form the basic feature in several traffic flow models (May, 1990). Reaction time can be defined as the time it takes the driver of the following vehicle to recognise that the leading vehicle started decelerating and that a closing speed has developed (Brackstone et al., 2002). Other researchers in the early models defined the reaction time as the summation of perception time and the time it take the foot to move to the brake pedal (Ma and Andréasson, 2006).

There are various factors that can influence the reaction time of a driver such as the speed of the vehicle, visibility, whether condition, age of the driver, vehicle characteristics, traffic conditions and the mental state of the driver. In psychological studies, as pointed out by (Ma and Andréasson, 2006), the driver reaction time process is characterised in four different stages of car-following which includes the driver's perception, recognition, decision and physical reaction. Reaction time is often assumed as a constant (or fixed) value (Ma and Andréasson, 2006) or a random variable as it is the case in many car-following models and not considered as differing and in reality to the drive's behaviour (Chang and Chong, 2005). Such assumptions restrict the models (Ma and Andréasson, 2006; Chang and Chong, 2005) and make it difficult for the models to adapt to different traffic conditions.

The reaction time has been estimated by several studies using data obtained from driving simulators (Mehmood and Easa, 2009), experiments carried out on test tracks (Chandler et al., 1958) and the use of human-driven and computer-controlled (robotic) vehicles (Orosz et al., 2011). For instance, in 2009 Mehmood and Easa conducted a study using data collected from a driving simulator to model the brake reaction time based on their

age and driving experience. A total of 60 subjects including 32 males and 28 females aged between 18 to 70 years were used in the study. Mehmood and Easa tested the subjects in three different driving conditions at different speed and distance. Since some of the data obtained was found to be biased, they used another set of participant and this time only 25 subjects including 16 males and 9 females aged between 18 and 70. Mehmood and Easa found that the brake reaction time of females were higher than the males and all age group recording high brake reaction times.

The estimated acceleration reaction time varied from 0.4 to 1.1 seconds for young drivers, 0.6 – 1.3 seconds for middle aged drivers and 0.6 – 1.5 seconds for old drivers (Mehmood and Easa, 2009). Following on from the 2009 study, Mehmood and Easa (2010) used 45 samples of data obtained from the Next Generation Simulation (NGSIM) program collected by Federal Highway Administration to validate driver brake reaction time (Mehmood and Easa, 2009) which they have incorporated in their proposed new car-following model. They found that the rate of change of speed for braking was higher than that of the non-braking in the deceleration scenarios and concluded that the vehicle in front reactions has a prominent impact on the actions of the driver of the vehicle following.

The estimation of reaction times with real time series traffic data has become possible due to the technological advancement. Different approaches to collect real time series data have been proposed by many researchers. Ozaki (1993) in the study of reaction and anticipation in the car-following behaviour developed a graphical method to ascertain the reaction time of the individual driver based on the difference in speed and acceleration profile. Chang and Chong (2005) used 5 vehicles equipped with tachometers and laptops to collect traffic data from some segments of Road Kangbyun buk in Korea. In all, ten subjects were used in the data collection which they grouped into five categories according to their driving experiences: under six months, one year, two years, five years and over five years. They made an assumption that the variety of drivers reflected in the data collected. Using lognormal distribution they obtained a reaction time of 0.5 seconds and 2.5 seconds for minimum speed of 3.6 km/h and maximum speed of 61.2 km/h respectively. The speed was measured by hand in order to reduce the abnormal speed and using discrete wavelet transform (DWT) in MatLab to correct the data collected (Chang and Chong, 2005). Measuring the speed by hand might not give accurate reading of some of the vehicles due to non-focus on the target vehicle due to external distraction and

tiredness of the hand. No mention of number of drivers under each categories to reflect the driving the data collected.

Ma and Andréasson (2006) used an advanced instrumented vehicle developed by Volvo Technical Development (VTD) to collect data on Swedish roads to estimate the reaction time or time delay. Using spectrum analysis method based on the Fourier analysis of the data obtained from 10 drivers and assuming a fixed reaction time, Ma and Andréasson estimated the reaction time ranging from 0.52 to 1.24 seconds. They reported that the method used in the estimation could give some inconsistent in the values of the estimations and that some of the reaction time estimation may give zero or even positive values. They reported a limited data was collected for the reaction or delay time estimation (Ma and Andréasson, 2006).

The spectrum analysis method used by Ma and Andréasson may have an advantage for estimating the reaction time delay from experimental data without any premises of the model form. However, the disadvantage of the spectrum analysis methods is that it is limited by the stationary and linear conjecture of the system and hence experiences some problems in practice in the spectral estimations. Ma and Andréasson (2006) reported that the estimated reaction time or time delay validation was not adequate, hence further studies required in the area of time series data analysis and in the aspects of psychology. The authors asserted that the assumption that the reaction time or delay is fixed put restrictions on the models (Chang and Chong, 2005) capabilities to replicate traffic in reality, hence analysing real traffic data quantitatively in terms of statistical or uncertainty term might improve this deficiency in the models capabilities. Hoogendoorn and Ossen (2006) estimated the reaction time for two-leader and one-leader (basic) car-following models as 1.54 seconds and 1.36 seconds respectively for a motorway driving in the Netherlands.

Orosz et al. (2011) in the study of reaction time delays of human verse robotic drivers revealed that reaction time delays can alter the frequency of arising oscillations and the wavelength of the transpiring traveling waves, leading to high-frequency/short-wavelength oscillations. The authors asserts that traffic congestion may occur by sufficiently large excitation; at the same time without these excitations the traffic flow remains smooth. This implies that each driver's behaviour in the traffic stream has a significant role in determining the condition of the whole traffic system. The authors concluded that research into the individual driver behaviour could assist to recognized the

characteristics of undesired human behaviour and allow researchers to shape the response of Autonomous Cruise Control (ACC) driven vehicles in such a way that they can lessen the impact of waves triggered by human drivers. Orosz et al. concluded that when vehicles interact with the nonlinearities in the system, the reaction time delays could make the dynamics of the traffic flow excitable, in such a way that waves may be triggered when the uniform traffic flow is linearly stable. Although the data sets collected are possible to use for analysis here, due to time limitation it was not analysed. In this current study, there was no analysis of reaction time (see further research in Chapter 11).

2.2.5 Time Headway/Time Gap and Safe Distances

Many car-following models were proposed based on a general assumption that describes the individual driver of a following vehicle's effort to attempt to maintain a safe and constant time headway at all time (Brackstone and McDonald, 2003; Van Winsum, 1999) in a car following situations. The general assumption may implies that, should the leading vehicle apply the maximum rate of braking in an attempt to slow down or stop, the following vehicle will eventually start to decelerate at a rate which is less than a critical threshold, and with a delay reaction time, will finally starts to slow down gradually until it comes to a stop at some distance behind the leading vehicle enough to avoid a collision. This assumption forms the basic principles of many car-following models, for instance Gipps (1981) and Gunay (2007) models. However, as pointed out by Brackstone and McDonald (2003), there is enough body of evidence to suggest that this assumption may not necessary be true. Brackstone and McDonald argues that time headways commonly described by the relationship as the inverse of the squared root of the vehicle speed ($1/\sqrt{v}$), but then also a considerable amount of time headways studied on a typical freeway may be considered 'unsafe', as 48 percent of the total time headways studied in an experiment were found to be below 1 seconds (e.g. Ayres et al., 2001).

Time headway can be defined as the time distance between successive vehicles travelling in the same direction with a specified point of reference (i.e. on the side) along the road as the vehicles passes the reference point, namely, from a specified point of reference of the leading vehicle (i.e. the front bumper) to the same specified point of reference of the following vehicle (i.e. the front bumper) (Gunay and Erdemir, 2011; Gunay, 2012). Van Winsum (1999) reported that there is a considerable evidence to suggest that human drivers adjust the time accessible to them as a control mechanism, and that in any

particular similar situation, the safe following distance the driver of a vehicle tries to maintain is primarily based on a time headway that is constant. He asserts that the preferred following distance D_p (in metres) that drivers attempt to maintain is given by:

$$D_p = t_p v_i \tag{2-23}$$

Where t_p is the preferred time headway in seconds and v_i is the vehicle driver's speed in metre per second (m/s). The principle underlying this rule he proposed was that drivers use time headway as a safety margin, and different drivers have different headways. When preferred distance D_p is smaller than the distance of separation to the lead vehicle, the driver do not have any safety related reason to accelerate until the preferred distance of the driver is reached. Time headways, that is comparatively constant with the driver of a vehicle depends on the skills of the driver, the state of the driver (i.e. fatigue), visual condition of the driver, psychological state and the concentration of the driver to the leading vehicle (Van Winsum, 1999).

Different experimental approaches have been adapted by many different researchers in the measurement of the time headways in car-following. Among the various approaches adapted are the video recording and the use of manual analysis of real traffic data (Gunay and Erdemir, 2011), driving simulators (Van Winsum and Heino, 1996), the use of the inductive loop detectors-with loops of wires (Ayres et al., 2001; Gunay and Erdemir, 2011) and the application of the automatic number plate recognition (Gunay, 2012) to study and observe the time headways of vehicles in a car-following situation. For instance, Van Winsum and Heino (1996) studied time headways using driving simulator during car-following and braking reaction of drivers. The authors found during the experiment that between the drivers, the time headway remained steady and constant above a range of speeds. They concluded that the time headway that each driver decides to follow is unrelated to the speed of the vehicle during car-following situation.

Ayres et al. (2001) carried out experiment to study the time headway preferred by highway drivers. Ayres et al. found that in the rush hour traffic, the time headway was in the range of 1 to 2 seconds between vehicles for different range of vehicular speed (from 20 to 60 mph). They assert that time headway below the limit of 1 second was observed in all traffic condition even though the volume of traffic did not required the drivers to drive at close distances. Ayres et al. found the time headway of 1 second for heavy traffic

i.e. the congested traffic. It is worth noting that the study did not mention the size of the data used to determine the time headways.

Gunay and Erdemir (2011) conducted an empirical studies to measure the time headways between vehicles in the neighbouring adjacent lane. They noticed that when the vehicles spacing on the same lane is in the range of 0 - 1.5 seconds (which is considered to be small), the number of neighbouring vehicles with a short time headways ranging from 0 – 1.5 seconds were less than when the spacing is between 1.5 – 2.5 seconds. This was translated to mean that a strong evidence of vehicular interactions with one another between two neighbouring lanes exist when the traffic is moving in the same direction, which is not considered in existing microscopic models. They found that a smaller number of drivers were prepared to retain the short headways with regard to the neighbouring lane vehicles when the same-lane time headways fall below a certain value. This, they argued could mean that drivers desire to pass or wait behind the neighbouring adjacent vehicle apart from when there is light traffic flow on the offside lane that is usually used by drivers for overtaking, instead of driving alongside (Gunay and Erdemir, 2011).

Following on from previous studies, Gunay (2012) used automatic number plate recognition (ANPR) camera technology to collect data in Thurles, the Republic of Northern Ireland to study the time headway of drivers taking into account the vehicles identities. A total of 10,024 single captured vehicles out of 34,332 vehicles for 20 sites recorded in a day were used in the study. He found that 17.2% of the vehicles maintained a time headway of 0.5 – 1.5 seconds in the first group of vehicle captured and 15.7% of the vehicles maintained a headway of 1.5 – 2.5 seconds for the second group captured. Gunay concluded that the headways distribution with regard to the time gaps in seconds was more or less biased towards the right when it was compared to the headways of the overall data distribution for all vehicular data with no specific reference to the identities of the individual vehicle. When identities of the individual vehicles were taken into account, he found that the standard deviation to the mean ratio of the time headways was less than that obtained from the overall data with no individual vehicular identities (Gunay, 2012).

2.2.6 Time to Collision

Traffic conflict investigation methods have shown that Time-to-Collision (TTC) has become a common vision feature used to evade obstacles (Jin et al., 2011) and an effective measure for evaluating the seriousness of traffic collisions and distinguishing critical from normal behaviour (Horst and Hogema, 1993). Time-To-Collision is broadly used in the study of driver behaviour and the evaluation of possible traffic collisions (Jin et al., 2011) in car-following and evidence in literature point straight to it use as a decision-making tool in traffic (Horst and Hogema, 1993). TTC as defined by Horst and Hogema (1993) is the time needed for two vehicles (i.e. following and leading) in a traffic stream travelling on the same road to collide if the two vehicles continue at their current speed in their travel path. It can also be defined as the distance of separation between the following and the leading vehicles divided by the difference in speed between the two vehicles. Time to collision can be expressed as the ratio of the relative distance between two vehicles to the relative speed between both vehicles in the same travel path. TTC can be formulated as (Jin et al., 2011; Bevrani et al., 2012; Brackstone and McDonald, 2003):

$$TTC\ (t) = \frac{\Delta x(t)}{\Delta v(t)} \tag{2-24}$$

Where $TTC\ (t)$ is the TTC for the vehicle following at time *t*. This relationship implies that a short TTC will occur when there is a larger relative speed and a smaller distance of separation between both vehicles. The smaller distance of separation (i.e. short headway) would not necessary lead to a collision since it has to happen together with the traffic unsteadiness in such a manner that the driver's response to the situation could not be prompt. Hence TTC is said to incorporate both a short headway and the traffic unsteadiness (i.e. the instability) at any given time (Bevrani et al., 2012). When the TTC is smaller, the foot movement to the brake pedal becomes faster, which is linked with a larger deceleration of the vehicle and as a results leads to maximum pressure been applied to the brake which is also linked with a larger deceleration of the following vehicle.

Van Winsum and Heino (1996) found no evidence that suggest that drivers following other vehicles with shorter headway will differ from the other drivers following with larger headway in their ability to perceived time to collision. On the other hand, evidence suggests that drivers with short following distance to the lead vehicle are better able to programme the intensity of braking to the levels required. Van Winsum and Heino (1996)

concluded that in the execution and programming of the brake reaction, the drivers who choose to follow the vehicle ahead in a short distance differs from the drivers that follow at a longer distance.

Jin et al. (2011) also defines TTC in terms of the visual angle of the following driver as the ratio of the angular size of the oncoming vehicle to its angular speed. This is formulated as:

$$TTC\ (t) = \frac{\varphi(t)}{\varphi'(t)} = -\ \frac{Z(t)}{Z'(t)} \tag{2-25}$$

where $\varphi(t)$ is the visual angle the nth vehicle driver observed at time t, $Z(t)$ is the distance between the following vehicle front bumper and the leading vehicle rear bumper. This imply that the following vehicle driver can observe the TTC as the ratio of the approaching vehicle leader's immediate visual angle to its rate of change. They showed that for a staggered (i.e. non-lane based) car-following (Gunay, 2007) the TTC can be expressed as a function of the visual information perceived by the driver that incorporated in the relative rate of dilation or constriction of the visual gap angle of the driver if no contour dilation element of the vehicle in front is present. This is formulated as:

$$\frac{1}{TTC} = \frac{\varphi'(t)}{\varphi\ (t)} - \frac{\theta'(t)}{\theta(t)} \tag{2-26}$$

where θ is the visual gap angle keeping the front vehicle apart from the collision position. The equation demonstrates that the driver of the vehicle is sensitive to the visual information of the leading vehicle's optical gap angle. They incorporated this formulation into the GHR model as a sensitivity term (Jin et al., 2011).

Time to collision and headway (expressed as $\Delta x/v$) are used as key safety indicators in many studies. For instance, Bevrani et al. (2012) conducted sensitivity test using the data obtained from the NGSIM database in attempt to examine how the acceleration prediction by the GHR model can changed the reproduced TTC. They found two interesting results from the analysis. Firstly, they found that any variation in the acceleration rate effects in nonlinear changes in the TTC since the relative distance and the relative speed are inter-correlated. Secondly, the TTC values were significantly influenced directly by the simulation step. This implies that when the simulation step is higher the TTC values increases. They found the TTC to be 0.14 seconds, 0.18 seconds and 1.10 seconds (which

were less than 3 seconds) for the GHR (Chandler et al., 1958), GHR (Ozaki, 1993) and GHR (Modified) models respectively (Bevrani et al., 2012).

Brackstone and McDonald (2003) used the data they collected in 1997 from the M27 and vehicle heading away from the City of Southampton in the UK to examined TTC in the speed range of 50 to 60 km/h the same as used by Van Winsum and Heino (1996) study and found that the TTCs were larger in the range of 21 – 58 seconds in general among the drivers. Van Winsum and Heino (1996) showed that the deceleration commenced by the driver was a function of the TTC as estimated by the driver, when the actual distance headway becomes smaller than the preferred distance. Van Winsum (1999) proposed a new car-following model incorporating the TTC estimated by the driver from psychological perspectives during the negative acceleration initiated by the driver in car-following situation. The model is formulated as follows:

$$a_i = cTTC_{est} + d + \varepsilon \tag{2-27}$$

And he defines the actual TTC and estimated TTC that the driver of a vehicle decides just how to decelerate as:

$$TTC = D_p/(RT\ x\ a_i) \tag{2-28}$$

$$TTC_{est} = eTTC^f \tag{2-29}$$

And the reaction time (RT) as:

$$RT = \sqrt{\left(2\ x\ \left(D_p - D_d\right)/-a_i\right)} \tag{2-30}$$

Where a_i = is the driver's deceleration, TTC_{est} is the TTC as estimated by the driver, c is a constant, d is a constant (<0), and ε is a random error term, D_p is the preferred following distance, D_d is the distance driver decides to decelerate, $D_p - D_d = -a_i * t^2$, RT is the reaction time, e and f is estimated as 1.04 and 0.72 respectively (Van Winsum, 1999). This model (equation 2-27) is such that when the TTC is smaller, it result in a higher negative deceleration a_i and hence, at a certain threshold of about 10 seconds the deceleration will be zero. He included the error term into the model on the assumption that pressing the brake pedal and or moving the foot from the acceleration pedal is as the result of the deceleration initiated by the driver (Van Winsum, 1999).

The braking response the driver of the vehicle initiates together with the brake control during the deceleration were both found to be affected by the time-to-collision at the moment the vehicle in front begun to apply the brake. Hence, TTC can be used as important information perceived by drivers in assessing when to start and control the braking when following another vehicle (Van Winsum and Heino, 1996). Van Winsum (1999) mentioned that the proposed model (i.e. equation 2-27) could be the basis for modelling the environmental effects and human behaviour factors on the flow of traffic, congestion and car-following, however he pointed out that the model has not been validated and calibrated with empirical data and as such its usefulness is limited.

Horst and Hogema (1993) for over year collected data for TTC and other traffic data using inductive loop detector together with nearby scatter type sensor on the A59 two-lane motorway near the city of Breda, Netherlands. They found that TTCs lower than 5 seconds were hardly noticed and the values of TTC tend to increase in fog condition when the visibility is poor. They asserted that the dynamics of car-following could not be studied well with inductive loop detector approach despite the advantage of gathering real traffic data instead they used traffic simulator to measure the TTC in car-following situation. The subjects were instructed to start braking the moment they approach a motionless object. They kept the visibility distance to 40, 80, 120 and 160 metres and the speed difference as 20 or 40 km/h.

Horst and Hogema found that drivers' decision to start braking and control of the braking could be as a result of the information of the TTC accessible to them from the optic flow field, this finding agrees with Van Winsum and Heino (1996) study. Horst and Hogema (1993) applying the least squared fit to the data obtained from the stimulation experiment proposed a new relationship between the TTC_{stim} (TTC in the simulator, the lead vehicle is visible at the determined visibility distance), TTC_{gas} (TTC at the moment gas pedal is fully released when lead vehicle is visible) and TTC_{min} (minimum TTC value as reach during the entire process). They obtained $TTC_{gas} = -1.15 + 0.83 * TTC_{stim}$ for r = 0.97, $TTC_{min} = -2.58 + 0.80 * TTC_{stim}$ for r = 0.92 and $TTC_{min} = -1.43 + 0.96 * TTC_{gas}$ for r = 0.93 (Horst and Hogema, 1993). Although, this is very important area of research, due to time limitations the data was not analysed in detail on TTC. The data collected could be used to either analysis the TTC of following vehicles or evaluate rear-end collision of vehicles for driver safety analysis (see further research in Chapter 11).

2.3 Data Collection Methods

There have been different approaches or methods developed to collect traffic flow data in transportation studies. For instance, the prominent methods commonly used in data collection such as inductive loop detectors (Ayres et. al., 2001), aerial photography (Hoogendoorn et al., 2003), video recordings (Ahmed, 1999; Gunay, 2004; Halkias and Colyar, 2006; Appiah, 2008) and instrumented vehicles (Brackstone et al., 1999; Kim, 2005) to calibrate and validate car following models have been improving over the years.

Many of these methods used in empirical studies have been conducted on test tracks (Chandler et al., 1958; Ranjitkar et al., 2005), in tunnels (Greenberg, 1959; Gazis et al., 1961), using driving simulators (Mehmood and Easa, 2009) and on the main roads in cities (Brackstone et al., 1999; Kim, 2005). All these data collection methods enable researchers to have better understanding of the traffic flow dynamics and the behaviour of individual vehicles in a platoon. In the past, less sophisticated methods were adapted in many transport studies. For instance, Greenberg (1959) conducted an experiment at the Lincoln Tunnel using a Simplex Productograph machine to collect traffic flow data to calibrate mathematical flow equations. Greenberg stationed one observer at the entrance and another observer to the exit to the Lincoln Tunnel. The machine was placed along a short length of the road and activated to record the time a vehicle passes each observer. In doing that the individual vehicle's velocity and the headway between the successive vehicles were accurately recorded. The resulted data were separated into speed groups and the average headway for each speed group calculated. In order to smooth the data obtained, Greenberg calculated the average speed (space mean speed) and average headway for all vehicles in the same time profile (Greenberg, 1959; Greenberg and Daou, 1960).

In a related experiment, Greenberg and Daou (1960) collected traffic data by placing observers with synchronised stop watches that runs continuously at various locations along the roadway. The observers marked the type of vehicle such as cars, trucks or buses that passes in front of them on the roadway in every 30 seconds. The time at which the individual vehicle passed each observer was easily obtained and the traffic flow rate calculated at each location. A more advanced methods have also been employed in transport research in recent years. For example, Mehmood and Easa (2009) used a driving simulator integrated into real car to collect data on driving variability among the driving population in Canada. The participants' driving behaviour were tested using STISIM

(System Technology Incorporated Simulator, a high fidelity interactive driving simulator which presents a 45 degree horizontal view) and projected onto an Epson EMP-S3 LCD screen. The participants aged between 18 to 70 years, were made to drive the integrated real car placed in front of the screen and equipped with steering, brake, accelerator and automatic transmission to capture their driving behaviour variability.

Instrumented vehicle was used by Ranjitkar et al. (2005) to performed an experiment on a two 1.2 km long test track. They used cars equipped with real time kinematic (RTK) GPS measuring device capable of measuring vehicular movement to collect driving behaviour data. The RTK GPS receiver measures the vehicle speed and position at an interval of 0.1 seconds. The GPS receiver has a vehicle position accuracy of 10 millimetre (mm) + 2 parts per million (ppm) and speed recording accuracy of less than 0.2 km/h. They used participants aged between 22 to 30 years to collect data for the study. Since the use of less sophisticated methods, there have been improvements in the techniques for data acquisition due to technological advancement. In the following sections, the most commonly used traffic data acquisition techniques researchers adapt in various transport studies are reviewed.

2.3.1 Inductive Loop Detector Data Collection Method

One of the most extensive methods often used in the field to measure traffic flow parameters, such as the volume, occupancy and speed of passing vehicles and currently being used in data acquisition is the inductive loop traffic detectors. The inductive loop detectors (ILD) operate on loops of wire placed on the surface (Gunay and Erdemir, 2011) or underneath the pavement (Ayres et. al., 2001) of roads on the principle of changing inductance caused by the movement of a large conductor, for example, vehicles. In operation, electrical pulses are generated when a vehicle pass over a loop detector with the resulting pulses counted and recorded by the detector loop system as the volume of traffic i.e. the number of vehicle per hour units (Ayres et. al., 2001). The occupancy described as the fraction of time that a vehicle is over the inductive loop detector (Wang et al., 2005) is determined when the detector system calculates a percent of the time that a vehicle passes over the detector by comparing the duration of the generated pulses to the time between the pulses (Ayres et. al., 2001). When a vehicle passes over a second inductive loop detector directly following a single loop detector separated by a short

(known) distance, the speed of the vehicle can be determined by the detector system by measuring the time between the pulses generated (Ayres et. al., 2001; Wolf, 1999).

Investigation was carried out by Ayres et. al. (2001) to study the time headways of drivers on highways in USA with data obtained from inductive loop detectors placed underneath four southbound lanes on a section of the Highway 101 in USA. The volume, speed and occupancy from the data (recorded at 30 seconds intervals) were categorised into three traffic groups. The first group, the free-flow traffic with average speed of 70 mph recorded low occupancy between 05:00 to 06:30 hours. The second group, the rush-hour traffic recorded a low speed with the speed dropping to 30 mph between 07:15 to 08:45 hours. They reported that the final group, the heavy traffic recorded a high volume of traffic with increase occupancy between 10:00 to 11:30 hours. Analysing the data further, they transformed the data into traffic parameters such as speed and following distance that could be controlled by individual driver in estimating the time headway in car following process.

In a separate study in Northern Ireland, Gunay and Erdemir (2011) used inductive loop surface detectors at two different sites on the A55 dual carriageway at the Southeast Belfast to collect data on inter-vehicular time headways in two adjacent lanes in the same direction. They collected 43,838 vehicle data sets at site 1 and 42,408 vehicle data sets at site 2. Inductive loop detectors have also been used in other applications such as microsimulation tools. For instance, Zhang and Kim (2005) created a ring road in simulation model and place three loop detectors at different locations at 270 metres, 540 metres and 810 metres with each detector having a length of 40 metres to measure the traffic density and the space-mean travel speed. Wang et al. (2005) also adapted similar method used by Zhang and Kim to collect data in simulation model. The use of inductive loop detectors in traffic studies and monitoring traffic flows are widespread, however, this is not the only known technique to observe and measure traffic flow (Wolf, 1999).

2.3.1.1 Limitations of Inductive Loop Detector Techniques

The inductive loop traffic detector data collection technology enable transport researchers to determine the volume of traffic, occupancy and the speed of the passing vehicles on a network. But due to the large size of data collected by this technique, manual analyses might not be possible (i.e., time consuming and errors) and therefore, a software has to be develop in order to save time and minimise errors and eliminate the possible human

errors in the analyses (Gunay and Erdemir, 2011). Moreover, this technique could not account for a following behaviour of vehicle pairs over longer period of time at different locations on the same stretched of road on the network since the loops are often installed at a particular location on the network. In addition to this techniques, the use of video cameras to record individual vehicle trajectories and study the traffic behaviour has been introduced in recent years. The next section review the use of video cameras in recording vehicle trajectories to collect traffic data for analyses.

2.3.2 Video Camera Recording of Traffic Flow Method

Digital video cameras mounted on buildings (Halkias and Colyar, 2006) and telescoping towers (Ervin et al., 2000) to record and observe vehicle trajectories and process the traffic data to create a database for car-following behaviour has been more apparent in recent years, for example the NGSIM (Halkias and Colyar, 2006) and SAVME (Ervin et al., 2000) databases.

The System for Assessment of the Vehicle Motion Environment (SAVME) data collection method which was initiated in 1992 through the collaboration of the University of Michigan Transportation Research Institute (UMTRI), Veridian ERIM International, and Nonlinear Dynamics Inc. for the National Highway Traffic Safety Administration uses video cameras to collect traffic data. The SAVME techniques collects dense digital video image data from several cameras mounted on roadside towers, processes and merge the video image data to produce one track file for every individual vehicle that passes through the selected road sites and compiles a database for individual vehicle trajectory. The SAVME database contains the measurement of about 30,500 vehicle trajectory data collected in a period of 18 hours (Ervin et al., 2000). The SAVME database has been used by other authors such as Mehmood et al. (2003) for different studies and applications. Mehmood et al. (2003) extracted 132 vehicle pairs of trajectory data from the SAVME database collected on a shoulder lane to develop and validate a new system dynamic car-following models.

The Next Generation Simulation (NGSIM) which was initiated by the US Federal Highway Administration (FHWA) in the early 2000 employs the use of digital video cameras mounted on top of buildings that overlooks some selected highways in the U.S. to record vehicle trajectory data for traffic studies (Figure 2-1) (Halkias and Colyar, 2006). Numerous experiments have been conducted using the NGSIM vehicles

trajectories database. Bevrani et al. (2012) extracted comprehensive vehicles trajectories data from the NGSIM database collected from the southbound U.S. Hollywood Motorway 101 in Los Angeles to evaluate and calibrate the GHR car-following model.

Figure 2-1: Typical digital video camera mounted on top of a building overlooking the highway to record vehicles trajectories data for NGSIM database (Source: Halkias and Colyar, 2006)

Farhi et al. (2012) also used vehicles trajectories data on a segment of U.S. Highway 101 from the NGSIM database for parameter identification of the new multi-anticipative car-following model they proposed. Mehmood and Easa (2010) extracted 80 vehicles trajectories data from the NGSIM database that was collected using video camera mounted on a 36-storey building situated adjacent to the U.S. Highway 101 and the Lankershim Boulevard interchange in the Universal City neighbourhood to calibrate and validate a new car-following model. The Lankershim NGSIM database was also used by Treiber and Kesting (2013) to calibrate and validate car-following models. Hamdar and Mahmassani (2008) used 4,733 vehicles trajectories data from the NGSIM database collected on Interstate 80 in Emeryville, California in their study to explore and assess accident free car-following models. Though the NGSIM data sets as well as the SAVME data sets which consist of detailed and accurate vehicles trajectories which are valuable to researchers (Halkias and Colyar, 2006), contains all sorts of data sets that cannot be used directly due to the inconsistencies and errors which could considerably influence the car-following model calibration outcomes, especially the models which are less robust (Treiber and Kesting, 2013).

Jin et al. (2011) used video camera mounted above the highway to record the lateral position of vehicles in Weixing Road, Changchun City, China, where they divided each lane into ten equal parts and literally recorded 583 traffic samples within an hour in the morning. Gates et al. (2007) mounted video camera (about 400 feet to 800 feet upstream) on a modular steel pole (18 feet long) at the roadside overlooking the intersection in Madsion area of Wisconsin to collect traffic data. At six different intersections, they used 8 millimetres analog video camera to record video images of vehicle movements continuously for about 2 to 4 hours during the day. Gates et al. (2007) processed the data using Sony Vegas Video 6.0 program and extracted a total of 898 vehicles trajectories for analysis (see Figure 2-2). However, mounting digital video cameras to record and observe traffic flow are not always possible at some locations. For example, in rural areas the cost involve in the required infrastructure will make it impossible for a short term traffic studies to be conducted. Not only that, the expensive mounting of equipment and placing of digital video cameras at strategic areas would be prohibited by lack of long-term commitment by researchers (Kanhere and Birchfield, 2008).

Low mount cameras have also been employed to study traffic flow, for example, Appiah (2008) collected data using digital video camera to record traffic flow at 2 signalised intersections in Edinburgh to investigate driver dilemma at signalised intersections. Ahmed (1999) collected data on traffic flow using standard video camera on the Interstate 93 at the Central Artery, in downtown Boston. Ahmed processed video data using Video Traffic Analysis System (VIVA) developed by Universitat Kaiserslautern in Germany which was capable of measuring vehicle positions from video images. Gunay (2004) observed traffic flow in Istanbul, Turkey using video camera mounted on a bridge supported a by tripod to investigate lane utilisation on Turkish highways.

Figure 2-2: Typical analog video camera mounted on signpost overlooking the intersection to record traffic flow (Source: Gates et al., 2007)

Greenshields (1935) conducted an empirical study using photographic method which involves a 16 millimetres Simplex movie camera (which was capable of taking single frames of images) to collect actual traffic flow data. Greenshields set up the 16 millimetres simplex movie camera at about 350 feet from U.S. 23 highway in Delaware, Ohio, so that individual vehicles that comes into the camera's view range and captured would appear in at least two successive images or frame. This method produced actual traffic flows per hour of vehicles passing the points of observation marked by short definite intervals of time and the measured distance travelled by these individual vehicles during one of these time intervals.

Aerial observation of traffic flow by helicopter for some sections of highways allows many consecutives vehicles to be observed at the same time (Brackstone and McDonald, 2003). The usefulness of the helicopter mounted with high resolution digital cameras also allows the movement of the individual vehicles in the platoon to be studied. Hoogendoorn et al. (2003) employed a helicopter mounted with a light sensitive camera with a resolution of 1300 by 1030 pixels with a maximum frequency of 8.6 Hz and a personal computer equipped with frame grabber attached to the camera to observe, measure and store the traffic data near the Dutch city of Utrecht. The camera was able to detect and track vehicles and capture images of up to 520 metres of road given the resolution and the spatial resolution (40 centimetres per pixel). They collected data during the afternoon peak hours (i.e. 15:30 – 17:30 hours) where they expected the type of bottleneck that causes congestion at the selected sites. In all, a total of 535 vehicles triples (i.e. car following involving three vehicles) were selected for the study out of 935 vehicles

trajectories collected for the period of 90 seconds (see Figure 2-3 for vehicles trajectories) (Ossen and Hoogendoorn, 2005, 2011; Hoogendoorn and Ossen, 2006).

Other researchers have also used aerial observation to observe and collect traffic flow data. For instance, in 1974 Treiterer and Myers used a helicopter mounted with a digital video camera that recorded images with a mean interval of 1.0 seconds. They observed and measured 70 vehicles platoon in a time of 238 seconds (Treiterer and Myers, 1974). The aerial observation method allows individual vehicles or platoon to be observed without the drivers being influenced. However, the instability of the cameras by the vibration of the helicopter may lead to data loss. Also, the inaccuracy in photogrammetric processing and the limited coverage area of the camera to capture each vehicle or platoon at a time on the stretch of road for a few minutes restrict its usefulness (Brackstone and McDonald, 2003). The data collection could also be affected by the weather condition such as wind speed, which could cause the instability of the helicopter and make it impossible to keep to a fixed position (Hoogendoorn et al., 2003) and thick clouds which could obstruct the camera's view thereby reducing the image quality. Digital video camera have also been employed in automatic number plate recognition technology (Gunay, 2012) to observe and record traffic data for use by researchers.

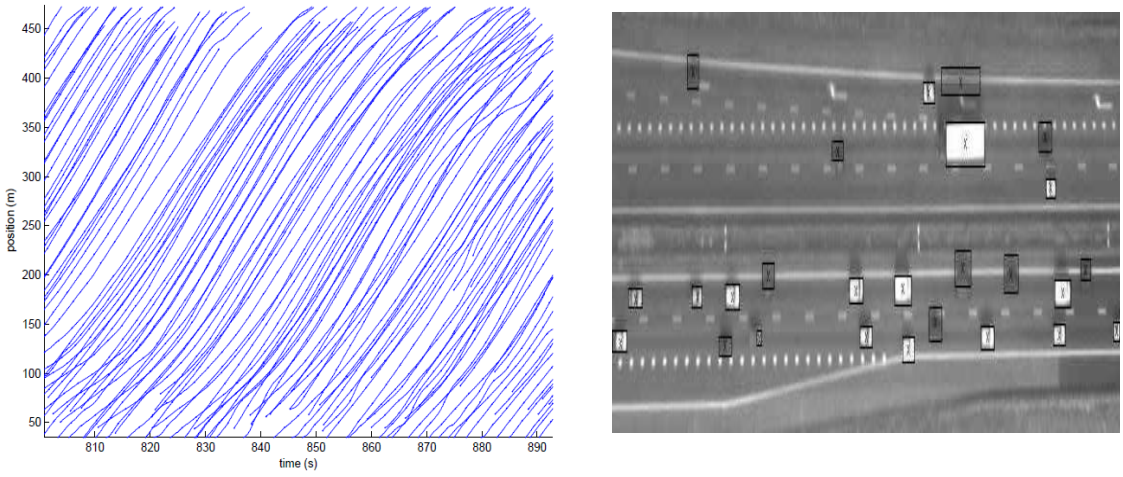

"Example showing 935 vehicle trajectories subset. Time instants are represented by small dots which are 2.5 seconds apart (Left), and a snapshot of the corresponding positions and dimensions of vehicles from vehicle detection recorded using helicopter (Right)".

Figure 2-3: Vehicle trajectories from a helicopter (Source: Hoogendoorn and Ossen, 2006; Hoogendoorn et al., 2003)

2.3.2.1 Limitations of Video Camera Recording Techniques

Video cameras as a tool for recording traffic flow have certainly improve traffic data collection and the study of individual driver behaviour. However, this techniques have some drawbacks, for instance, cameras mounted high on the side of the road or helicopter can only cover, capture and record the vehicle trajectories for a specific stretch of the road in the camera's view but not the vehicle interactions on the entire network. Bad weather conditions such as thick clouds which could obstruct the camera's view (e.g. high mounted cameras (Gates et al., 2007)) and wind speed that could cause instability (e.g. helicopter (Hoogendoorn and Ossen, 2006)) may result in very poor image quality that would make it difficult to analysed.

The poor image quality and other factors may result in some inconsistencies and errors in creating database such as NGSIM vehicles trajectories (Halkias and Colyar, 2006), which may render some of the data not been used for analysis since they could affect the car-following results as reported by Treiber and Kesting (2013) when using only video cameras to create database. Also, the high cost involve in mounting the camera so high to record wide area makes it impossible for a short time experiment to be conducted, especially in rural areas (Kanhere and Birchfield, 2008).

Aside the drawbacks of video cameras in traffic recordings, it helps in recording permanently the driver behaviour interactions and variability in car following as well as the types of vehicle interactions in a network. The next section review the use of vehicles equipped with devices such as video-audio camera to record traffic flow data for various traffic studies.

2.3.3 Instrumented Vehicle Data Collection Methods

The increase in investment and research, particularly in the area of driver assistance systems such as Adaptive Cruise Control (ACC) vehicle distance detector sensors (Brackstone and McDonald, 2003) have revolutionised the way researchers observe and study vehicle movements in traffic stream and collect real traffic data using tools such as instrumented vehicles. Instrumented vehicles as a tool used in traffic research to collect data are not something new since its introduction in the late 1950s, however, many different types of instrumented vehicle have been developed to conduct different experiment (Brackstone et al., 1999). In recent years, more advanced devices such as lidar

sensors (Ma and Andreasson, 2005), radar sensors (Brackstone et al., 1999; Chakroborty and Kikuchi, 1999; Kim, 2005), Deferential Global Position Systems (Kim, 2005) and digital cameras have been used to equipped vehicles to observe and record traffic flow and improve real time series data collection for microsimulation modelling and other applications.

Chandler et al. (1958) performed an experiment on a test track using an instrumented vehicle (i.e. car) that was linked to series of lead vehicles with wire to collect quantitative data regarding driver-car performance on a two-lane highway. The instrumented vehicle was equipped with a reel wound with fine wire and a power unit on a small platform which was fastened to the front bumper. The end of the wire was fastened on the rear bumper of the lead car. A slipping friction clutch provided a constant wire tension as the test vehicle and the lead vehicle were driven around the test track. A multiple turn potentiometer geared to a reel shaft and tachometer operating off the shaft measured the following distance and the relative speed between the two vehicles. Accelerometer which was mounted in the vehicle measured the longitudinal acceleration of the test vehicle. The speed of the test vehicle was measured by a fifth wheel attached to the test vehicle. All the experimental data were recorded and stored by an oscillograph installed in the back seat of the test vehicle (Figure 2-4) (Gazis et al., 1961).

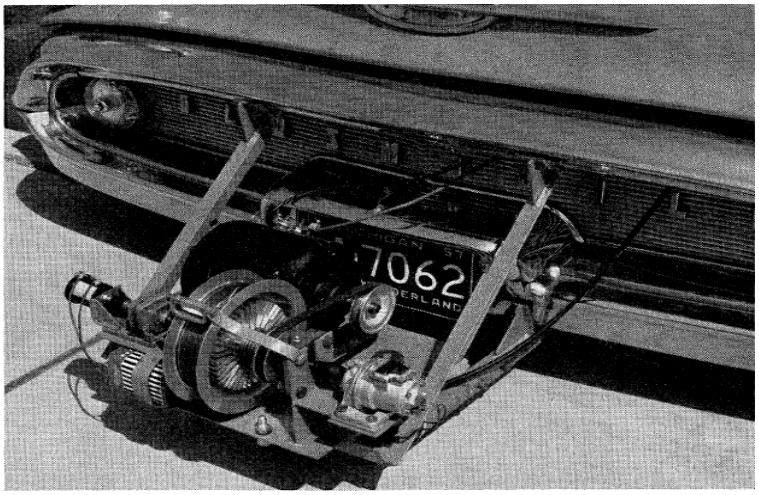

Figure 2-4: Instrumented vehicle used by Chandler et al. (1958) to collect time series data

Instrumented vehicles have been improving since the study by Chandler et al. (1958) due to the technological advancement over the years. Many well-known organisations and institutions such as The Robert Bosch GmbH Research Group in Germany have

developed instrumented vehicle with some of the sophisticated equipment to collect data which have been used by many authors such as Panwai and Dia (2005), Al-Jameel (2010).

Soria et al. (2014) used an instrumented vehicle developed by the University of Florida-Transportation Research Centre (TRC) which was equipped with Honeywell mobile digital recorder system capable of recording four cameras at the same time (i.e. cameras installed on the front, rear and both side of the vehicle), a Global Positioning Systems (GPS) (which can record the position and the speed) and an on-board computer to record information from the devices on board the vehicle to collect data to evaluate four existing car-following models. In all, 31 drivers of different gender and age were observed driving the instrumented vehicle during the morning and afternoon peak hour (Soria et al., 2014). The second by second snapshot analysis for estimating the distance headway between the vehicles and the computation of the speed of the leading vehicle from video frames (Soria et al., 2014) might leads to inaccuracies in the data obtain. In fact, this inaccuracies in the data could be addressed by introducing distance and speed measuring device such as lidar sensor (Ma and Andreasson, 2005) or radar sensor (Brackstone et al., 1999).

In 1999, Chakroborty and Kikuchi used an instrumented vehicle equipped with laser radar and speed measuring devices to measure and collect data on the distance headway between the leading and the following vehicles and the speed of the test vehicle at a continuous rate of 50 milliseconds. The instrumented vehicle was driven on the arterial roads in and around Newark, Delaware by two-man team to collect time series data (Chakroborty and Kikuchi, 1999).

The Transport Research Group (TRG) of University of Southampton developed an instrumented vehicle in 1993 to study driver behaviour and driver response to intelligent transports systems (ITS) (Brackstone et al., 1999). The vehicle was equipped with an optical speedometer to measure the ground speed of the test vehicle with an accuracy of ±0.02 m/s, radar rangefinder (fitted either to the front or the back of the vehicle) to measure the relative distance and the relative speed of the following vehicle, video-audio monitoring systems that permanently records each experiment for later analysis and an on-board computer to log the data coming from the devices. The radar rangefinder used by the TRG has an operational range in excess of 100 metres and a distance measurement accuracy of ±0.2 metres in range and the relative speed accuracy of ±0.4 m/s. The radar has a frequency rate of 10 Hz which sent information to the on-board controller PC and recorded in 5 minutes block (Brackstone et al., 2002).

The TRG Southampton instrumented vehicle was used to conduct experiment on both two-lane motorway and three-lane motorway of the M3 and the M27 with a speed limit in excess of 60 mph near Southampton in the United Kingdom (UK) to observe and collect driver behaviour real time series data during the morning peak hour (7:00 AM to 8:30 AM) and the evening peak hour (17:00 to 18:00). They used either the 'passive' mode where the sensor is mounted at the rear of the vehicle or 'active' mode where the sensor is mounted on the front of the vehicle to collect car-following data (McDonald et al., 1999; Brackstone et al., 1999; Brackstone et al., 2000, 2002; Brackstone, 2003; Piao and McDonald, 2003; Brackstone et al., 2009).

Further studies were conducted using the TRG Southampton instrumented vehicle on major European cities to conduct comparative microscopic studies on speed flow relationship and measure car following characteristics that might be influenced by national driving behaviours. The TRG instrumented vehicle collected car-following data from 30 UK drivers on the M3 motorway near London in 1997, 99 French drivers on the A1 road near Lille in the north (peripherique encircling Paris) in 1997 and 148 German drivers on a range of Autobahns (mainly A1) in the Hamburg area in the north in 1998 (Brackstone et al., 1999). In 2002, TRG Southampton instrumented vehicle was used to collect data in Oslo (Norway), Paris (France) and Southampton (UK) (Piao and McDonald, 2003). The TRG Southampton instructmented vehicle could not define the vehicle's position during the entire experiment as there was no GPS based devices on-board to define and record the actual position of the vehicle at every point in time. Moreover, the instruments on-board the test vehicle could not measure the acceleration of the test vehicle which has to be derived by computation from the ground speed.

Ma and Andreasson (2005) employed an instrumented vehicle that was developed by Volvo Technical Development (VTD) to conduct a study on Swedish roads. The vehicle was equipped with a Global Position System (GPS) based navigation system, two lidar sensors, video cameras to observe vehicles in both the front and the rear of the test vehicle and an advanced on-board trip computer installed with Volvo ERS software that records the speed, distance, travel time and fuel economy. The two-dimensional lidar sensors which was installed at the front and the back of the vehicle can each observe up to four vehicles or objects at the same time and continuously measure the distance between the instrumented vehicle and the vehicle being observed at a maximal frequency of 50 Hz (with measuring accuracy interval of 0.02 seconds) within a distance range of 1 metre to about 150 metres. They used the vehicle equipped with the devices mostly on Swedish

motorway section of Road E18 near Stockholm, where the speed limits were 70 km/h, 90 km/h and 110 km/h to observe and collect car-following driver behaviour data. The time series data were collected on both single lane road and two-lane road sections of the E18 motorway (Ma and Andréasson, 2006a, 2006b, 2007; Ma, 2007).

However, there are some limitations of the lidar sensors, in that the noise measurement of lidar sensor (1% to 5% of the range) will be amplified when deriving its differentials (Ma, 2007), which might result in certain delay in the time series when using filtering algorithms software, such as the Volvo ERS to smooth the readings which might not be smooth enough for the car following studies (Ma and Andréasson, 2006a; 2006b). Also, the lidar sensors has a distance measurement range of up to 150 metres which restrict its usefulness when considering studies that requires long range distance measurement. Kim (2005) introduced a distance measuring instrument integrated with Differential Global Position System (DGPS) into his instrumented vehicle to collect real time series data on I-295 and I-495 freeways in the USA. He equipped the vehicle with infrared radar sensor to measure the distance and the relative speed of the following vehicles, DGPS based distance measuring device to predict the position, speed and acceleration of the test vehicle, video-audio camera (Brackstone et al., 1999) to record the charateristics of the following driver and an on-board computer to store the data from the on-board devices. The radar sensor has an operational distance range of 2 metres to 150 metres with measuring accuracy of ±1.0 metres and -20 m/s to 60 m/s in relative velocity with measuring accuracy of ±0.3 m/s.

Kim used one video-audio camera which was mounted facing the back of the vehicle and mounted the radar sensor to the back bumper of the vehicle i.e. “passive” mode (Brackstone et al., 2002). The instrumented vehicle was used mainly on the I-295 (two-lane) and I-495 (four-lane) freeway in Maryland near the Washington D.C. area to collect car-following data during the rush hour and non-rush hour (Kim, 2005). Although Kim employed the most up to date technology in his data colection methods, only “passive” mode of data collection was used. Morever, only one video-audio camera mounted at the back of the test vehicle was used in the data collection and not taking into consideration of what was happening in front of the test vehicle. The radar sensor range of about 150 metres restrict it usefulness for capturing data outside of this detection range. Saleh and Lawson (2013) equipped a 2000 BMW 3-series car with a performancebox (PB) to collect traffic data on driving cycle in Edinburgh. The test vehicle was driven through some selected intersections on urban roads during the evening peak hour (i.e. between 4.00 pm

– 6.00 pm) and data were collected at a frequency of 10 Hz. The use of performancebox by Saleh and Lawson gave accurate data collection of the test vehicle's speed, acceleration and distance travel since the performancebox is a GPS based measuring device with universal coordinated time (UTC) to provide the location of the test vehicle at every point in time.

2.3.3.1 Limitations of Instrumented Vehicle Techniques

Using vehicles equipped with data measuring devices to collect traffic data by floating vehicle amongst the traffic stream has revolutionised the way researchers observe and collect driver behaviour data. However, there are some limitations of the types of technology employed or installed in the test vehicle to collect traffic data. For instance, the short range of the radar sensors (i.e. from 2 metres to 150 metres) used to measure relative speed and distance between any vehicle pairs restrict its usefulness in capturing data outside the detection range of the sensors e.g. 180 metres.

Also most of the data collection (i.e. relative speed) was limited to either the front or the back of the test vehicle since the radar sensors were either installed at the front or the back of the test vehicle restricting the data collection on both side at the same time. Moreover, since the video recorders were not GPS based to link to the position of the test vehicle, any computation using the video recordings may result in errors and may not reflect the actual computation.

To address some of the limitations in this research, an instrumented vehicle as a data collection tool where two radar sensors are mounted at the front and the back of the test vehicle to simultaneously record traffic data is used. The range of the radar sensors used for this research is 200 metres long, which is capable of capturing more data in the far range. Moreover, a GPS base video-audio recording device (i.e. Video VBOX) that is capable of recording the speed, acceleration, position, distance and travel time of the test vehicle is used in the instrumented vehicle setup.

It is important to note that during the period from 1960 to 1997 no major advances or techniques were reported on the methods of data collection relating to car-following. For instance, Blaauw (1982) used fixed-based vehicle simulator and an instrumented car on the road to evaluate the absolute and relative validities of simulator system in terms of system performance and driver behaviour for drivers who were inexperienced and

experienced, who were instructed to perform lateral and longitudinal vehicle control for both the vehicle simulator and the instrumented vehicle under the same road conditions. Hoberock (1976) in a study placed selected subjects in moving vehicles or laboratory devices and exposed them to various motion changes. The participants were asked to record their feelings about the motion on a questionnaire. This data collection technique was used by Hoberock to assess the subjects comfort in a moving vehicle. Lee-Gosselin (1995) reviewed a number of travel survey data collection techniques used in transportation research from the 1970s to the nineties. Several transport related data collection techniques were developed in the seventies (Wright, 1973; Kitamura, 1988).

2.4 Review of Analytical Approaches

Over the years, researchers have applied different analytical methods including handling and sorting of traffic flow data in calibration and assessment of statistical significance of parameters of traffic flow models, such as car following models. In calibration of models, regression analysis have been used in traffic flow analysis to estimate the relationships between different parameters of car following model (e.g. see Ma and Andréasson, 2007; Hoogendoorn and Ossen, 2006; Mehmood and Easa, 2010; Gates et al., 2007). Several authors have applied regression analysis method in the study of car following behaviour, for example, Gates et al. (2007) analysed traffic flow data using multilinear regression method to estimate the parameters of vehicle deceleration rate and brake-response time at different intersections. They found that among the dependent variables analysed, the speed of the approaching vehicle and distance from the intersection have significant effect on the deceleration rate and the brake-response time. Ma and Andréasson (2007) used multilinear regression method to examine the relationship between the acceleration and the perceptual parameters of different car following behaviour regimes.

In comparative experimental studies, researchers have over the years used analysis of variance (ANOVA) (e.g., Kim, 2005; Brackstone et al., 2009; Mehmood et al., 2003) to determine the statistical significance of traffic flow experiments. In 2003, Piao and McDonald used one-way ANOVA method to analyse the time gaps difference between three European cities (i.e. Oslo, Paris and Southampton) in two different speed bands of 10-20 km/h and 20-30 km/h. They found from the F-test results that there were significant time gap differences in the two speed bands between the three European cities they studied (Piao and McDonald, 2003).

In spite of the shortfalls of F-test used as a preliminary test of data analyses addressed by Markowski and Markowski (1990), F-test is still used as a comparative analysis of data for different driver behaviour variability in car-following. For example, Kim (2005) analysed the variability in car following behaviour using one-way ANOVA method to differentiate the relationships between causal factors (i.e., human and environmental factors) and the behaviour of the following vehicle. Kim performed a series of F-test analysis on the effect of different casual factors on following behaviour and asserted that there were statistical significance differences between the different causal factors and the car following behaviour. Other statistical methods have been used to validate models by many researchers. For instance, Kumar (2009) used the sums of the relative error to select a representative candidate cycle for motorcycle driving cycle model developed in a study conducted in Edinburgh.

In traffic flow analysis, numerous models parameters have been calibrated by different authors using the least-squares method (e.g., Greenberg, 1959; Gazis et al., 1959; Ossen and Hoogendoorn, 2005), which minimizes the sum of the squared residuals (i.e. between the observe and predicted values) of a model. For instance, Greenberg and Daou (1960) used a least-squares method to obtain a relationship between traffic speed and traffic density. Greenberg (1959) applied the least-squares fit to verify the flow theory relation between the headway and the traffic velocity. Ossen and Hoogendoorn (2005) used the least-squares method to analyse traffic data to estimate the optimal sensitivity parameters for different versions of the GHR model for separate following behaviours. They found that 80 percent of the data established statistical relation between the model's response and the stimuli for all instances of driver-vehicle combination. The calibration parameters of nonlinear driver behaviour models have been estimated using different approaches (for review see Brackstone and McDonald (1999)) but there is not much evidence in literature for the use of multilinear (or linear) regression method for calibrating nonlinear car following models calibration parameters.

Correlation analysis is one of the commonly used methods to find the relationship between the response and the other dependent variables of car following models. For example, Brackstone (2002) applied bi-variate 2-tailed correlation analysis in examining the correlation between driver psychology and car following. He found degree of correlation existing between different measures and dependent variables (respondents) namely; driver externality (DE), driver internality (DI) and sensation seeking scale V (SSSV) he examined. Brackstone obtained a Pearson coefficient of correlation of -0.69

for the link between the DE and DI, -0.618 for DE and SSS and finally 0.634 for passivity/aggressiveness (P/A) and slow to fast (S/F) for driving speed. Chandler et al. (1958) used correlation analysis to determine the relationship between the response (acceleration function) and the respondents (i.e. space and relative speed function) of the basic linear car following model. They found a correlation between the acceleration and the relative speed function with a resulting coefficient of correlation in the range of 0.8 to 0.9. However, they did not establish any correlation with the space dependent function of the model and therefore dropped the space dependent function from the final model formulation.

Authors such as Barceló and Casas, 2005; Panwai and Dia, 2005; Al-Jameel, 2010 and Toledo et al., 2003 have used error metric (EM) and root mean squared error (RMSE) method to analyse data to test the validity and measure the accuracy of new models between field experimental data and the simulated values. Toledo et al. (2003) applied the root mean squared normalise error (RMSNE) to measure and quantify the traffic flow relationship between simulated values and observed data obtained from Stockholm in Sweden. They obtained RMSE values ranging from 0.05 to 0.17 for different locations between the simulated values and the observed data and concluded that the simulation travel time reproduced the observed travel patterns at peak times for most of the locations in Stockholm (Toledo et al., 2003).

Other methods of data analysis such as descriptive statistics (i.e. standard deviation) and graphical representation of data (i.e. scatter plot) have been employed by many researchers to interpret the results of traffic flow experiments (see for example, Ossen and Hoogendoorn, 2005; Kim, 2005; Gates et al., 2007; Gunay and Erdemir, 2011). Graphical representation of data enable researchers to observe and compare the pattern of results of experiments for different behaviours at a time. For example, Kim (2005) used charts to show the oscillatory process (i.e. the variation in following distance and relative speed relation (Brackstone et al., 2009)) and traffic hysteresis phenomenon (i.e. the description of occurrence of acceleration and deceleration procedures having different asymmetric speed-density curve) in car following behaviour for drivers keeping the required following distance at different driving manoeuvres (Kim, 2005) (see also Brackstone et al., 2002).

2.4.1 The Analytical Approaches Proposed for this Current Research

A combination of different statistical approaches discussed in this section including other statistical methods are used in this research data analysis. In this research, multilinear regression method is used to calibrate existing and new car following models. T-test statistical analysis method is used to validate existing and new models developed in this research. The use of descriptive statistics and graphical representations such as charts (see for example; Ossen and Hoogendoorn, 2005; Kim, 2005; Gates et al., 2007; Gunay and Erdemir, 2011) are used for comparative analysis. Error measurement analysis is used in the selection of the appropriate sensors' elevation angle for used in the data collection.

The data collection for this research involve the use of private vehicle equipped with traffic data measuring devices such as radar sensors. PCAN Explorer 5 (Peak Controller-Area-Network Explorer) (Peak-System, 2014b) used as a general tool to monitor CAN messages worldwide and also available for both commercial and industrial use is introduced to monitor CAN messages from the radar sensors. The application of CAN data monitoring software is not something new to researchers or traffic engineers, this is because different applications have been used in different studies (see Brackstone et al., 2002; Kim, 2005), but there are insufficient or no evidence of PCAN Explorer 5 (for brief review see Gajdos, 2008) used in research of this kind to monitor data traffic from two radar sensors simultaneously.

Although PCAN Explorer 5 is a universal tool, its application in literature for traffic data monitoring for car following research is very limited. This tool provides all the necessary features that makes it useful as an advanced CAN bus traffic data monitoring. With the incorporation of integrated data logger, the PCAN Explorer 5 allows data to be recorded, analysed and stored throughout the experimental period (Peak-System, 2014; Gajdos, 2008). Other software used in this research is the VBOXTools and PerformanceTools developed by Racelogic Ltd to process the test vehicle's data obtained using the Video Velocity Box (Video VBOX) and the PerformanceBox (PB). These two software are easy to use and available for use for this research.

2.5 Summary

In this chapter, the literature review on car following models and data collection techniques used in collecting driver behaviour and traffic flow data as well as analytical

approaches used in data analysis were discussed. This is addressed under research question 1. The backgrounds of car following models and different types of the car following models including the fundamentals of traffic flow dynamics were discussed. The literature review found that different versions of the GHR car following model have been produced. It found that broad range of values of calibration parameters from -0.8 to 3.2 of the GHR car following model were produced because of experimental simplicity and reliability of data. Very few of these versions of the GHR models were found to be reliable models. Apart from that, no reported agreement have been reached for a general set of calibration parameters of the GHR model that best describe driver behaviour. In this work, new set of calibration parameters estimates of the GHR model are being produced using a more reliable data. This is addressed under research question 2.

It was revealed that most of the car following models proposed in the literature use the prediction of the following vehicle's acceleration to describe the driver behaviour. Very few models use the safe or desired following distance of the following vehicle to predict or describe the driver behaviour. There has been lack of attention of models that predict the desired following distance behaviour of vehicles in the available literature. In this work, car following model is developed to predict the relative or desired following distance between two consecutive vehicles to describe the driver behaviour. The model takes into consideration the relative acceleration between the two consecutive vehicles in predicting the desired following distance of the following vehicle. This is addressed under research question 2.

The literature review found that the existing two-leader car following models were proposed using existing car following models as the basis of the models development. Evidence suggests that most of the two-leader car following models were developed from studies that were based on non-scientific arguments (Hoogendoorn and Ossen, 2006). Moreover, these models largely predict the acceleration of the following vehicle but little or no evidence to support the models prediction of the desired following distance of the following vehicle. In this work, two-leader car following model is developed that describes the desired following distance of following vehicle in a three consecutive vehicles movement in a car following situation. The model developed in this work is an improvement of the two-leader car following model formulation in the available literature. This is addressed under research question 2.

The reaction time, the time headway or time gap and time to collision of the driver of the following vehicles were reviewed. It was found that these parameters of driver behaviour were mostly estimated using simple experimental data, which at times does not replicate actual driving behaviour. The headway, time to collision and reaction time discussed in this chapter are safety indicators or variables in car following. These safety indicators in relation to car following are independent of each other. Research have showed that small headways in car following create potentially unsafe conditions (Vogel, 2003). TTC instead is a parameter that distinguish between the actual occurrences of unsafe and safe situation in car following (Vogel, 2003; Sultan and McDonald, 2003). The minimum time headway of two seconds that drivers are advice to maintain following the lead vehicle is based on the drivers reaction time (SWOV, 2012). The reaction time of drivers is considered an important factor in human driving behaviour (Gunay, 2007; Kesting and Treiber, 2008) and forms the basic feature in several car following or traffic flow models (May, 1990). Due to time limitations there was no analysis of reaction time and time to collision carried out in this work. Although, data was collected but these parameters analysis in car following have been recommended for further research. The review found that the effects of socioeconomic and other parameters on the accuracy of existing car following models predictions were lacking in the available literature. This is addressed under research question 3.

The data collection techniques reviewed in this chapter were found to have a number of limitations that restrict its effective use in a number of experiments. For instance, the inductive loop detector system can only be used at a fixed position. Also poor image quality, poor weather condition and limited length of the field of view of the video camera techniques limit its application in a number of studies. The previous instrumented vehicle techniques only use rear mounted short range radar sensors and does not allow instantaneous updates of sensor settings to correct any malfunction in the course of its operation. In this work, an instrumented vehicle equipped with front and rear advanced long range radar sensors, both forward and rear facing video-audio recorder connected to GPS based time series speed and distance measuring device, in-vehicle computer logging vehicle speed and a CAN (Controller Area Network) monitoring interface user program to provide real time monitoring and display of data is developed to collect much more reliable driver behaviour data. This is addressed under research question 1.

The review found that different researchers used different statistical approaches to analyse data based on the study objectives and what the researcher wants to achieve in

the experiment. In this work, combination of different analytical approaches including descriptive statistics and graphical representation, regression analysis and the statistical significance analysis methods are used to analyse the data and calibrate models in this current research. This is addressed under research question 2. The next chapter discusses the methodology of this research. It discusses the study design, the experimental procedure that involve the development of the instrumented vehicle utilised for data collection. It also discusses the data collection process for this research.

CHAPTER 3 METHODOLOGY: STUDY DESIGN, EXPERIMENTAL PROCEDURE AND DATA COLLECTION

3.1 Introduction

Chapter 2 discussed the review of literature on car following models, the data collection techniques used in transportation research and analytical approaches used in data analysis. The City of Edinburgh and the neighbouring towns has been chosen as the case study for this study. The city can boast of good public bus services with the largest and most successful municipal or public own Bus Company (Lothian Buses) in the United Kingdom. Due to the fast economic growth, the city has seen an increase in car use over three decades (Edinburgh Census, 2013) making it one of the busiest and congested cities in Scotland and UK as a whole.

New instrumented vehicle that enable the collection of driver behaviour data of three consecutive vehicles in motion within the traffic stream was developed. The instrumented vehicle is capable of measuring the relative distance and relative speed between the tracked or subject vehicles and instrumented test vehicle as well as the relative acceleration between them. The instrumented vehicle provide the opportunity to collect additional data including the subject vehicles drivers' characteristics such as gender, in-vehicle activities such as smoking, vehicle occupancy (i.e. following vehicles only), vehicle characteristics, weather condition, road and traffic characteristics. In addition, the instrumented vehicle's own speed, acceleration, distance and time travelled are measured by the on-board speed measuring device. To optimise data collection for this research, a series of performance testings of the instrumented vehicle were carried out. Preliminary surveys were carried out within and around the City of Edinburgh (i.e. the study area) to assess the traffic conditions on the selected traffic corridors prior to the main or final data collection. The performance testing and traffic surveys enabled the efficient and effective planning and preparation for the study's main data collection.

In this chapter, Section 3.2 discusses the study design. It also discusses the car usage situation in Edinburgh in the last decade. Section 3.3 discusses the experimental procedure used in this study, which involves the instrumentation of the private vehicle used for the data collection for this study. The data collection process of this study is discussed in Section 3.4. Finally, Section 3.5 summarises the discussions of this chapter.

3.2 The Study Design

The study design discusses the case study setting and corridor types identified and selected for use in the data collection for this study. The City of Edinburgh, the capital of Scotland in the United Kingdom (UK), is the seat of the Scottish Government and Parliament. Edinburgh is located in Lothian between the Pentland Hills and the southern shore of the Firth of Forth with a total residential population of 476,626 (Edinburgh Census, 2013). Edinburgh is well known for its ancient and historic architectural buildings as well as the International Arts and Fringe Festivals. Edinburgh serves as one of Europe's cultural and historical centres. The city's Old Town and New Town dating back to the 18th century are recognised as World Heritage Site by United Nations Educational, Scientific and Cultural Organization. The City of Edinburgh serves as the financial hub of Scotland and one of the fastest growing economy in the UK. The economy of Edinburgh is mostly centred on banking and finance, hospitality, services and education (i.e. home to four universities).

There are a number of major roads surrounding the main city forming a boundary between the city and neighbouring counties. The A720 (The Edinburgh City Bypass) and A1 are the two major roads that surrounds Edinburgh. The A90 (Queensferry Road), A902 (Maybury Road, Telford Road, Ferry Road) and A199 connects the A720 at the northwest of the city (i.e. Gogar) to the A1 at the northeast of the city (i.e. Brunstane), making the A720, A1, A90, A902 and A199 the main trunk roads forming a ring road around the City of Edinburgh. The A7, A8, A70, A71, A701, A702, A900 (Leith Walk) and A901 (see Figure 3-1a) are the main arterial roads that connects to the trunk roads to the neighbouring towns and cities. Because of the City of Edinburgh's historical nature and buildings in the Old and New Towns, the roads in the inner part of Edinburgh are quite narrow. Some of the roads in Edinburgh are quite steep due to the hilly nature of some part of the city, which may affect the speed of vehicles. Edinburgh roads has different speed limits for vehicles across the entire city ranging from 20 mph (inner city and some residential areas) to 40 mph maximum (outer city).

In this section, the car usage in Edinburgh is discussed in Section 3.2.1. The study area and selected traffic corridors are discussed in Section 3.2.2. A bus following study was undertaken to investigate commuter bus drivers' driving speed variability and to model bus following behaviour. The bus following data collection corridor description is discussed in Section 3.2.3.

3.2.1 Car Usage in Edinburgh

The economic growth in Edinburgh has come with significant challenges for the city to keep up with the transport needs of its residents and the surrounding areas. The economic growth has also attracted more people from outside of Edinburgh to work in the city, mostly travelling by cars. The number of households in the City of Edinburgh without access to own car or do not have a car was less than Glasgow and Dundee and above the Scottish national average of 34%. Glasgow recorded 51% and Dundee recorded 42% compared with almost 40% of the households in Edinburgh having no access to own car (Edinburgh Census, 2013), this indicates that nearly 60% of the households in Edinburgh own or have access to own car or van.

Over the last three decades, car ownership for the residents in the City of Edinburgh has nearly doubled from 94,000 cars in 1981 to 181,000 cars in 2011, resulting in an increase of about 48.07% cars. 60.1% of the households in Edinburgh own one or more cars or vans and 66.4% of the households in both Edinburgh and the surrounding Lothian Counties own cars or vans compared with the Scottish average of 69.5% of household car ownership level. In recent years, fewer residents in Edinburgh drove to work in 2011 (i.e. based on place of residence) compared to 2001 in spite of the increase in car ownership over the last decades. However, car journeys into Edinburgh has increased significantly due to significant growth in car travel in some of the neighbouring local authority areas (Edinburgh Census, 2013), resulting in heavy traffic and congestion in some part of the city.

The City of Edinburgh council recognises that the most productive way to embark on many trips is by the use of car (ELTS, 2014), however, car journeys also come with heavy traffic and congestion. In managing the car use and the associated traffic congestion in the central business centre, the City Council has implemented measures such as parking management in some areas, car clubs promotions, given support for priority for ‘high occupancy vehicle’ and car sharing for people going to similar places to try and encourage efficient car use in order to reduce car usage and traffic congestion (ELTS, 2014).

3.2.2 Study Area and Selected Traffic Corridors

The study area has a mix traffic flow, mix traffic lanes in some part of the study route, traffic congestion during the peak hour periods and free flow traffic mostly at the outer

part of the city leading to the neighbouring towns and cities. Some part of the study area has dedicated bus lanes (namely, the Greenways) and tram lanes, which force all other traffic to join the single adjacent roads during the restricted lanes operational times. This usually result in slow moving traffic and/or stop-start traffic situation, which sometimes leads to traffic congestion, resulting in different car following driving behaviours. The study area has different speed limits ranging from 20 mph (32 km/h) at the inner city to 70 mph (113 km/h) maximum at the outer city's trunk roads. The different speed limits within the study area enable different car following driving behaviours to be observed. There is a mix of single and double lane roads on the study routes where all vehicle types are allowed to use. The study area also has a heavy commercial activities, shopping malls and universities within the inner city and along some of the routes selected which contributes to the heavy flow of traffic on the corridors.

Major and minor truck and arterial roads within and outside of Edinburgh has been selected for this study to collect traffic data especially during congested and uncongested periods including stop and start traffic. The A720 bypass has been chosen as a special case test route due to the amount of traffic flow and the high speed (over 50 mph) nature of the road during the morning, afternoon and evening peak hours. This enable the collection of data on two-lane high speed roads together with the low speed single lane roads within the City of Edinburgh. The corridors selected for the study has different road characteristics and speed limits. The corridors were carefully selected to enable the observation of different car following behaviours in a slow moving traffic stream, stop and start urban driving behaviour, single and double lanes traffic stream for both congested and uncongested driving conditions. The selected corridors also enable the observation of off-road activities (such as pedestrians crossing at undesignated crossing sites) and effect on car following behaviour since most part of the corridors passes through the commercial centres.

In order to classify the road types identified and selected for this study into urban, rural and highways, Christidis and Rivas (2012) road classification approach was adopted. Christidis and Rivas (2012) tested different moving averages of speed measurement data from European study, and found that one (1) hour and three (3) hours moving averages gave a more realistic representation of duration of the peak periods within the networks considered, but that could not accurately reflect whether a road was urban or not urban. Using the free flow speed as a good substitute regarding the road type and characteristics, they classified the roads into three groups. They classified roads with speed below 50

km/h (31 mph) as urban, roads with speed above 100 km/h (62 mph) to represent local and inter-urban links and finally, roads with free flow speed above 80 km/h (50 mph) as highways in order to analyse inter-urban traffic with few highways.

Christidis and Rivas (2012) estimated congestion threshold value using average delay per kilometres as a congestion indicator since it provide a physical interpretation, because it allows direct estimate of particular trip's total delay. They found that a speed reduction from 50 km/h to 40 km/h produced 0.3 minutes per kilometre delay and a speed reduction from 100 km/h to 80 km/h resulted in a 0.15 km/h delay to indicate congestion in the system. The reduction in the speed from 50 km/h to 40 km/h and 100 km/h to 80 km/h shows a 20% speed reduction in both cases that is generating the travel delay estimated by Christidis and Rivas, which provide an indication of congestion in the network. By this estimation, Christidis and Rivas (2012) set the congestion threshold to speeds below 20% of the designated speed of each of the classified roads used in the European study.

Hence, for this study, the selected corridors or study routes are classified into three groups, namely; urban, rural and highways. The roads within and around the city centre of Edinburgh with speed below 40 mph are classified as urban roads. The roads outskirt of Edinburgh which links the city to the neighbouring towns and villages with speed from 40 mph up to 50 mph are classified as rural roads. The roads with speed above 50 mph linking Edinburgh to other cities and major towns are classified as highways. The traffic volumes on each identified routes were observed using both the forward and rear facing cameras mounted on the instrumented vehicle. The traffic flow observed were classified into congested and uncongested flows in order to analyse the effect of the traffic flow on driving behaviour discussed in Chapter 5. The traffic volumes captured on the cameras were analysed and based on the traffic flow or speed, the data was grouped into congested or uncongested flow.

For this study, the congestion indicator of 20% below the designated road speed estimated by Christidis and Rivas (2012) is applied and used as the basis for the traffic flow volumes categorisation into congested and uncongested flow. For this study, congested flow is considered when the vehicular flow speed is below 20% of the legal road designed speed, and uncongested flow is considered when the vehicular free flow speed is above 20% and up to or over the legal road designed speed. For instance, roads with 30 mph legal designed speed with traffic flow speed below 24 mph (i.e. below 20% of 30 mph) will cause travel delay that is used as congestion indicator. The routes selected for this study

are classified as traffic corridors 1, 2, 3 and 4. The study corridors are discussed in the following sections.

3.2.2.1 Traffic Corridor 1

This corridor comprises the A1 and B1350 roads. Brief characteristics of these roads are discussed in this section. The A1 trunk road is one of the major trunk roads in the United Kingdom which runs from the south of England (from New Change at St. Paul's Cathedral in central London) and to the city centre of Edinburgh. A1 links the A7 and the A900 roads at the east end of the Princes Street in central business area of Edinburgh. A1 has many distinct characteristics, possibly due to the road considered as the longest road in the United Kingdom. A1 serves as inner city route, dual and single carriageway urban and rural motorway routes for cities, towns and communities along its route. The A1 runs from the Edinburgh city centre as single lane arterial road to double lane road (section of road with dedicated bus only lane) through Edinburgh suburbs (i.e., via Willowbrae Road, Milton Road and Milton Link, which is a high speed dual carriageway trunk road with no restriction on lane use) to Old Craighall Roundabout linking the A720 where this corridor end (see Figure 3-1b, white line on map (a)). The B1350 (London Road) serves as a link between the A900 and the A1. The B1350 link is a short double lane road with dedicated bus lane. It serves as one of the main routes from the east end of Edinburgh to the retail centre at Meadowbank.

Corridor 1 starts from London Road (B1350/A1) from the City Centre through A1 to Old Craighall Roundabout (Eastfield Wood) where it meets the Southbound of A720 (Figure 3-1b). This traffic corridor combine urban single lane and two–lane high speed roads with speed limits ranging from 30 mph to a maximum of 50 mph. The corridor has a total distance of 6 miles (9.7 km) from start (point A) to finish (point B). Corridor 1 is considered as urban traffic corridor due to the characteristics of the roads within the corridor.

3.2.2.2 Traffic Corridor 2

This corridor comprise of the A720. The characteristics of the A720 are briefly discussed in this section. The A720 trunk road commonly known as The City of Edinburgh Bypass serving Edinburgh and its surrounding towns and nearby cities was completed in 1990

(May et al., 1992). The A720 is a dual carriageway that runs from the Old Craighall Roundabout in the east of Edinburgh, where it meets with the A1 to form a ring road around the city, to Gogar Roundabout in the north of the city. It is considered one of the major trunk roads in Scotland. The A720 has 12 intersections including two roundabouts at both ends, Old Craighall Roundabout to the southeast and Gogar Roundabout to the northeast. The A720 has one major roundabout, the Sheriffhall Roundabout directly on its path, whereas the other junctions/intersections are fly-overs for entry and exit ramps to and from the carriageway.

The A720 is partitioned into 9 different sections. The sections from 1 to 9 include: Old Craighall to Sheriffhall Roundabout which include Millerhill Junction (3.502 km), Sheriffhall Roundabout to Gilmerton Junction (1.670 km), Gilmerton Junction to Lasswade Junction (1.614 km), Lasswade Junction to Straiton Junction (0.882 km), Straiton Junction to Lothianburn Junction (2.697 km), Lothianburn Junction to Dreghorn Junction (1.985 km), Dreghorn Junction to Baberton Junction (3.721 km), Baberton Junction to Calder Junction (1.848 km), and Calder Junction to Hermiston Junction (2.252 km) (Transportscotland.gov.uk). Only the Gilmerton to Lasswade Junction allows for vehicular exit and entry ramps from and/or to the northbound traffic but does not allow entry and exit ramps to and/or from the southbound traffic. The A720 has a number of emergency lay-bys at certain locations and hard shoulders along the route with only one service station at Dreghorn Junction. It serves as a link to most of the major roads in Edinburgh and Scotland (see Figure 3-1e, brown line on map (a)).

Corridor 2 starts from the Southbound at Gogar Roundabout of A720 (point A) to the Northbound at Old Craighall (Eastfield Wood) Roundabout (point B) for the entire high speed dual carriageway road on both direction of travel as shown in Figure 3-1e. The corridor has speed limits ranging from 50 mph to 70 mph. The standard dual carriageway throughout the corridor enable more vehicle passing manoeuvres and different driver behaviours to be observed. The total distance from the start of the corridor at the south (point A) to the end point at the north (point B) is 13.1 miles (21.1 km) (i.e. one way). This corridor is the only dual carriageway bypass in Edinburgh where most of the vehicles entering and leaving the city connect to from the neighbouring cities and towns. This corridor is classified as highway due to the high traffic flow speed and the characteristics of the road.

3.2.2.3 Traffic Corridor 3

This corridor comprises the A900 and the A71. The individual roads characteristics are briefly discussed in this section. The A900 is considered one of the busiest roads in central Edinburgh, running from the east end of city centre at the Princess Street through Constitution Street to A199. The A900 has a mix of dual carriageway with dedicated bus only lane use and single lanes. The A900 links the A901 at the bottom of Leith Walk (Great Junction Street - Duke Street intersection). Some section of the A900 forms part of the study corridor (see Figure 3-1d, blue line on map (a)).

The A71 is considered one of the major arterial roads in Scotland, which runs from Gorgie Road (Dalry – Gorgie suburbs) in the south west of central Edinburgh to Irvine town centre (A737 - Ayr Road) in Ayrshire, the west coast of Scotland. The A71 is a mix of single and dual carriageway. From central Edinburgh, the A71 changes from a single lane to dual carriageway (with dedicated bus only lane) and changes to rural arterial single lane road to Oakbank roundabout (i.e. corridor end point). Between central Edinburgh at the start of the A71 through to Oakbank roundabout, there are eleven (11) roundabouts on the road. The section of A71 from Dalry-Gorgie suburb to Oakbank roundabout forms part of corridor 3.

Corridor 3 start from Leith Walk (A900) through Edinburgh suburbs roads (i.e. Queen Street, North/South Charlotte Street, Lothian Road, West Approach Road, Gorgie Road, Stenhouse Road and Calder Road) to Oakbank roundabout (A71) at Livingstone (see Figure 3-1d). This corridor has speed limit ranging from 30 mph to 50 mph. The total distance of this corridor from the start (point A) to the finish (point B) is 15.7 miles (25.3 km). The corridor is one of the main arterial road in Edinburgh that passes through the commercial centre. It is used by many motorist travelling to Kilmarnock and Ayrshire at the west coast of Scotland. This corridor is considered as part urban and part rural based on the traffic flow speed and the road characteristics and therefore, classified as urban-rural corridor for this study.

3.2.2.4 Traffic Corridor 4

Corridor 4 is a combination of traffic corridors 1 and 2 to form one traffic corridor. The corridor combine highway and urban driving conditions. It starts from the northeast of the A720 through the entire stretch of the highway to London Road (B1350) in Edinburgh

city centre via the A1 (see Figure 3-1c, brown-white line on map (a)). It has varied speed limits ranging from 30 mph to 70 mph with total distance of 20 miles (32.2 km) from the northeast of A720 (point A) to the city centre of Edinburgh (point B). The corridor comprises both the urban and highway driving characteristics. This corridor is classified as urban-highway corridor.

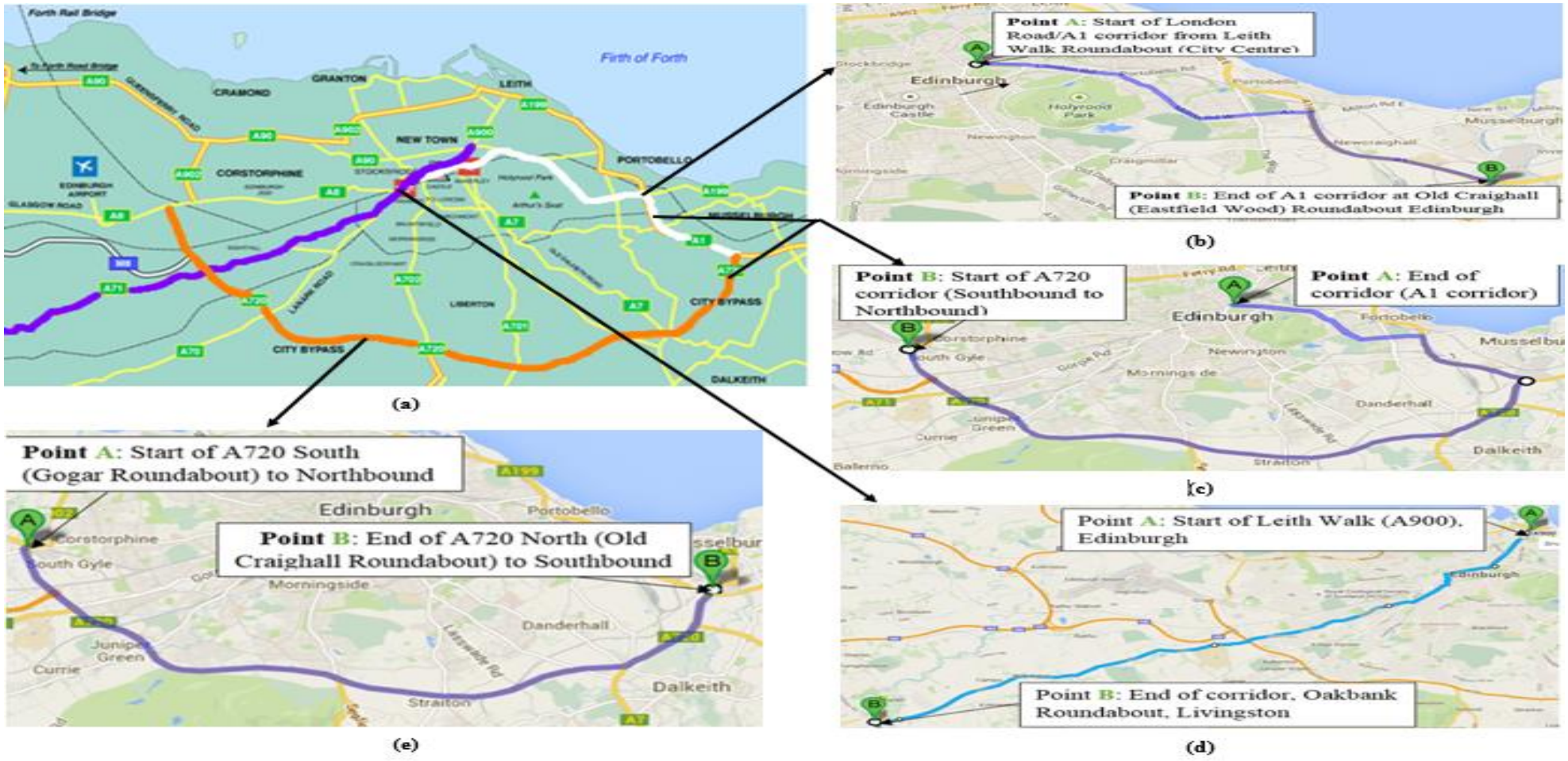

(a) Ring and major road networks in Edinburgh (Source: www.edinburgh-stockbridge.com); (b) Corridor 1 (White on map (a)); (c) Corridor 4 (Brown-White on map (a)), (d) Corridor 2 (Blue on map (a)), (e) Corridor 3 (Brown on map (a)).

Figure 3-1: Edinburgh major road networks and Study Corridors

3.2.3 Bus Following Corridor Description

A busy traffic corridor that stretches from Edinburgh city centre in the southwest through the rural arterial roads in the neighbouring towns to Gorebridge town centre was selected for the bus following data acquisition for this study. This traffic corridor connects Edinburgh to Gorebridge town centre via Gilmerton, Newbattle and Gowkshill towns. This corridor is one of the busiest traffic corridor from Edinburgh to the surrounding towns. Most of the roads are single lane with mixed traffic flow which passes through the A772 highway (a major A-road). The corridor begins from the A772 (A701 intersection at Nether Liberton) and end at Birkenside in Gorebridge via Gilmerton Road, Drum Street, B6482 (Dalhousie Road), B703 (Main Street), A7, B704 and B6372 (Powdermill Brae) with speed limit at 30 mph (see Figure 3-2).

This corridor was selected because there was no bus lane restrictions on the corridor. This enabled buses to be followed without any difficulties. The corridor has an urban and rural driving conditions which enable vehicles to be followed for longer periods before the vehicles changes direction. The traffic corridor selected has a total distance of 10.6 miles one way from the start in Edinburgh to the end at Gorebridge. The heavy traffic on the corridor ensured that all vehicles in the stream stay in lane without the possibility of overtaking the lead vehicle, enabling continuous bus (or car) following during the data collection.

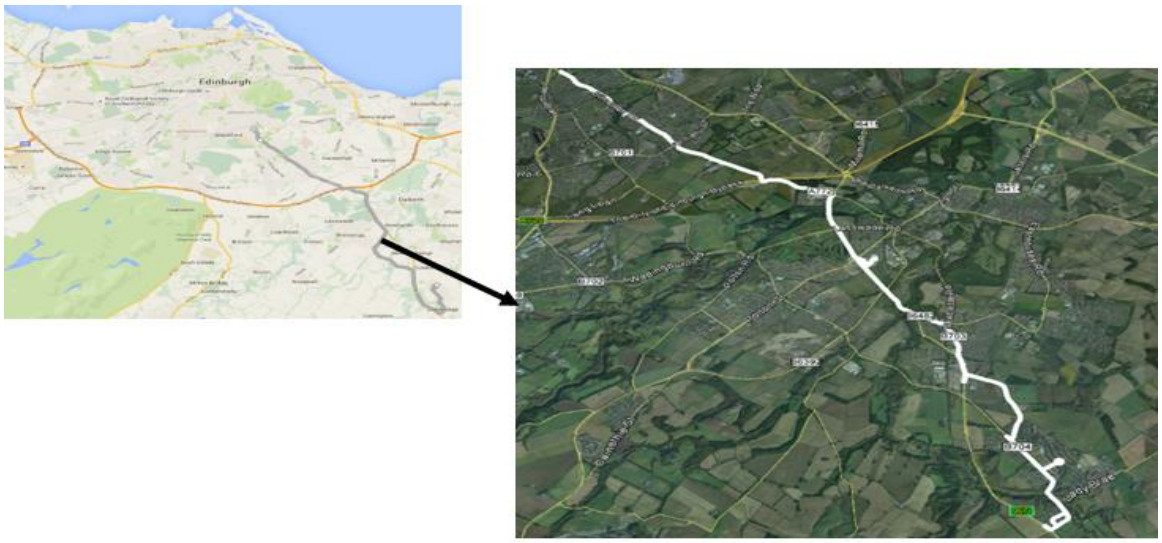

Figure 3-2: The map of study area and the route (white) commuter buses were followed by the instrumented vehicle

3.3 Experimental Procedure:

An instrumented vehicle was developed and utilised to collect traffic and driving behaviour data for this study. The equipment used to equip the instrumented vehicle include the ARS 308-2 Long Range Radar Sensors (77GHz), GPS based Video VBOX and PerformanceBox, Sony Video Camcorder Camera, Advanced Laptop Computer and CAN-Bus. This section discusses the details of the instrumented vehicle setup utilised in this study. The data measuring devices and basic functions are discussed in Section 3.3.2. The radar sensors and CAN-bus cables termination process are discussed in Section 3.3.3. The mounting of devices on the test vehicle is discussed in Section 3.3.4. The operation of the instrumented vehicle as used in the data collection is discussed in Section 3.3.5.

3.3.1 The Vehicle Instrumentation

A private vehicle was equipped with Front and Rear advanced ARS 308-2 Long Range Radar Sensors with 77 GHz (i.e. the type used in Adaptive Cruise Control vehicles), both Forward and Rear facing video-audio recorders connected to GPS based time series speed and distance measurement device (i.e. Video Velocity Box), in-vehicle computer logging vehicle speed and a CAN monitoring interface user program to provide real time monitoring and display of data.

3.3.2 Data Measuring Devices and Basic Functions

The basic functions of the various elements of the measuring instruments and software tools used in this research are presented in Table 3-1. The general description, characteristics and functions of each of the measuring devices used to equip the instrumented vehicle are presented in Appendix 3.3.2.

Table 3-1: The various instruments, software tools and their brief basic function

Instrument	Brief Function
Radar Sensor ARS 308-2 Long Range Sensor (77GHz)	For measuring relative distance, relative speed and relative acceleration. It provides additional information such as vehicle type, width etc.
PCAN-Buses (PCAN – USB Pro and PCAN-USB)	They serves as the communication channels between the radar sensors, the instrumented vehicle OBD-II port and the on-board computer (laptop)
Video Velocity BOX (Video VBOX)	For measuring the speed, acceleration, distance and time travel of the test vehicle. Provides visual video recordings of driver and vehicle characteristics of both leading and following vehicles, environmental and weather conditions.
Sony video camcorder	For recording rear following driver's characteristics such as gender, vehicle characteristics and in-vehicle activities such as number of occupants. To identify vehicles and verify sensor data for any abnormality.
PerformanceBox Performance Meter	For measuring the acceleration and deceleration (i.e. G-force), speed, distance, time travel and mapping of test vehicle path (onto Google Earth). As a backup for the Video VBOX data. Used for test vehicle speed re-engineering test.
Laptop computer (On-board computer)	Serves as the data monitoring station and communication hub for the devices used for the experiment. Receive, process and store experimental data.
Vehicle (Ford Mondeo 2002 model)	Housed all the measuring instruments for data collection. Used as test vehicle
PCAN-Explorer 5 software	Provides the platform for monitoring live signal data from the radar sensors and test vehicle OBD-II port. For receiving and transmission of signal data. Providing the platform for changing default settings of the radar sensors for efficient operation and display of the sensor status during operation.
Video VBOX Setup, VBOXTools and PerformanceTools programs	Provides the platforms to make changes to the Video VBOX basic settings and create Scene for the VBOX. Provides the platform for Video VBOX and PerformanceBox data extraction, processing and exporting to Microsoft Excel for further analysis. Provides the platform for mapping the vehicle's path onto Google Earth for analysis.

3.3.3 Termination of Radar Sensor - CAN-Bus Cables

Two 5-metre power supply high-speed CAN bus – radar sensor cables and one 1-metre high-speed CAN-OBD-II diagnostics cable to access the CAN lines of the instrumented vehicle were used for this study (Figure 3-3). These CAN-bus cables were acquired without termination resistors at both ends for the 5-metre power supply high-speed CAN bus – sensor cable and one end of the CAN-OBD-II diagnostic cable. The PCAN-USB Pro and the PCAN-USB adapters used for the experiment do not have an internal termination resistors, hence the need for all the cables connected to these adapters to be terminated with 120 Ohms resistors at both ends of the cable for it to work. Without the termination of the cables at both ends with 120 Ohms resistors, the interfering signal reflections and transceivers of the connected CAN nodes (i.e. CAN interface, control device) will not work (Peak-System, 2013). Moreover, the CAN-bus (ISO 11898-2) cables are twisted and shielded, and required to be terminated with the same impedance value to minimise the reflected waves that occur from miss-matched impedances (Corrigan, 2008). Figure 3-4 is an example of sensor cable of ARS 308-2X terminated at one end with a 120 Ohms resistor with the same impedance as the twisted wires.

The 5-metre high-speed CAN bus - sensor cables supply 12V DC power to the ARS 308-2 radar sensors used for this study. The cables are twisted and shielded with 9-pin, SUB-D F sockets. Both ends of the two 5-metre high-speed CAN bus – sensor cables were terminated with 120 Ohms resistors, and the 9-pin socket end of the CAN-OBD-II diagnostic cable terminated with 120 Ohms resistor. This was done by opening up the socket ends of the cables and connecting the CAN 1 high (Pin 3 – Red) and CAN 1 low (Pin 6 – Black) with the 120 Ohms resistor (see Figure 3-4). The other Pins in the cables were not touched as the termination is only required on CAN high (Pin 3) and CAN low (Pin 6) for the CAN bus to work properly. The sensor-plug ends of the two 5-metre cables were taped with black adhesive sellotape to insulate both ends of the cable and also to prevent the breaking of the 120 Ohms resistors as a result of excessive twisting at ends of the cables during operation. Figure 3-5 shows the termination diagram of the CAN bus cable and connections to the PCAN adapters.

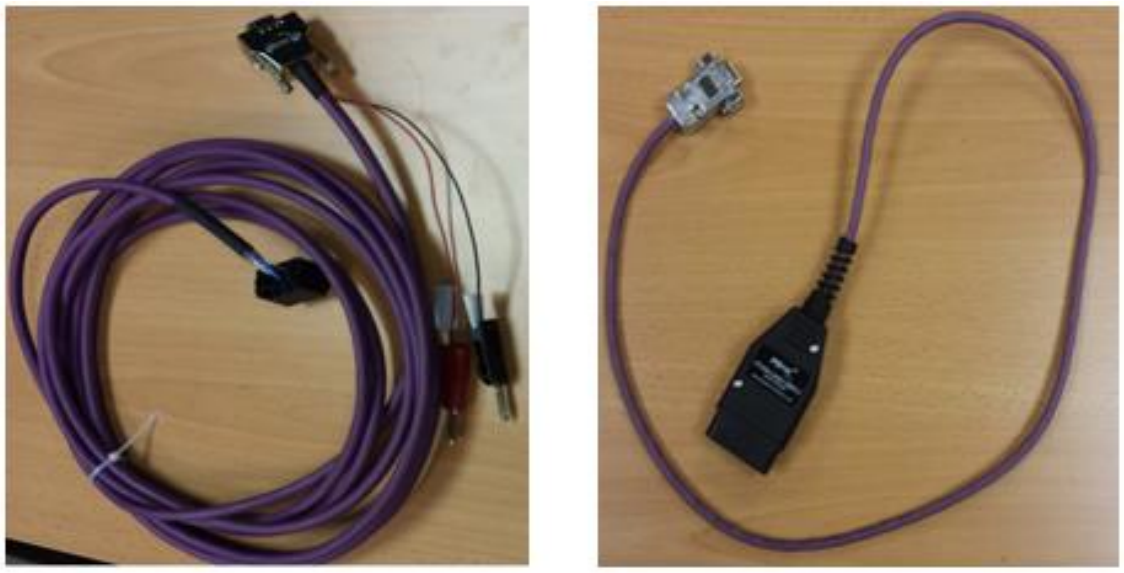

Figure 3-3: The 5-metre power supply high-speed Radar Sensor - CAN-Bus cable (left) and CAN-OBD-II diagnostic 1-metre cable (right)

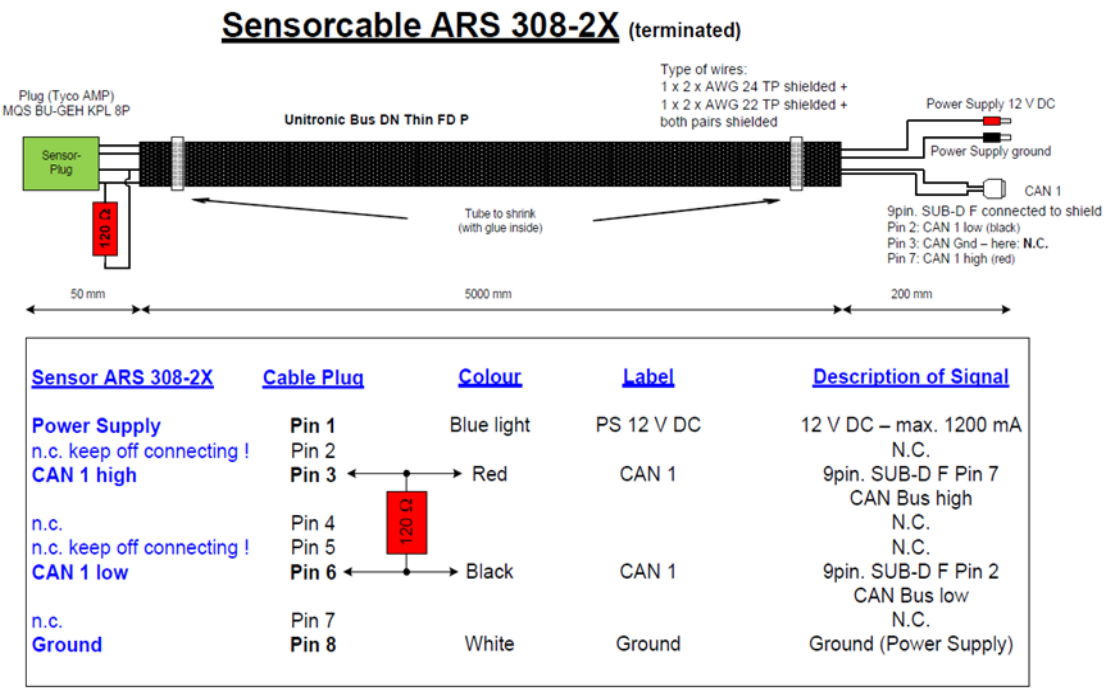

Sensor ARS 308-2X	Cable Plug	Colour	Label	Description of Signal
Power Supply	**Pin 1**	Blue light	PS 12 V DC	12 V DC – max. 1200 mA
n.c. keep off connecting !	Pin 2			N.C.
CAN 1 high	**Pin 3**	Red	CAN 1	9pin. SUB-D F Pin 7 CAN Bus high
n.c.	Pin 4			N.C.
n.c. keep off connecting !	Pin 5			N.C.
CAN 1 low	**Pin 6**	Black	CAN 1	9pin. SUB-D F Pin 2 CAN Bus low
n.c.	Pin 7			N.C.
Ground	**Pin 8**	White	Ground	Ground (Power Supply)

120 Ω

Figure 3-4: Example of CAN-Bus power supply cable terminated showing the Pins, colour and description (Continental, 2014)

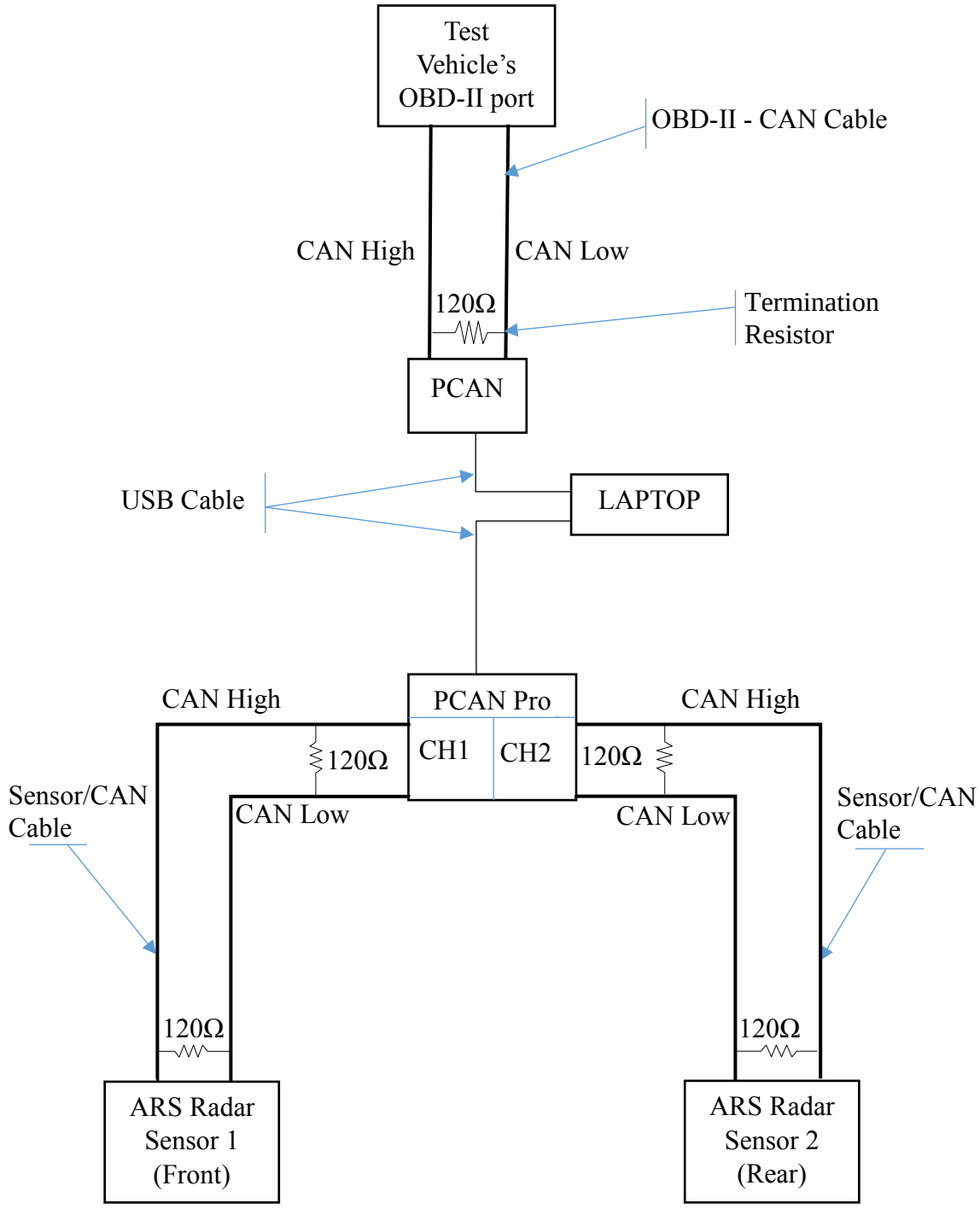

Figure 3-5: The standard termination of the CAN-bus cables and the connection to the PCAN adapters, OBD-II and Laptop (CH = Channel)

3.3.4 The Test Vehicle Instrumentation Setup (Mounting of Equipment)

After the laboratory testing of the equipment (see Appendix 3.3.4), the instrumentation were setup in the test vehicle (Figure 3-6). Two metal plates were moulded to hold the two radar sensors on the test vehicle's bumpers. One radar sensor was mounted behind the front bumper underneath the bonnet inside the vehicle engine compartment, and another mounted below the rear bumper of the test vehicle at a height of 24 centimetres and 20 centimetres parallel to the ground respectively. The two radar sensors were connected to the PCAN-USB Pro CAN-bus using the separate 5-metre CAN bus – sensor cables. The PCAN-USB Pro CAN adapter was placed in between the front passenger seat and the test vehicle gearshift control handle compartment, and powered by an extension cigarette plug made specifically for powering the two radar sensors. The CAN-OBD-II diagnostic cable was connected to the OBD-II port of the test vehicle's Engine Control Unit interface under the dashboard above the test vehicle's foot pedals and the PCAN-USB adapter. The PCAN-USB Pro and PCAN-USB CAN-buses were connected to the on-board laptop computer (with PCAN-Explorer 5 installed and copy protection dongle plugged-in) which provides power to the PCAN-USB CAN adapters.

The PerformanceBox (PB) mounting bracket was securely mounted low down in the corner of the windscreen facing the passenger seat using the three windscreen suction cups. The mounting bracket enable the sliding forward and backward to adjust the position of the PerformanceBox when mounted. The power cable and the external GPS antenna were connected to the PerformanceBox. The PerformanceBox was slide into position in the windscreen mounting bracket. The Video VBOX two cameras (with directional microphone) were mounted at the centre of the windscreens where they have unobstructed views from the front and rear of the test vehicle. One forward facing camera (marked HI RES) securely mounted at the centre of the front windscreen and one rear facing camera (marked LOW RES) securely mounted at centre of the back windscreen using the suction cups. The cameras were adjusted to ensure the label marked 'top' was facing up to have the correct orientation of the cameras. The video cameras were connected to the VBOX CAM sockets (i.e. front for CAM2, rear for CAM1 (main)), no effect on camera display size as the two-camera mode elements was included in the Video VBOX Scene created and uploaded into the VBOX.

The Video VBOX preview OLED (organic light emitting diode) screen (or monitor) mounted low down in the centre of the front windscreen with special windscreen sticker.

The position and adjustment settings of the cameras were done with the preview monitor when Video VBOX was powered up. The preview monitor, the power plug, the GPS antenna cables were connected to the Video VBOX 'AOUT', power and GPS sockets respectively. The Video VBOX and the PerformanceBox antennas were mounted at the centre of the roof of the test vehicle with few centimetre apart and away from objects that may interfere with the GPS signals. The Video VBOX was placed in a secured place in between the front passenger seat and the test vehicle gearshift control handle compartment. The PerformanceBox and the Video VBOX were connected to a standalone car battery at back of the front passenger seat, which was fully charged before the start of each and every experiment.

The high resolution Sony digital video camera was mounted on a tripod (as a support) at the back centre of the test vehicle facing the rear. The tripod was tied to the middle rear passenger seat headrest, the tripod stand was extended to the floor of the vehicle to give it move stability and prevent it from vibration during operation. This positioned the camera above the headrest and at the centre of the rear windscreen to provide good view of the rear following vehicles. The test vehicle instrumentation showing all the equipment setup is shown in Figure 3-6. The pictorial view of both the external and internal of the instrumented vehicle setup is presented in Appendix 3.3.4.

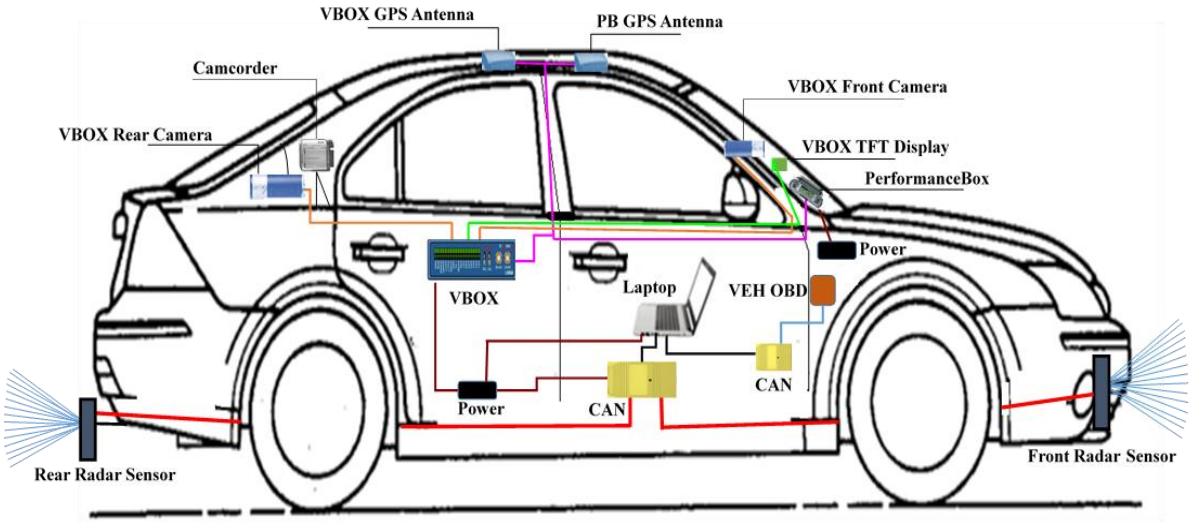

Figure 3-6: The Instrumented Vehicle Connectivity Diagram

3.3.5 The Operation of the Instrumented Vehicle (Systems Operations)

For the setup of the instrumented vehicle to operate and work as required, there are certain processes that is required to be carried out prior to it being fully functional. The following processes describe the operations of the instrumented vehicle setup.

3.3.5.1 Net Configuration and Project Creation

A PCAN Net Configuration was created in the PCAN-Explorer 5 (PE5) for all the three connected CAN Network hardware (i.e. the two radar sensors and the test vehicle OBD). The PCAN Net Configuration allows the PCAN-Explorer 5 (or PCAN program), that serves as the client, to connect to the CAN Network hardware. Without the Net Configuration, the CAN hardware connections will not be recognisable and the PE5 cannot monitor the live signals or CAN messages from the connected CAN Networks. The PCAN Net Configuration is essential for the PE5 interface to be fully functional in monitoring CAN messages from the CAN networks. A PCAN-Explorer Project was created for the experiment. The Project allows the efficient management of all the associated items that are required to monitor and visualize the CAN networks during operation, such as the bus connections, folders and files, and the filters. In order to identify each experiment carried out during the trial testing, a number of different projects were created for each pilot testing and the final data collection.

3.3.5.2 Symbols Creation

Symbols file (or text file) also referred to Database Container (DBC) (Continental, 2013) contains the definition of the Symbolic interpretation of the CAN messages (Peak-System, 2014a), which when applied to CAN messages, brings the messages into a form that enables the user to understand the messages easily. The symbols are created in the text editor of the PE5 and helps in identifying each CAN messages that are received or transmitted. The CAN messages are normally received and transmitted in a specific format with values of different application variables (e.g. device power status, direction, speed). Each values contained in the symbol files covers a bit group of variables of its own in the message's data bytes. With the symbol files created, the PE5 can extract the transferred values out of the data bytes and show the variables with their identifier and

with their values in the messages, and present the messages in the form that is easy to understand during the live monitoring of the CAN networks (Peak-System, 2014a).

For this research, the radar sensor manufacture's default channel database, DBC (i.e. symbol files) created for the radar sensor operations and signal monitoring within the PE5 were modified and updated. The modified DBC and symbols definitions added precisely to suit the research data collection through a series of investigations. The default symbols files contains values of variables that allows the sensor configuration to be changed as and when required and as an individual or multi combinations elements within the PE5. New symbols file was created for the test vehicle CAN interface signal messages for transmission of the test vehicle speed configuration to the sensors during operation. A typical symbols file for each value in a CAN message identifier contains the following variable properties: name, unit, data type, factor, offset, bit start, bit length, data format, display mode, output format, minimum, maximum, default value and enum including the long name (i.e. to give further description of identifier's name) and comment (i.e. any preferred user comments).

The symbols files, DBC (containing the different bit groups in the CAN message's data bytes), were assigned to the created Projects before the start of each and every experiment. Different symbols files were created for each connected CAN-Bus (i.e. the two radar sensors, the test vehicle CAN line) since they all operate independently. A prefix of "F" for front and "B" for back sensors assigned to the value identifier names in the symbols files. Even though, the radar sensors CAN-Bus symbols files were created the same with the same values of variables, the prefix "F" and "B" to the symbols value identifier names help to differentiate both sensors CAN messages from the PCAN USB Pro bus connected to the radar sensors. This also helps not to confuse the two independent trace data during the analysis of the radar sensors data since all the CAN connections signals are saved in the same trace files within the PE5 (see Appendix 3.3.5.2 for DBC detail).

3.3.5.3 Instrumented Vehicle System Operation

When all the installed measuring equipment are powered up, the Net Configuration and Project in the PCAN-Explorer 5 (installed on the PC) establish network connections with the three (3) independent PCAN connections (i.e. the two radar sensors and the test vehicle OBD-II), the symbols files (containing scaling information for CAN frames and

signal definition) are then assigned to the three (3) CAN networks messages or signals. When this process is complete then the system operation process begins.

The test vehicle speed information contain in the ID 201 is extracted from the test vehicle's engine via the vehicle's OBD-II port through the PCAN-USB bus, which serves as a communication tool between the test vehicle OBD-II port and the on-board laptop computer. The PE5 processes the ID 201, converts the speed in kilometre per hour (km/h) to metre/second (m/s) (sensors only receive the input speed in m/s) in the information signal received and sent out the ID 201 to each radar sensor's ID 300 and ID 301 through special Visual Basic macro (VBmacro) codes written purposely for this process. The VBmacro codes processes the ID 201 and extract the necessary input signals and automatically sent out the signals to each radar sensor's ID 300 and ID 301 continuously as the ID 201 is being received at 20 microseconds.

The radar sensors only accept the ID 300 and ID 301 as input signals. Each sensor has its own independent ID 300 and ID 301 and each operates independent. Each ID 300 and ID 301 after receiving the ID 201 as input signal from the test vehicle, are then transmitted together with ID 200 (Sensor Configuration) to the front and back mounted radar sensors through the PCAN-USB Pro CAN-Bus. The PCAN-USB Pro CAN-Bus serves as a communication channel between the front and back radar sensors and the on-board laptop computer running the PE5. Again, each sensor contains its own ID 200 which contains the Sensor Configuration settings, which when transmitted (i.e. sent out) to the radar sensors either as an individual or as combination elements causes changes to the sensor's default settings during operation. Any default changes caused by ID 200 and accepted will have a value of successful in the ID 201*. The ID 300, ID 301 and ID 200 are transmitted at a rate of 50 microseconds (cycle time) to the radar sensors. The ID 200 can be transmitted once if only required to change a particular default settings for a particular application, such as radar range length or continuously if the settings requires continuous updates. Higher cycle time than required by the radar sensors will make the sensors go quite (i.e. stop sending signals).

The two radar sensors after receiving the input signal ID 300, ID 301 and ID 200 processes the signals, and continuously radiate the signal to analyse its surroundings every cycle at a rate of 66 microseconds (ms). The reflected signals are processed and becomes available in the form of Targets or Objects depending on the radar output type. The radar output type was sent as Objects for this research since the vehicles are required

to be tracked. The tracked object's position is calculated relative to an assumed vehicle course which is determined by using the speed and yaw rate information contained in ID 300 and ID 301. The returned reflected signal information about an object contained in ID 60A, ID 60B, ID 60C, ID 700 and the sensor state contained in ID 201* for each radar sensor is then transmitted on CAN1 of the radar sensors through the PCAN-USB Pro adapter to the on-board laptop computer running the PE5. The ID 60A, ID 60B, ID 60C, ID 700 and ID 201* are received by the PE5 at rate of 66 ms. The PE5 display and monitor live all the messages or signals including radar sensors state that are received and transmitted during operation of the system.

The PE5 after receiving the ID 60A, ID 60B, ID 60C, ID 700 and ID 201* as traces, process them and together with ID 201 from the test vehicle are then saved in a trace file with a time stamped. A VBmacro codes running behind the PE5 saves the traces automatically which can also be saved manually. The process continues until the operation is stopped or terminated. The trace files are then exported as a comma separated values (CSV) file format for offline analysis. The flowchart of the process is shown in Figure 3-7. Table 3-2 shows the CAN IDs and its content definition.

The Video VBOX and the PerformanceBox operate similarly apart from the video recording features of the Video VBOX. The Video VBOX external GPS receives GPS signals to the Video VBOX through the GPS Engine (10 Hz). The video cameras (both forward and rear facing) starts to record video and audio data. An indicator flash lights lit to show all the connected systems are working. The input video data is sent out to the preview OLED monitor connected to the Video VBOX to display live images of the recordings. The input video data with associated audio data and the speed information of the test vehicle received from the satellite tracking via the GPS antenna are simultaneously stored on a 32GB High Capacity Integral ultima pro SD card. This process continues and repeats itself until the end of the experiment. The 32GB SD (secure digital) card then taken offline onto the laptop computer (VBOXTools installed) for data extraction and data export to CSV or Excel file format, a more understandable form for further analysis. The maximum 32GB SD card required for the Video VBOX was used for this research because it can record data for several hours. The flowchart of the operation process is shown in Figure 3-8.

The PerformanceBox external antenna receives GPS signals to the PerformanceBox that tracks the test vehicle's movement. A large digital speed value is displayed in real time

on the back-lit LCD (liquid-crystal display) speed display screen of the PerformanceBox as it is being received. The speed information then stored on the 2GB Integral SD card. The process repeats itself until the experiment is completed. The 2GB SD card then taken offline onto the laptop computer (PerformanceTools installed) for data extraction and data export to CSV or Excel file format, a more understandable form for further analysis (see Figure 3-8 for the flow chart of the process). The Sony digital video camera at the back of the vehicle begins to record at the start of the experiment. The video records the rear images of the experiment and data stored onto an internal 30GB memory. The video data then transferred to the laptop computer after the experiment through a data cable connection for further analysis.

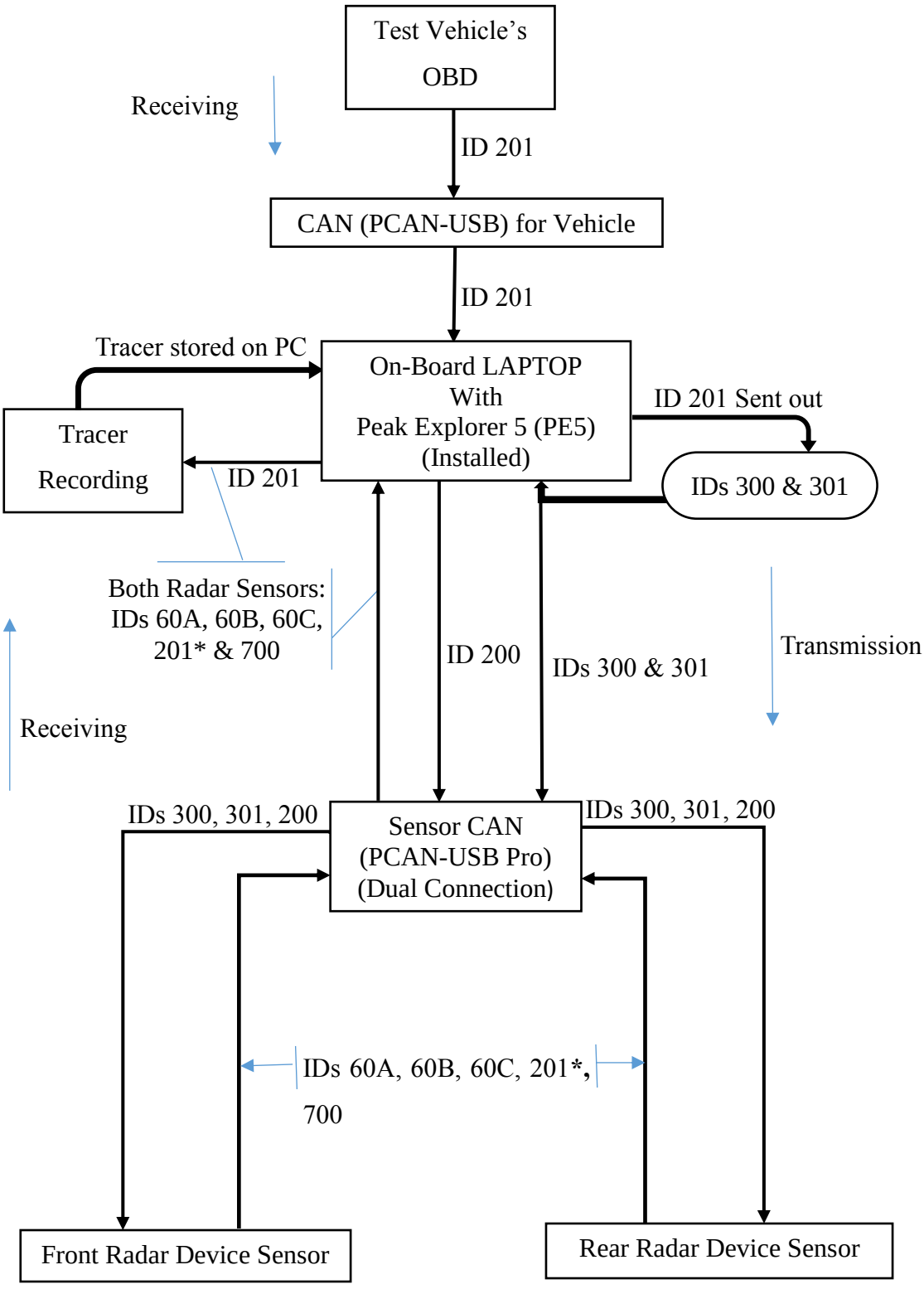

Figure 3-7: The system process diagram of the Instrumented Vehicle

Table 3-2: The CAN IDs message names, content definition and transmission status

Message ID	Message Name	Message Content	Receive/ Transmit Cycle and Status
200	Radar Configuration	Radar elevation angle, Radar output type, Radar range length, Radar service start align and radar align mode.	50 ms Transmit
201*	Radar State	Contains signals that report and verify the state of the sensor. Current range length, Current elevation, Radar power reduction, NVMwrite status, Sensor temperature, Sensor ID etc.	66 ms Receive
201	Vehicle Speed Configuration and Information	Test vehicle speed, Yaw rate, RPMH, Gas pedal position	20 ms Receive and Transmit
300	Speed Information	Radar device speed Radar device speed direction	50 ms Transmit
301	Yaw Rate Information	Radar device speed direction Yaw rate information – measured by yaw rate sensor in the radar sensors	50 ms Transmit
60A	Object Status	No of objects – number of measured objects, Measurement Counter – increases 1 per cycle, Number of lanes right, Number of lanes left, Sensor misaligned, sensor defective, Sensor switched off, Sensor supply voltage, Sensor output reduced, Sensor RxInvalid, Sensor external disturbed and Interface version number	66 ms Receive
60B	Object Information 1	Rolling counter – increase every cycle by one, Object ID – gives ID to any tracked object, Relative longitudinal speed, Relative longitudinal acceleration, probability of existence, Dynamic property – object movement status, Lateral displacement, Object length, Object width, Object measurement status – object detection and recorded status.	66 ms Receive
60C	Object Information 2	Radar cross section (RCS), Object lateral velocity, Object obstacle probability	66 ms Receive
700	Object List Interface Version	Major release number, minor release, Patch level	66 ms Receive

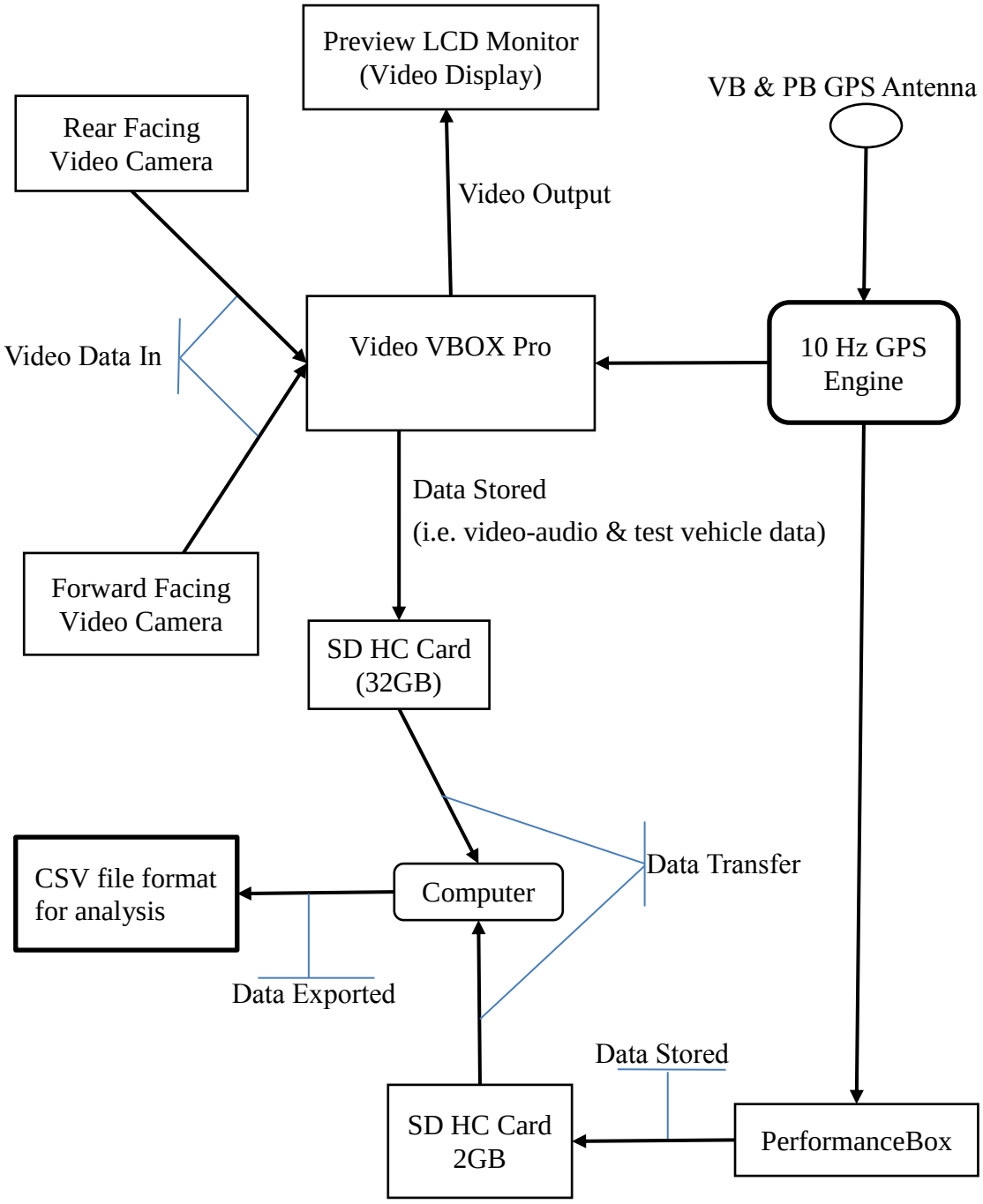

Figure 3-8: The operation process diagram of Video VBOX and PerformanceBox

3.4 Data Collection

This section discusses the data collection process carried out for this study. The calibration of the radar sensor beam elevation angle is discussed in Section 3.4.1. Discussed in Section 3.4.2 is the reversed engineering of the test vehicle speed. Section 3.4.3 discusses the radar sensor speed direction settings. The pilot data collection is discussed in Section 3.4.4. The main data collection for this study is discussed in Section

3.4.5. Section 3.4.6 discusses the data parameters measured during the experiment and finally Section 3.4.7 discusses the bus following data acquisition.

3.4.1 Calibration of the Elevation Angle of the Radar Beam

The right operational elevation angle of the radar radiation of the sensors mounted on the front and rear of the test vehicle is paramount to the quality of data collection and the success of this research. To calibrate and determine the correct elevation angle of the radar beam based on the mounted heights of the sensors on the test vehicle, a number of on-street field test using private parked vehicles were carried out. The elevation angle of the radar sensor's plate ranges from 0 degree to 32 degrees. The elevation angle of 0 degree indicates that the radar radiation or beam is inclined towards the sky, and the 32 degrees elevation angle indicates that the radar beam is inclined towards the road (Continental, 2013). The radar sensor's plate is set to a default elevation angle of 16^{o} horizontal around which the sensor's plate moves towards the sky or towards the road depending on the sensors mounted heights. The elevation of the radar beam or radiation can be changed in a certain range through the radar sensor configuration (Continental, 2013) by transmitting the changed signal to the radar sensor via the PE5 interface.

The front and rear radar sensors were mounted on the instrumented vehicle at a height of 24 centimetres and 20 centimetres (cm) respectively, measured from the bottom of the sensors to the ground. Because the radar sensor's plate can be changed via the configuration of the radar sensor, the mounted heights were not that significant to hinder its effective operation. However, there was a need to calibrate and determine the correct elevation angle of the radar radiation corresponding to the mounted heights of both the front and the rear radar sensors. To begin with, four different parked (i.e. stationary) vehicles on different public roads at different locations in a quiet residential area in the City of Edinburgh were used. For each subject stationary vehicle, a 50 metre (165 feet) long fiberglass ranger tape measure with metric (metre, m) and imperial (feet) scale (with long winding lever and easy grip knob quick rewinding) was used to measure distances from the bumper of the parked subject vehicles from 10 metres, 20 metres, 30 metres, 40 metres and 50 metres to the test vehicle.

The distances of 10 metres, 20 metres, 30 metres, 40 metres and 50 metres measured from the bumper of the parked vehicles were marked with heavy tool coloured boxes on the side of the road. During the calibration field test, the test vehicle was parked behind or in

front of the stationary vehicles along the road at distances of 10 metres, 20 metres, 30 metres, 40 metres and 50 metres whilst varying the angle of elevation of the sensor at each marked distance. During the field experiment, the test vehicle either moves backwards (reversing) away from or forward towards the stationary (parked) subject vehicles depending on the start of the measured distance. To begin with the front sensor, the test vehicle was guided to align the front radar sensor with the coloured boxes which marks the measured distances by the second research team member before the start of each experiment.

At each marked distance, the angle of elevation of the radar sensor is varied from 14.50^{o} to 16.0^{o} with gradual interval increments of 0.25^{o} (i.e. 14.50^{o}, 14.75^{o}, 15.00^{o}, 15.25^{o}, 15.75^{o} and 16.00^{o}) to measure the distance from the front sensor to the parked subject vehicles. This process is repeated until all the marked distances are completed. The process is then repeated with the rear mounted sensor. The test vehicle turns around and reverses towards the subject parked same vehicle that was used for the front sensor test: beginning the test from the 50 metre mark to 10 metre mark points with the radar elevation angle changing from 14.50^{o} to 16.0^{o} with an interval increments of 0.25^{o} at each measured distance. The same process is repeated for all the four subject stationary vehicles identified at different locations within the study area. The test vehicle speed information was not needed at this stage, because the test vehicle was always stationary when the test is being carried out to measure the distances using the radar sensors with varying radar elevation angle. The table of results of the distance measurement are presented in Appendix 3.4.1.

The measured distances, after the experiment, were taken for offline analysis to determine the right calibration elevation angle of the radar radiation appropriate to the mounted heights of the radar sensors. To determine the correct elevation angle suitable for the mounted heights of the radar sensors on the test vehicle, the Root Mean Square Error (RMSE) method was applied to calculate the error margin between the actual marked distances and the radar sensor measured distances from the subject vehicles. The RMSE is expressed as:

$$\mathrm{RMSE} = \sqrt{\frac{1}{\mathrm{N}}\sum_{\mathrm{i}=1}^{\mathrm{N}}(\mathrm{m}_i - a_{\mathrm{i}})^2} \tag{3-1}$$

where m_i and a_i are the measured radar distance and the actual marked distance values respectively and N is the number of observations. The plots of the result of the RMSE calculations for the front and rear sensors are presented in Figure 3-9 and Figure 3-10.

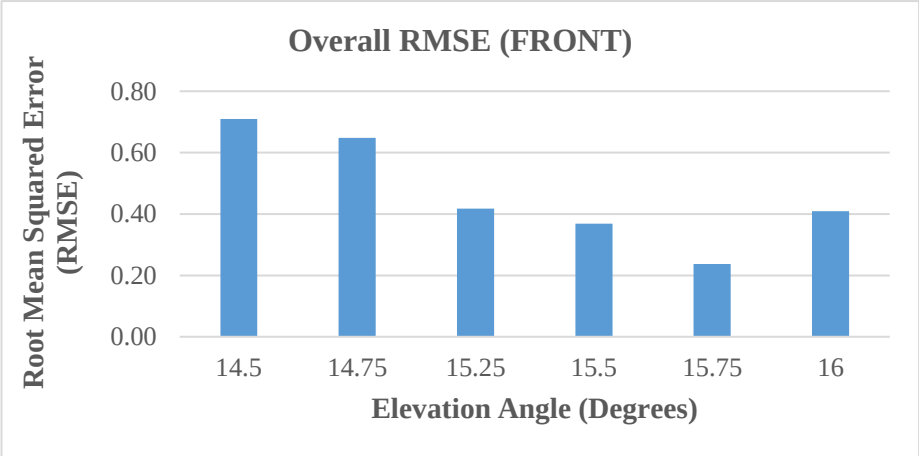

Figure 3-9: The front radar sensor elevation angle RMSE comparison for all 4 vehicles

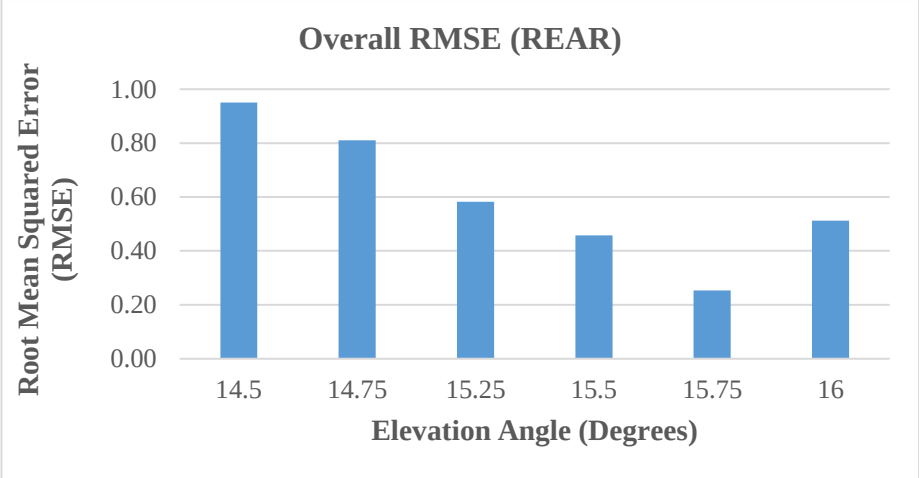

Figure 3-10: The rear radar sensor elevation angle RMSE comparison for all 4 vehicles

From the analysis, the elevation angle of 15.75^o was found to produce more reliable data for all the measured distances corresponding to the mounted heights of both the front and the rear sensors, and consistent with the road characteristics of the test site, which is the same within the study area. Also, from the RMSE graphs, it shows clearly that 15.75^o is the best sensor beam elevation angle suitable for the mounted heights of the radar sensors on the test vehicle.

3.4.2 Reverse (Re)-Engineering of the Test Vehicle Speed Configuration and Information

The speed configuration from the test vehicle's CAN signals was not readily available to incorporate into the radar sensors' set up for use in the data collection. In order to configure the speed information from the test vehicle CAN signals, a series of requests were made to Ford Motors, the manufacturer of the test vehicle (Ford Mondeo), to assist with the release of the test vehicle's speed configuration and information. The requests were not successful. There was a need to re-engineer (i.e. reverse-engineer) the test vehicle CAN data to determine the speed configuration before the data collection stage could commence. The radar sensors requires input signals, which contain the test vehicle's speed and yaw rate information that are used to evaluate the test vehicle's course to determine the movement of any detected objects and their respective position in relation to the course of the test vehicle. It was essential for this research to obtain the speed configuration of the test vehicle and continuously transmit it as input signal to the radar sensors during the experiment.

To begin the process of reversed-engineering of the test vehicle's speed configuration, the PerformanceBox time and the Laptop computer time (with Peak Explorer 5 installed to monitor the CAN messages) were synchronised to ensure both measuring devices have the same operational times. The display speed information of the PerformanceBox (PB) was used to compare and validate the speed of the test vehicle during the experiment. It was appropriate to use the PB in the experiment due to the large display screen showing the test vehicle speed information. The OBD-II port of the Engine Control Unit (ECU) of the test vehicle was connected to the on-board laptop computer via the PCAN-USB Bus using the OBD-II CAN cable. Communication between the Laptop computer and the test vehicle's OBD-II were established as CAN signals or messages were received by the Laptop computer. The symbols file generated for the purpose of the reversed-engineering experiment was applied and assigned to the CAN messages for easy message identification. Changes in the received signals or messages were clearly visible and noticeable on the laptop screen because the Peak Explorer 5 displays and monitors the messages live for the user.

A series of field experiments were carried out after the setup was completed by driving around within the study area in order to re-engineer the speed configuration of the test vehicle. During the test runs, CAN message IDs that were not needed for this research

but shown up during the experiment were eliminated until the required CAN message ID was identified. With continuous updating and adjustments of the symbols file applied to the CAN messages, the correct speed configuration and information were obtained. All throughout the test runs, the re-engineered test vehicle speed was compared with the PB speed data in a validation process. In order to further validate the re-engineered vehicle speed, a further test runs was carried out with the Video VBOX connected to the test vehicle CAN via the Racelogic OBD-II cable.

The Video VBOX uploaded with a re-engineered (or decrypted) symbol file of the test vehicle speed information from Racelogic was used for the test runs. A step by step instruction experiment with the Video VBOX designed by Racelogic for this research was followed in order for Racelogic to re-engineer the test vehicle speed configuration (see Appendix 3.4.2). The test result including voice and video data was sent out to Racelogic to re-engineer (or decrypt) the test vehicle speed information. The returned decrypted symbol file of the test vehicle speed information from Racelogic was uploaded onto the Video VBOX. The result of the Video VBOX test runs were compared with the earlier PCAN-Bus experiment and found that the two experiments produced the same speed in all speed ranges. Further experiment was carried out to obtain the angular velocity (i.e. yaw rate) information of the test vehicle. The data was analysed, reformatted and incorporated in the sensors setup.

The test vehicle speed configuration was incorporated into the radar sensors setup after the validation process was completed. The generated symbols file for the test vehicle speed configuration was modified to convert the speed from kilometre per hour (km/h) or mile per hour (mph) to metre per second (m/s) as the CAN message is being received since the radar sensors input speed unit is m/s. Visual Basic macro codes were developed to automatically sent out the test vehicle speed information to the radar sensors CAN IDs 300 and 301, in order to evaluate the course of the test vehicle during the data collection experiment.

3.4.3 Radar Sensor Speed Direction Settings

The ARS 308-2 long range radar sensors used for this research has four operational radar device speed direction (i.e. 0 = Standstill, 1 = Forward, 2 = Reverse and 3 = irrelevant/unused) that indicates radar direction while looking into the positive straight ahead direction with each having different effects on the radar output. The Standstill

indicates no movement in any direction and the Forward indicates the movement of the radar in the positive straight ahead direction. The Reverse, however, indicates the radar movement against the positive forward direction (i.e. backwards), whiles irrelevant/unused indicates no use, no matter how high or low of the radar beam (Continental, 2013).

Since the test vehicle normally moves forward, the radar device speed direction of the front sensor was default set to a value of 1 = Forward for its operation. Because the radar sensor was not originally designed to be used at the rear of the host vehicle, its efficient and operational use at the rear should mimic the front sensor's operational use as if it is mounted at the front of the host vehicle. To do this, the rear radar sensor was mounted at 180^{o} from the normal mounting position as used at the front of the host vehicle. Doing this, enabled the rear radar sensor to operate the same way as the front sensor without requiring any additional software or special program written for it to perform tasks in order to mimic the front sensor's operation. The rear sensor was mounted below the rear bumper of the test vehicle.

In order not to change the sign of the speed of the rear radar sensor during the experiment because it is mounted at the back of the test vehicle, the radar device speed direction was set to a default value of 2 = Reverse. Under this circumstance, the speed calculations of the rear radar sensor will be correct regarding what it detects in the backside. The front and the rear sensors with the correct radar device speed directions set as default, the sensors now operates efficiently to track and detect objects with the correct speed calculations throughout the experiment.

3.4.4 Pilot Data Collection

Preliminary acquisition of data and survey of traffic were carried out on a number of traffic corridors within Edinburgh and the surrounding areas during the morning and afternoon peak and off peak periods. Prior to the preliminary data collection, the test vehicle's on-board instrumentation were tested to ensure proper functioning of the devices (see Appendix 3.4.4). The pilot data acquisition was initially carried out outside the research's main identified traffic corridors to observe the general driving behaviour of vehicles across the City of Edinburgh. An initial three days extensive pilot data acquisition and traffic survey was carried out across different locations within three months on 24 October 2014, 25 November 2014 and 03 December 2014, mainly within

and outskirts of the City of Edinburgh on urban and rural roads during the morning and afternoon peak and off peak periods (see Figure 3-11). The initial data acquisition enabled better understanding of the data structure and the data output of the radar sensors in tracking subject vehicles. Initial analysis of the sensors data showed that a number of different vehicles were tracked at the same time by both the front and the rear sensors in addition to the immediate leading and following vehicles.

Vehicles to the left or right of the instrumented vehicle in the adjacent lane in the same direction of travel and the approaching vehicles in the opposite lanes were tracked and captured by the sensors, but not analysed in this study. The data parameters or variables captured by the radar sensors were time stamped making it easier to keep track of each parameters and relate to other parameters. The video analysis of the front and rear view cameras showed different driving behaviours and manoeuvres across different range of vehicle types. The natural driving behaviours amongst the drivers captured were observed and identified the most common driving behaviours and manoeuvres under real driving conditions in car following situations. The subsequent pilot data acquisition was focused more on the common driving behaviours that were identified in the initial data acquisition.

Series of pilot data collection continued mainly on the three main selected traffic corridors within the study area to observe in detail the driving behaviours under different driving conditions in a car following situation and also, to validate the data collected on other corridors. The pilot data collection completed at the end of June 2015. Throughout the preliminary data collection, the instrumentation that needed to be adjusted to suit the driving conditions on the corridors were carried out. For instance, the initial video analysis revealed that the recordings of the in-vehicle activities of the rear following vehicles could be improved if the rear view cameras were focused directly on the following vehicle. To improve the recordings of the rear following in-vehicle activities including the occupancy, the Sony camcorder video camera was zoomed in and focused directly at the centre of the immediate following vehicle's windscreen. The Video VBOX rear camera remained unadjusted since it recorded the relevant information. The preliminary analysis of the front video camera suggest that most vehicles tend to accelerate faster in an uncongested traffic when leading the traffic stream. However, in congested traffic, some of the leading vehicles tend to brake early before slowing down to a stop or with the brake lights staying on longer while in motion.

The preliminary survey and data acquisition during the morning and afternoon peak and off peak periods in all traffic and weather conditions helped to plan for the main data collection. Enough information were gathered on the factors that could affect the car following situation, such as the weather condition, road characteristics, traffic conditions and human characteristics. The conditions at which individual vehicles, both leading and following the test vehicle terminates the car following process that influence the following duration were identified. The preliminary surveys improved the data collection techniques, helped to identify the data type and the common driving manoeuvres to concentrate on more during the main final data collection.

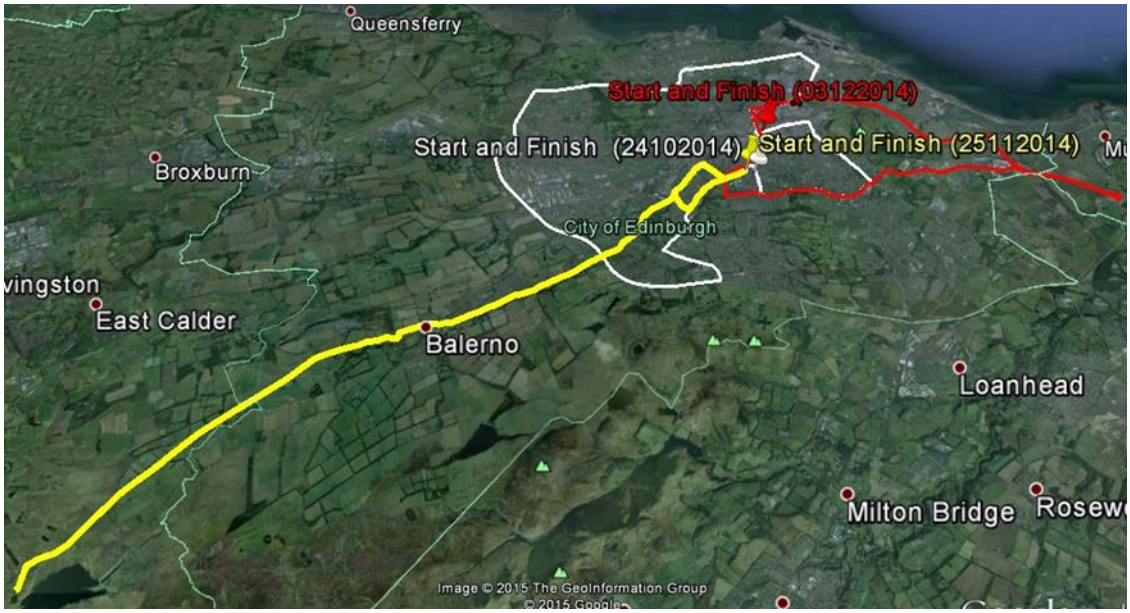

Figure 3-11: Route map of initial days of the preliminary data acquisition and surveys

3.4.5 Main Data Collection

The field data collection on car following was carried out from July 2015 through to October 2015 during the morning peak (rush) hours and afternoon off-peak (non-rush) hours. The data was collected mainly on the selected four traffic corridors (that includes the combined traffic corridors 1 and 2) within the City of Edinburgh and the surrounding areas on an urban, rural and highway arterials. Additional data were collected on different traffic corridors (designated as other corridors) within Edinburgh Township and the M8 Motorway from Edinburgh to Glasgow link. These additional data were not analysed in this study due to time limitation.

The instrumented vehicle was always manned with two-man team, comprising the driver of the test vehicle and the data analyst who was monitoring all the instrumentation on-board and the feeds from the radar sensors and video cameras to ensure they were all working properly at all time during the experiment. The instrumented vehicle at every point in the experiment tracks the front leading and the rear following vehicles at the same time as in a three consecutive vehicles in motion scenario as shown in Figure 3-12. The data collection was designed in this manner in order for all the vehicles the instrumented test vehicle encounters, both leading and following, to be monitored and tracked at same time. In order to differentiate the data of the front and rear radar sensors, all signals or CAN messages (data) from the front leading vehicles were prefixed with the letter "F" for "Front" and all signals or CAN messages (data) from the rear following vehicles were prefixed with the letter "B" for "Back". The tracked vehicles CAN messages (data) were fed into the on-board Laptop computer installed with PCAN Explorer 5 and displays live on the computer showing the states of each sensor's tracked messages.

The PCAN Explorer 5 processes the messages and automatically store them as traces in a trace file format (.trc) on the Laptop computer with a storage capacity of 1TB. This process continues throughout the duration of the experiment. The stored files are then taken offline for analysis by exporting the files to a more readable comma separated values (CSV) file format easy to interpret the data. Apart from the immediate leading and following vehicles that the sensors tracks, each sensor tracked a number of multiple objects detected on its track simultaneously. The radar sensors detects all objects (i.e. pedestrians, bicycles, motorbikes, cars, trucks including buses) in its field of view (FoV) with a high detection measurement accuracy.

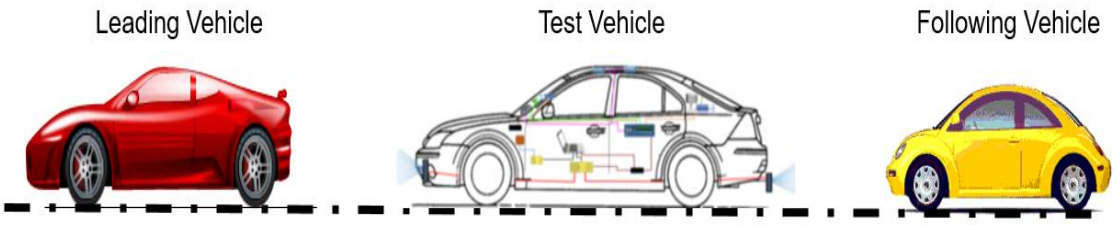

Figure 3-12: Three consecutive vehicles movement in a car following situation.

The Video VBOX Scene created to display the front and rear view cameras (same size) side by side, the speed of the test vehicle, the speedometer, UK summer time with the number of satellite tracking, the UTC time and the date of the experiment. The feeds from the video cameras and test vehicle speed information from the GPS were displayed live

on the preview OLED display screen fixed at the bottom centre of the front windscreen. The traffic activities recorded by the video cameras were merged and saved into one video file linked with the test vehicle recorded speed data by the Video VBOX.

The data collection on each day was covered by the morning peak (rush) from 08:00 to 09:30 (or 08:00 to 10:00 for the longer corridors) and afternoon off peak (non-rush) from 14:00 to 16:00 (British Standard Time (BST)) periods. The data collection times takes into accounts the different driving variations of the traffic on the corridors. Different driving characteristics were expected at different times of the day, partly due to the different activities and weather conditions of the day. A final all day testing and validation of the instrumented test vehicle was carried out before the start of the data collection. The data collection was undertaken on one selected traffic corridor (route) per day at a time, spanning a total of twenty (22) days to complete the car following data acquisition. In all, a total of seven (7) days of data acquisition was undertaken on Traffic Corridor 1, five (5) days on Traffic Corridor 2, five (5) days on Traffic Corridor 3, two (2) days for Traffic Corridors 4 and three (3) days for the other Traffic Corridors considered for this research. Each day morning peak and afternoon off-peak data acquisition comprises two (2) test runs each (i.e. from the start point to the end point and returned journey to the start point of the route) resulting in four (4) test runs in a day covering both direction of travel. In all, a total of two sets of eighty-four (84) or a set of one hundred and sixty-eight (168) test runs were undertaken for the entire data acquisitions for this research. The test runs are the main or actual data collection runs for this study.

For each selected traffic routes, an initial three (3) days of data collection were undertaken before moving on to another selected traffic routes. After the initial data collection, the rest of the data collection on each routes were undertaken on different days on different routes. This enabled the capture of driving behaviours under different driving conditions on the same route in the same week or month. A number of observations were made under car following situation during the experiment. Different factors that affects car following behaviour were observed including different manoeuvres that were captured by the video cameras. Different vehicles were leading or following the instrumented vehicle at different periods as a result of the termination of the car following process during the experiment (see Appendix 3.4.5).

3.4.6 Data Parameters Measured

Different factors that affects car following situation were captured or measured by the instrumented vehicle throughout the data acquisition process. Some of the car following data collection parameters were either captured (measured) directly by the radar sensors and the video cameras including other on-board devices or calculated offline. The car following variables or parameters that were captured or measured, and/or calculated for each car following time sequence for each leading and following vehicles that the instrumented vehicle encountered are shown in Table 3-3 and Table 3-4.

Table 3-3: Measured and calculated data variables obtained for data analysis

Measured Variables	Calculated Variables
• Relative Longitudinal Acceleration	• Leading Vehicle Speed
• Relative Longitudinal Distance	• Following Vehicle Speed
• Relative Longitudinal Speed	• Leading Vehicle Acceleration
• Instrumented Vehicle Speed	• Following Vehicle Acceleration
• Instrumented Vehicle Acceleration	• Distance Headway
• Distance Travel	• Time Headway
• Lateral Speed	• Time Gap
• Lateral Displacement	• Time To Collision (TTC)

Table 3-4: Data parameters/variables obtained using the Instrumented Vehicle

Variables Obtained	Leading Vehicle	Instrumented Vehicle	Following Vehicle
Relative Longitudinal Acceleration	√	√	√
Relative Longitudinal Displacement	√	√	√
Relative Longitudinal Speed	√	√	√
Vehicle Speed	√	√	√
Vehicle Acceleration	√	√	√
Distance Travel	√	√	√
Lateral Speed	√	x	√
Lateral Displacement	√	x	√
Distance Headway	x	√	√
Time Headway	x	√	√
Time Gap	x	√	√
Time To Collision	x	√	√
Time Duration in the Car following	√	√	√
Vehicle and Other Characteristics:			
• Vehicle Type	√	x	√
• Driver's Gender	x	x	√
• Vehicle Occupancy	x	x	√
• In-Vehicle Activities such as drinking	x	x	√
Environmental Condition	√	√	√
Road Traffic Condition such as traffic flow (obtained from the video)	√	√	√
Traffic Corridor such as number of lane	√	√	√

* Key: √ = applicable; x = not applicable

3.4.7 Bus Following Data Acquisition

The instrumented vehicle was used in the data acquisition of the bus following experiment. The commuter buses that were followed for the data acquisition were a double decker commuter buses operated and owned by the Lothian Bus Company, a publicly owned local bus company with the major shareholder being the Edinburgh City Council. The data was collected in a period of two consecutive days during the evening peak (17:00 – 18:30) (rush) hours where the traffic on the corridor was at its heaviest in both direction of travel. The data was collected in both dry and wet conditions in the month of August 2015. The test driver (different driver) was an experienced driver with several years of driving experience on the road and who was familiar with the instrumented vehicle. The test driver was instructed to drive the test vehicle freely and

the way the driver would normally drive for all the runs of the data collection. The instrumented vehicle covered a total distance of 21.2 miles each day (start point to finish point and return journey to start point).

The instrumented vehicle followed several double decker commuter buses (with length of 11.3 metres) on the traffic corridor from Edinburgh through to the busy rural roads to Gorebridge town centre, a town in the outskirt of the City of Edinburgh (see Figure 3-2) and back to Edinburgh. Different buses were followed on the returned journey from Gorebridge town centre to Edinburgh city centre. In all, eight (8) different male drivers of double decker buses were followed in two consecutive days during the PM peak hours. The bus drivers including drivers of the vehicles following the instrumented vehicle were not made aware of being followed and taking part in the study. This was to ensure that the driving behaviour of all vehicle drivers being monitored are not affected by the presence of the instrumented vehicle. The radar signal monitoring software used for this research monitors the data live and it is capable of handling several live radar signal data from several radar devices. The data collection time plan for the research is presented in Appendix 3.4.7.

3.5 Summary

In this chapter, the study design, the experimental procedure and data collection methodology were discussed. Edinburgh and the neighbouring towns were chosen as the case study area. The major roads within the study area were discussed. Four major traffic corridors (i.e. roads) with different road characteristics were identified and selected as this study's main data collection routes. In addition, one of the busiest public bus routes within the study area was selected for the collection of bus following data used for the bus following study discussed in Chapter 10. The traffic corridors (i.e. roads) used in this study have a combined speed limits from 30 mph to 70 mph.

New instrumented vehicle that is capable of observing the activities of both the front leading vehicle and the rear following vehicle was developed and used for data collection. The instrumented vehicle developed is capable of measuring the relative distance, relative speed and relative acceleration between the tracked vehicles and the test vehicle both at the front and the rear. In addition to these, the data type collected by the instrumented vehicle includes the subject vehicles drivers and vehicle occupancy characteristics (rear

vehicles only) such as gender. The process involving the termination of the CAN-Bus communication cables that enable the CAN interface and control device to work to enable the entire system to properly function was discussed.

The data acquisition for this research was discussed in this chapter. Calibration of data collection equipment were carried out to enhance the quality of the data collected. The right elevation plate of the radar sensors beam was essential regardless of the mounting heights of the radar sensors on the instrumented vehicle. Trial experiment was carried out to determine the appropriate angle of elevation of the radar plate suitable for the mounting heights of the sensors on the instrumented vehicle. Since the radar sensors required the test vehicle's own speed information to determine the course of the test vehicle, this study reversed-engineered the test vehicle's speed through field experiment. A visual basic macro program was developed to automate the transmission of the test vehicle's speed information to the radar sensors for their effective operation during the experiment. Preliminary pilot data collection was carried out which enabled the effective planning of the data collection and the kind of driver behaviour variables to be collected during the main data collection. The driving behaviour data including the bus following data were collected on week days for all four identified traffic corridors including the bus corridor.

The next chapter discusses the data cleaning and data preparation analysis of this study. It discusses the data description, preliminary cleaning and filtering of radar sensors data, data preparation and the general statistics of this study.

CHAPTER 4 DATA CLEANING AND PREPARATION ANALYSIS

4.1 Introduction

In Chapter 3, the study design, experimental procedure and data collection methodology were discussed. The case study area and corridors used in this study including vehicle instrumentation were discussed in Chapter 3.

In order to ensure that the data collected is made ready for analysis, the data cleaning and preparation process were carried out and discussed in this chapter. The data storage format, the data extraction and processing are discussed. Because the radar sensors were capable of tracking and measuring objects in its field of view (either in-motion or stationary), the raw data from the sensors needed to be cleaned before the data could be used for analysis. In doing so, a preliminary data cleaning and data filtering (i.e. screening) process was undertaken to eliminate all the non-essential records from the data sets. This is discussed in this chapter. The final preparation of the data is discussed. The general data statistics is discussed and presented in this chapter.

4.2 The Data Description

Due to the sheer volume of data collected for this study, the handling and processing of the raw data for further analysis has been very demanding and time consuming tasks undertaken for this study. The raw data include the radar sensors (front and rear) data, the video (both front and rear) recordings and the corresponding Video VBOX host vehicle measured data for all the 82 pairs of experimental runs. The data sets were obtained from synchronised measuring devices, so data from one device is easily matched up with data from another measuring device with the same time sequence. The Video VBOX and the PerformanceBox display times were synchronised with the on-board Laptop computer display time (i.e. the radar sensor data time stamp). This was done before the experiment to ensure that data from all the measuring devices can be merged together for analysis. The video recordings from the three (3) video cameras were first analysed. From the video data, the total number of vehicles including the car following duration for each vehicle observed for all the four traffic corridors on daily basis were obtained. The total following duration for the individual vehicle following behaviour were needed to extract the

required corresponding individual vehicle's data captured by the radar sensors. The data from the Video VBOX and the radar sensors were subsequently analysed.

4.2.1 The Data Storage Format

There were 600 signals or CAN messages that were received from each radar sensor per second. The CAN messages from the radar sensors were processed by the PCAN Explorer 5 as traces and saved in a trace file format (*.trc*). Both the front and the rear radar sensors' messages were stored in one file with the same message variables (i.e. message or data parameters). Both sensors use the same algorithms and are only distinguished by a pre-defined prefix letters to each message variable. In order to distinguish between the data parameters from each radar sensor, the letters "F" and "B" were prefixed to the individual CAN message variables contained in the symbols file for the front and the back radar sensors respectively for easy identification during the experiment and data extraction process. Though both radar sensors messages were saved together in one trace file, the front sensor message variables were separated from the rear sensor message variables within the same file, which makes it easy to identify, select and export the individual radar sensor's data separately for further analysis.

The CAN messages were stored automatically in smaller file sizes so it can be handled by a third party applications such as Excel spreadsheets for processing. The trace files were then exported to a more readable comma separated value (CSV) file format for further data analysis. The Video VBOX data was saved in a Racelogic space delimited text format that can be imported easily into a third party data processing applications such as CSV spreadsheets (Racelogic, 2012). The video recordings were saved in a video (AVI) format while the data (i.e. test vehicle's speed information from the VBox) is saved in a data (VBO) file format. The video files are linked to the data files in the same 'media' folder where they are saved. The recordings from the rear view Sony camcorder video camera were stored by the camera's 64GB internal memory and transferred to the laptop computer via high definition video transfer cable for further analysis after each experiment.

4.2.2 The Video Data Output and Extraction, VBOX and PB Data Processing

The scene of the Video VBOX was created to display the front and the rear video side by side, the BST and UTC times including the date and test vehicle's speed in miles per hour (mph) (see Appendix 3.3.2.9). With the videos sitting side by side, it makes it easier to analyse and extract the required video data from the front and rear recordings at the same time. The video recordings for each run were played back to extract the data. The data sets for each captured vehicle were extracted, and the car following duration for each vehicle determined using the difference in the times the individual vehicle appeared and disappeared in the video recordings. The number of times each individual vehicle stopped and moved off during the car following process were extracted. This was to enable the estimation of the actual car following duration for each captured vehicle less the stop/start duration (i.e. duration of following without stopping). Other data extracted from the video recordings include the vehicle types for both the leading and following vehicles, the gender of the driver and the vehicle occupancy together with the in-vehicle driving activities such as smoking while driving specifically for the following vehicles, the weather condition, the traffic flow (i.e. congested and uncongested) and bus lane (or green way) availability on the corridors which restrict a 2-lane traffic to a single lane traffic.

The camcorder video camera was played back side by side with the Video VBOX video recordings to extract the gender, the vehicle occupancy and the in-vehicle activities of the following vehicles observed. The extraction of the video data were first recorded manually on printed work templates (see Appendix 4.2.2), and later transferred onto Excel spreadsheet for further data analysis to determine the actual car following duration for each vehicle observed during the experiment. To determine the total car following duration without any stopping for each vehicle observed, the total time each vehicle spent in the car following process were calculated which included all the stopping/stationary duration of each vehicle. The total time each vehicle stopped/stationary during the entire car following process then subtracted from the overall total car following duration of each vehicle. The templates for the final calculations of the total vehicle following durations are presented in Appendix 4.2.2. The start time and termination time of the car following process recorded for each observed vehicles were then used to extract the corresponding individual vehicle's radar sensor data during the radar sensors' data analysis.

The instrumented test vehicle's speed information data obtained by the Video VBOX and PB saved in space delimited text format were uploaded into a more readable format using

a VBOXTools, a specialised software for the data processing. The readable data sets were exported to a CSV spreadsheet format and analysed. The UTC time stamp, acceleration, speed and distance travelled by the test vehicle were extracted from the raw data and processed. The UTC time stamp of the data were reformatted to the same format as the radar sensors' time stamp format, which was later used for joining up with the test vehicle's actual speed data captured by the PCAN Explorer 5 CAN message monitoring application.

4.2.3 The Radar Sensor Message Output and Extraction

In a typical cycle, each radar sensor sent 40 message pairs for any identified objects it detects in its field of view. Each identified objects that the radar sensor tracks are assigned an ID from 1 to 40 in every cycle. The same ID is assigned to the same object tracked continuously in every cycle until the object is out of the field of view of the radar sensors. For a typical cycle, 40 assigned object IDs are returned from the radar sensor at every cycle in a 15 cycles per second resulting in 600 messages received per second. Not all detected objects with object IDs in a cycle are valid objects, hence the repeated cycle process will confirm and measure the objects it detects for the third time as valid objects.

Detected objects are validated in a cycle through the object measurement status (OBS) process. Every new objects detected in the initial cycle are assigned OBS value of one (1). When the same objects are detected in the next cycle, they are assigned OBS value of two (2) indicating the objects seen but not measured (i.e. stored in the radar sensors' temporal memory). When the same objects are detected in the third cycle they are assigned the OBS value of three (3), which indicates that the objects are measured (i.e. stored in the radar sensors' memory) and confirmed their validity in the cycle. The objects will be continuously assigned OBS value of 3 in all the subsequent cycles until the objects are out of the field of view of the radar sensors. The number of measured objects expressed in the listing of each cycle are identified in the No_Of_Objects (NOB) variable in the data set. It is important to note that the of number of measured objects in the total listing of tracked objects could be higher than the listings in the NOB variable since some of the old objects which were not measured but still tracked in every cycle still exist in the listings (Continental, 2013).

The valid detected objects are assigned Object Dynamic Property (ODP) value in every cycle to indicate the measured objects movement status during the tracking process. ODP

value of three (3) was assigned to the measured objects tracked moving in the same positive direction of the radar sensor and a value of four (4) assigned to the measured objects approaching in the opposing lane moving against the radar sensor's forward positive direction for the front radar sensor. For the purpose of this study, the rear radar sensor dynamic property of measured objects were assigned ODP value of four (4) since the speed direction of the rear radar sensor was reversed to function as if it was facing the forward positive direction, and a value of three (3) to the measured objects in the opposing lane moving against the positive direction of the rear radar sensor.

The dynamic property status is very important in extracting the preferred measured objects from the data listing. Two sets of raw data were extracted and exported from the radar sensors' output files to a comma separated values (*.csv*) file format: the overall radar sensors data sets including the radar sensor configuration and selected variable data sets for both the front and the rear radar sensors. The selected messages or signals descriptions of the listing exported to spreadsheet in a comma separated values format are shown in Table 4-1. The front and the rear radar sensors data sets were exported separately for analysis.

Table 4-1: Message outputs of the radar sensor

a) Radar signal or message output description and variable values range (Continental, 2013).

Messages	Description	Variable Value Range
No. Of Objects	Number of tracked objects in the listing in every cycle	0 – 255 Typical cycle: 1 - 40
Object Roll Count	Increases by 1 per cycle after each sent CAN cycle	0 – 3
Object ID	Numerical ID assigned to each identified object per cycle	0 – 63 Typical cycle: 1 - 40
Object Longitudinal Displacement	Longitudinal relative distance between the object and the test vehicle	0 – 240 metres (m)
Object Relative Longitudinal Speed	Difference in speed between the object and the test vehicle	-128 m/s – +127.9375 m/s
Object Relative Longitudinal Acceleration	Difference in acceleration between the object and the test vehicle	-16 m/s^2 – 15.9675 m/s^2
Object Probability of Existence	Existence probability calculation for an object that was tracked and/or measured	• 0: invalid • 1: < 25 % • 2: < 50 % • 3: < 75 % • 4: < 90 % • 5: < 99 % • 6: < 99.9 % • 7: < 99.99%
Object Dynamic Property	Shows the object motion state in relation to the test vehicle	• 0: unclassified • 1: standing • 2: stopped • 3: moving • 4: oncoming
Object Length	The length of the object tracked	• 0: unknown • 1: < 0.5 m • 2: < 2 m • 3: < 4 m • 4: < 6 m • 5: < 10 m • 6: < 20 m • 7: exceeds

b) Message outputs of the radar sensor (continuation)

Messages	Description	Variable Value Range
Object width	The width of the object tracked	• 0: unknown • 1: < 0.5 m (pedestrian) • 2: < 1 m (bike) • 3: < 2 m (car) • 4: < 3 m (truck) • 5: < 4 m • 6: < 6 m • 7: exceeds
Object Measurement Status	The Object measurement status shows the presence of an Object in a cycle	• 0: no object • 1: new object • 2: object not measured • 3: object measured
Object Lateral Displacement	The lateral displacement of an object tracked	-51.9 m – 52 m
Object Lateral Speed	The lateral speed of an object tracked	-32 m/s – 31.75 m/s
Object to Left	The number of tracked object to the left of the test vehicle	
Object to right	The number of tracked object to the right of the test vehicle	

4.3 Preliminary Cleaning and Filtering of Radar Sensors Data

The cleaning and filtering of both radar sensors' data were divided into four stages. Each stage comprises at least one written computer program or Visual Basic for Application macro (VBmacro) program to speed up the cleaning and filtering process. Two different VBmacro programs were written and used to clean the front and the rear sensors data at different stages of the cleaning and filtering process. This is because the ODP parameter and other calculations such as following vehicles' acceleration were different for the leading and the following vehicles.

Stage 1: As mentioned earlier, the traces from the radar sensors were saved in smaller files sizes due to the volume of data received per second. The data were exported to a comma separated values file format for further processing. All the *CSV* files were further split into two separate files A and B by running the files through a special spreadsheet file split computer program, developed for this research to split the files further into smaller sizes due to the large amount of data contained in each *CSV* file. This enabled the processing of the data sets on a spreadsheet with least difficulties.

Stage 2: Within the data set, each data parameter in a column have a corresponding time stamp. Also, not all the data parameter in a column, such as the NOB and the test vehicle speed (i.e. radar speed), have the same pattern with the larger data sets due to the rate at which the CAN messages were transmitted and received during the experiment. The data sets needed to be of the same pattern without the individual parameter time stamps except the base time selected (i.e. relative acceleration time stamp) before proceeding with further analysis. Running VBmacro program with the data sets, all the time stamps of each column data parameter were removed, the NOB and the radar speed matched up with rest of the data sets. The data at this stage have only one column time stamp used as the base time for all analysis.

Stage 3: The measured objects (i.e. leading and following vehicles tracked) needed to be extracted from the raw data sets at this stage to be analysed further. To extract the valid measured vehicles from the data sets, the following data filtering criteria were used for the leading and following vehicles:

- Object dynamic property value of 3 for the front radar sensor data for leading vehicles.
- Object dynamic property value of 4 for the rear radar sensor data for the following vehicles.
- Object measurement status of 3 (measured) for both the front and the rear radar sensors data.
- Object property of existence of 3 – 7 (i.e. 75% - 99.99%) (see Table 4-1a) for both the front and the rear radar sensors data.

Running VBmacro program with the above filtering criteria, all the measured leading and following vehicles data were extracted from the raw data sets and all other irrelevant data eliminated from the data sets.

Stage 4: At this stage, the data sets contained in each file have become smaller in size and easy to handle. All the separate data set for each CSV files were manually combined together as one complete data set for each day's experiment. Different VBmacro programs were run at this stage to remove all the duplicated data and eliminate all the non-essential data from the data sets, such as the roll counter. Then the Video VBOX data (i.e. the test vehicle's acceleration) joined to the radar sensors' data and finally calculates the tracked vehicle's speed information including the time gaps, time (and distance) headways for the following vehicles.

To ensure the data quality, manual inspections and checks were carried out on the data sets after every stage of the data cleaning and filtering process.

4.4 Data Preparation

The final data preparation involves the extraction of each vehicle data from the data sets and eliminate further all non-essential data within the individual vehicle data sets. The individual vehicle data filtering process required manually extracting each tracked vehicle's data from the data sets since there were no available software to extract each vehicle's data from the data sets. Using the start and termination times of each following vehicle observed in the video data and the corresponding radar sensors data sets base times, all the individual tracked vehicles were extracted from the data sets obtained by the radar sensors. Individual vehicles data sets extracted were manually inspected and further eliminated the non-essential data within the data sets. The data sets for the individual vehicles were manually inspected again and checks done by plotting series of chats to observe any abnormality in the data sets. All these were done to ensure the quality of data to be used for the analysis.

Since each tracked same vehicle was assigned the same object ID throughout the tracking process, it was easy to extract the individual vehicle's data from the data sets. After further cleaning of the data, all the individual vehicle's data sets captured on each traffic corridor were manually joined together from the individual files in sequential order using the vehicle IDs. The time sequence data sets for the Out runs for each traffic corridor were grouped together and the Return runs for each traffic corridors were also grouped together, creating two separate database for the car following experiment for both the leading and the following vehicles for the AM and PM study. A final database was also created by combing all the time sequence data sets for the Out runs and Return runs together as one complete data set for each traffic corridor considered in this study. Separate combined data sets for the AM and PM for both the leading and following vehicles for each corridor were created. Note that, the AM and PM data sets were analysed separately for the leading vehicles and the following vehicles.

The data from the Video VBOX (i.e. the test vehicle acceleration and distance travelled) were matched up with the final radar sensor data sets using the base time of each data sets to complete the data preparation process. The complete data sets contains the captured vehicles data and the test vehicle data.

4.5 General Statistics

An overview of the general statistics of the data is discussed in this section. Section 4.5.1 discusses the vehicle type composition, Section 4.5.2 discusses the data statistics and Section 4.5.3 discusses the setting of the following distance threshold used for models formulations.

4.5.1 Vehicle Types Composition

As a result of data loss due to the radar sensors going quite few times during the experiment, not all the vehicles observed and captured by the video recordings and tracked by the radar sensors were successful for the data analysis. In all, a total of 1,387 individual vehicles either leading or following the test vehicle were observed and captured on all the four traffic corridors during the morning (AM) and afternoon (PM) study. Out of the total vehicles observed, 702 individual vehicles were captured in the AM and 685 individual vehicles captured in the PM. A total of 1,203 individual vehicles out of the 1,387 individual vehicles captured were successful for the analysis. Vehicles captured following or leading the test vehicle for a very short period or distance including when the sensor was quite were excluded from the analysis.

For the individual vehicles captured that were successful for the analysis, a total of 621 and 582 vehicles in a car following situation out of the total 1,203 vehicles were observed in the AM and PM respectively. For the AM study, 274 vehicles of the 621 captured individual vehicles were following the test vehicle and 347 vehicles were leading the test vehicle. Again, for the PM study, 251 vehicles of the 582 captured individual vehicles were following the test vehicle and 331 vehicles leading the test vehicle. A summary of the individual vehicles observed and analysed for each traffic corridor is shown in Table 4-2. The vehicles were categorised into different vehicle types such as cars, vans, trucks, buses and motorbikes, see Figure 4-1 and Figure 4-2.

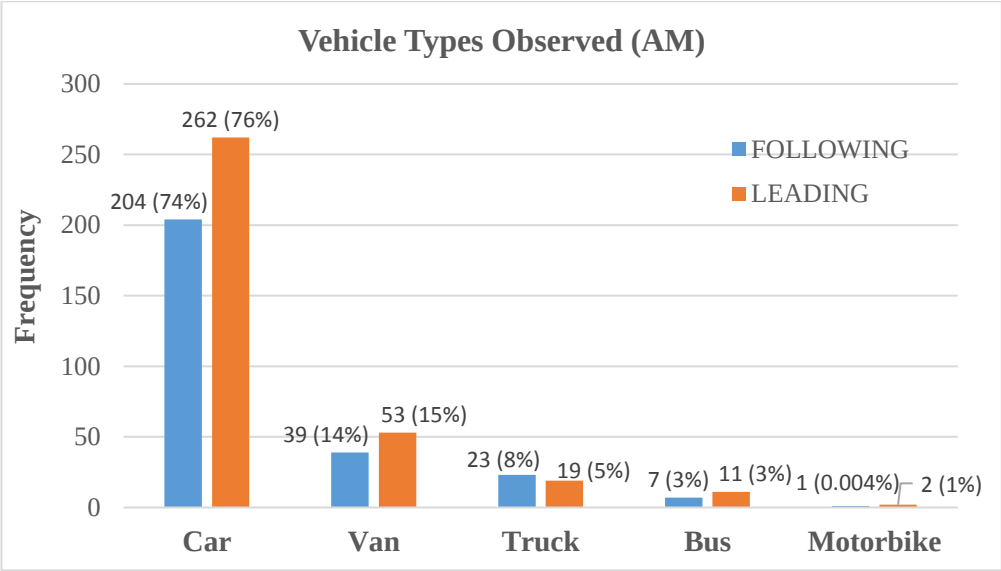

Figure 4-1: Types of vehicle classification for the AM

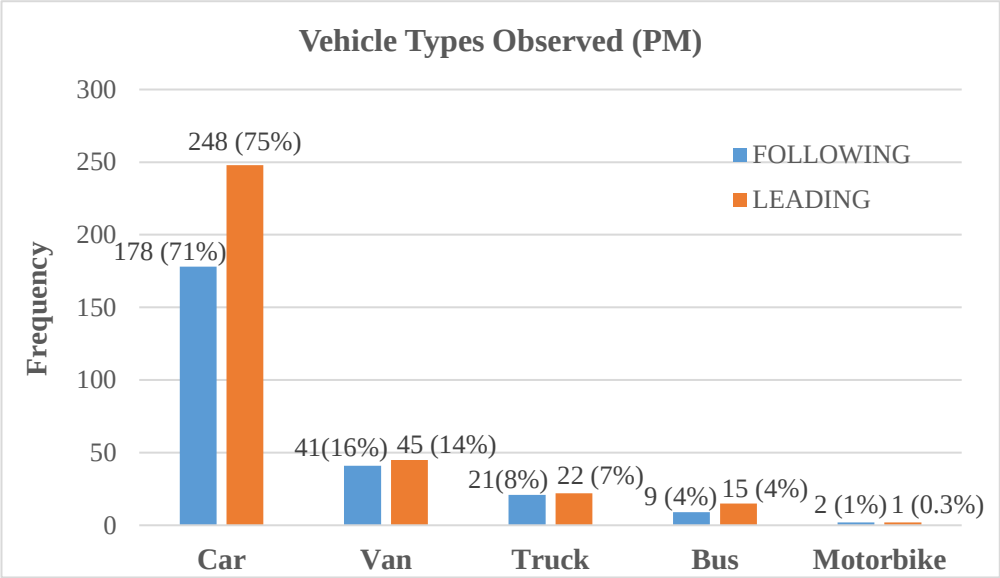

Figure 4-2: Types of vehicle classification for the PM

Table 4-2: Number of vehicles captured for each Traffic Corridor for both the AM and PM

Traffic Corridor	Run Number	No. of Days	Run	Length of Corridor (km)	No. of Lanes	Total Number of Vehicles Observed							
						AM				PM			
						Following		Leading		Following		Leading	
1	1	5	Out	9.7	2[a]	26	47	36	65	21	46	28	57
	2	5	Return	9.7		21		29		25		29	
2	3	4	Out	20.9	2	27	59	35	76	22	54	28	67
	4	4	Return	20.9		32		41		32		39	
3	5	5	Out	25.7	1 and 2[b]	61	125	57	123	51	112	60	129
	6	5	Return	25.7		64		66		61		69	
4	7	2	Out	32.2	2[a]	20	43	45	83	16	39	28	78
	8	2	Return	32.2		23		38		23		50	

[a] Part of the corridor is a dedicated bus lane within the city peripheral with few kilometres of the corridor designated as a single lane

[b] Corridor is a combined 1 and 2 lanes with the dedicated bus lane within the city part of the corridor with half of the corridor designated as a single lane

4.5.2 Data Statistics

As mentioned earlier, the Out run and Return run time sequence data sets for each traffic corridor was obtained. All the Out runs data sets and all the Return runs data sets for each traffic corridor were combined and then analysed separately. For this analysis, the bus following corridor data sets was excluded, which is discussed in Chapter 10. The data sets were analysed in two-fold. Firstly, the instrumented test vehicle as the leading vehicle and secondly, the test vehicle as the following vehicle for both the AM and PM study for all the four traffic corridors under investigation. The values of other car following parameters that were not directly obtained by the radar sensors, such as the time headway were computed. The time gap TG (s) is measured from the rear bumper of the lead vehicle to the front bumper of the following vehicle. It is defined as the ratio of the following distance Δx (m) to the following speed *v* (m/s) and expressed as;

$$TG = \frac{\Delta x}{v} \tag{4-1}$$

Again, knowing the length of the test vehicle (L_{TV} = 4.731 metres), the time headway (TH) or distance headway (DH) of the following vehicles were computed. The headways (TH or DH) were computed only when the test vehicle was the leading vehicle, this is because the length of the vehicles that were directly ahead of the test vehicle were not readily available. TH or DH is the time or distance between the leading and the following vehicles taken into consideration the full length of the leading vehicle. It is defined as the time or distance measured between the same common point of the leading and the following vehicles (i.e. the front bumpers) as the two vehicles passes or arrives at a designated test point on the roadway. The time headway (TH) expressed as the ratio of the distance headway ($L_{TV} + \Delta x$) (m) to the following vehicle's speed *v* (m):

$$TH = \frac{L_{TV} + \Delta x}{v} \tag{4-2}$$

The Time to Collision *TTC* (s) which is a function of the relative distance Δv (m) and relative speed Δv (m/s) was computed. The TTC is expressed as the ratio of the relative distance to the relative speed:

$$TTC = \frac{\Delta x}{\Delta v} \tag{4-3}$$

The mean and standard deviation were computed for each speed parameter. For the test vehicle leading: the overall average relative distance for Corridors 1, 2, 3 and 4 are 10.36 m, 14.99 m, 9.05 m and 15.31 m respectively. Corridor 3 recorded overall lowest following distance compared with the other Corridors. Corridor 4 recorded the lowest average time gap (TG) of 1.89 seconds with a standard deviation of 1.40 seconds than all the other Traffic Corridors. Corridor 2 recorded the highest observed overall average TG of 1.92 seconds and a standard deviation of 1.41 seconds. In all, the time gap for all the Corridors investigated ranges from an average of 1.89 seconds to 1.92 seconds, which is less than 2 seconds.

Similarly, Corridor 4 was found to have the lowest average time headway of 2.96 seconds and a standard deviation (st. dev.) of 2.04 seconds than all the other Traffic Corridors. The Corridor with the lowest TTC was found to be Corridor 3 with an average TTC of 26.94 seconds than the other Corridors considered in this study. For the TTC, it was observed that the TTC increases with decrease in the relative speed between two consecutives vehicles. This, at times produces a high TTC values even with a minimal increase or decrease in the relative distance between the two consecutive vehicles. It often result in a higher overall standard deviation of the mean TTC value. In effect, a smaller relative speed result in a higher TTC value. The distance headways for all the Corridors under investigation were found to be ranging from 13.65 m to 23.01 m for vehicles following the test vehicle (see Table 4-3 and Table 4-4).

For the test vehicle following: the overall average relative distance for Corridors 1, 2, 3 and 4 are 23.28 m, 25.08 m, 21.84 m and 29.75 m respectively. Corridor 4 had the lowest average time gap of 2.32 seconds (st. dev. of 1.85) than all the other Corridors investigated. The average time gap of the test vehicle ranges from 2.32 seconds to 2.38 seconds which is higher than 2 seconds but less than 2.5 seconds for all the Corridors. TTC of 63.47 seconds for Corridor 1 was found to be less amongst all the Corridors under investigation. The Corridor with highest TTC was found to be Corridor 2 with 67.45 seconds compared with the other Corridors (see Table 4-5 and Table 4-6). As observed, the larger the relative distance or smaller the relative speed result in higher value of the TTC of the following vehicle. This analysis could be further extended to include other vehicles in the vicinity of the test vehicle such as vehicles in the adjacent lanes. An overview of the general statistics results are presented in Table 4-3 and Table 4-4 for when test vehicle was leading, and Table 4-5 and Table 4-6 for when test vehicle was

following. Motorbikes were excluded in the tables as there were not enough motorbikes observed during the experiment for this study.

The average overall duration of vehicles following the test vehicle and vehicles leading the test vehicle for Corridor 1, Corridor 2, Corridor 3 and Corridor 4 for both the AM and PM are presented in Figure 4-3 and Figure 4-4. The overview of vehicles observed during the experiment from 31 July 2015 to 17 September 2015 are presented in Table 4-7 and Table 4-8.

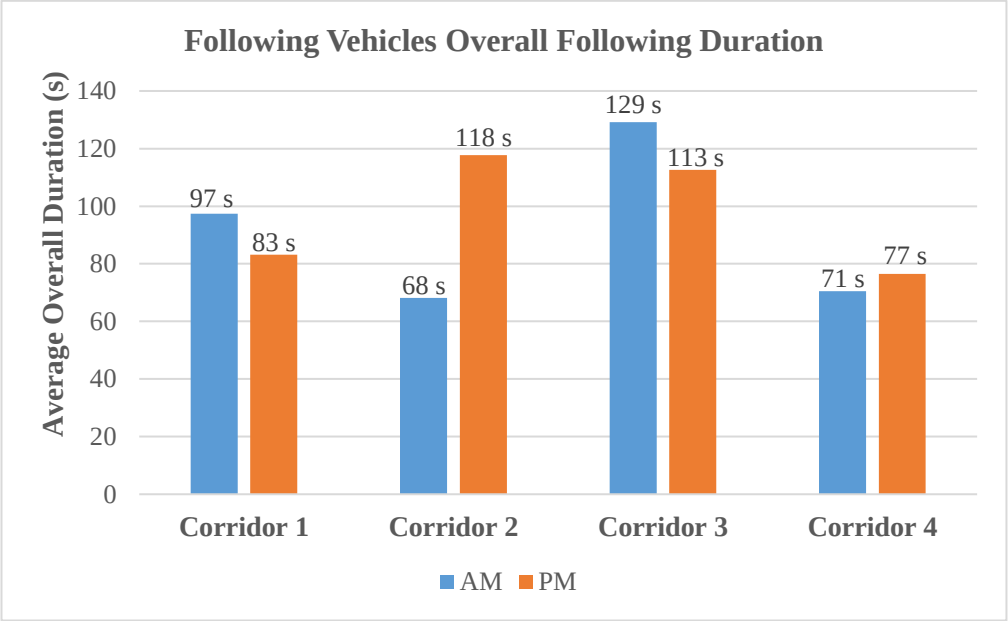

Figure 4-3: Average vehicle following overall duration when Test Vehicle was leading

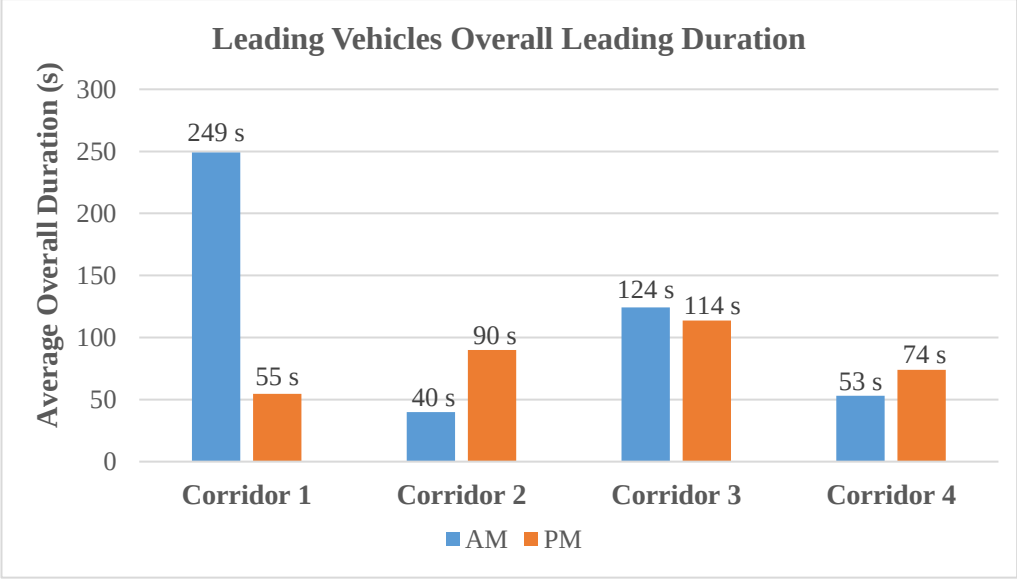

Figure 4-4: Average vehicle leading overall duration when Test Vehicle was following

4.5.3 Setting the Following Distance Threshold for Model Formulations

In this section, a description of the setting of the relative distance threshold for the data sets at which to include the following vehicles observed during the experiment for the development of car following models is given. As discussed in Chapter 3, the instrumented vehicle developed for data collection is capable of observing and tracking target vehicles as far as 200 metres for both upstream and downstream of the traffic. Therefore, it is important to set a threshold at which the following distance of the target vehicles will have more effect on the driving behaviour. As discussed in Chapter 2, Ossen and Hoogendoorn (2005) set a maximum mean gross safe distance headway threshold value for a following vehicle to be influenced by the lead vehicle at 70 metres. They adapted a formula to calculate the safe distance headway. This study adapt the same formula used by Ossen and Hoogendoorn (2005) to calculate the minimum safe distance headway, and based on that set the threshold value at which the following vehicles distance will be included in all car following models analysis for this study. The minimum safe distance headway (SDH) formulation adapted by Ossen and Hoogendoorn (2005) is expressed as:

$$\text{SDH} = \text{overall reaction time} * v(t) + l_{sf} \tag{4-2}$$

Where $v(t)$ is the speed of the following vehicle and l_{sf} represent the vehicle length plus the reserve safety distance at rest. The safe distance headway calculation is based on the assumption that all the vehicles have nearly the same braking distances. In setting the threshold value at 70 metres, Ossen and Hoogendoorn (2005) calculated the minimum safe headway distance value to be 30.5 metres to 55.5 metres for a vehicle travelling at 25 m/s with an assumed vehicle length of 4.5 metres and reserved safety distance of 1 metre and assumed reaction time of between 1 and 2 seconds. The approach used by Ossen and Hoogendoorn (2005) is used to determine the minimum distance threshold value for this study.

To set the threshold value, we take, for example, a vehicle travelling at 30 m/s and assumed reaction time of between 1.2 seconds and 2 seconds and lead vehicle length of 4.7 metres (actual length of test vehicle) with a reserve safety distance of 1 metre. The minimum SDH estimate is equal to 41.7 metres to 65.7 metres for those reaction times respectively. Now considering the minimum SDH calculation, the threshold of the following distance is set to 75 metres as the maximum for the analysis of this study. This

is to ensure that most of the vehicles captured during the experiment are included in the analysis for the models development. The following distance threshold set to 75 metres is applied to all the data sets used for the car following models development discussed in Chapter 7.

Table 4-3: Test vehicle leading: – overview of the general statistics for Corridors 1 and 2*

Traffic Corridor	Run	Time of Day	Average Relative Acceleration	Average Relative Distance	Average Relative Speed	Average Speed		Average Time Gap	Average Time To Collision (Δx/Δv)	Average Headway		Average Acceleration	
						Test Vehicle	Following Vehicle			Time	Distance	Test Vehicle	Following Vehicle
			m/s^2	m	m/s	m/s	m/s	s	s	s	m	m/s^2	m/s^2
1	Out	AM	-0.03 (0.84)	11.78 (11.81)	-0.12 (1.56)	7.58 (5.73)	7.70 (5.58)	1.83 (1.11)	21.63 (40.14)	2.88 (1.71)	16.51 (11.81)	-0.01 (0.76)	0.02 (1.04)
		PM	-0.05 (0.87)	9.75 (5.87)	-0.35 (1.51)	6.47 (4.60)	6.82 (4.63)	1.99 (1.70)	19.44 (29.26)	3.20 (2.45)	14.48 (5.87)	0.11 (0.83)	0.16 (1.10)
	Return	AM	-0.03 (0.74	8.92 (8.33)	-0.11 (1.19)	5.56 (3.56)	5.68 (3.44)	1.80 (1.34)	24.06 (31.51)	2.92 (1.77)	13.65 (8.33)	-0.04 (0.76)	-0.02 (0.98)
		PM	0.02 (0.83)	10.98 (12.38)	-0.20 (1.33)	5.84 (3.93)	6.04 (3.79)	1.96 (1.57)	23.46 (46.92)	3.11 (1.93)	15.71 (12.38)	0.12 (0.89)	0.10 (1.12)
2	Out	AM	-0.04 (0.63)	14.50 (15.26)	-0.11 (1.70)	12.04 (9.35)	12.16 (9.41)	1.86 (1.49)	28.09 (49.82)	2.90 (2.42)	19.24 (15.26)	0.02 (0.54)	0.07 (0.81)
		PM	-0.02 (0.54)	18.02 (21.40)	-0.04 (1.45)	11.26 (9.25)	11.30 (9.06)	2.00 (1.21)	40.63 (59.67)	2.77 (1.61)	22.75 (21.40)	-0.003 (0.64)	0.02 (0.10)
	Return	AM	0.01 (0.56)	14.85 (24.66)	0.21 (1.68)	8.21 (8.70)	8.00 (7.93)	2.58 (1.82)	33.80 (85.97)	3.99 (2.72)	19.58 (24.66)	0.02 (0.50)	0.01 (0.73)
		PM	-0.01 (0.54)	12.57 (8.11)	-0.40 (1.45)	10.77 (9.39)	11.16 (9.75)	1.99 (1.80)	32.85 (50.48)	3.02 (2.41)	17.30 (8.11)	0.02 (0.51)	0.03 (0.74)

*( ) = Standard Deviation values, m = metres, m/s = metre/second, s = seconds

Table 4-4: Test vehicle leading: – overview of the general statistics for Corridors 3 and 4*

Traffic Corridor	Run	Time of Day	Average Relative Acceleration	Average Relative Distance	Average Relative Speed	Average Speed		Average Time Gap	Average Time To Collision (Δx/Δv)	Average Headway		Average Acceleration	
						Test Vehicle	Following Vehicle			Time	Distance	Test Vehicle	Following. Vehicle
			m/s^2	m	m/s	m/s	m/s	s	s	s	m	m/s^2	m/s^2
3	Out	AM	0.01 (0.77)	8.42 (3.83)	-0.06 (10.4)	6.85 (3.58)	6.91 (3.52)	1.46 (0.95)	24.37 (37.11)	2.42 (1.54)	13.15 (3.83)	0.01 (0.69)	-0.01 (1.00)
		PM	0.06 (0.69)	8.82 (4.77)	-0.05 (1.10)	5.49 (3.62)	5.55 (3.43)	2.02 (1.02)	21.45 (29.49)	3.33 (2.02)	13.55 (4.77)	0.01 (0.71)	-0.05 (0.95)
	Return	AM	0.07 (0.76)	10.17 (6.08)	0.14 (1.36)	6.76 (3.52)	6.61 (3.22)	1.79 (1.16)	25.53 (40.75)	2.74 (1.59)	14.91 (6.08)	0.01 (0.68)	-0.06 (0.99)
		PM	0.03 (0.82)	8.79 (4.52)	-0.08 (1.40)	5.45 (3.29)	5.53 (3.14)	1.94 (1.04)	20.85 (35.52)	3.18 (1.75)	13.52 (4.52)	0.01 (0.70)	-0.02 (1.04)
4	Out	AM	-0.02 (0.71)	11.11 (12.85)	-0.12 (1.12)	6.22 (6.43)	6.34 (6.15)	2.14 (1.72)	29.56 (65.50)	3.45 (2.15)	15.84 (12.85)	0.01 (0.60)	0.03 (0.91)
		PM	-0.03 (0.83)	16.29 (16.35)	-0.12 (1.88)	13.69 (8.52)	13.81 (8.59)	1.26 (0.79)	32.78 (79.22)	1.86 (1.17)	21.02 (16.35)	0.03 (0.52)	0.05 (0.94)
	Return	AM	0.12 (0.74)	18.28 (11.31)	0.43 (1.92)	15.81 (9.90)	15.38 (9.62)	1.61 (1.30)	34.55 (66.36)	2.22 (1.81)	23.01 (11.31)	0.03 (0.66)	-0.09 (0.97)
		PM	-0.01 (0.69)	15.56 (14.94)	-0.15 (1.60)	12.81 (8.97)	12.96 (8.97)	1.54 (1.18)	34.01 (76.94)	2.29 (1.76)	20.30 (14.94)	0.001 (0.45)	0.01 (0.82)

*( ) = Standard Deviation values, m = metres, m/s = metre/second, s = seconds

Table 4-5: Test vehicle following: – overview of the general statistics for Corridors 1 and 2*

Traffic Corridor	Run	Time of Day	Average Relative Acceleration	Average Relative Distance	Average Relative Speed	Average Speed		Average Time Gap	Average Time-To-Collision (Δx/Δv)	Average Acceleration	
						Test Vehicle	Lead Vehicle			Test Vehicle	Lead Vehicle
			m/s^2	m	m/s	m/s	m/s	s	s	m/s^2	m/s^2
1	Out	AM	-0.04 (0.74)	22.03 (13.62)	0.17 (1.53)	11.74 (5.65)	11.91 (5.81)	2.29 (2.79)	51.57 (81.85)	0.04 (0.72)	-0.01 (0.97)
		PM	-0.06 (0.69)	25.00 (16.55)	-0.02 (1.67)	11.31 (5.62)	11.29 (5.60)	2.56 (2.25)	56.28 (98.61)	-0.05 (0.76)	-0.11 (0.99)
	Return	AM	-0.06 (0.70)	20.60 (13.04)	-0.01 (1.34)	10.19 (5.60)	10.18 (5.65)	2.39 (2.16)	54.25 (90.63)	0.02 (1.11)	-0.04 (1.29)
		PM	-0.06 (0.76)	25.5 (14.17)	0.15 (1.67)	12.40 (5.68)	12.55 (5.84)	2.35 (2.31)	59.29 (97.62)	-0.06 (0.75)	-0.12 (1.03)
2	Out	AM	-0.03 (0.60)	42.93 (30.11)	0.61 (2.21)	19.77 (8.49)	20.38 (8.80)	2.29 (1.57)	78.97 (155.55)	0.03 (0.55)	0.00 (0.80)
		PM	-0.02 (0.51)	32.33 (16.44)	-0.06 (1.36)	19.77 (7.55)	19.71 (7.59)	1.81 (1.00)	97.36 (135.10)	0.00 (0.60)	-0.02 (0.78)
	Return	AM	-0.01 (0.55)	36.03 (28.76)	-0.05 (1.39)	15.67 (10.76)	15.61 (10.57)	2.95 (2.06)	88.54 (162.07)	-0.01 (0.50)	-0.01 (0.74)
		PM	-0.01 (0.54)	29.04 (16.18)	0.02 (1.24)	16.46 (8.85)	16.48 (8.81)	2.29 (1.58)	83.78 (123.19)	0.01 (0.56)	0.00 (0.76)

*( ) = Standard Deviation values, m = metres, m/s = metre/second, s = seconds

Table 4-6: Test vehicle following: – overview of the general statistics for Corridors 3 and 4*

Traffic Corridor	Run	Time of Day	Average Relative Acceleration	Average Relative Distance	Average Relative Speed	Average Speed		Average Time Gap	Average Time-To-Collision (Δx/Δv)	Average Acceleration	
						Test Vehicle	Lead Vehicle			Test Vehicle	Lead Vehicle
			m/s^2	m	m/s	m/s	m/s	s	s	m/s^2	m/s^2
3	Out	AM	-0.05 (0.69)	21.00 (11.65)	0.04 (1.27)	11.35 (5.44)	11.39 (5.46)	2.04 (1.35)	60.50 (96.88)	-0.002 (0.70)	-0.05 (0.95)
		PM	-0.03 (0.74)	23.04 (13.65)	0.03 (1.39)	10.48 (6.21)	10.51 (6.20)	2.61 (1.96)	54.88 (91.12)	-0.02 (0.98)	0.01 (0.71)
	Return	AM	-0.04 (0.71)	21.52 (12.81)	-0.01 (1.27)	11.55 (5.76)	11.54 (5.87)	1.98 (1.00)	58.51 (92.02)	-0.002 (0.70)	-0.04 (0.96)
		PM	-0.04 (0.73)	21.81 (12.59)	-0.002 (1.31)	11.62 (5.89)	11.62 (5.92)	2.16 (1.53)	58.26 (93.14)	0.003 (0.71)	-0.03 (0.98)
4	Out	AM	-0.04 (0.66)	31.15 (21.54)	-0.08 (1.76)	12.95 (8.94)	12.86 (8.84)	2.98 (2.26)	70.16 (135.04)	0.001 (0.61)	-0.04 (0.88)
		PM	-0.04 (0.65)	26.09 (17.72)	0.11 (1.53)	15.40 (7.85)	15.15 (8.12)	1.79 (0.98)	62.86 (104.04)	0.003 (0.49)	-0.03 (0.80)
	Return	AM	-0.05 (0.59)	37.86 (18.35)	0.15 (1.86)	17.48 (7.16)	17.63 (7.54)	2.35 (1.33)	84.66 (147.77)	0.001 (0.61)	-0.05 (0.83)
		PM	-0.02 (0.64)	23.90 (12.26)	0.004 (1.32)	14.84 (8.11)	14.84 (8.03)	2.14 (2.11)	62.89 (91.42)	0.01 (0.47)	-0.01 (0.78)

*( ) = Standard Deviation values, m = metres, m/s = metre/second, s = seconds

Table 4-7: Summary of following vehicles observed (and analysed) during the AM and PM Study from 31 July 2015 – 17 September 2015 – Test vehicle leading*

Date	Total Vehicle Following	Time of Day (No. of Vehicle)		Average Following Duration (s)		Total number of Vehicle Type								Corridor	Weather Condition		Day of Week
						AM				PM							
		AM	PM	AM	PM	Car	Van	Truck	Bus	Car	Van	Truck	Bus		AM	PM	
31/07	53	25	28	151	100	16	4	3	2	20	4	1	3	C3	Dry	Dry	Fri
04/08	41	23	18	77	70	16	6	1	-	13	3	1	1	C3	Dry	Dry	Tue
05/08	39	22	17	107	119	16	3	2	1	13	3	-	1	C3	Dry	Wet	Wed
06/08	21	8	13	169	94	6	1	-	-	10	2	1	-	C1	Wet	Dry	Thu
07/08	19	10	9	116	127	4	-	1	1	7	1	1	-	C1	Dry	Dry	Fri
19/08	47	27	20	136	169	23	2	2	-	13	5	1	1	C3	Dry	Dry	Wed
24/08	16	8	8	249	121	5	1	-	-	8	-	-	-	C1	Dry	Dry	Mon
25/08	20	12	8	188	121	8	2	1	1	7	1	-	-	C1	Dry	Dry	Tue
28/08	31	15	16	99	149	8	3	4	-	13	1	2	-	C2	Dry	Dry	Fri
04/09	36	17	19	64	130	14	2	1	-	9	5	3	1	C2	Dry	Dry	Fri
07/09	20	10	10	40	41	6	1	3	-	8	1	1	-	C2	Dry	Dry	Mon
08/09	40	16	24	53	74	13	1	1	-	13	5	5	-	C4	Dry	Dry	Tue
09/08	42	27	15	71	117	25	-	2	-	8	6	1	-	C4	Dry	Dry	Wed
10/09	26	17	9	214	90	13	3	1	-	6	2	1	-	C2	Dry	Dry	Thu
16/09	57	28	29	150	111	16	9	1	2	22	2	3	2	C3	Dry	Dry	Wed
17/09	17	9	8	125	109	8	-	-	8	-	-	-	-	C1	Dry	Dry	Thu

*Excludes a total of three (3) Motorbikes data

Table 4-8: Summary of leading vehicles observed (and analysed) during the AM and PM Study from 31 July 2015 – 17 September 2015 – Test vehicle following*

Date	Total Vehicle Leading	Time of Day (No. of Vehicle)		Average Leading Duration (s)		Total number of Vehicle Type								Corridor	Weather Condition		Day of Week
						AM				PM							
		AM	PM	AM	PM	Car	Van	Truck	Bus	Car	Van	Truck	Bus		AM	PM	
31/07	52	28	24	131	155	22	4	1	1	18	3	1	2	C3	Dry	Dry	Fri
04/08	49	24	25	127	134	20	3	-	1	14	5	2	4	C3	Dry	Dry	Tue
05/08	57	23	34	133	19	3	1	-	-	22	6	3	2	C3	Dry	Wet	Wed
06/08	20	11	9	87	142	8	3	-	-	8	1	-	-	C1	Wet	Dry	Thu
07/08	23	14	9	69	109	10	2	-	2	8	1	-	-	C1	Dry	Dry	Fri
19/08	50	23	27	129	107	14	4	1	3	16	7	4	-	C3	Dry	Dry	Wed
24/08	23	10	13	146	77	9	1	-	-	12	1	-	-	C1	Dry	Dry	Mon
25/08	27	16	11	96	92	9	3	1	3	10	-	1	-	C1	Dry	Dry	Tue
28/08	40	20	20	87	111	14	3	3	-	17	3	-	-	C2	Dry	Dry	Fri
04/09	40	21	19	67	161	12	4	5	-	11	6	1	1	C2	Dry	Dry	Fri
07/09	37	21	16	76	109	17	3	1	-	14	1	1	-	C2	Dry	Dry	Mon
08/09	76	36	40	71	76	30	3	3	-	33	3	3	1	C4	Dry	Dry	Tue
09/08	85	47	38	70	77	41	5	-	1	31	4	2	1	C4	Dry	Dry	Wed
10/09	26	14	12	111	90	9	4	1	-	7	2	3	-	C2	Dry	Dry	Thu
16/09	44	25	19	126	148	17	6	1	-	16	2	1	-	C3	Dry	Dry	Wed
17/09	29	14	15	89	79	11	2	1	-	11	1	1	2	C1	Dry	Dry	Thu

*Excludes a total of three (3) Motorbikes data

4.6 Summary

In this chapter, the structure of the data obtained for the analysis of this study including the storage format of the data were discussed. The processes involved in the extraction of individual vehicle's data from the video recordings and the corresponding radar sensors data were discussed. An extensive preliminary data cleaning and filtering of non-essential data from the raw data sets were carried out. In order to make the data cleaning less complicated, although time consuming, a four stage approach in cleaning the data sets was adapted using a series of computer program and visual basic macro program developed for the processing of the data sets. At each stage of the processes, a manual inspection was carried out to ensure that the appropriate data is processed and the expected output results were obtained. Further and more intensive data preparation by extracting the final individual vehicle's data set as captured by the radar sensors and seen in the video data were carried out.

An overview of the general statistics of the data sets was presented in this chapter. The data sets was grouped into different vehicle types and the vehicle composition determined. Cars were found to be more than other vehicle types for both situations where the test vehicle was either leading or following other vehicles. The speed information of all the observed vehicles that were not directly captured or recorded by the radar sensors were calculated. The general overview of the data statistics were presented in Table 4-2 to Table 4-8. Further analysis of the corridor types investigated found Corridor 3 with the lowest vehicle following distance and speed among all the four corridors. The overall time gap for all the corridors was found to range from 1.89 seconds to 1.92 seconds, less than the UK or EU guidelines for minimum following time gap of 2 seconds for following vehicles. In the case of the test vehicle following other vehicle types, the average time gap ranges from 2.32 seconds to 2.38 seconds which is higher than 2 seconds but less than 2.5 seconds for all the Corridors. Corridor 3 was observed to have the lowest combined TTC of 26.94 seconds and Corridor 1 with the combined highest TTC of 29.49 seconds for all vehicle types following the test vehicle. It was observed that the TTC value increases significantly with a small decrease in the relative distance between any two consecutive vehicles.

The data sets used in this study was obtained using an instrumented vehicle capable of tracking vehicles as far as 200 metres away from the test vehicle to the target vehicles. Therefore, setting the safe distance threshold at 75 metres maximum at which to include

the target vehicles in the data sets for the models development was very important. The process of calculating the safe distance threshold was discussed in this chapter. In the next chapter, the general analysis of the data sets obtained for this study is discussed. Factors that influence driver behaviour are also discussed in the next chapter.

CHAPTER 5 GENERAL ANALYSIS OF DATA

5.1 Introduction

Chapter 4 discussed the cleaning and preparation of the data sets obtained for this study. Better understanding of driver behaviour under different traffic conditions in car following scenario enables better and reliable driver behaviour models to be developed. For this study, an instrumented vehicle equipped with advanced measuring devices was used as a floating test vehicle within different traffic streams under different traffic conditions to collect microscopic driving behaviour data. The data collected was analysed to provide better understanding of driver behaviour. Both the front leading vehicles and the rear following vehicles to the instrumented test vehicle were observed during the experiment. The data obtained was processed and analysed. The vehicles following the test vehicle data sets and the vehicles leading the test vehicle data sets were separately analysed. This is because the leading and the following vehicles data sets were obtained independently during the experiment, even though, both data sets were obtained with the same time stamp and as three consecutive vehicles movements with different speed profiles.

In this chapter, the overall analysis of the data set is discussed in two main sections. The first section discusses the general overview analysis of car following behaviour observed during the experiment. The second section discusses the driving behaviour of following vehicles captured under different car following scenarios. All the models used in this study are developed based on the data obtained when the instrumented vehicle was leading the following vehicles, except Chapter 10 where the following vehicle was the instrumented vehicle.

5.2 The General Overview Analysis

In this section, a brief overview analysis of vehicle following process between two successive vehicles and three consecutive vehicles, which form the basis of this study are discussed. The following speed – distance gap relationship of vehicles observed during the experiment are also discussed. Car following is often describe as the interactions between two successive vehicles moving in the same direction of travel in a single lane of traffic. The interactions between vehicles in the car following process result in the

following driver's attempt to maintain a desired distance following headway or time gap behind the leading vehicle directly ahead of the following vehicle through the adjustment of the following vehicle's acceleration. As the process of following interactions continue, over time, the change in the speed of the following vehicle at some stage becomes greater than the speed of the lead vehicle as the following driver tries to close the distance gap in an attempt to maintain the desired following distance or time gap.

The continued increases in the speed of the following vehicle will narrow the distance gap and bring the following vehicle closer and closer to the lead vehicle until the driver's perceived desired distance gap is reached, the driver then begins to decelerate again thereby drifting backwards. The process repeats again throughout the following process until vehicle following termination occurs. The continuous speed and acceleration adjustments of the following vehicle during the following process, over time, result in the coil or hysteresis (Kim, 2005) or spiral (Brackstone et al., 2009) found in typical vehicle following behaviour as shown in Figure 5-1, Figure 5-2 and Figure 5-3. The relative distance verses the relative speed plot result in the Δx-Δv plane (i.e. the ratio of the relative distance to the relative speed, $\Delta x/\Delta v$), which expresses the time to collision of the following vehicle to the lead vehicle. The typical coil like shape following interactions between two vehicles have implications for drivers safety and network capacity as a whole, particularly, where traffic demands are high (Brackstone et al., 2009).

The typical following behaviour observed varies depending on the type of vehicle following the leading test vehicle. For instance, Figure 5-1 shows a typical following interaction between a van and the test vehicle. The van (i.e. vehicle with ID124) was observed following the test vehicle in the morning of 04 August 2015 on Corridor 3. The duration of the following process was 300 seconds. Figure 5-2 shows a truck following the test vehicle with a following duration of 80 seconds. The truck (i.e. vehicle with ID103) was observed in the morning of 31 July 2015 on Corridor 3. Figure 5-3 shows a typical following interaction between two cars with a following duration of 134 seconds. The car (i.e. vehicle with ID26) was observed following the test vehicle in the morning of 25 August 2015 on Corridor 1. It can be seen in Figure 5-1, Figure 5-2 and Figure 5-3 that the following behaviour in the Δx-Δv relationship vary among all the three following vehicle types observed during the experiment. The van following distance vary from approximately (~) 3 metres to ~13 metres, that of the car following distance vary from ~3 metres to ~10 metres and the truck following distance vary from about 5 metres to ~15 metres. All the following vehicles relative speed varying from ~ -3 m/s to ~4 m/s. The

result show that the following behaviour differs from the vehicle type following and varies among different drivers.

Figure 5-4 shows the lateral displacement and lateral speed of all the following vehicles observed during the experiment. The analysis found that the lateral speed of the following vehicles varies from ~ -16 m/s to ~10 m/s and the lateral displacement varies from ~ -15 metres to ~21 metres. Three consecutive vehicles movements of car following data were collected during the experiment. A typical three consecutive vehicles movement was selected from the data sets and analysed. Figure 5-5, Figure 5-6 and Figure 5-7 shows the speed profile, the following relative distance and the time gap charts respectively for the typical three consecutive vehicles movement observed during the experiment involving vehicles with ID6, ID8 and the test vehicle. Vehicle with ID6 observed following the test vehicle (i.e. first leader) and the test vehicle following vehicle with ID8 leading (i.e. second Leader) in a three consecutive vehicles movement in a time of 120 seconds. The triple vehicles movement was observed in the morning of 06 August 2015 on Corridor 1.

It can be seen from Figure 5-5, Figure 5-6 and Figure 5-7 that there are variation between the speeds of all the three vehicles involved in the three consecutive vehicles movement. The average speed of the following vehicle, the first leader (test vehicle) and the second leader were 30 km/h, 31 km/h and 32 km/h respectively (see Figure 5-5). It was observed that the following vehicle followed closer to the test vehicle (i.e. first leader) than the test vehicle following the second leading vehicle at all speed ranges. The following vehicle (ID6) recorded average following distance of 7.34 metres and that of the test vehicle recorded 15.68 metres (see Figure 5-6). Similarly, the time gap between the following vehicle (ID6) and the test vehicle was, on average, less than the time gap for the test vehicle to the second leading vehicle (ID8). The average time gap of following vehicle (ID6) was 0.96 seconds (i.e. ~1 seconds) and the time gap of test vehicle was 2 seconds (see Figure 5-7).

Figure 5-8 shows the speed profile of two cars following process. Car with ID26 observed following the test vehicle on 25 August 2015 in the morning on Corridor 1 with a following duration of 134 seconds. The following car (ID26) followed the test vehicle with average separation distance of 6.64 metres and average following speed of 16.56 km/h and test vehicle (i.e. leading) recorded average speed of 16.47 km/h. The time gap, distance headway and time headway of the following car (ID26) was found to be 1.7 seconds, 11.37 metres and 2.9 seconds respectively. The time gap and distribution of the

time gap of all the following vehicles observed during the experiment and analysed are shown in Figure 5-9 and Figure 5-10 respectively. It can be seen in Figure 5-9 and Figure 5-10 that, in general, the time gaps decreases with increase in the following vehicles speed.

The time gap vary across all speed ranges. As observed, lower speed result in larger time gap for all the following vehicles analysed. The average overall time gap for all the following vehicles analysed (i.e. 489 vehicles observed) in this study is 1.86 seconds (i.e. ~1.9 seconds). Figure 5-11 and Figure 5-12 shows the time gap and distribution of time gap of the test vehicle following all leading vehicles observed and analysed for this study. In general, the time gap decreases with increase in the speed of the test vehicle. Again, lower speed of the test vehicle resulted in a larger time gap and higher speed resulted in lower time gap of the test vehicle. The average overall time gap of the test vehicle is 2.29 seconds (i.e. ~2.3 seconds).

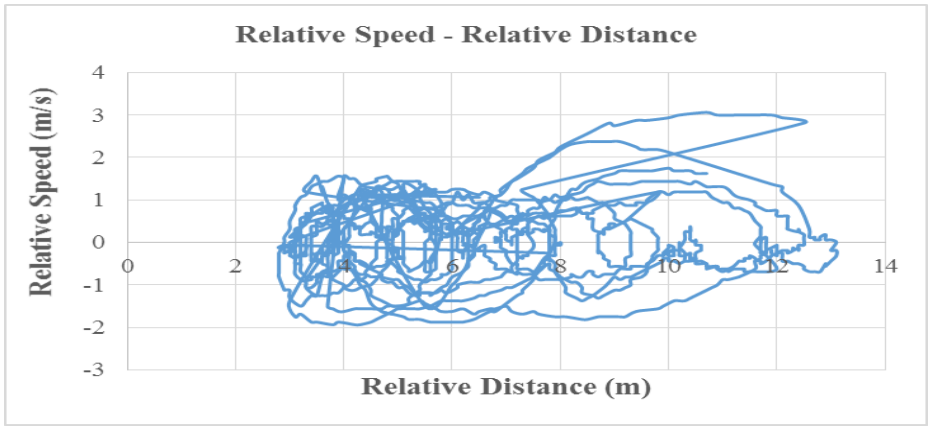

Figure 5-1: Relative speed and relative distance for Van following test vehicle

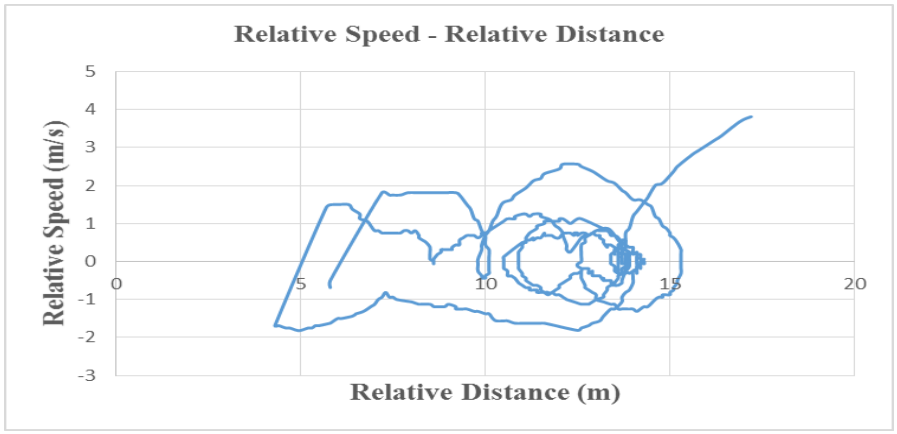

Figure 5-2: Relative speed and relative distance for Truck following test vehicle

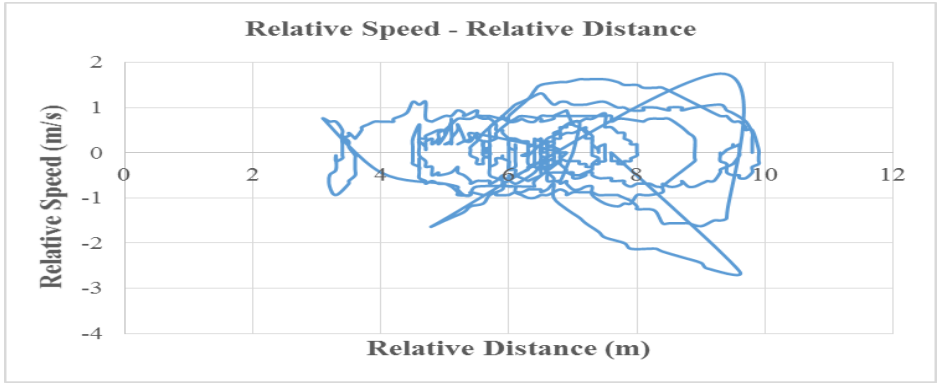

Figure 5-3: Relative speed and relative distance for Car following test vehicle

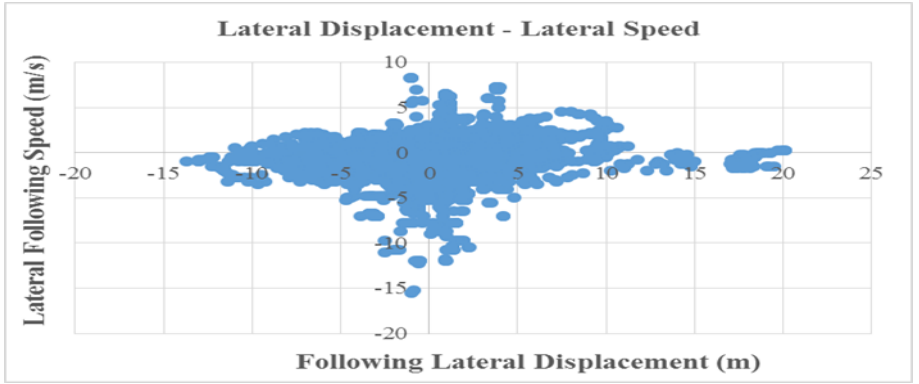

Figure 5-4: Lateral speed and lateral displacement of all following vehicles

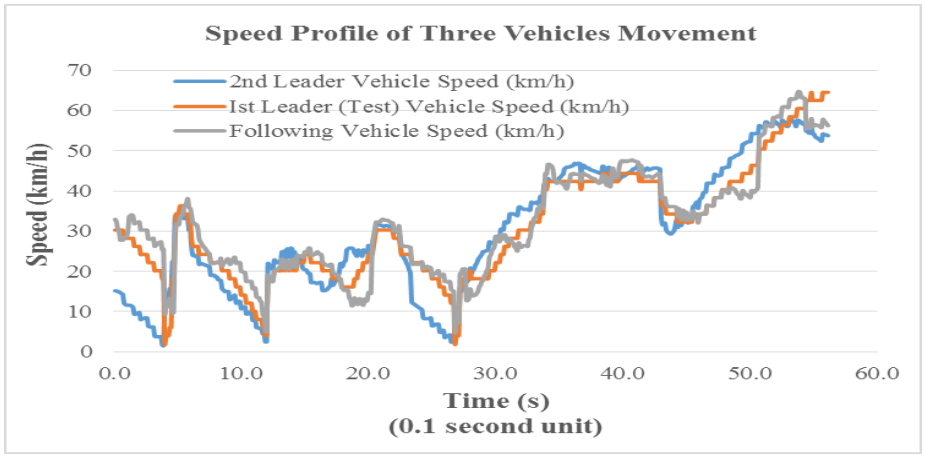

Figure 5-5: Speed profile of three consecutive cars following behaviour

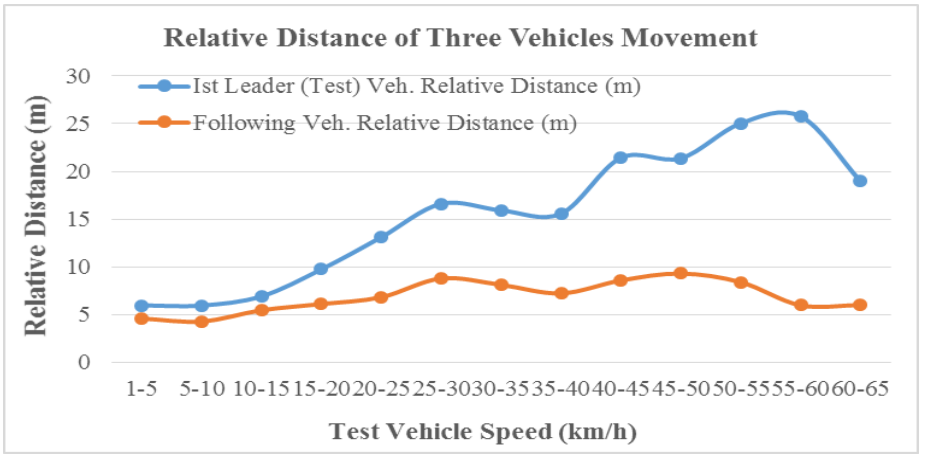

Figure 5-6: Rel. distance of three consecutive cars following behaviour

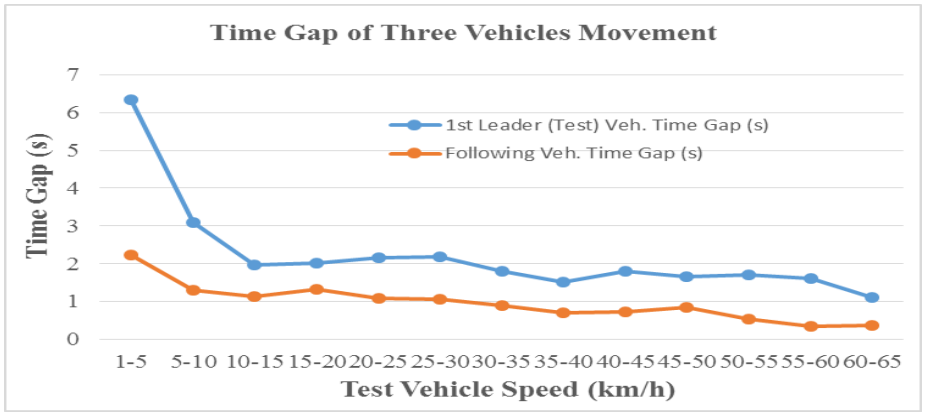

Figure 5-7: Time gap of three consecutive cars following behaviour

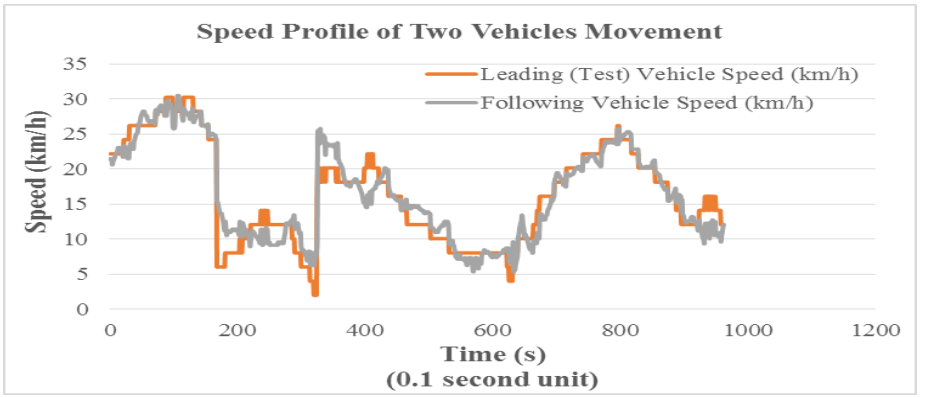

Figure 5-8: Speed profile of two cars following behaviour

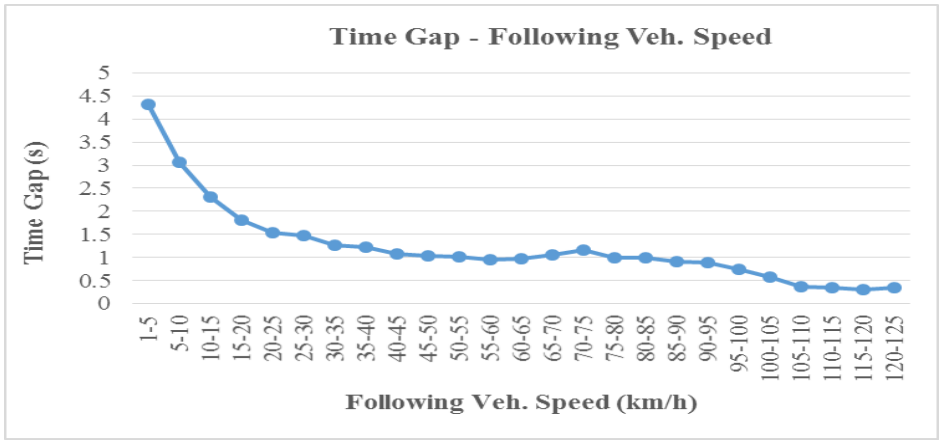

Figure 5-9: Time gap and speed of all following vehicles

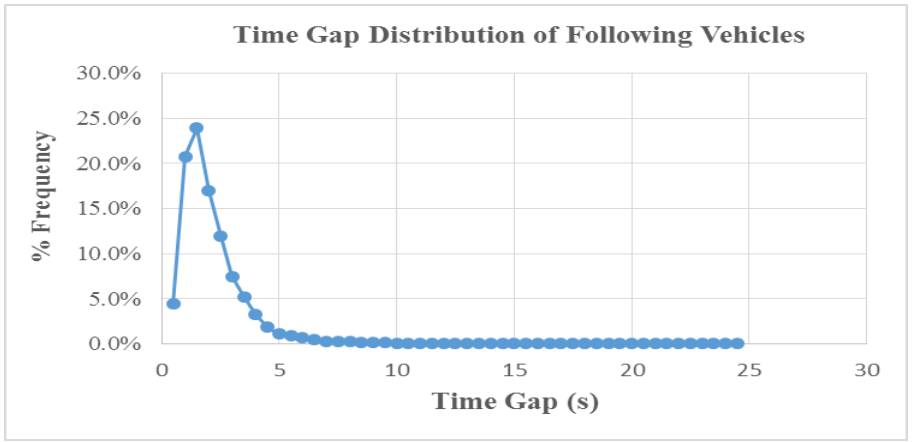

Figure 5-10: Time gap distribution of all following vehicles

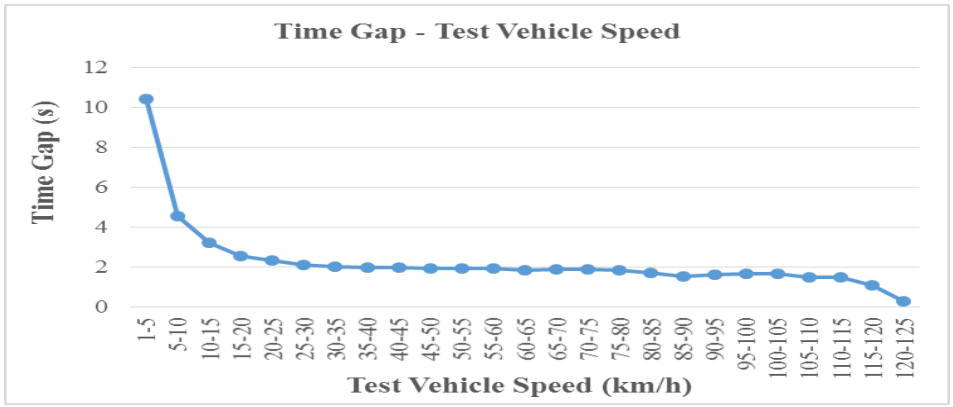

Figure 5-11: Time gap and speed of test vehicle following all leading vehicles

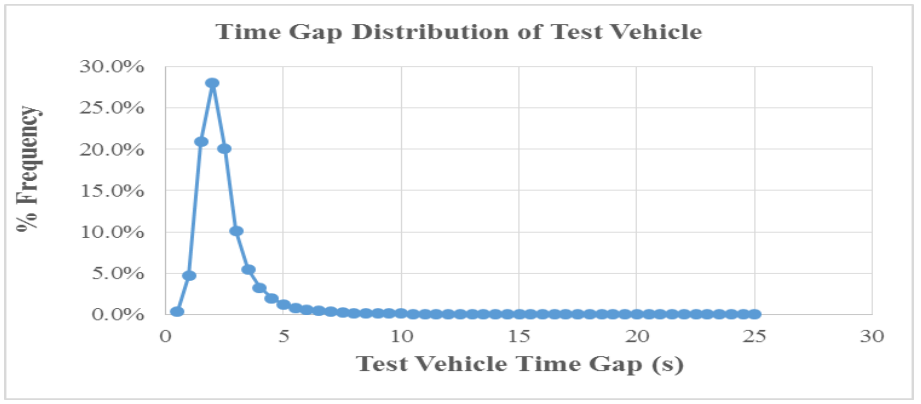

Figure 5-12: Time gap distribution of test vehicle following all leading vehicles

5.3 Car Following Analysis

In this section, the vehicles observed following the test vehicle were analysed. Factors that could affects the driving behaviour of the following vehicles were analysed in this section. These factors include human and vehicle characteristics (such as the gender, vehicle occupancy and vehicle type characteristics), environmental and other characteristics (such as the weather condition, time of day and day of the week characteristics) and traffic and road characteristics (such as the number of driving lanes, traffic flow, bus lane availability on the corridor, characteristics of corridor and data collection run).

5.3.1 Gender Characteristics

Male and female drivers car following behaviour are analysed. Not many female drivers were observed following the test vehicle during the experiment. In all, a total of 76 female and 324 male drivers' data were extracted and analysed. Figure 5-13 and Figure 5-14 shows the relative distance comparisons for both male and female drivers. It can be seen from Figure 5-13 and Figure 5-14 that, in general, the relative distance increases as the speed increase for both male and female drivers. At lower speed range, female drivers tend to follow closer to the lead vehicle than the male drivers. At higher speed range, male drivers tend to follow closer to lead vehicle than female counterpart does. At speed below 20 km/h, similar following distances for male and female drivers were observed.

Figure 5-15 shows the time gap comparisons between male and female drivers. The time gaps of male and female drivers decreases as the speed increase. Higher time gaps were observed at speed below 30 km/h for both male and female drivers. Again, male drivers seem to have larger time gap than female drivers for most of the speed ranges. As observed, lower speed encourages longer following distance resulting in larger time gap and for the case of male drivers, it gives them more variability in driving than the female counterparts. The result suggests that female drivers are more cautious and in control of vehicle when driving, partly, because of the steady following distance and time gap following other vehicles.

5.3.2 Vehicle Occupancy Characteristics

The effect of vehicle occupancy on the following distance in a car following scenario was analysed. A total of 289 following vehicles with occupancy of one (i.e. driver as a sole occupant) and 114 following vehicles with occupancy of two or more (i.e. occupancy of 2+ including the driver) were extracted from the data sets and analysed. Figure 5-16 shows the relative distance comparisons for occupancy of one (1) and occupancy of 2+ vehicles. At speed below 60 km/h, the relative distance steadily increases as the speed increase for both vehicle occupancy groups. At speed above 60 km/h, there was variation in the relative distance for the two occupancy groups as the following vehicle speed increases. Occupancy of 2+ vehicles have lower following distances across the higher speed ranges than the driver only occupancy vehicles. Figure 5-17 shows the time gaps of the vehicle occupancy groups. The time gaps, in general, decreases with increase in the following speed. Large time gaps were observed at lower speed ranges for both vehicle occupancy groups. The driver only vehicle occupancy group was found, in general, with shorter relative distance than the two or more vehicle occupancy group in car following situation.

5.3.3 Vehicle Type Characteristics

This section analyses the vehicle type effect on following distance in car following situation. There were 13 buses, 283 cars, 34 trucks and 65 vans data extracted from the data sets and analysed for vehicles observed following the test vehicle. Because there were bus lane restrictions enforced within the inner city of the study area at the time of the experiment, not many buses were observed following the test vehicle. This is because the buses use the bus lanes for most of the bus journeys within the city. Figure 5-18 shows the relative distance comparisons for different vehicle types. Figure 5-19 shows the relative distance with the test vehicle speed for all the vehicle types observed. The relative distance, in general, increases with increase in the speed of both the following vehicles and the test vehicle as shown in Figure 5-18 and Figure 5-19 respectively. Trucks were observed to follow with longer relative distance across most of the higher speed ranges. In general, the average relative distance of vans was shorter than all the other vehicle types considered in this study.

The average relative distance of cars, vans, trucks and buses was calculated to be 8.71 metres, 6.50 metres, 9.6 metres and 7.18 metres respectively. Figure 5-20 shows the time gaps of all the vehicle types considered. It can be seen that the time gap of all the vehicle types decreases with increase in the following vehicle speed. At speed below 15 km/h, large time gap greater than 2 seconds for all the following vehicle types was observed. At speed below 40 km/h, buses were found to follow with larger time gaps. A situation that might be attributed to the slow movement of the buses travelling within the inner city due to the possibility of stopping for passengers to embark and disembark. The average time gaps of cars, vans, trucks and buses were found to be 1.8 seconds, 1.6 seconds, 2.3 seconds and 2.4 seconds respectively. Apart from the buses following with larger time gaps at lower speed, trucks were, in general, following with large time gaps than cars and vans. In all, vans were found to follow with shorter time gaps than all the vehicle types observed following the test vehicle.

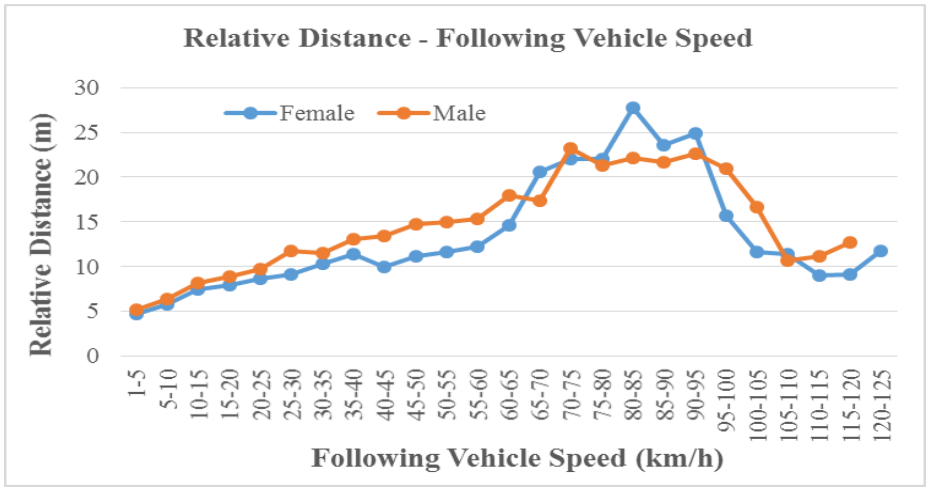

Figure 5-13: Relative distance and speed for Gender characteristics

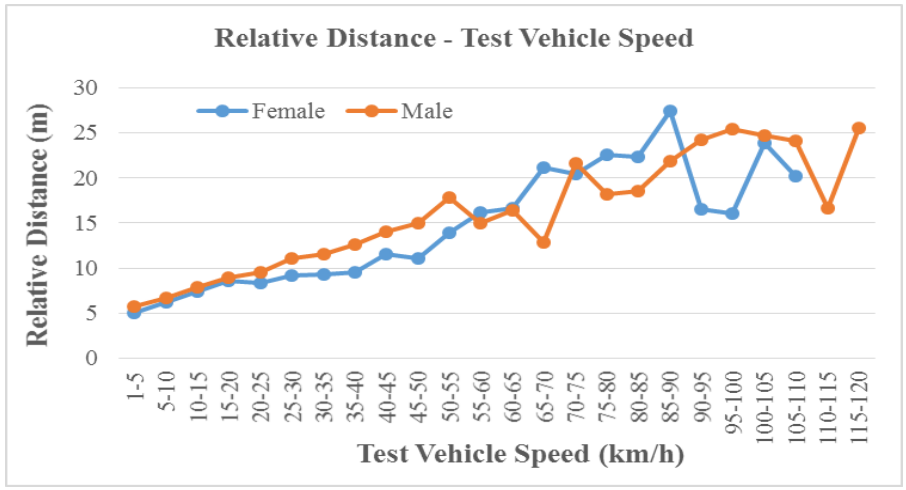

Figure 5-14: Relative distance and test vehicle speed for Gender (following vehicle)

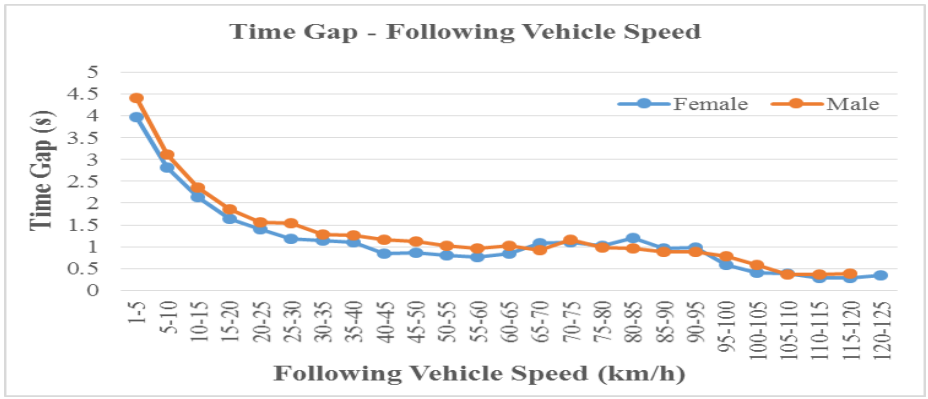

Figure 5-15: Time gap and speed for Gender characteristics

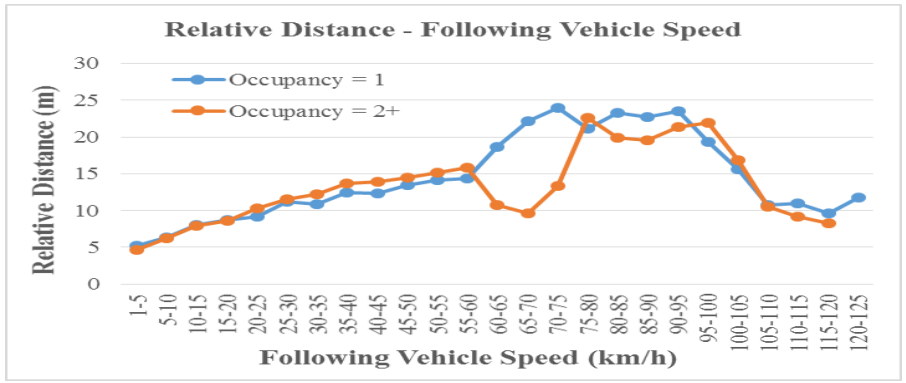

Figure 5-16: Relative distance and speed for Vehicle Occupancy characteristics

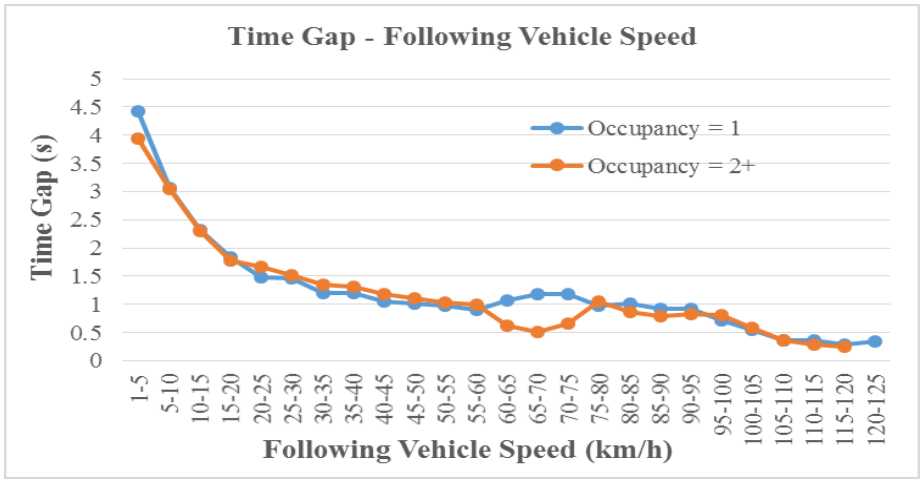

Figure 5-17: Time gap and speed for Occupancy characteristics

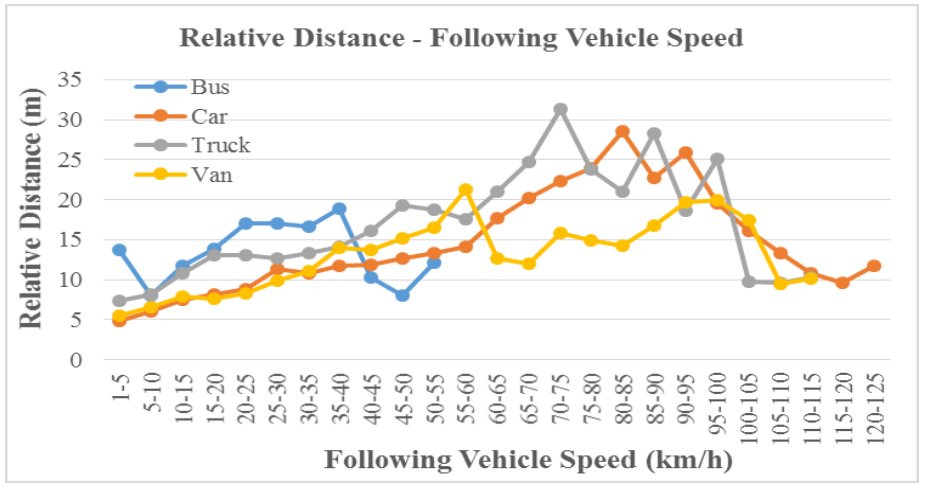

Figure 5-18: Relative distance and speed for Vehicle type characteristics

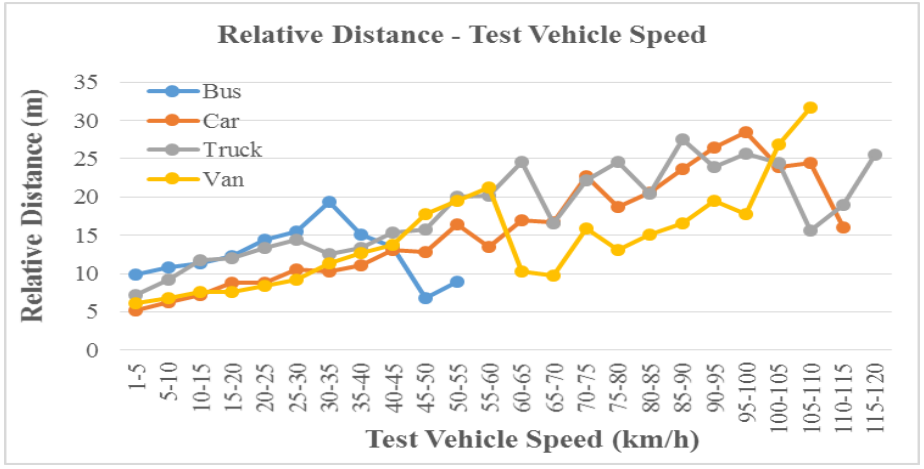

Figure 5-19: Rel. distance and test vehicle speed for all Vehicle type

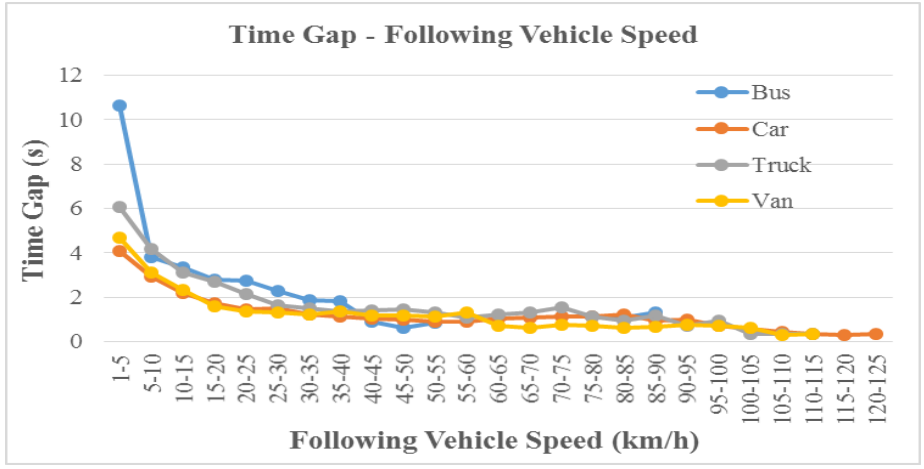

Figure 5-20: Time and speed for Vehicle type characteristics

5.3.4 Weather Condition

The weather condition effect on the following distance of vehicles in car following situation was analysed. The experiment was conducted mostly in the UK summer months through to October 2015 and not much rainfall was observed. When there was rain during the time of the experiment, the rainfall was not heavy and for a short duration. In all, there were 32 vehicles observed during the wet periods and 366 vehicles observed during the dry periods. Figure 5-21 shows the relative distance differences for both weather conditions. The relative distance increases with increase in the speed of the following vehicles in both the wet and dry conditions. The analysis found that vehicles followed with shorter relative distances in the dry conditions than in the wet conditions. Figure 5-22 shows the differences in time gap for dry and wet conditions. Large time gap was observed at low speed ranges for the wet and the dry conditions. The time gaps for the wet and dry conditions decreases with increase in the following vehicle speed.

5.3.5 Time of Day Characteristics

The time of day driving effect on the following distance of vehicles in car following scenario was analysed. A total of 206 and 198 vehicles data were extracted from the data sets for vehicles observed in the morning peak and afternoon off-peak hours respectively. It can be seen in Figure 5-23 that the following distance vary across all the speed ranges for both the AM peak and the PM off-peak periods. At speed above 60 km/h, there was wide variation in the following distance that can be observed between the morning peak and the afternoon off-peak periods as the speed increase. Vehicles travelling in the morning peak periods tend to follow closer to the lead vehicles than the afternoon off-peak periods. Increase in traffic volume during the peak hours encourages shorter following distance between vehicles, which maximises the use of the available road space. The average following distance of vehicles for the morning peak and afternoon off-peak periods are 10.25 metres and 11.26 metres respectively. Similar following time gaps were observed for both the morning peak and the afternoon off-peak periods as shown in Figure 5-24. The average time gap for both the morning peak periods and the afternoon off-peak periods was found to be 1.86 seconds (~1.9 seconds).

5.3.6 Day of the Week Characteristics

The data sets used for this analysis was collected during the weekdays, which include Mondays, Tuesdays, Wednesdays, Thursdays and Fridays. The effect of the day of the week on the following distance of vehicles in car following scenario was analysed. This is because, there might be differences in the driving behaviour for each day of the week due to possible changes in the traffic flow on daily basis. The data set was categorised into the day of the week in which the experiment was conducted. In all, there were 31 vehicles for Monday, 102 vehicles for Tuesday, 81 vehicles for Wednesday, 60 vehicles for Thursday and 124 vehicles for Friday extracted from the data sets and considered for this analysis. As shown in Figure 5-25, the following distances increases, in general, with increase in the following vehicle speed. From Figure 5-26, it can be seen that the time gaps decreases with increase in the following speed. At speed below 55 km/h, similar following distance behaviour was observed for all the days of the week. At speed above 55 km/h, it can be seen that there was significant variation in the following distances among all the days of the week considered for this study.

Above the speed of 65 km/h to 95 km/h, Tuesday, on average, tend to have the longest following distance than the other days of the week. In general, Wednesday and Thursday tend to have shorter following distances than the other days of the week. Monday also have shorter following distance than Tuesday and Friday. The average following distance for Monday, Tuesday, Wednesday, Thursday and Friday were 10.26 metres, 11.11 metres, 9.82 metres, 9.54 metres and 11.82 metres respectively. The average time gap for Tuesday, Wednesday and Friday were less than 2 seconds and that of Monday and Thursday were between 2 seconds and 2.2 seconds.

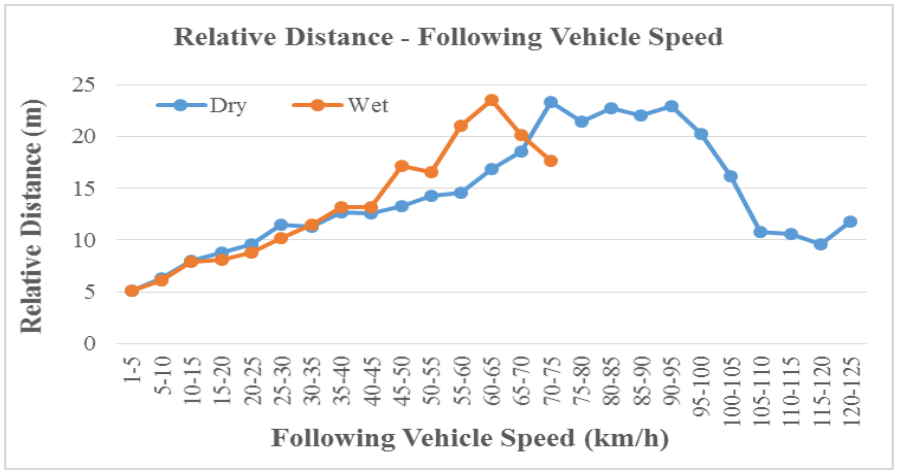

Figure 5-21: Relative distance and speed for Weather characteristics

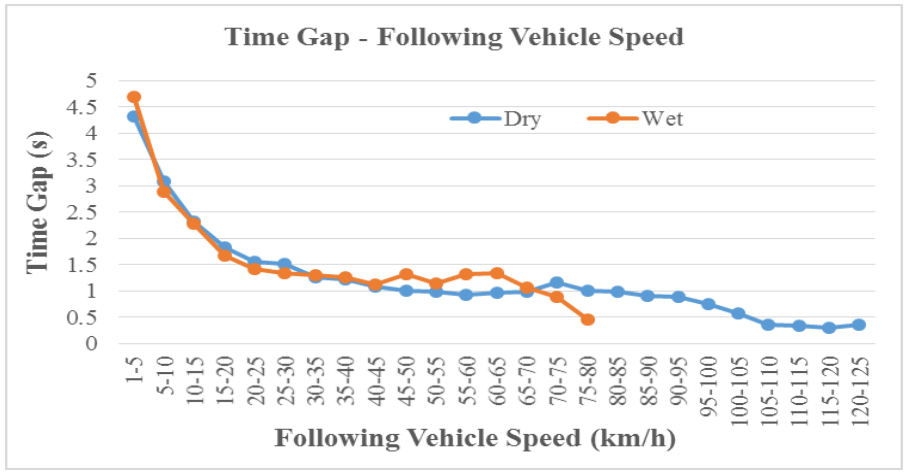

Figure 5-22: Time gap and speed for Weather characteristics

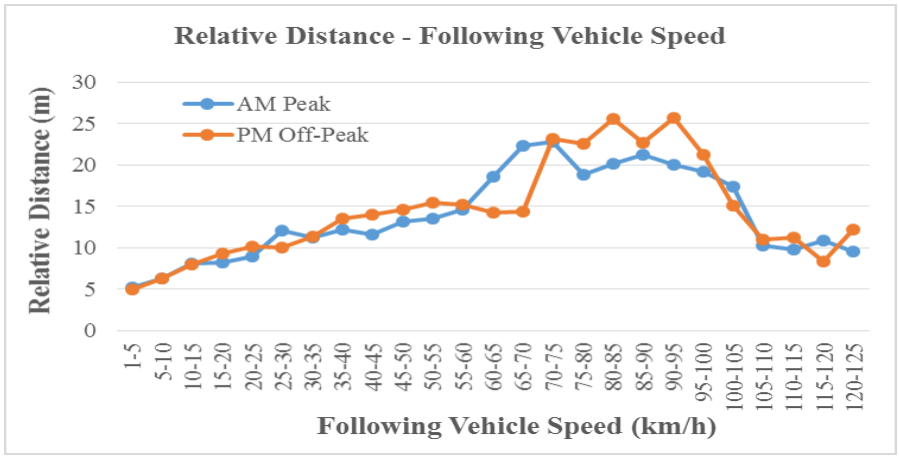

Figure 5-23: Relative distance and speed for Time of Day characteristics

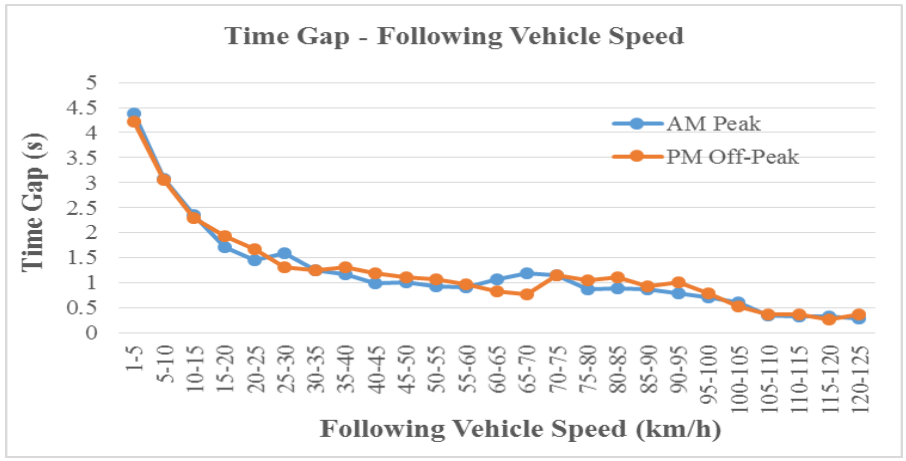

Figure 5-24: Time gap and speed for Time of Day characteristics

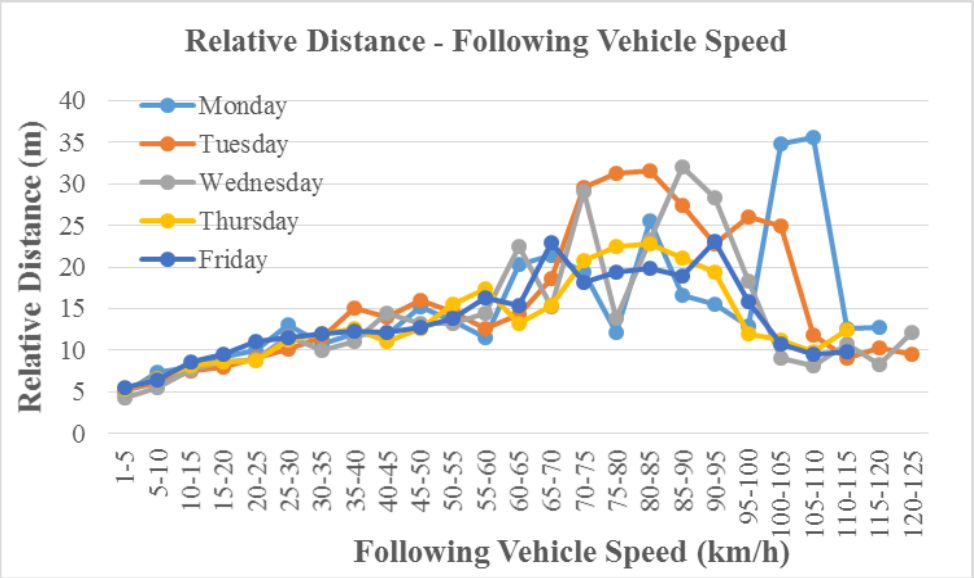

Figure 5-25: Relative distance and speed for Day of the Week characteristics

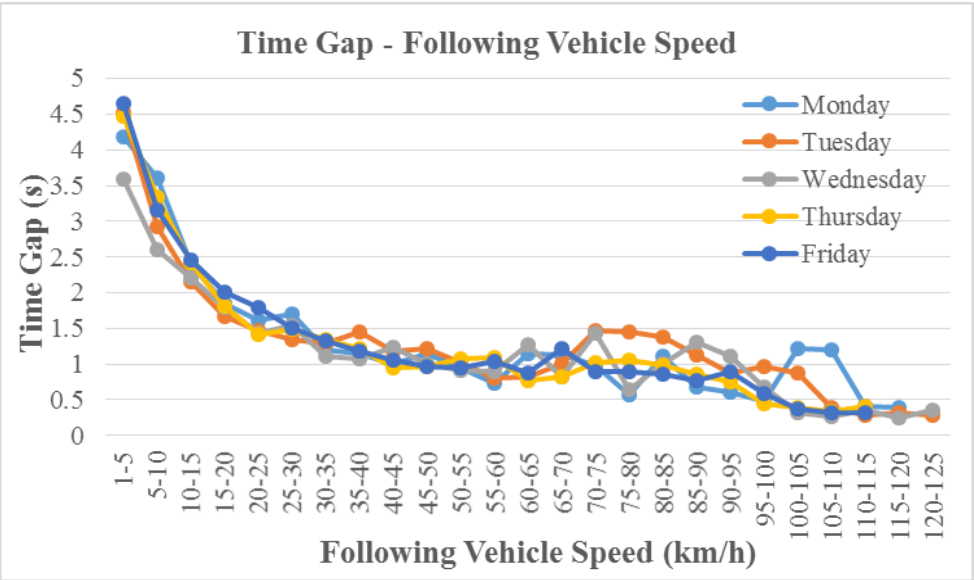

Figure 5-26: Time gap and speed for Day of the Week characteristics

5.3.7 Number of Driving Lanes

In this section, the driving lanes of the study corridors were analysed to ascertain their effect on the following distance of vehicles in car following scenario. The driving lanes considered in this study are not the driving lane of the test vehicle but the corridors total driving lanes in the same direction of travel excluding the opposing lanes. The lanes were categorised into single lanes and double (2) lanes. Three of the four corridors used for this study have a combination of one and two lanes within the length of the corridors. The

total number of vehicles extracted and analysed for the single lanes sections of the corridors were 51 vehicles and that of the double (2) lanes were 349 vehicles. Figure 5-27 and Figure 5-28 shows the relative distance and time gap respectively for the single lane and two-lane roads comparisons. Visually, there was no much difference in the following distance between the single lane and the double lane roads at speed below 40 km/h. The relative distance for both road lane groups increases with increase in the following vehicle speed, however, at speed above 95 km/h, the two-lane roads following distance decreases with increase in the following speed.

The standard deviation of the single lane corridors (5.3 metres) were found to be less than that of the two-lane corridors (8.9 metres). In general, single lane roads tend to have vehicles following with shorter following distances than double lane roads. Drivers travelling on double lane roads tend to be more cautious in their driving behaviour following other vehicles due to the possibility of vehicles in the neighbouring lane traffic stream cutting in or joining in front of other vehicles, which often result in sudden slow of vehicular movements. This situation, most of the time, makes drivers drive less defensive, hence tend to have longer following distances on double lanes than on single lanes traffic stream. The average following distance of the singe lane traffic corridors was 9.54 metres and double lane corridors was 10.91 metres. The average time gap of single lane corridors was 1.76 seconds (~1.8 seconds) less than that of the double lane corridors of 1.88 seconds (~1.9 seconds).

5.3.8 Traffic Flow Characteristics

As discussed in Chapter 3, congested traffic flow was classified as flow speed of below 20% of the legal road designed speed and uncongested traffic flow was classified as flow speed above the 20% below the designed speed and up to or over the legal designed road speed. The traffic flow characteristics considered in this section is categorised into congested and uncongested traffic flow phases. The car following behaviour during the congested and uncongested traffic flow was analysed to ascertain the difference in the following distance of vehicles observed following the test vehicle. On several occasions, same vehicles were observed within the same corridor following the test vehicle in both the congested and uncongested traffic flow phases during the experiment. The number of vehicles observed and analysed following in the congested phase was 229 vehicles and vehicles observed in the uncongested phase was 279 vehicles. Figure 5-29 and Figure 5-

30 shows the comparisons of relative distance between the congested and the uncongested phases. There was clear differences observed in the relative distance between the uncongested and congested phases as the following vehicle speed increases. It shows clearly that vehicles follow closer in the congested phase than in the uncongested phase. As expected, in congested phase, the traffic slow down forcing all vehicles to reduce speed which encourages shorter following distances of the following vehicles. However, in uncongested phase, the traffic flow freely with increasing vehicle speed which also encourages longer following distances of the following vehicles.

The standard deviation of the relative distance for the congested phase (4.7 metres) was found to be less than that of the uncongested phase (11.1 metres). The average following distance for the congested and the uncongested phases were 8.22 metres and 14.39 metres respectively. Figure 5-31 and Figure 5-32 shows the time gap and the standard deviation of the time gap with the following vehicle speed respectively for the congested and the uncongested traffic flow phases. In general, the time gap and the standard deviation of the time gap decreases with increase in the following vehicle speed for both the congested and the uncongested phases. The standard deviation of the time gap of the uncongested traffic was found to be larger than the congested traffic across all the speed ranges except at 25-30 km/h speed range. The result of the analysis suggests that drivers, in general, tend to be more cautious and in control of the vehicle driving during the congested phase than in the uncongested phase due to the possibility of sudden disturbance in the traffic flow.

5.3.9 Bus Lane Availability on Corridor

The experiment was carried out in areas within the inner city of Edinburgh that has bus only lane restrictions enforced. Other areas did not have lane restrictions in place and therefore, it is important to investigate the effect of bus lane availability on the following distance of vehicles in car following scenario. There were many occasions where the same vehicles were observed following in areas with bus lane restrictions enforced into areas without bus lane restrictions on the corridors. In all, 266 vehicles were observed on the part of the corridors without bus lane restrictions and 155 vehicles on corridors with bus lane restrictions enforced. Vehicles observed in areas with the bus lane restrictions enforced were found to follow at closer following distances across most of the speed ranges as shown in Figure 5-33. Also, there was unsteady increases in the following

distance for the bus lane areas compared to the no-bus lane areas as the following vehicle speed increase.

Vehicles following in areas where there were bus lane restrictions enforced tend to have shorter following distance than vehicles following in areas without bus lane restrictions in place. The average following distance of 8.94 metres and standard deviation of 6.4 metres of bus lane restricted areas on the study corridors was found to be less than that of the no-bus lane restricted areas with average following distance of 11.71 metres and standard deviation of 9.3 metres. The time gap of both the bus lane restricted areas and no-bus lane restricted areas generally decreases with increase in the following speed as shown in Figure 5-34. Again, the vehicles following in the areas with bus lane restrictions enforced tend to have lower time gaps than the no-bus lane restricted areas. The short following distance and time gap of the bus lane restricted areas may be as a result of vehicles being forced to use or join the single lane of traffic, which reduces the inter-vehicle spacing as the traffic volume increases. The result showed that bus lane restricted areas do have effect on the following behaviour of vehicles in car following situation due to the lack of road space to carry out certain driving manoeuvres.

5.3.10 Type of Corridor Characteristics

As discussed in Chapter 3, the selected traffic corridors within the study area were classified into three groups such as urban, rural and highways. The roads within and around the city centre of Edinburgh with speed below 40 mph were classified as urban roads. The roads outskirt of The City of Edinburgh that links Edinburgh to the neighbouring towns and villages with speed from 40 mph up to 50 mph were classified as rural roads. The roads with speed above 50 mph linking Edinburgh to other cities and major towns were classified as highways. These roads classifications were identified with each corridor as urban for Corridor 1, highway for Corridor 2, urban-rural for Corridor 3 and urban-highway for Corridor 4. The corridor type characteristics effect on the following distance of vehicles in car following situation was analysed. There are four traffic corridor types with different characteristics considered in this analysis. There were 121 vehicles for Corridor 1, 142 vehicles for Corridor 2, 159 vehicles for Corridor 3 and 157 vehicles for Corridor 4 extracted from the data sets and analysed for vehicles observed following the test vehicle during the experiment.

Figure 5-35 and Figure 5-36 shows the differences in the following distance and time gap for the corridor types considered in this study respectively. There was clear differences in the following distance observed between the corridor types at speed above 60 km/h. It can be seen that at speed above 80 km/h, the following distance between all the corridor types decreases with increase in the following vehicle speed. However, at speed below 80 km/h, the relative distance increases with increase in speed for all the corridor types considered. The time gaps of all four the corridors decreases with increase in the following speed. Time gaps above 2 seconds were found at speed below 15 km/h for all corridor types. Among the four corridors considered in this analysis, Corridor 3 tend to have vehicles with shorter following distance and shorter time gap than the rest of the corridors. The result showed that the characteristics of the road or corridor affect the following distance between vehicles in car following situations.

5.3.11 Data Collection Run (Direction of Travel)

The data collection run i.e. the direction of the test vehicle travel during the experiment is analysed in this section. The traffic moving from the city centre to the outskirts of Edinburgh during the experimental runs were classified as the Out runs and the traffic moving towards Edinburgh city centre from the neighbouring towns were classified as the Return runs. A total of 185 vehicles and 214 vehicles data were extracted from the data sets and analysed for the Out run and the Return run respectively. Figure 5-37 and Figure 5-38 shows the relative distance and the time gap comparisons for both data collection runs respectively. There was, relatively, clear differences in the following distances between the Out run and the Return run as the speed increases above 20-25 km/h speed range. Below the speed of 25 km/h, similar following distances were observed between the Out run and the Return run.

The time gap decreases with increase in the following vehicle speed across most of the speed ranges as shown in Figure 5-38. Large time gaps are observed at lower speed ranges. In general, the Out runs tend to have lower following distance and time gap across most of the speed ranges than the Return runs. The average relative distance of the Out run and the Return run are 10.55 metres and 10.87 metres respectively. The average time gap of the Out run (~1.8 seconds) was less than that of the Return run (~2 seconds). The heavy traffic volume within the city centre contributes to the low speed driving, which encourages longer following distances between vehicles, hence traffic moving towards

the city centre tend to have longer following distances. The result showed that the direction of traffic flow from and/or to the city centre affects the vehicular following distance in car following situations.

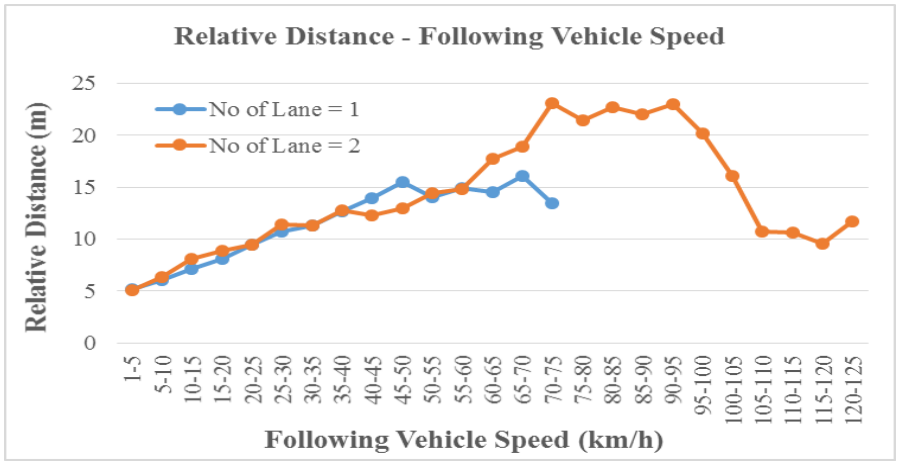

Figure 5-27: Relative distance and speed for Number of Lane

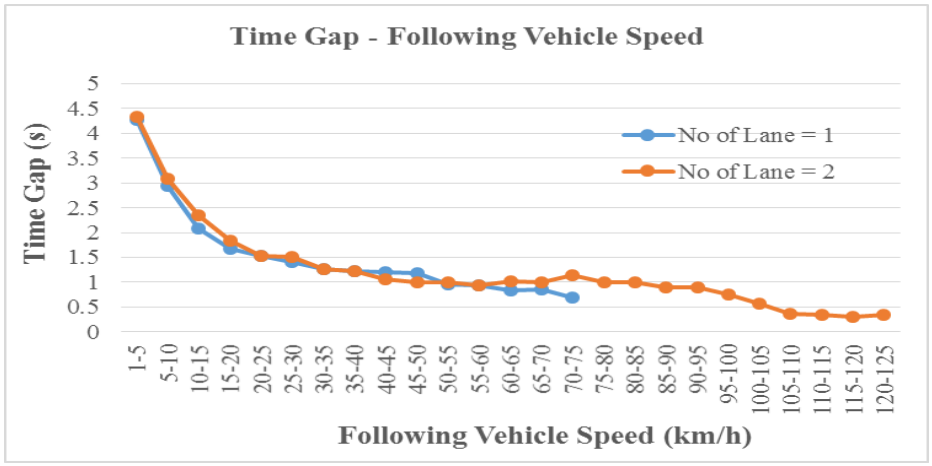

Figure 5-28: Time gap and speed for Number of Lane

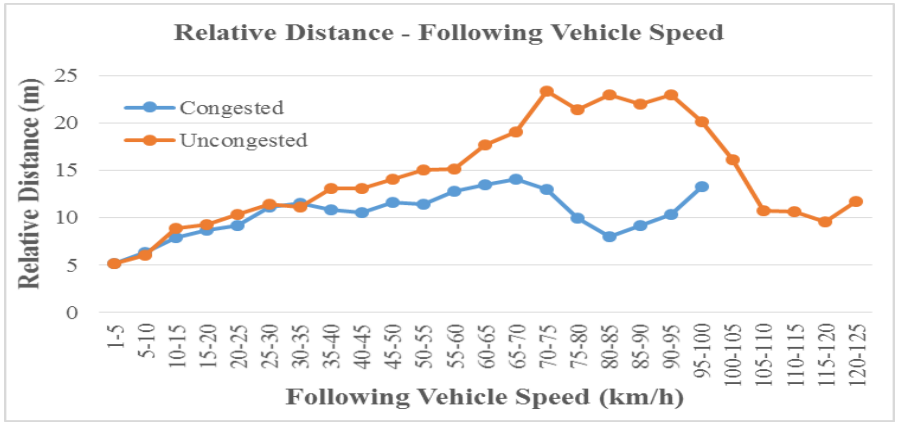

Figure 5-29: Relative distance and speed for Flow characteristics

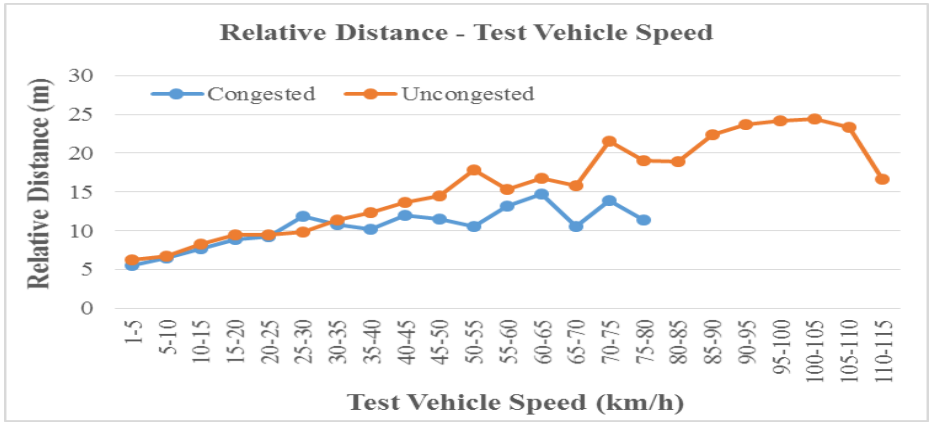

Figure 5-30: Relative distance and test vehicle speed for Flow characteristics

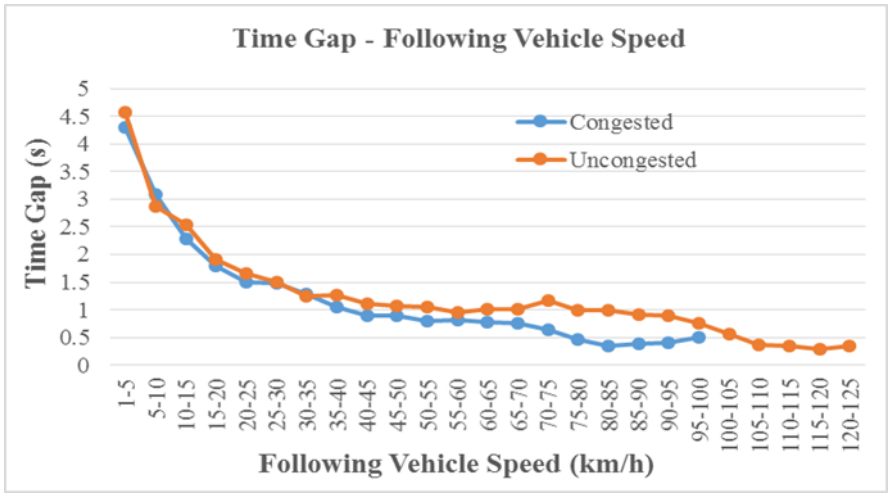

Figure 5-31: Time gap and speed for Flow characteristics

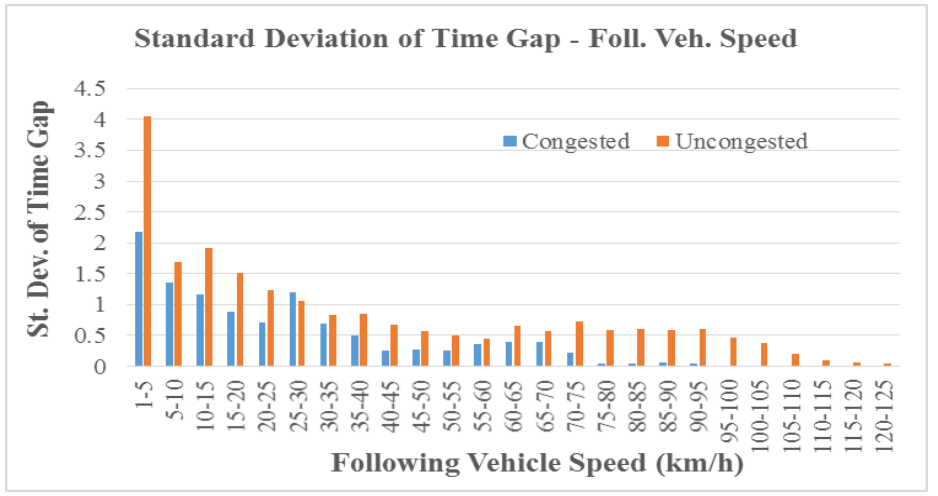

Figure 5-32: St. deviation of time gap and speed for Flow characteristics

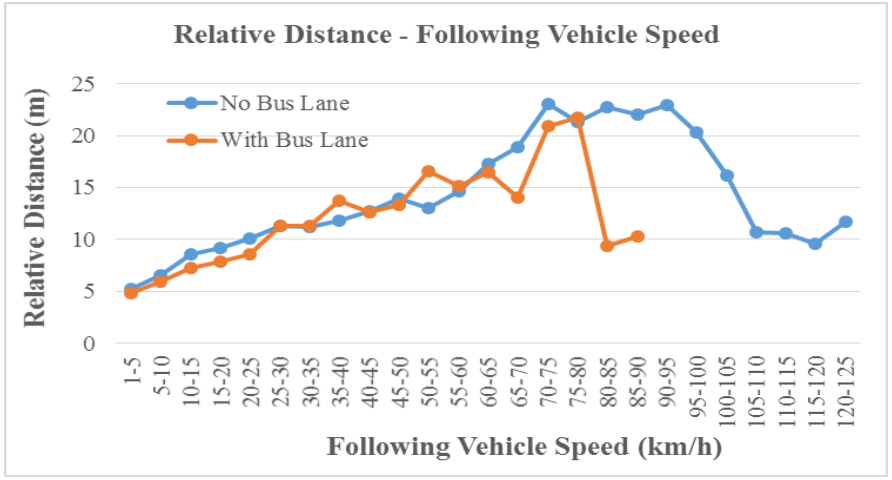

Figure 5-33: Relative distance and speed for Bus Lane Availability

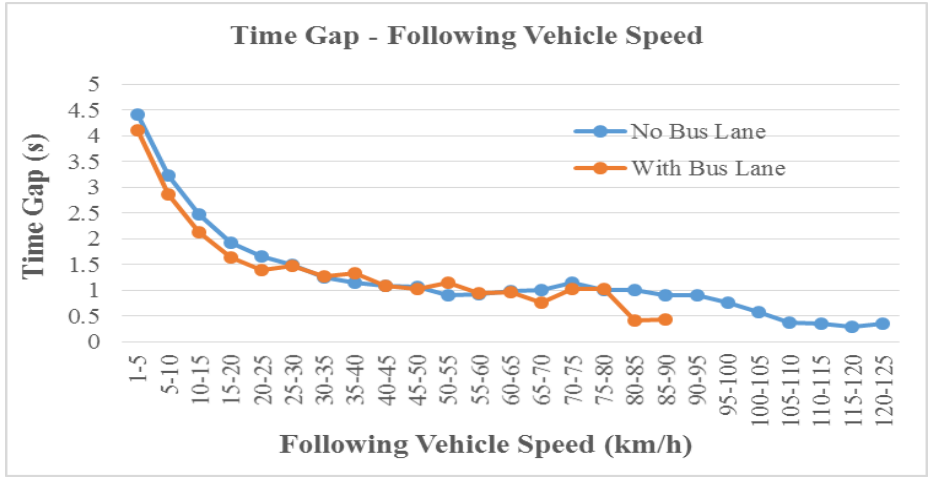

Figure 5-34: Time gap and speed for Bus Lane Availability

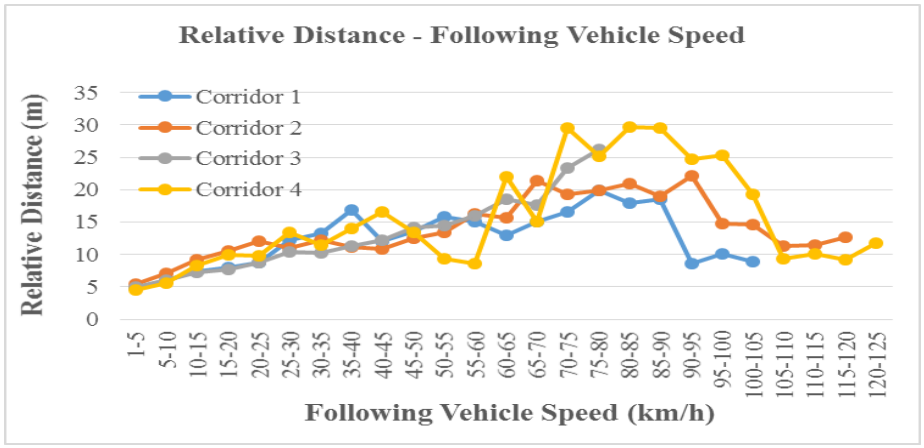

Figure 5-35: Relative distance and speed for Corridor Type characteristics

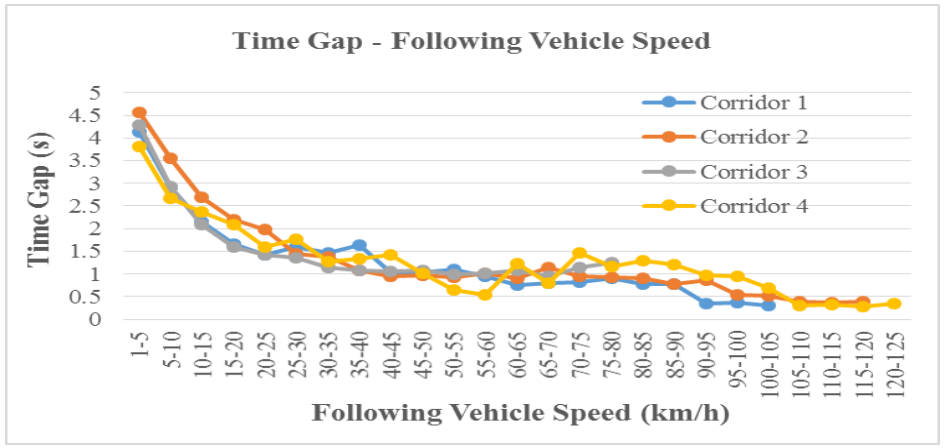

Figure 5-36: Time gap and speed for Corridor Type characteristics

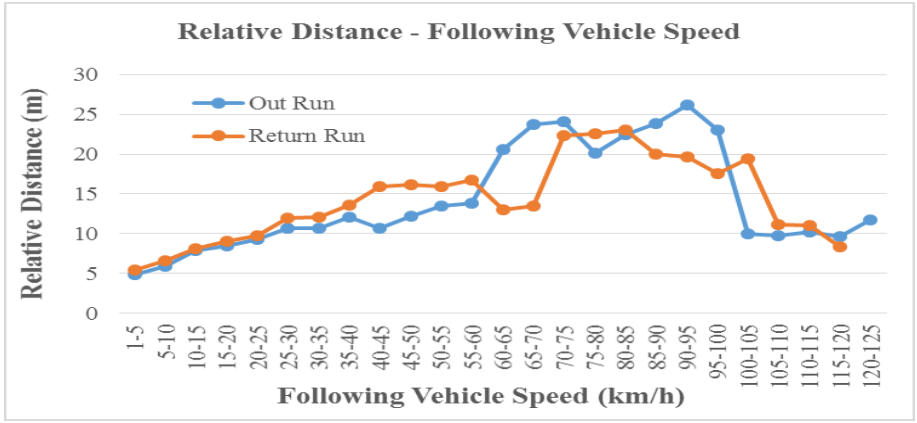

Figure 5-37: Relative distance and speed for Direction of Travel – Data Collection Run

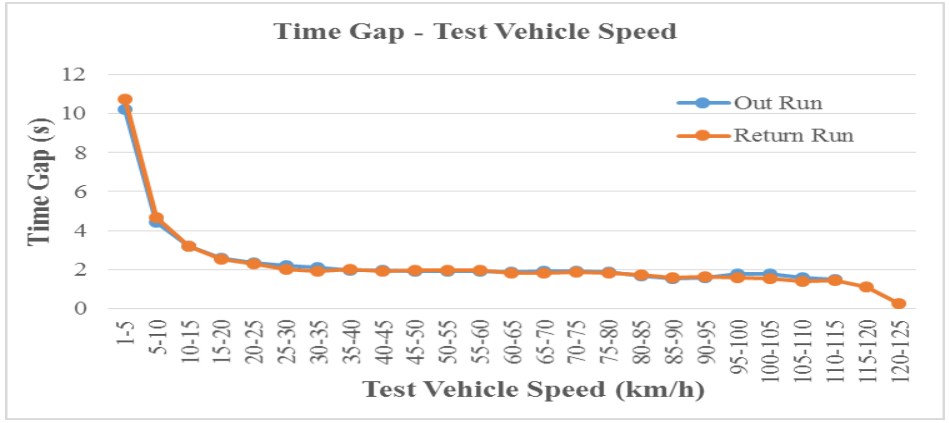

Figure 5-38: Time gap and speed for Direction of Travel – Data Collection Run

5.4 Summary

In this chapter, the data collected for this study was analysed. This chapter discussed the general overview of the data analysis. The analysis showed that there was variability in the driver behaviour across the drivers observed, and that, each driver follows their own different driving rules instead of following a set of deterministic driving rules. It also showed that drivers were inconsistent in their driving behaviour in keeping a safe or desired following distance and time gap following other vehicles. The average overall time gap measured for all the following vehicles was found to be 1.86 seconds (i.e., ~1.9 seconds), which is less than the UK guidelines for the minimum following time gap of 2 seconds including the Netherlands, EU (SWOV, 2012) that drivers are advised to maintain on the road.

In this chapter, factors that were classified as human and vehicle characteristics, environmental and other characteristics, and traffic and road characteristics that affect driving behaviour in a car following situation were analysed and discussed. The analysis showed that the different factors or characteristics considered in this study influence driver behaviour in keeping a safe or desired following distance and time gap in car following situations.

The next chapter discusses the analysis of the GHR car following model calibration and validation. It also discusses the analysis of driver-vehicle interactions involving different vehicle types.

CHAPTER 6 ANALYSIS OF GHR CAR FOLLOWING MODEL CALIBRATION AND VALIDATION

6.1 Introduction

The general overview of the research data collected was discussed in Chapter 5. Also discussed in Chapter 5 was the car following behaviour of vehicles observed following the test vehicle during the experiment. The review of car following models development in the relevant literature was discussed in Chapter 2. It was found that the lack of appropriate car following data in the area of microscopic data acquisition (Ossen and Hoogendoorn, 2005) has resulted in the development of different car following models whose reliability to replicate actual inter-vehicle interactions in a car following scenario uncertain. It is evident in the relevant literature that, different versions of the GHR model have been proposed (Brackstone and McDonald, 1999). Different data acquisitions used to calibrate the GHR model resulted in different versions of the model, with each intended to describe the driver-vehicle interactions between two adjacent vehicles. To understand the driver-vehicle interactions within an urban-rural driving condition, the GHR car following model is considered in this chapter.

A number of gaps were identified in the literature reviewed and discussed in Chapter 2. Firstly, the review identified that little recent research on car following model have been studied on multiple leader car following models. The very few available multiple leader models were developed as extension of existing car following models that does not necessarily describe the actual driving behaviour of multiple leader car following scenarios. Secondly, most of the previous work on car following models use the acceleration of the following vehicle to describe the driving behaviour and very little work on models that describe the safe or desired following distance of the following vehicle. Evidence in the literature suggest that distance-based car following models lacks the needed attention required in recent years. Thirdly, the data collection techniques used in most studies, in many cases, does not give adequate and quality microscopic data that warrant proper study of driver behaviour that requires continuous longitudinal measurements over long period of travel distance within a network. For instance, the use of observers stationed at temporal locations or points and video camera recordings situated at fixed locations or points limits the data collection from these techniques that may not be representative of driver behaviour over a long travel distance.

Furthermore, the review also found that there have been very little or no work including socioeconomic variables investigated in the previous car following models. Empirical evidence showing that the existing car following models certainly provide a better description of the effect of socioeconomic variables on car following was, however, missing in the current models. Finally, the different versions of the GHR model were found to be calibrated using data obtained from car following car, but little or no attention have been given to the calibration of the GHR model using data obtained from truck following car or car following truck. For instance, evidence in the relevant literature suggests the need for more reliable and accurate driver behaviour data to calibrate the GHR model to produce a more reliable and acceptable model calibration parameters that best describe individual driving behaviour of car following car for urban-rural and highway driving conditions. This is because different data sets have produced different versions of the GHR model, but very few have been found to be most reliable and yet no reported agreement have been reached for a more general acceptable set of model calibration parameters. This chapter, Chapters 7, 8 and 9 discuss in detail how these gaps identified were investigated and the gaps filled in the literature to contribute to the body of knowledge.

In this chapter, new versions of the GHR model that best describe driver-vehicle interactions within an urban-rural area for a car following a car, for truck following a car and for car following a truck are proposed. In this chapter, the GHR model calibration and validation process that take into account the position of the test vehicle in the car following process is discussed. Also discussed in this chapter is the driver-vehicle interactions during the car-following process. Finally, the summary of the analysis of this chapter is given.

6.1.1 Car Following Model Description

Car following models formulations developed in this study and all the tested scenarios of car following models discussed in Chapters 6, 7, 8, 9 and 10 are presented in Table 6-1 and Table 6-2. Each model is identified by the model code that defines the models developed and all the scenarios tested in this study. The whole data sets (containing 96,873 individual time series data points with increment of 0.1 seconds) used for the calibration and validation of the GHR car following model discussed in this chapter was split randomly into different data sets as shown in Figure 6-1. The split data sets were

used to test different scenarios of the GHR model calibration discussed in this chapter. Similar data split processes are also presented in Chapters 10, 11 and 12 for models calibration and validation.

Table 6-1: Distance-based car following models formulation codes and models descriptions

Model	Model Description	Chapter
GHR Model Calibration		
Scenario 1	Passenger-Car following Test Vehicle	Chapter 6
	Truck following Test Vehicle	
Scenario 2	Test Vehicle following Passenger-Car	
	Test Vehicle following Truck	
Distance-based Car Following Model		
Model A	Basic Distance Model with Relative Acceleration and Time Gap	Chapters 7 and 8
Model B	Basic Distance Model with Relative Acceleration and Time Headway	
Model C	Basic Distance Model with Acceleration of Following Vehicle and Time Gap	
Model D	Basic Distance Model with Acceleration of Following Vehicle and Time Headway	
Model A-1	Distance Model with Gender	
Model A-2	Distance Model with Vehicle Occupancy	
Model A-3	Distance Model with Corridor Type	
Model A-4	Distance Model with Gender and Vehicle Occupancy	Chapter 8
Model A-5	Distance Model with Gender, Vehicle Occupancy and Corridor Type	
Model A-6	Corridor 1 Model with Gender and Vehicle Occupancy	
Model A-7	Corridor 2 Model with Gender and Vehicle Occupancy	
Model A-8	Corridor 3 Model with Gender and Vehicle Occupancy	

Table 6-2: Car following models formulation assigned codes and description of the models (continue)

Model	Model Description	Chapter
Distance-based Two-Leader Car Following Model		
Model A2	Basic Distance Two-Leader Model with Acceleration of Following Vehicle	Chapters 7 and 9
Model B2	Basic Distance Two-Leader Model with No Acceleration of Following Vehicle	
Model A2-1	Car-Car-Car Model[1]	Chapter 9
Model A2-2	Large Vehicle-Car-Car Model[2]	
Model A2-3	Car-Car-Large Vehicle Model[3]	
Model A2-4	Large Vehicle-Car-Large Vehicle Model[4]	
Model A2-5	Two-Leader Model with Gender	Chapters 7 and 9
Model A2-6	Two-Leader Model with Vehicle Occupancy	
Model A2-7	Two-Leader Model with Corridor Type	
Model A2-8	Two-Leader Model with Gender and Vehicle Occupancy	Chapter 9
Model A2-9	Two-Leader Model with Corridor Type, Gender and Vehicle Occupancy	
Distance-based Bus Following Model		
Model B1-1	Basic Distance Bus Model with Following Vehicle Speed	Chapters 7 and 10
Model B1-2	Basic Distance Bus Model with Leading Vehicle Speed	
Model B1-3	Basic Distance Bus Model with Following Vehicle and Leading Vehicle Speed	

[1]Car-Car-Car Model = Car following first leading Car (Test Vehicle) and second leading Car
[2]Large Vehicle-Car-Car Model = Large Vehicle following first leading Car and second leading Car
[3]Car-Car-Large Vehicle Model = Car following first Leading Car and second leading Large Vehicle
[4]Large Vehicle-Car-Large Vehicle Model = Large Vehicle following first leading Car and second leading Large Vehicle

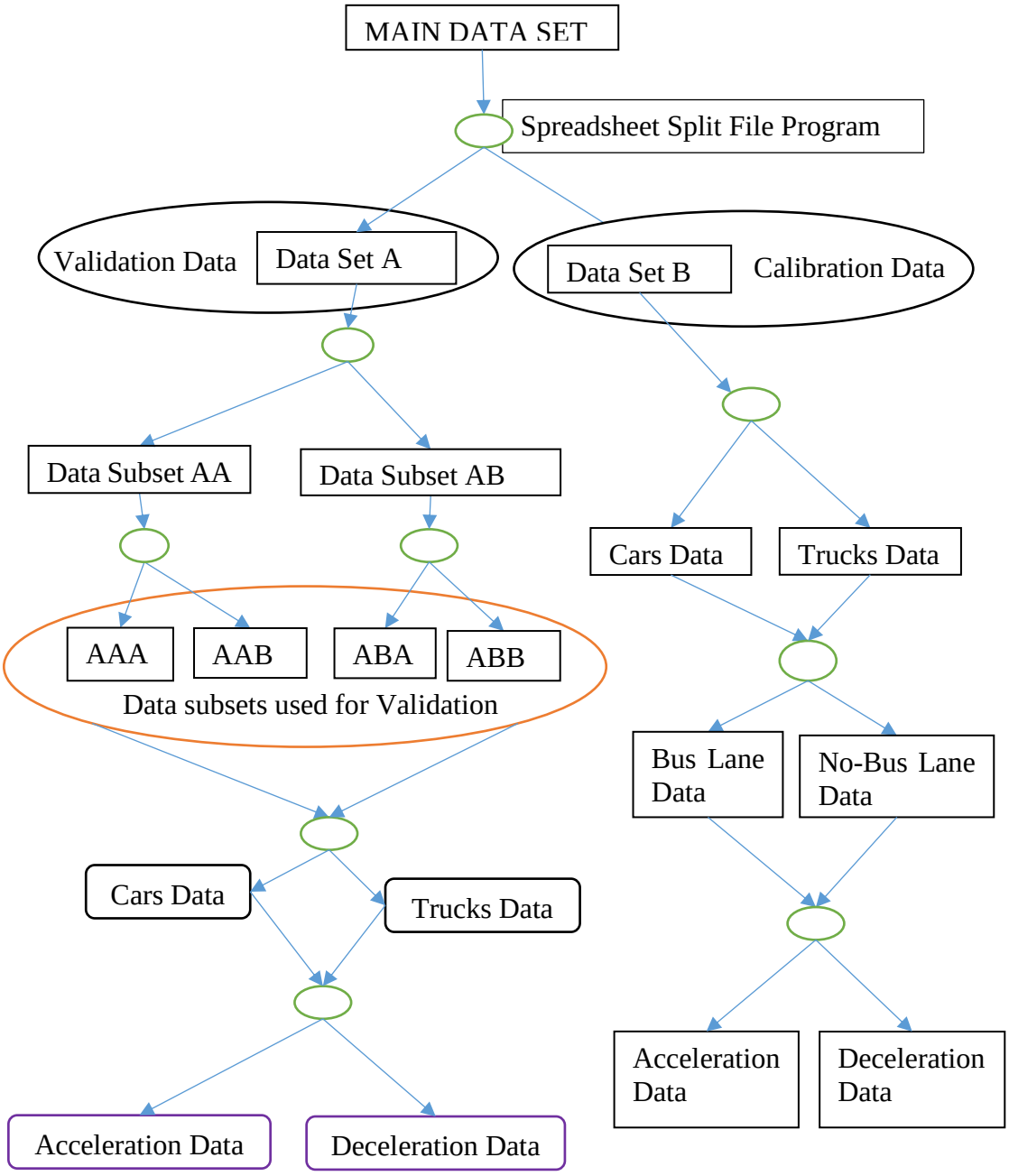

Data Set A and Data Set B	Subset data of the Main Data Set that comprises Out/Return runs for all AM and PM data
Data AA and AB	Subset data of Sub Data Set A
Data AAA and AAB	Subset data of Sub Data Set AA
Data ABA and ABB	Subset data of Sub Data Set AB

Figure 6-1: Flowchart of data sets used for the GHR model calibration and validation

6.2 Model Calibration and Validation

In this chapter, the novelty include the calibration of truck following car (i.e. car - truck) and the driver-vehicle behaviour analysis as well as the data types. In this analysis, two cases of the GHR car following model (Gazis et al., 1961) are considered. The first case considered is the calibration of the GHR model for a car following a car, a truck following a car as well as a car following a truck, and present an appropriate GHR car following model calibration parameters that best describe the driving behaviour within an urban-rural traffic condition. The second case involve using the new sets of the calibration parameters of the GHR model proposed to evaluate the driver-vehicle interactions between two sets of vehicle type when the leader is:

- the test-car followed by either a passenger-car or truck.
- a truck or passenger-car followed by the test-car.

The effect of the type of lead vehicle on the following vehicle (i.e. test vehicle) and the effect of lead vehicle (i.e. test vehicle) on the type of following vehicle are then analysed.

For this study, there was no analysis of reaction time, hence the following drivers observed reaction times were not estimated and used for this study. Therefore, the reaction time τ used for the calibration of the GHR model is set to zero as used in the relevant literature (Kesting and Treiber, 2008b). For this study, the driving behaviour data sets obtained were from vehicles constantly in motion without stopping (i.e. all stopped vehicles data were removed) during the car following process. The real driving behaviour data sets obtained have a time increment of 0.1 seconds, as used in the relevant literature (Brockfeld, 2004) at each stage of the following process. These data sets were used to calibrate the GHR model.

6.3 Case I: GHR Model Calibration

Considering the GHR car following model (Gazis et al., 1961):

$$a_n(t) = cv_n^m(t)\frac{\Delta v(t-\tau)}{\Delta x^l(t-\tau)} \tag{6-1}$$

Re-arranging the above equation (6-1), the model is expressed as:

$$\frac{a_n(t)}{\Delta v(t-\tau)} = \frac{c v_n^m(t)}{\Delta x^l(t-\tau)} \quad (6\text{-}2)$$

In order to determine the model parameters using multiple linear regression method, logarithm is applied to equation (6-2) and the model is expressed as (Appiah et al., 2015; Ranjitkar et al., 2005):

$$log\left[\frac{|a_n(t)|}{|\Delta v(t-\tau)|}\right] = \log c + mlog[v_n(t)] - llog[\Delta x_n(t-\tau)]$$

and for $\log c = x$, then c is given by: $c = 10^x$ (6-3)

Where $|a_n(t)|$ and $|\Delta v(t)|$ are the absolute values of the acceleration of the following vehicle $a_n(t)$ and the relative velocity between the leading and following vehicles $\Delta v(t)$ respectively, $\Delta x(t)$ is the relative distance between the leading and following vehicles, c, m, l are the calibration parameters, τ is the reaction time (τ = 0) and x is the intercept.

The whole data set (containing 96,872 individual points) was equally split into two different data sets: Data set A and Data set B as shown in Figure 6-1 with each having 48,436 individual data points. The data set used to calibrate the model is designated as Data set B. As discussed in Chapter 4, the data sets are in two classifications: the Out-run and the Return-run for both the morning (i.e. AM) and afternoon (i.e. PM) data sets. Each data classification (within Data set B) was split into two groups of vehicle type excluding buses (discussed in Chapter 10): cars group and trucks group (i.e. including all van type). Separating and grouping the vehicle types enabled the evaluation of the effect of each vehicle type on driving behaviour. Again, in order to evaluate the effect of bus lane (i.e. green lanes) availability on driving behaviour of each vehicle type in the car following process, each vehicle type data sets were further divided into bus lane availability and no-bus lane availability data sets. Each data sets (i.e. bus lane) for each vehicle type were further split into two groups of data sets: acceleration and deceleration phases for each test run of each corridor (see Figure 6-1). Because it is presumed that driving behaviour may vary depending on the traffic flow dynamics, different models of the same following vehicle could be establish to describe each situation.

Using multiple linear regression analysis method, equation (6-3) is applied to each of the data sets and each analysed separately to obtain different calibration parameters for both the acceleration and the deceleration phases for all the vehicle type classification with or

without the bus lane for both the AM and PM situations. This resulted in four (4) different models (i.e. 4 sets of calibration parameters) for each corridor and sixteen (16) models in total for all corridors for both the acceleration and the deceleration phases. The models calibration parameters estimates included in this analysis all have a *p*-value < 0.05. The models parameters estimates were then refined in three stages using the relative error method (equation 6-4) and the sum of the relative error (S_r) method (equation 6-5).

In order to obtain or define a set of model parameters estimates that best represent all the models parameters, the relative error and the sum of the relative errors methods were applied to refine the models parameters. For each Out or Return run, the sum of the relative errors calculated for both the acceleration and the deceleration phases by summing up the relative errors of each model parameters estimates for any given run for each corridor. The relative error (Δz_p) and the sum of the relative errors (S_r) equations are as follows:

$$\Delta z_p = \frac{\bar{Y} - Y_{rpn}}{\bar{Y}} \tag{6-4}$$

$$S_r = \sum_{z_p=1}^{n} |\Delta z_p| \tag{6-5}$$

where z_p is the assessment parameter (z_p ranging from 1 to 3; 1 = *m*, 2 = *l* and 3 = *c*) and Δz_p is the relative error value for parameter z_p. $\bar{Y}$ is the overall mean value of the parameter. Y_{rpn} is the parameter with a value of corridor *r* (ranging from 1 and 4), parameter type *p* (ranging from 1 to 3, 1 = *m*, 2 = *l*, 3 = *c*) and *n* the number of test runs for all corridors (ranging from 1 to 16 for stage 1, and 1 to 4 for stage 3). S_r is the sum of the values of the relative errors for each run.

At the first stage, the sums of the relative error of each sets of model parameters estimates were calculated and the two minimum values of the sums of the relative error of each corridor selected, thereby reducing the sixteen models to eight (8) models (two per corridor). At the second stage, the mean value of the two selected sets of model parameters estimates (with the least minimum values of Sr) for each corridor were calculated, and obtained a single set of model parameters estimates that represent each corridor for all the data set in both the acceleration and the deceleration phases. At the third stage of the model parameters estimates refining, again equations (6-4) and (6-5) applied and the two minimum values of the S_r of the four refined sets of model parameters

estimates selected. The process was repeated again for the two minimum selected models parameters estimates. A single set of model parameters estimates was then obtain for both the acceleration and the deceleration phases for each vehicle type (i.e. car and truck) with or without bus lane (see Table 6-4 and Table 6-6).

Because the test vehicle was capable of tracking vehicles directly in front and directly behind, the data sets was analysed in two different scenarios of car following based on the position of the test vehicle, i.e. the test vehicle as a leading vehicle and the test vehicle as a following vehicle. The resulting model parameters estimates were analysed separately for when the following vehicle was either a passenger-car or a truck (i.e. leader was test vehicle) and when the leading vehicle was either a passenger-car or a truck (i.e. follower was test vehicle) under the road characteristics with or without bus lane in both the acceleration and deceleration phases. It is worth noting that the speed of the vehicles used for the model parameters estimation was expressed as metre per second (m/s).

6.3.1 Data Parameters used for Model Calibration

The relative distance Δx_n (m), relative speed Δv_n (m/s) and the relative acceleration Δa_n (m/s^2) were measured directly by the radar sensors. The following vehicle speed v_n (m/s) was calculated using the directly measured relative speed and the test vehicle's speed v_t (m/s) are measured directly from the test vehicle's engine via the OBD-II port connection to the on-board laptop computer (i.e. $v_n = v_t - \Delta v_n$). The following vehicle acceleration a_n (m/s^2) was calculated using the directly measured relative acceleration and the test vehicle' acceleration measured by the Video VBOX (i.e. $a_n = a_t - a_n$). The log ($|a_n/\Delta v_n|$), log v_n and log Δx_n were then calculated as shown in Table 6-3. The resulting values were then used to calibrate the model (eqn. 6-3) using multiple linear regression to determine the calibration parameters *m*, *l* and *c*.

Table 6-3: Illustrate sample of the data set used for the calibration of the GHR car following model.

Time [s]	Veh_ID	Δa_n [m/s²]	Δx_n [m]	Δv_n [m/s]	v_t [m/s]	v_n [m/s]	a_n [m/s²]	$\lvert a_n/\Delta v \rvert$	$\text{Log}(\lvert a_n/\Delta v_n \rvert)$	$\text{Log}(v_n)$	$\text{Log}(\Delta x_n)$
0.1	1	-0.375	7.1	-0.6875	3.92	4.6075	0.025	0.036364	-1.43933	0.663465	0.851258
0.2	1	-0.25	11.3	-0.4375	10.08	10.5175	0.03	0.068571	-1.16386	1.021913	1.053078
0.3	1	-0.25	11.2	-0.5	10.08	10.58	0.03	0.06	-1.22185	1.024486	1.049218
0.4	1	-0.25	11.2	-0.5625	10.08	10.6425	0.03	0.053333	-1.273	1.027044	1.049218
0.5	1	-0.4375	6.7	-0.8125	2.8	3.6125	0.0875	0.107692	-0.96782	0.557808	0.826075
0.6	1	1	6.4	2	4.48	2.48	0.09	0.045	-1.34679	0.394452	0.80618
0.7	1	-0.3125	11.3	-0.5	10.08	10.58	0.0925	0.185	-0.73283	1.024486	1.053078
0.8	1	-0.4375	6	-0.6875	2.24	2.9275	0.1375	0.2	-0.69897	0.466497	0.778151
0.9	1	0	10.8	-0.125	10.64	10.765	0.18	1.44	0.158362	1.032014	1.033424
1.0	1	-0.5	6.4	-0.8125	2.8	3.6125	0.2	0.246154	-0.60879	0.557808	0.80618
1.1	1	-0.0625	10.8	-0.1875	10.64	10.8275	0.2425	1.293333	0.11171	1.034528	1.033424
1.2	1	-0.0625	10.8	-0.1875	10.64	10.8275	0.2425	1.293333	0.11171	1.034528	1.033424
1.3	1	-0.0625	10.8	-0.25	10.64	10.89	0.2425	0.97	-0.01323	1.037028	1.033424

6.3.2 Scenario I: Following Vehicle was either a Passenger-car or a Truck (i.e. Test Vehicle Leading)

The scenario where the following vehicle was either a passenger-car or a truck and the leading vehicle was a test vehicle was first considered during the acceleration and deceleration phases. Table 6-4 shows the set of model parameters estimates of the following vehicles (a passenger-car and a truck) following the test vehicle on roads with different lane characteristics. Firstly, considering roads with no-bus lane, it was observed that the model parameters estimates of passenger-car was higher than the model parameters estimates of truck in both the acceleration and deceleration phases. The sensitivity coefficient of the trucks, c = 1.29 and 0.69 are less than that of the passenger-car, c = 1.73 and 3.18 for the acceleration and the deceleration phases respectively. This suggests that trucks response less than passenger-car when the lead vehicle is a passenger-car (test vehicle) on roads with no-bus lane.

Secondly, the case where there was bus lane was considered. It was observed that the model parameters estimates of passenger-car was higher than the model parameters estimates of the truck in both the acceleration and deceleration phases. It also suggests that drivers of trucks response less than passenger-car drivers when following a passenger-car (test vehicle) with a lesser sensitivity coefficient estimates. This is generally due to the truck drivers being able to see beyond and around the car directly in front compared to the passenger-car drivers. The less sensitivity coefficient of the trucks to the passenger-car in both cases of road type suggests that the bus lane or no-bus lane availability has no or little effect on the vehicle type following.

When the same vehicle type was considered, the sensitivity coefficient for roads without bus lane was higher than roads with bus lane for both the passenger-cars and the trucks in the acceleration phase. However, the sensitivity coefficient for roads without bus lane was less than roads with bus lane for both the passenger-cars and the trucks during the deceleration phase.

Table 6-4: Model parameters estimates result (Test Vehicle Leading)

Leader	Follower	Bus Lane	Acceleration			Deceleration		
			m	*l*	*c*	*m*	*l*	*c*
Test Vehicle	Car	No	-0.11	0.25	1.73	-0.05	0.67	3.18
Test Vehicle	Car	Yes	-0.13	0.13	1.50	0.18	0.82	3.73
Test Vehicle	Truck	No	-0.25	-0.04	1.29	-0.43	-0.30	0.69
Test Vehicle	Truck	Yes	-0.08	0.19	1.19	0.72	1.15	1.78

Now, the final set of model parameters estimates that best describe and represent a passenger-car following the test vehicle and a truck following the test vehicle for any given road type (i.e. with or without bus-lane) is proposed. To propose the final model parameters estimates, the two sets of models parameters estimates were combined for passenger-cars only or trucks following the test vehicle under the different road characteristics. The values for each model parameters estimates for when car and truck following were determined. Presented in Table 6-5 are the proposed new versions of the GHR car following models for when the test vehicle was leading either a passenger-car or a truck. The final proposed model parameters estimates showed that in the acceleration phase, the model parameters estimates of passenger-car was higher than that of a truck when the test vehicle is leading. However, in the deceleration phase, all the model parameters estimates were higher for a passenger-car than for a truck with the exception of the model parameter *m* (i.e., 0.07 for passenger-car, 0.15 for truck). The effect of the driver-vehicle interactions in the car following process is discussed further in detail in Section 6.2.2 of this chapter.

Table 6-5: The final GHR model parameters estimates (Test Vehicle Leading)

Leader	Follower	Acceleration			Deceleration		
		m	*l*	*c*	*m*	*l*	*c*
Test Vehicle	Car	-0.12	0.19	1.62	0.07	0.75	3.45
Test Vehicle	Truck	-0.16	0.07	1.24	0.15	0.43	1.24

6.3.3 Scenario II: Leading Vehicle was either a Passenger-car or a Truck (Test Vehicle Following)

The scenario where the leading vehicle was either a passenger-car or a truck followed by the test vehicle was considered in this section. The test vehicle followed several different vehicle types (i.e. 678 vehicles) on different roads with different traffic conditions whose

driving behaviours varies. These lead vehicles driving behaviours will influence the driving behaviour of the test vehicle's driving behaviour regardless of the number of test vehicle drivers used. It is, therefore, important to evaluate the driving behaviour of the test vehicle following these vehicle types and estimates model parameters for the case where the test vehicle was following. Table 6-6 shows the overview of the model parameters estimates when the leading vehicle was either a passenger-car or a truck followed by the test vehicle. First, the situation where there was no-bus lane during the following process was considered. It was observed that during the acceleration phase, the models parameters estimates with the exception of parameter *m* were less for the passenger-car than for a truck leading the test vehicle.

The higher sensitivity coefficient of trucks to the passenger-cars suggests that vehicle following trucks response stronger than when following passenger-cars of similar sizes. The reason may be that the following vehicle driver not being able to see beyond the trucks to assess the traffic condition ahead may prompt the driver to concentrate solely on the trucks directly in front, hence the high response to the trucks in the following process. In the deceleration phase, however, the models parameters estimates were less for trucks than for passenger-cars when the test vehicle was following. The sensitivity coefficient was less for a truck as a leader than a passenger-car suggesting more response to the passenger-car than the truck during deceleration phase.

Furthermore, the situation where there was bus lane was considered. In both the acceleration and deceleration phases, the sensitivity coefficients of passenger-car were less than that of a truck leading. This also suggests that availability of bus lane has little or no effect on the following process when the leading vehicle was either a truck or passenger-car. Again, a scenario where a passenger-car was leading in all the road characteristics was considered. It was observed that the sensitivity coefficients were less on roads with bus lane than roads without bus lane in both the acceleration and deceleration phases. However, for a truck leading in all road characteristics, the sensitivity coefficients were less on roads having no-bus lane than when there was bus lane availability in both the acceleration and deceleration phases.

Again, both cases of road type data sets (with or without bus lane) combined and new models parameters estimates produced that best describe the following process when the leading vehicle was either a passenger-car or a truck followed by the test vehicle. The two

sets of model parameters estimates were combined for each road type for when the leader was a passenger-car and a truck. The individual models parameters estimates for car and truck leading were determined. Presented in Table 6-7 are the final proposed models parameters estimates for when the leading vehicle was either a passenger-car or a truck followed by the test vehicle. The final models parameters estimates showed that the sensitivity coefficients for when the leader was a truck were higher than when the leader was a passenger-car. What it means is that, a driver exhibits strong response or reaction to when following trucks or large vehicles since their field of view of traffic downstream are obstructed by the size of the large vehicles, hence tend to concentrate more on the vehicle directly in front compared with following small vehicles of similar size.

Table 6-6: Overview of model parameters estimates result (Test Vehicle Following)

Leader	Follower	Bus Lane	Acceleration			Deceleration		
			m	*l*	*c*	*m*	*l*	*c*
Car	Test Vehicle	No	0.32	0.44	0.76	0.25	0.34	0.75
Car	Test Vehicle	Yes	0.57	0.51	0.52	0.86	0.71	0.47
Truck	Test Vehicle	No	0.31	0.61	1.81	0.22	0.29	0.55
Truck	Test Vehicle	Yes	0.27	0.58	2.23	0.36	0.39	0.77

Table 6-7*:* The final version of GHR model parameters estimates for test vehicle following

Leader	Follower	Acceleration			Deceleration		
		m	*l*	*c*	*m*	*l*	*c*
Car	Test Vehicle	0.45	0.47	0.64	0.55	0.52	0.61
Truck	Test Vehicle	0.29	0.60	2.02	0.29	0.34	0.66

6.3.4 Comparison of Model Parameters Estimates for Scenario I and Scenario II

From the first case, the sensitivity coefficient *c* was higher when the test vehicle was leading passenger-car in both the acceleration and deceleration phases than when the test vehicle was following passenger-car. However, for the second case where a truck followed the test vehicle, the sensitivity coefficient *c* was less than when the test vehicle was following a truck in the acceleration phase but higher in the deceleration phase (see Table 6-8). The low sensitivity coefficient of the test driver following a truck in the deceleration phase may due to the fact that the following driver's (i.e. test driver)

awareness of being part of the experiment may influence the driving behaviour compared with drivers of other following vehicles not directly involved in the experiment.

In addition, with the reduced speed of the large vehicles, the test driver may be able to anticipate that the leading vehicle may be decelerating and hence decides to decelerate earlier than anticipated, resulting in a less response to the large vehicles behaviour in the deceleration phase compared with during the acceleration phase. The final GHR model parameters estimates proposed in this study for passenger-car following test vehicle, truck following test vehicle and test vehicle following truck are presented in Table 6-9.

Table 6-8: Models parameters estimates comparison for different following scenarios

Leader	Follower	Acceleration			Deceleration		
		m	*l*	*c*	*m*	*l*	*c*
Test Vehicle	Passenger-Car	-0.12	0.19	1.62	0.07	0.75	3.45
Passenger-Car	Test Vehicle	0.45	0.47	0.64	0.55	0.52	0.61
Test Vehicle	Truck	-0.16	0.07	1.24	0.15	0.43	1.24
Truck	Test Vehicle	0.29	0.60	2.02	0.29	0.34	0.66

Table 6-9: The final GHR model parameters estimates proposed for different car following scenarios

Leader	Follower	Acceleration			Deceleration		
		m	*l*	*c*	*m*	*l*	*c*
Test Vehicle	Passenger-Car	-0.12	0.19	1.62	0.07	0.75	3.45
Test Vehicle	Truck	-0.16	0.07	1.24	0.15	0.43	1.24
Truck	Test Vehicle	0.29	0.60	2.02	0.29	0.34	0.66

6.3.5 Comparison with other GHR Car Following Models

Evidence in the relevant literature (Chandler et al., 1958; Herman and Potts, 1959; Edie, 1961; Gazis et al., 1961; Herman and Rothery, 1962) suggests that all the most reliable versions of the GHR model (Brackstone and McDonald, 1999) used data obtained from experiment that involves person (or passenger) cars excluding all other types of vehicle to calibrate the GHR model. It is appropriate to use the car following car GHR model parameters estimates proposed in this study to compare with the most reliable models that Blackstone and McDonald reviewed.

Considering Scenario I and Scenario II of the car following car process, it is appropriate to suggests that the driving behaviour of the test vehicle as the following vehicle (Scenario II, i.e. test vehicle following other passenger-cars) may be influenced by the idea of being part of the experiment. Considering Scenario I case (i.e. test vehicle leading), drivers are believed to drive naturally without their driving behaviour being affected by the experiment, since the following vehicle drivers were not made aware of the experiment and being directly involved with the experiment. It is evident that the driving behaviour of the following vehicles were more of a representative of the general driving population since different drivers were following at different times during the car following process when the test vehicle was leading. For this reason, the models parameters estimates of the following vehicles are considered as the final proposed model parameters estimates for this study's version of the GHR model for car following test car and for truck following test car (i.e. Scenario I).

Because the test vehicle following trucks (i.e. large vehicles) was a unique situation, the model parameters estimates of the test vehicle following trucks (i.e. Scenario II) is also considered as this study's final version of the GHR model for car following truck (i.e. large vehicle). The calibration parameters estimates that this study proposed for a car following the test car closely agrees with the parameters estimates proposed by Ozaki (1993) with m = -0.2 and l = 0.2 for the acceleration phase. The Ozaki estimate of parameter c = 1.1 is slightly different to the current study's estimate of parameter c = 1.62, but it is closer to the Ozaki estimate than the other researchers' reliable estimate of parameter c in the acceleration phase (see Table 6-10). In the deceleration phase, this current study's parameters estimates of m = 0.07 (~0.1) and l = 0.75 (~0.8) closely agrees with the parameters estimates proposed by Hoefs (1972) (m = 0.2 and l = 0.9). The values obtained for this current study's parameters estimates were 0.1 less than the parameters estimates proposed by Hoefs. In the deceleration phase, the model parameter estimate proposed by Ozaki (l = 1), however, agrees with this current research parameter estimate (l = 0.75 (~1)).

The model parameters values obtained for this current study varies from other parameters values proposed by Chandler et al., Herman and Potts, and Treiterer and Myers in both the acceleration and deceleration phases (see Table 6-10). In comparing this current study's GHR model parameters values with the most reliable values of the GHR model parameters (Brackstone and McDonald, 1999), the Ozaki and Hoefs model parameters

values closely relates to this current study's parameters values in the acceleration and the deceleration phases respectively. This shows that the model parameters values obtained for a car following a car are reliable in the urban-rural and highway traffic conditions. It can be inferred that the GHR model parameters values obtained for a truck following a car and a car following a truck are most reliable and best describe driving behaviour within urban-rural and highway driving conditions for a truck-car following interactions.

Table 6-10: Comparison of calibration paramters values of the current study and the most reliable GHR model (Brackstone and McDonald, 1999)

Source	*m*	*l*	*c*
Chandler et al. (1958)	0	0	0.17 - 0.74 /s
Herman & Potts (1959)	0	1	19.8 ft/s
Hoefs (1972) (accn/decn) *	0.6/0.2	3.2/0.9	-
Treiterer and Myers (1974) (accn/decn) *	0.2/0.7	1.6/2.5	-
Ozaki (1993) (accn/decn) *	-0.2/0.9	0.2/1	1.1
Values obtained from the current study (accn/decn) *	-0.12/0.07	0.19/0.75	1.62/3.45

*accn/decn: acceleration/deceleration

6.3.6 Validation of the Model Parameters Estimates

As earlier discussed in this chapter, new versions of the GHR model that best describe a car following a car, a truck following a car and a car following a truck within urban-rural and highway traffic conditions were proposed for this study. To begin the validation of the GHR model, half of the main data set designated as Data set A (containing 48,436 individual data points) discussed in Section 6.1.1 was used for the model validation. The data file A was split randomly into two subset data (i.e. data subset AA and data subset AB) files using the spreadsheet split file program developed and used for the data processing discussed in Chapter 4 Section 4.3.

Again, each individual data subset (AA and AB) files were randomly split into two new data set files, creating four new sub data sets (AAA, AAB, ABA and ABB) files. In all, a total of four randomly split data subsets (AAA, ABB, ABA, ABB) with each consisting of at least 12,109 individual time series data points with time increment of 0.1 seconds were used for the validation. Each of the four data sets were further divided into cars and

trucks data sets. In order to perform the t-test on the acceleration and the deceleration phases of each vehicle type (i.e. cars and trucks), the data sets were further grouped into acceleration and deceleration phases based on the following vehicle's acceleration rate (see Figure 6-1). The absolute values of the relative speed was use in the model validation process. This was to ensure that the models simulation runs produced only acceleration values for the acceleration phases and deceleration values for the deceleration phases. The models were simulated using the four data sets to produce the predicted acceleration and deceleration values for all the vehicle following scenarios (i.e. car following car, truck following car and car following truck) considered in this study.

One of the useful statistical approach used for testing research hypotheses is the t-test statistics, which is a form of the statistical hypothesis test with a standardised value that is computed from sample data or observations during hypothesis test. The means of two groups with paired observations can be compared with a two-sample test, and the mean of a sample data can be compared with a set value using one-sample t-test. There are a number of assumptions that underpin the use of the t-test statistics in general. The assumptions are that, the data should be normally distributed, mean should be known, small sample size, and independent and random sample observations (McClave et al., 2008: Daly et al., 1991; Baldi and Long, 2001; Laerd, 2017; ENU, 2017)

In order to validate the models, a *t*-test statistics was performed to determine whether there were statistical significant mean difference between the observed and the models predicted data sets for the acceleration and deceleration phases for all the vehicle following scenarios discussed in this chapter. Performing the t-test statistical analysis validates the models parameters estimates against the field data sets to ascertain the models reliability to real world car following situations. Since the observed data was used to generate the corresponding models predicted data sets for each drivers observed, the paired t-test statistics was considered more appropriate for testing the statistical significance difference between the two groups of data sets for this study.

For a paired two-sample for means t-test statistics given:

$$\mu_o - \mu_p = \mu_d \quad ; \quad \mu_d = 0 \tag{6-6}$$

the null ($H_{o)}$ and the alternative (H_a) hypotheses are therefore given as:

$$H_0: \mu_d = 0 \quad ; \quad H_a: \mu_d > 0 \tag{6-7}$$

the computation of the t-test t-value for the paired two-sample groups is given by:

$$t = \frac{\overline{d} - \mu_d}{S_d/\sqrt{n}} \tag{6-8}$$

where $\overline{d}$ is the sample mean of the differences in the means between the two groups of data. S_d is the standard deviation of the differences in the standard deviations between the two groups of data and n is the sample size, μ_d is the population mean of the differences in the means between the two groups of data. μ_o is the observed true population mean and μ_p is the predicted true population mean (McClave et al., 2008: Daly et al., 1991; Anderson et el., 2010; ENU, 2017). The degree of freedom is given by the sample size minus 1 (i.e. $n - 1$). Based on the significance level, usually at 95% (i.e., p-value ≤ 0.05), and the degree of freedom (df), a decision is made about the research hypothesis (i.e., either to accept or reject the null hypothesis). The p-value can be computed using Microsoft Excel formula, which is given by:

$$p = TDIST\ (x, df, tails) \tag{6-9}$$

where is *x* is the t-test t-value (t-stat), tails is either one-tailed or two-tailed distribution. For this study, Microsoft Excel data analysis tool was used to computes the t-test t-values and the p-values for all the models validation analyses discussed in this study.

Since the data set used for the validation was very large, the data was divided into four set of blocks. The four blocks of data were used to validate the model resulting in four models. Each of the four set of blocks contains at least 12,109 data points, which is very large for a t-test statistical analysis. One of the assumptions of the t-test statistical analysis is that the sample size should be small. Therefore, it was appropriate to use the averages of each block of data sets to perform the t-test for the models validation process. In view of that, the averages of the observed and the models predicted data of the four blocks of data were used for the t-test analysis. The same approach was used for all the models validation process discussed in this study. The average observed and the corresponding predicted acceleration and deceleration data sets for each vehicle following scenario for each simulation runs were computed and the results presented in Table 6-11 to Table 6-

13. To perform the t-test at 95% (i.e. p-value ≤ 0.05) confidence level (cl), two hypothetical questions for the t-test analysis were set out:

H_0: There is no significant difference between the observed and the model predicted acceleration or deceleration data sets (i.e., $H_0: \mu_d = 0$).
Ha: There is significant difference between the observed and the model predicted acceleration or deceleration data sets (i.e., $H_a: \mu_d \neq 0$).

The hypotheses stated above makes the paired two-sample for means t-test a two-tail hypothesis test, therefore, a two-tail t-test analysis was performed for the models validation. The t-test statistics was computed using Microsoft Excel data analysis tool for the acceleration and deceleration phases for all the vehicle following scenarios discussed. The outputs of the t-test statistics are presented in Table 6-11 to Table 6-13.

For degree of freedom (df) of 3 (i.e. 4 - 1), the two-tailed t-test statistics p-value of 0.28 and t-stat value of -1.318 for the acceleration phase, and p-value of 0.74 and t-stat value of -0.371 for the deceleration phase were obtained for the car following car scenario. For the truck following car scenario, the t-test statistics p-value of 0.29, t-stat value of -1.273 for acceleration phase, and p-value of 0.85 and t-stat value of 0.199 for deceleration phase were obtained. Finally, for the car following truck scenario, the t-test statistics p-value of 0.20, t-stat value of -1.634 for the acceleration phase, and p-value of 0.32, t-stat value of -1.176 for the deceleration phase were obtained. It can be seen that the p-values for all the three different vehicle following scenarios were greater than the p-value of 0.05 (i.e. 95% confidence level). Similarly, the t-stat values for all the three different vehicle following scenarios were also less than the two-tail t-critical of 3.182 (for df = 3, at 96% cl). The t-test statistics results showed that there was no enough evidence in the mean differences between the observed and predicted data to suggest the rejection of the null hypothesis and therefore, the alternative hypothesis was rejected since no significant differences were observed in the two groups of data sets.

The t-test statistics was used to test the significant differences between the observed and the predicted acceleration and deceleration phases of the proposed models parameters estimates for car following car, truck following car and car following truck. The analysis found that at p-value of 0.05 (i.e. 95%) confidence level, there was no statistical significant differences observed between the observed (or measured) and the models predicted data sets to suggest the rejection of the null hypothesis (H_0). Therefore, we

conclude that there is no statistical significant difference between the observed and the predicted data sets for the car following car ([t(3) = -1.318, p-value > 0.05, 2-tail] for acceleration and [t(3) = -0.371, p-value > 0.05, 2-tail] for deceleration), the truck following car ([t(3) = -1.273, p-value > 0.05, 2-tail] for acceleration and [t(3) = 0.199, p-value > 0.05, 2-tail] for deceleration) and the car following truck ([t(3) = -1.634, p-value > 0.05, 2-tail] for acceleration and [t(3) = -1.176, p-value > 0.05, 2-tail] for deceleration) for both the acceleration and deceleration phases.

Table 6-11: Paired two sample means t-test results for car following test car

Acceleration					
Data Set	Observed	Predicted	T-Test Result		
				Observed	Predicted
AAA	0.60	1.37	Mean	0.648	0.8975
AAB	0.64	0.93	Variance	0.003256	0.11863
ABA	0.73	0.69	Observations	4	4
ABB	0.62	0.60	Pearson Correlation	-0.54648	
			Hypothesized Mean Difference	0	
			df	3	
			t Stat	-1.317908	
			P(T<=t) one-tail	0.139567	
			t Critical one-tail	2.353363	
			P(T<=t) two-tail	0.279134	
			t Critical two-tail	3.182446	
Deceleration					
Data Set	Observed	Predicted	T-Test Result		
				Observed	Predicted
AAA	0.58	0.98	Mean	0.6125	0.66
AAB	0.65	0.70	Variance	0.001892	0.06433
ABA	0.65	0.59	Observations	4	4
ABB	0.57	0.37	Pearson Correlation	0.024173	
			Hypothesized Mean Difference	0	
			df	3	
			t Stat	-0.370654	
			P(T<=t) one-tail	0.36776	
			t Critical one-tail	2.353363	
			P(T<=t) two-tail	0.73552	
			t Critical two-tail	3.182446	

Table 6-12: Paired two sample means t-test results for truck following car

Acceleration					
Data Set	Observed	Predicted	T-Test Result		
				Observed	Predicted
AAA	0.68	1.14	Mean	0.575	0.72
AAB	0.51	0.67	Variance	0.0055	0.0826
ABA	0.57	0.52	Observations	4	4
ABB	0.54	0.55	Pearson Correlation	0.84919	
			Hypothesized Mean Difference	0	
			df	3	
			t Stat	-1.273	
			P(T<=t) one-tail	0.14636	
			t Critical one-tail	2.35336	
			P(T<=t) two-tail	0.29272	
			t Critical two-tail	3.18245	

Deceleration					
Data Set	Observed	Predicted	T-Test Result		
				Observed	Predicted
AAA	0.60	0.81	Mean	0.525	0.51
AAB	0.49	0.42	Variance	0.00257	0.04007
ABA	0.50	0.40	Observations	4	4
ABB	0.51	0.41	Pearson Correlation	0.98282	
			Hypothesized Mean Difference	0	
			df	3	
			t Stat	0.19912	
			P(T<=t) one-tail	0.42745	
			t Critical one-tail	2.35336	
			P(T<=t) two-tail	0.8549	
			t Critical two-tail	3.18245	

Table 6-13: Paired two sample means t-test results for car following truck

Acceleration					
Data Set	Observed	Predicted	T-Test Result		
				Observed	Predicted
AAA	0.36	1.05	Mean	0.4075	0.6725
AAB	0.39	0.63	Variance	0.0039583	0.100558333
ABA	0.38	0.28	Observations	4	4
ABB	0.50	0.73	Pearson Correlation	-0.0179606	
			Hypothesized Mean Difference	0	
			df	3	
			t Stat	-1.6338012	
			P(T<=t) one-tail	0.1004049	
			t Critical one-tail	2.3533634	
			P(T<=t) two-tail	0.2008098	
			t Critical two-tail	3.1824463	
Deceleration					
Data Set	Observed	Predicted	T-Test Result		
				Observed	Predicted
AAA	0.36	0.82	Mean	0.3725	0.5325
AAB	0.35	0.60	Variance	0.0020917	0.078091667
ABA	0.34	0.15	Observations	4	4
ABB	0.44	0.56	Pearson Correlation	0.2392964	
			Hypothesized Mean Difference	0	
			df	3	
			t Stat	-1.1758139	
			P(T<=t) one-tail	0.1622429	
			t Critical one-tail	2.3533634	
			P(T<=t) two-tail	0.3244858	
			t Critical two-tail	3.1824463	

6.4 Case II: Analysis of Inter-Vehicle Interactions

Some differences in the inter-vehicle interactions in the models parameters estimates when the leader is the test vehicle followed by a car or the test vehicle followed by a truck or a truck followed by the test vehicle were observed. To gain more insight into these differences, the driver-vehicle interactions were evaluated using the sensitivities of the following drivers in this analysis. To begin with, each corridor data (both the Out runs

and the Return runs) were combined as one corridor data set and then each data separated into car and truck (all van types included) under acceleration and deceleration phases.

The basic driver-vehicle interaction proposed by Gazis et al. (1961) that explained how a driver response to a given stimulus was considered (equation (2-4)). The response-stimulus equation expressed as:

$$\text{Response (t)} = \text{Sensitivity (t)} \times \text{Stimulus (t)} \tag{6-10}$$

The sensitivity expressed as a function of the following vehicle's speed and following distance. Given the response – stimulus model (equation (2-11)), the formulation of the sensitivity (λ) of a driver of a following vehicle is given as:

$$\lambda = \mathrm{c}\frac{v_n^m(t)}{\Delta \mathrm{x}^{\mathrm{l}}(\mathrm{t})} \tag{6-11}$$

where *m*, *l*, *c* are the sensitivity parameters. To estimate the sensitivity value for the driver-vehicle interactions, equation (6-11) is applied to the models parameters estimates in Table 6-5 and Table 6-7, and the average sensitivity values for each corridor calculated (i.e. AM and PM separately). Eight (8) sets of sensitivity values (i.e. two (2) for each corridor, one (1) for AM and one (1) for PM) were obtained for all the corridors for both the acceleration and the deceleration phases.

To refine the sensitivity values for each of the corridors, the absolute relative error method ($|\Delta z|$) (i.e. equation 6-4) was applied to the sensitivity data sets, and the least minimum values from each corridor were selected. The resulting four (4) sensitivity values were then averaged to obtain a mean sensitivity value that is representative of all the corridors for all vehicle type under investigation for both the acceleration and deceleration phases. The sensitivity values for the two different scenarios were then estimated, and separately obtained the values for when the test vehicle was leading and when the test vehicle was following other vehicle types. Table 6-14 shows the overview of the mean sensitivity estimates of driver-vehicle interactions in both the acceleration and the deceleration phases. To gain more insight into the effect of the type of leading or following vehicle might have on the driving behaviour in the car following process, two scenarios were considered where the test vehicle was leading a passenger-car or a truck, and test vehicle following a passenger-car or a truck.

6.4.1 Scenario I: Test Vehicle Followed by a Passenger-car or a Truck

Case I (see Table 6-14), when the test vehicle was leading either a passenger-car or a truck for both the acceleration and deceleration phases is now considered. The analysis found, on average, that the sensitivity estimates of 0.901 and 0.854 for a passenger-car were higher than the sensitivity estimates of 0.769 and 0.623 for a truck in both the acceleration and deceleration phases respectively. A study by Hoogendoorn and Ossen (2006) using different model calibration parameters values obtained from experiment for the estimation of the drivers sensitivity, also reported a lesser sensitivity estimate when the follower was a truck than that of a person-car when comparing the differences between a follower as a person-car or a truck. They attributed the driving behaviour differences to the drivers' experiences between the two different driver groups. The lesser sensitivity of truck drivers, in both the acceleration and deceleration phases, can be explained by the high viewpoint of truck drivers that is associated with the added ability to see further ahead of the traffic downstream. This makes the truck drivers able to anticipate any disturbance in the traffic flow, hence response or reacts less to the vehicle directly ahead.

Although, the driver of the passenger-car following directly behind a car of similar size can see beyond and around the car, but compared that to a truck driver following similar car, the passenger-car driver will have a shorter view of the traffic ahead or downstream than that of the truck driver. This lack of ability for the passenger-car to see further ahead enable them to concentrate more on the immediate vehicles downstream and as a result response or reacts slightly stronger to the vehicle directly following. As expected, truck drivers will have less response to vehicles they are following because of their slow rate of deceleration and longer braking distance before coming to a stop. They will normally follow other vehicles with a considerable distance between them compared with that of a passenger-car considered to have a shorter braking distance.

6.4.2 Scenario II: Passenger-car or Truck Followed by Test Vehicle

With respect to Case II (see Table 6-14), the situation where the lead vehicle was either a passenger-car or a truck followed by the test vehicle was investigated. It was found that, in the acceleration phase, the sensitivity estimates for a passenger-car (0.446) was less than when the leader was a truck (0.660). As it is generally the case when a passenger-

car is following a large vehicle, the view of the passenger-car is normally obscured to the traffic downstream due to the size of the truck. As a result, the passenger-car driver will normally pay more attention to the truck that is leading, which might adversely affects driver's driving behaviour. This behavioural effect enable the passenger-car driver react stronger to the behaviour or speed profile of the lead truck than that of a lead passenger-car.

Hoogendoorn and Ossen in a study conducted in 2006, analysed the sensitivity of two-leader vehicle following behaviour in a car following situation using data obtained from a helicopter mounted with video camera monitoring vehicle trajectories on highways in the Netherlands. They considered the case of the following vehicles to only the first leader as a truck or a car and found that the following vehicles' sensitivity to the leading trucks (0.219) was higher than that of a person-car sensitivity (0.185). In relation to this investigation, a similar trend was observed when the leading vehicle was a truck. The sensitivity of the test vehicle was larger to the truck than to that of the passenger-car when following both vehicles. This can be explained by the lack of the following driver not being able to look beyond and around the trucks due to its size to process the traffic information downstream to make an informed judgement of the traffic flow condition. Hence, the following driver tend to spend most of the driving concentrating more on the leading trucks, resulting in larger sensitivity or stronger response to the trucks than that of a passenger-car.

However, the opposite of this behaviour was noticed during the deceleration phase. The sensitivity estimate of the passenger-car as the leader was higher than the sensitivity estimate of the truck as the leader. The deceleration sensitivity of the truck (0.459) as leader was less than that of the passenger-car (0.484) as a leader. One possible explanation may be the driver's experience and awareness of the slow deceleration rate (i.e. longer braking distance) of large vehicles and the reduced speed during deceleration phase, which may prompt the driver to begin anticipating that the traffic downstream is also coming to a halt, hence decides to react earlier than expected to the large vehicle in front.

Table 6-14: An overview of the sensitivity estimates results of driver-vehicle interactions

Driver-Vehicle Interaction			Acceleration		Deceleration	
			Sensitivity		Sensitivity	
Case	Leader	Follower	λ (st. dev.)	Error	λ (st. dev.)	Error
I	Test Vehicle	Car	0.901 (0.011)	0.012	0.854 (0.025)	0.028
	Test Vehicle	Truck	0.769 (0.023)	0.032	0.623 (0.027)	0.041
II	Car	Test Vehicle	0.446 (0.017)	0.036	0.484 (0.018)	0.033
	Truck	Test Vehicle	0.660 (0.033)	0.043	0.459 (0.018)	0.031

To investigate further the driver-vehicle interactions of the two scenarios (i.e. Case I and Case II) for a situation where there is one single acceleration (i.e. acceleration/deceleration combined), the data sets were combined and a new sensitivity parameters estimated for both cases (see Table 6-15). It was observed, for instance, in Case I that the truck drivers tend to response less with lower sensitivity compared to the drivers of passenger-cars as they follow the test vehicle. In Case II, however, it was observed that the test vehicle response stronger with larger sensitivity when following trucks compared to following passenger-cars of similar size with lower sensitivity. This is because of the limited visibility of the test vehicle driver's ability to see beyond and around the trucks. The results of the two cases investigated were expected. In general, the sensitivity of all the following drivers analysed were found to be varying following the leading vehicles for all the vehicle following scenarios considered. A study by Ranjitkar el al. (2005) using data from car following experiment conducted on a test track found the sensitivity of drivers varying towards their speed and spacing from the lead vehicles they were observed following (see also Treiterer and Myers, 1974).

It is worth noting that a single driver drove the test vehicle to collect data used in this analysis. As stated in Section 6.2.1.5, the test vehicle driver's behaviour following other vehicles may be influenced by the idea of being part of the experiment. The analysis of test vehicle following behaviour is valid for a single driver following a number of different vehicle types. It should be noted also that, the test vehicle followed 678 vehicles (i.e. 513 cars and 165 large vehicles) over several hours over a period from July to October the same year. A single driver following different types of vehicles at different times of the day, and on different days of the month will not have the same observed driving behaviour following about 678 vehicle types. The lead vehicles' driving behaviour will certainly influence the behaviour of the single driver at each point in time following these vehicles, hence different driving behaviours of the following vehicle will be observed

regardless of who is at the driving seat. Moreover, the weather condition, traffic flow, the type of road and the time of day or day of week during the driving process will certainly influence the driving behaviour of the same driver. The same driver driving under the influence of these factors will not have the same driving behaviour over long period of driving. Since the test vehicle followed several vehicle types under different driving or traffic conditions on several days in different months, different driving behaviours will be observed for the same driver, hence, it is appropriate to include the model in this study.

Table 6-15: Sensitivity estimates results for inter-vehicle interaction in car following situation

Scenario			Sensitivity	St. Dev.	Error
	Leader	Follower	(λ)		
I	Test Vehicle	Car	0.878	0.024	0.020
	Test Vehicle	Truck	0.696	0.073	0.037
II	Car	Test Vehicle	0.465	0.019	0.035
	Truck	Test Vehicle	0.560	0.101	0.037

6.5 Summary

Evidence in the available literature suggest that no or little attention have been given to the calibration of the GHR model using data obtained from truck following car or car following truck. There was also the need for more reliable and accurate driver behaviour data to calibrate the GHR model to produce a more reliable and acceptable model calibration parameters that best describe individual driving behaviour of car following car. This is because different data sets have produced different versions of the GHR model, but very few have been found to be most reliable and yet no reported agreement have been reached for a more general acceptable sets of model calibration parameters. The main contributions in this chapter have been the calibration of the GHR model with more reliable and accurate data sets to produce new sets of calibration parameters values for truck following car, car following truck and car following car for urban-rural and highway driving conditions.

In this chapter, the calibration and validation of the GHR car following model, which mostly serves as the basis for the development of most of the existing car following models were discussed. With evidence in literature pointing to the fact that the calibration of the existing models were based on a car following a car, there was a need to calibrate

the model with other vehicle types as the leader or as the follower. In view of that, the calibration of the GHR model using two main scenarios where the test vehicle was either the following or the leading vehicle were carried out. Data acquired by the use of an instrumented vehicle on a number of urban-rural and highway traffic corridors were used to calibrate and validate the model. The model calibration was done based on a number of scenarios including where a passenger-car was following the test vehicle, where truck was following the test vehicle and where the test vehicle was following a truck.

New sets of GHR model calibration parameters estimates or values for the three car following scenarios that best describes urban-rural and highway driving conditions were proposed. Half of the whole data set acquired was used to validate the model for this study. Using t-test statistics for the validation process, the test results revealed that there were no statistical significant differences in the observed data and the predicted data sets. In addition to proposing new versions of the GHR model, model comparisons (i.e. where a passenger-car was following the test vehicle) with the most reliable existing GHR models reviewed by Brackstone and McDonald (1999) were carried out to ascertain which of the existing GHR models best relates to the new version of the GHR model proposed. In comparison, the results showed that the new model parameters estimates relates closely to the Ozaki (1993) GHR model for the acceleration phase and Hoefs (1972) GHR model for the deceleration phase.

Further investigations were carried out involving driver-vehicle interactions mainly when the test vehicle was leading and when the test vehicle was following different vehicle types (i.e. cars and trucks). The investigations showed that, in both the acceleration phase and deceleration phase when the test vehicle was leading, the response of the passenger-car driver in terms of the following behaviour was much stronger than the response of the truck driver. It also revealed that, the response of the test vehicle as a follower was much stronger with high sensitivity to the leading trucks than that of the leading passenger-car in the acceleration phase.

The findings of the driver-vehicle interactions for this study are in agreement with the study conducted by Hoogendoorn and Ossen (2006) in the analysis of the two-leader car following situation when considering only the first leader and the following vehicles. In the deceleration phase, the findings revealed that the response of the test vehicle when following the trucks was less than that of the passenger-cars. One possible explanation

could be that of the driver's awareness of the slow deceleration rate (i.e. longer braking distance) of large vehicles and the reduced speed during deceleration. This might have prompted the driver to begin to anticipate that the traffic downstream was also coming to a stop, hence to decide to react earlier than expected to the large vehicle in front.

The next chapter discusses the formulation of car following models proposed in this study. It discusses the formulation of car following models and two-leader car following models including the models extension to include gender, vehicle occupancy and corridor (road) type characteristics. It also discusses the formulation of bus following models.

CHAPTER 7 DISTANCE-BASED CAR FOLLOWING MODELS: FORMULATION OF MODELS

7.1 Introduction

In Chapter 6, the calibration of the GHR car following model that produced new sets of calibration parameters for different vehicle type following behaviour were discussed. The response of following vehicles to leading vehicles in car following scenarios was also discussed in Chapter 6. Most of the existing car following models proposed in the available literature were developed with data usually obtained from an uncertain experimental methods (Kim and Lovell, 2003) or simple experiment. Most importantly, data from test tracks (Chandler et. al., 1958; Brockfeld et al., 2004) and video cameras placed at fixed positions and on tall buildings or on a helicopter (Mehmood and Easa, 2010; Gunay and Woodward 2007; Hoogendoorn et al., 2003), which usually come with limitations with the length or distance that can be covered tracking the same target vehicles.

The complexity involved in the video analysis also have some drawbacks and limit the size of data that can be analysed (Gunay and Erdemir, 2011). Other models are also developed before calibration and validation (Kim, 2005), which could make it difficult to ascertain it's reliability in predicting real world scenarios. Evidence in the literature suggest that most of the car following models were developed based on the acceleration of the following vehicles, with very few models developed based on the safe or desired following distance of the following vehicles (see Brackstone and McDonald, 1999).

The gaps identified in the literature for this study are briefly discussed in Chapter 6. In this chapter, the novelty include the formulation of distance-based car following model, distance-based two-leader car following model and distance-based bus following model. Other novelty in this chapter include the extended model formulation of the distance-based car following models to incorporate other socioeconomic variables that influence driving behaviour. The code names and descriptions of the model formulations developed in this chapter are presented in Chapter 6 Section 6.1.1.

In this chapter, distance-based car following models formulations are discussed. Section 7.2 discusses the development of a distance-based car following model, which often refers

to as follow the leader model. Vehicle characteristics, traffic corridor types and driver characteristics effect on following behaviour are investigated and discussed in this chapter. In a car following process, it has been found that drivers does not only concentrate on the vehicle immediately in front, but response to the second vehicle ahead (Hoogendoorn and Ossen, 2006). Section 7.4 of this chapter discusses the two-leader car following process. It discusses the formulation or development of a new distance-based two-leader car following model that best describes the driving behaviour on a number of traffic corridors. New car following models that incorporates gender, vehicle occupancy and corridor type are proposed and discussed in Sections 7.3 and 7.5.

With growing interest in the use of public transport, major cities around the world are introducing more bus services into the networks that are already congested. In some areas, for instance, vehicles share the same road spaces with public buses and these vehicles are, in some cases, forced to follow the public buses in their commutes. Vehicles following buses presents their own challenges to the drivers because of the slow movement and most often, the stop-start-and-go process of the buses. Section 7.8 investigates the bus following behaviour. A distance-based bus following model is proposed and discussed in this section. Finally, Section 7.9 summaries the analysis of this chapter.

7.2 Distance-Based Car Following Model Formulation

A new distance-based car following model for this study is proposed and forms the basic model for all extended models development. To begin with, a description of the data sets used for the modelling of the car following is given. Only the data sets obtained for the following vehicles (i.e. when the test vehicle was leading) are used for the car following modelling in this study. The whole data set was initially use to calibrate the model to determine the final model parameters. The data set consists of 525 individual uninterrupted vehicle-following situations. As discussed in Chapter 4, the relative distance of the following vehicles to be included in the car following modelling was set to 75 metres.

The maximum safe distance headway threshold of 75 metres was applied to the whole data set, resulting in obtaining 403 individual uninterrupted following vehicles. This represents 96,052 individual time series data points with a time step of 0.1 seconds for vehicles following the test vehicle. The final data set referred to as the Main Data Set then

split into two equal halves: Data File 1 and Data File 2 (see Figure 7-2) using the spreadsheet split file program discussed in Chapter 6. Data File 1 consists of 214 individual uninterrupted following vehicles and Data File 2 consists of 189 individual uninterrupted following vehicles representing 48,027 and 48,026 individual time series data points respectively. Data set (i.e. Data File) 1 was used in the car-following model calibration and Data set 2 was used to validate the model discussed in Section 7.2.3.

Studies have shown that car following models numerically perform well with the time step or update time step (Kesting and Treiber, 2008b) in car following models in place of reaction time. For instance, Gipps (1981) in the derivative of the car following model, sets the time step to equal to the reaction time of the drivers. Gipps observed numerically that the model performs well with the iteration or simulation with the time step (Wilson, 2001; Kesting and Treiber, 2008b). For example, the traffic microsimulation model AIMSUM that implements the Gipps model uses the following driver's reaction time equal to the simulation time step, hence at every time step, drivers following react immediately to the leading drivers actions (Olstam and Tapani, 2004). Newell (1961) model is an example of iterated coupled map model that incorporates the time step (Kesting and Treiber, 2008b). For this study, the driving behaviour data obtained are from vehicles (both leading and following the test vehicle) constantly in motion without stopping (i.e. stopped vehicles data were excluded from the final data set) during the car following process. The real driving behaviour data obtained have a time step or increment of 0.1 seconds at each stage of the following process, which reflects the actual driving behaviour of individual vehicles observed. These data sets were used in all the models calibrations discussed in this chapter. Hence, for this study, the time step was used instead of the reaction time for all the models formulation discussed in this chapter. A time step Δt of 0.1 seconds (Brockfeld, 2004), the rate at which the driving behaviour data were obtained was used for all model calibrations in this study.

7.2.1 The General Model Formulation

Now to develop the basic car following model, we consider the dynamic equations using the simple car following scenario shown in Figure 7-1 as follows:

$$\Delta x_n = x_{n-1} - x_n \tag{7-1}$$

$$\frac{dx}{dt} = \dot{x} = v \quad ; \quad \frac{dv}{dt} = \ddot{x} = a \tag{7-2}$$

$$\Delta v_n = v_{n-1} - v_n \; ; \quad \Delta a_n = a_{n-1} - a_n \tag{7-3}$$

Where:

x_n and x_{n-1} - are the positions (m) of the following and the leading vehicles respectively,

Δx_n - is the relative distance (m) between the leading and the following vehicles,

v_n and v_{n-1} - are the speed (km/h) of the following and leading vehicles respectively,

Δv_n - is the relative speed (m/s) between the leading and the following vehicles,

a_n and a_{n-1} - are the acceleration (m/s^2) of the following and leading vehicles respectively,

Δa_n - is the relative acceleration (m/s^2) between the leading and the following vehicles respectively.

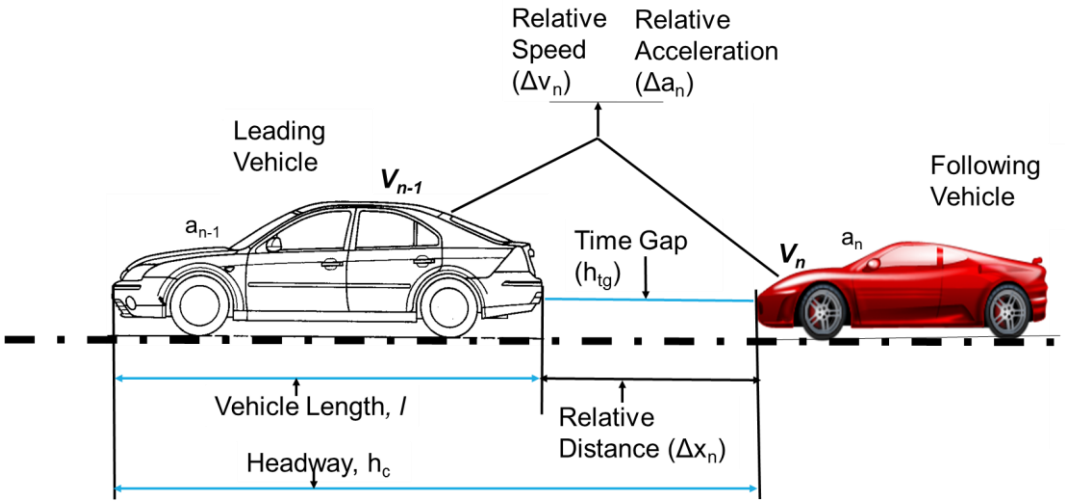

Figure 7-1: Simple car following process

The main motivation in this analysis is to model the safe or desired relative (following) distance between two vehicles following one another in a car following scenario. In order to determine the final parameters of the basic model, a preliminary model formulation was carried out with the whole data set. The model parameters that were not statistically significant at 95% (i.e. p-value > 0.05) confidence level were eliminated, and the process repeated until all the individual model parameters produced statistically significant estimates with p-values < 0.05 (95% confidence level). Two basic car following models are proposed. The new proposed models describes the following (relative) distance as a

function of the relative acceleration or acceleration of the following vehicle, relative speed, the speed of the following vehicle and the time gap (h_{tg}) or the time headway (h_c) of the following vehicle. The basic model is expressed as:

$$\Delta x(t) = f\left(\Delta a_n, \Delta v_n, v_n, h_{tg}, (h_c)\right) \ or\ f\left(a_n, \Delta v_n, v_n, h_{tg}, (\ h_c)\right) \tag{7-4}$$

The general formulations of the models are expressed as follows:

Model A: $$\Delta x(t+\Delta t) = \alpha_0 \Delta v_n(t+\Delta t) + \alpha_1 \Delta a_n(t+\Delta t) + \alpha_2 v_n(t) + \alpha_3 h_{tg}(t) + \varepsilon \tag{7-5}$$

Model B: $$\Delta x(t+\Delta t) = \alpha_0 \Delta v_n(t+\Delta t) + \alpha_1 \Delta a_n(t+\Delta t) + \alpha_2 v_n(t) + \alpha_3 h_c(t) + \varepsilon \tag{7-6}$$

Model C: $$\Delta x(t+\Delta t) = \alpha_0 \Delta v_n(t+\Delta t) + \alpha_1 a_n(t+\Delta t) + \alpha_2 v_n(t) + \alpha_3 h_{tg}(t) + \varepsilon \tag{7-7}$$

Model D: $$\Delta x(t+\Delta t) = \alpha_0 \Delta v_n(t+\Delta t) + \alpha_1 a_n(t+\Delta t) + \alpha_2 v_n(t) + \alpha_3 h_c(t) + \varepsilon \tag{7-8}$$

where $\alpha_0,\ \alpha_1,\ \alpha_2,\ \alpha_3$ are the calibration parameters to be determined and ε is the error term, h_{tg} and h_c are the time gap and the time headway in seconds respectively, Δt is the time step or increment in seconds and t is the time in seconds. Carrying out further analysis of the above models, Model A (eqn. 7-5) and Model C (eqn. 7-7) with the time gap produced better models with larger R^2 value than that of Model B (eqn. 7-6) and Model D (eqn. 7-8) with the time headway. For this analysis, Model A and Model C with the time gap are developed further as the basic or general car following model for this study. The general model estimation where b_o is constant is given by:

Model A:

$$\Delta x(t+\Delta t) = \alpha_0 \Delta v_n(t+\Delta t) + \alpha_1 \Delta a_n(t+\Delta t) + \alpha_2 v_n(t) + \alpha_3 h_{tg}(t) + b_o \tag{7-9}$$

Model C:

$$\Delta x(t+\Delta t) = \alpha_0 \Delta v_n(t+\Delta t) + \alpha_1 a_n(t+\Delta t) + \alpha_2 v_n(t) + \alpha_3 h_{tg}(t) + b_o \quad (7\text{-}10)$$

7.2.2 Model Parameters

The general model describes the following distance as a function of the relative speed, the speed of the following vehicle, the time gap and the relative acceleration between two vehicles for Model A or the following vehicle acceleration for Model C. The relative distance Δx_n (m), relative speed Δv_n (m/s), the relative acceleration Δa_n (m/s^2), the following vehicle speed v_n (km/h) and the following vehicle acceleration a_n measurements or calculations are discussed in Chapter 6 Section 6.2.1.1. In addition to these parameters, the time gap h_{tg} (s) measured from the rear bumper of the test vehicle to the front bumper of the target following vehicle. It is calculated as the ratio of the following (relative) distance to the speed of the following vehicle. The parameters such as the gender, the corridor type and the vehicle occupancy considered in the general model extension were obtained from the video-recorded data during the field experiment. These parameters obtained during the experiment were used in the modelling of the car following models. Table 7-1 shows a sample of the data set used to calibrate the distance-based car following models.

Table 7-1: Illustrate sample of the data set used to calibrate the distance-based car following models

Time [s]	Veh_ID	Δx [m]	Δa_n [m/s²]	Δv_n [m/s]	v_n [km/h]	h_{tg} [s]	Occupancy	Gender	Corridor (Cdr) Type		
							Occ 1= 1	Male = 1	Cdr 1	Cdr 2	Cdr 3
2.1	1	11.1	-0.19	-1.25	32.724	1.22112	1	1	1	0	0
2.2	1	11	-0.31	-1.3125	32.949	1.20186	1	1	1	0	0
2.3	1	10.8	-0.31	-1.4375	33.399	1.16411	1	1	1	0	0
2.4	1	10.8	-0.19	-1.375	31.158	1.24783	1	1	1	0	0
2.5	1	10.7	-0.88	-1.4375	31.383	1.22742	1	1	1	0	0
2.6	1	10.5	-0.63	-1.375	31.158	1.21317	1	1	1	0	0
2.7	1	10.3	-0.38	-1.4375	31.383	1.18153	1	1	1	0	0
2.8	1	10.2	-0.38	-1.4375	31.383	1.17006	1	1	1	0	0
2.9	1	10.1	-0.31	-1.4375	31.383	1.15859	1	1	1	0	0
3.0	1	10	-0.13	-1.375	29.142	1.23533	1	1	1	0	0
3.1	1	9.8	-0.81	-1.4375	29.367	1.20135	1	1	1	0	0
3.2	1	9.5	-0.31	-1.375	29.142	1.17356	1	1	1	0	0
3.3	1	9.4	-0.25	-1.375	29.142	1.16121	1	1	1	0	0
3.4	1	9.3	-0.4375	-1.4375	27.351	1.22409	1	1	1	0	0
3.5	1	9.1	-0.6875	-1.5625	27.801	1.17838	1	1	1	0	0
3.6	1	9	-0.6875	-1.5625	27.801	1.16543	1	1	1	0	0
3.7	1	8.9	-0.375	-1.5	27.576	1.16188	1	1	1	0	0

7.2.3 Model Validation: Modelled Against Observed Data

There was a need to validate the proposed general car following models to ascertain its reliability to predict accurately the real world scenarios of car following behaviour. To carry out the validation process, a t-test statistical significance testing method discussed in Chapter 6 was used to determine the significant differences between the empirical data obtained from the field and the predicted data from the general models. As already discussed in Section 7.2, one-half of the split data was used for the model validation process. Data set 2 (designated as Data set File A) that consists of 189 individual uninterrupted following vehicles, representing 48,026 individual time series data points with a step of 0.1 seconds was used for the model validation. To begin the validation process, the Data set 2 (A) file was further split into four different sets of data files. The data file A was initially split into two separate equal halves to produce new sets of data files, namely: Data file AA and Data file AB. Each sub data files were further split into two equal separate halves, given four new sets of different data files (i.e. sub data sets AAA, AAB, ABA and ABB with each containing 12,007 individual data points) used for the validation process (see Figure 7-2). Further detailed discussions on the models validation are presented in Chapter 8.

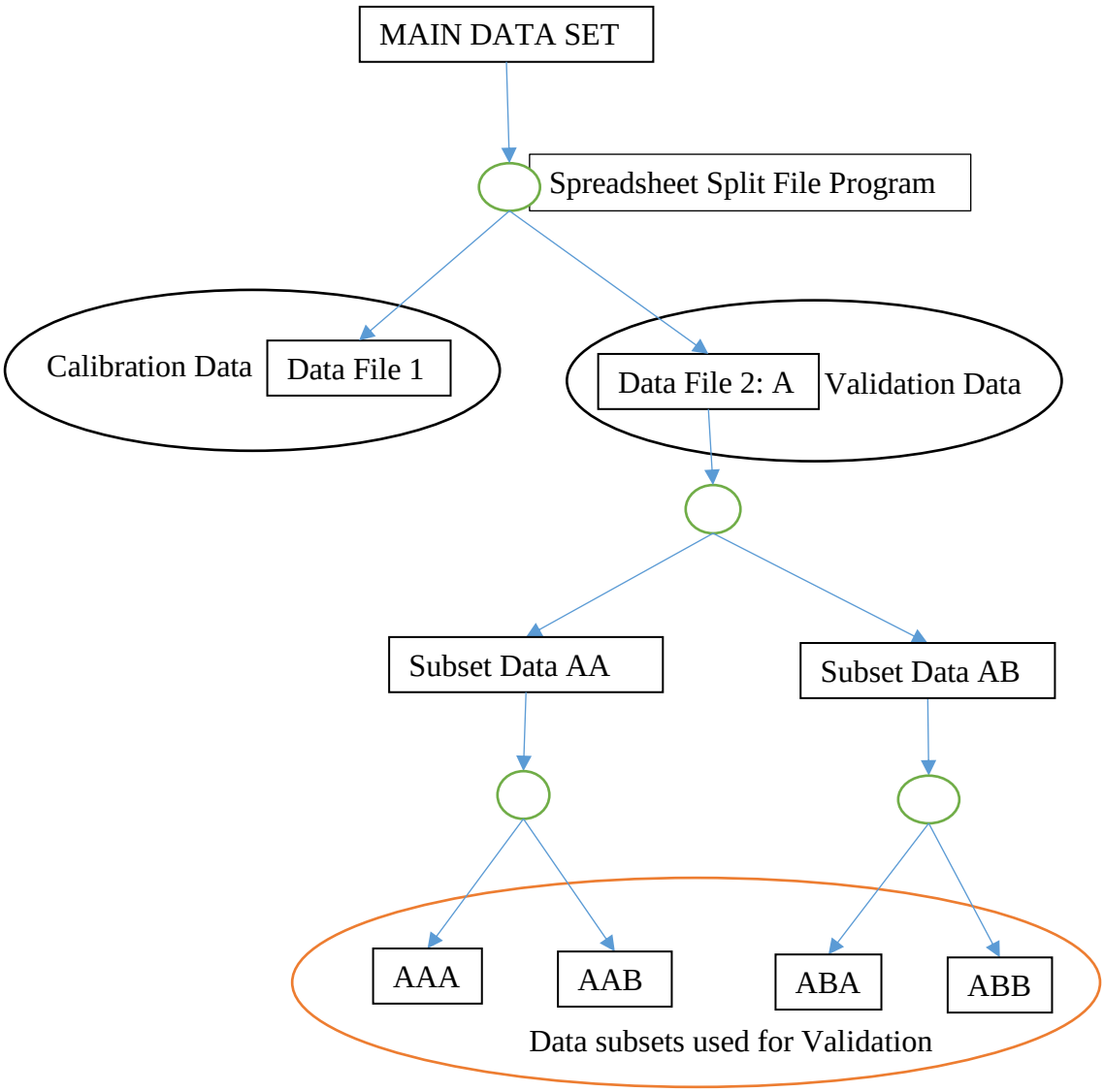

Data File 1 and Data File 2 (A)	Subset data of Main Data Set that comprises the Out and Return runs for all the AM and the PM data sets
Data AA and AB	Subset data sets of Data File 2: A
Data AAA, AAB and ABA, ABB	Subset data sets of Sub Data sets AA and AB respectively

Figure 7-2: Flowchart of data sets used for the calibration and validation of distance-based car following models

7.2.4 Model Simulation

It is essential to simulate the model with a number of some selected following vehicle pairs data and compare the performances of the simulation model results with that of the individual following vehicle's field observed data in car following scenario. To carry out the simulation process, a selected number of field data obtained from four individual following vehicles (i.e. vehicle drivers identified as 117, 102, 129 and 8) from different

traffic corridors under different conditions were used for the model simulation. The vehicles used in this analysis recorded a minimum car following duration of 35 seconds. The data sets for the four vehicles were collected in the morning peak hour period between 08:20 am and 09:20 am.

The car following microscopic data sets for Driver 117 and Driver 102 was collected on 31 July 2015 with each driver's data set consisting of 120 and 524 individual time sequence data points respectively. The data set for Driver 129 was obtained on 04 August 2015 and consists of 601 individual time sequence data points. The data set for Driver 8 was obtained on 07 August 2015 and consists of 127 individual time sequence data points. Each individual driver's data set were simulated using the proposed general Model A and the resulting simulation outputs plotted in comparison with the individual drivers' field observed data. The following distances for the simulation model and the field data were compared and analysed. Further detailed analysis is discussed in Chapter 8.

7.3 Model Extension Formulation

The general Model A was extended to incorporate the gender, vehicle occupancy and corridor type characteristics. Sections 7.3.1, 7.3.2 and 7.3.3 discusses the model extension formulation or development with these individual variables.

7.3.1 Car Following Model by Gender

To ascertain the gender effect and its significance on the following distance, a new model is proposed that takes into account the gender of the following vehicle driver. The proposed model is an extension of the general Model A proposed in this chapter. The whole data set was used in calibrating the gender model (Model A-1) discussed in Chapter 8. In all, 77 individual vehicles with female drivers and 326 individual vehicles with male drivers were observed following the test vehicle uninterrupted on all the four traffic corridors considered for this study. The data set consists of 96,052 individual time sequence data points at a time step of 0.1 seconds for the model calibration. A dummy variable or indicator variable to represent the gender of the driver is introduced into the general Model A. The generalised baseline model formulation (i.e. Model A-1) is as follows:

$$\Delta x(t+\Delta t) = \alpha_0 \Delta v_n(t+\Delta t) + \alpha_1 \Delta a_n(t+\Delta t) + \alpha_2 v_n(t) + \alpha_3 h_{tg}(t) + \alpha_4 g + \varepsilon \quad (7\text{-}11)$$

where g is the gender of the driver as a dummy or indicator variable. Since linear regression models takes numerical values, a binary value of 1 or 0 is assigned to the indicator variable. Since the gender has two categories, two scenarios can result from assigning the value of 1 or 0 to each category depending on which category of the gender is define in the model. The two scenarios the binary value can be assigned to the gender dummy variable in model development is as follows:

Scenario 1: Male = 1 and Female = 0
Scenario 2: Male = 0 and Female = 1

As already mentioned, these scenarios depend on the category of the gender defined in the model equation. For the purpose of this study, male is assigned 1 and female is assigned 0. Now, the estimate of the generalised baseline model is given by:

Model A-1:

$$\Delta x(t+\Delta t) = \alpha_0 \Delta v_n(t+\Delta t) + \alpha_1 \Delta a_n(t+\Delta t) + \alpha_2 v_n(t) + \alpha_3 h_{tg}(t) + \alpha_4 g + b_0 \quad (7\text{-}12)$$

7.3.2 Car Following Model by Vehicle Occupancy

To investigate the effect of the vehicle occupancy on the driving behaviour, an extension of the general Model A is proposed to include the vehicle occupancy. The vehicle occupancy is categorised into two groups: vehicle occupancy of one (1) (i.e. driver only) and vehicle occupancy of two or more (2+) passengers including the driver. The vehicle occupancy = 1 category consists of only the driver of the vehicle following and the vehicle occupancy = 2+ includes buses and all other vehicles following with more than one passenger on board.

In all, the data set for the model calibration consists of 289 individual following vehicles with occupancy of 1 and 114 individual following vehicles with occupancy of 2+. A dummy variable is introduced to represent the vehicle occupancy category in the general Model A. The proposed model (i.e. Model A-2) in the generalised form is as follows:

$$\Delta x(t+\Delta t) = \alpha_0 \Delta v_n(t+\Delta t) + \alpha_1 \Delta a_n(t+\Delta t) + \alpha_2 v_n(t) + \alpha_3 h_{tg}(t) + \alpha_4 oc + \varepsilon \quad (7\text{-}13)$$

where *oc* is the vehicle occupancy as an indicator variable in the model. A binary value of 1 or 0 was assigned to the vehicle occupancy indicator variable. Again, there can be two scenarios resulting from assigning the binary variable to the vehicle occupancy depending on the definition of the category in the proposed model. For the purpose of this model, vehicle occupancy of 1 assigned the value of 1 and vehicle occupancy of 2+ assigned the value of 0. The generalised model estimate equation is given by:

Model A-2:

$$\Delta x(t+\Delta t) = \alpha_0 \Delta v_n(t+\Delta t) + \alpha_1 \Delta a_n(t+\Delta t) + \alpha_2 v_n(t) + \alpha_3 h_{tg}(t) + \alpha_4 oc + b_o \quad (7\text{-}14)$$

7.3.3 Car Following Model by Corridor Type

To investigate the effect of corridor (road) type on car following behaviour, an extension of Model A is proposed to include the corridor type characteristics. Four different traffic corridor types were considered for this study. Corridor 1 is defined as urban traffic condition, Corridor 2 is defined as highway traffic condition, Corridor 3 is defined as urban-rural traffic condition and finally, Corridor 4 is defined as highway-urban traffic condition. These corridor types classification are discussed in Chapter 3. The data set used for the corridor type model calibration consists of 75, 111, 134 and 82 individual following vehicles for Corridor 1, Corridor 2, Corridor 3 and Corridor 4 respectively.

In order to assess the significant effect of the corridor type on the car following behaviour, dummy variables are introduced for each of the corridor type category under investigation. To prevent the dummy variables or the indicator variables (k = categories) terms adding up to one (1) in the model and interfere with the intercept term of the model, a multiple dummy variable equation, $k - 1$, was used to determine the number of variables to be included in the model development. For k = 4 traffic corridor type, $k - 1 = 4 - 1$ equals to 3 dummy variables to be included in the model development. Corridor 4 is a highway-urban traffic condition, which is a combination of Corridor 1 (urban) and Corridor 2 (highway) as one complete corridor. It is appropriate, therefore,

to eliminate Corridor 4 from the model formulation as dummy variable, as it is a combination of Corridor 1 and Corridor 2 considered in the model. The generalised model (i.e. Model A-3) equation is as follows:

$$\Delta x(t+\Delta t) = \alpha_0 \Delta v_n(t+\Delta t) + \alpha_1 \Delta a_n(t+\Delta t) + \alpha_2 v_n(t) + \alpha_3 h_{tg}(t) + \alpha_4 cr1 + \alpha_5 cr2 + \alpha_6 cr3 + \varepsilon \quad (7\text{-}15)$$

where $cr1$, $cr2$, and $cr3$ are the dummy variables representing traffic corridor 1, traffic corridor 2 and traffic corridor 3 respectively and ε is the error term. Binary value of 1 or 0 is assigned to the dummies and defined in the model formulation as follows:

Traffic corridor 1 ($cr1$) = 1, all other traffic corridors = 0
Traffic corridor 2 ($cr2$) = 1, all other traffic corridors = 0
Traffic corridor 3 ($cr3$) = 1, all other traffic corridors = 0

The proposed model estimate is given by:

Model A-3:

$$\Delta x(t+\Delta t) = \alpha_0 \Delta v_n(t+\Delta t) + \alpha_1 \Delta a_n(t+\Delta t) + \alpha_2 v_n(t) + \alpha_3 h_{tg}(t) + \alpha_4 cr1 + \alpha_5 cr2 + \alpha_6 cr3 + b_o \quad (7\text{-}16)$$

7.4 Distance-Based Two-Leader Car Following Model Formulation

A study by Hoogendoorn and Ossen (2006) suggests that following drivers does not only response to the vehicle directly ahead, but the leader to the first leader (i.e. the second leader) in a three vehicles movement. Literature supports the need for better and reliable car following models (Brockfeld et al., 2004), but silence on a robust two-leader car following models when evidence suggest that drivers do response to vehicle two or three ahead. Also, for drivers to be aware of one additional vehicle ahead of them does affects their distance gap (Sayer et al., 2000) to the immediate vehicle in front in a car following situation.

The existing two-leader car following models in the literature were developed based on an extension of the existing one-leader car following models (Bexelius, 1968; Lenz et al., 1999; Zhou and Li, 2012; Farhi et al., 2012), which evidence suggests that most of these

models were theoretically developed first before calibration of the models. Again, almost all the existing two-leader models describe the acceleration of the following vehicles when, in fact, other studies suggests that additional vehicle ahead of the immediate lead vehicle affects the following distance, yet the existing models do not address this following behaviour. Evidence supports the need for a two-leader car following model that is capable of predicting the following distance of a vehicle in a three vehicles movement. In this section, a two-leader car following model that is capable of predicting the desired following distance in a three vehicles movement is proposed. The proposed model was not developed as an extension of existing one-leader car following model. The model was developed using empirical data. The two-leader model formulation is discussed in this section.

7.4.1 Model Data Description

Using the video camera recordings for both the leading and following vehicles, all cases of three consecutive vehicles movements in car following scenarios were identified in the video and the corresponding radar sensors' numerical data for all three consecutive vehicles movements were extracted and processed. As discussed in Chapter 3, the instrumented vehicle used for this study was capable of observing three consecutive vehicles movement as seen in Figure 7-3. With the identified three vehicles movements, the rear following vehicles data sets (i.e. when the test vehicle was leading) were manually synchronised with the front leading vehicles data sets (i.e. when the test vehicle was following) using the system time stamp as the baseline reference for the synchronisation process. The two data sets (i.e. leading and following data sets) joined to form one complete data set.

Because the front and the rear radar sensors mounted on the test vehicle operates and processes data independently during the experiment, data from both the front and the rear target vehicles contain the same test vehicle's speed and acceleration data. At every time step of 0.1 seconds, the test vehicle's speed information was the same in both the front and rear vehicles' radar sensors' data sets for any three consecutive vehicles movement observed involving the immediate leading and following vehicles throughout the following process. Additional manual checks were carried out using the test vehicle's speed and acceleration columns of both the leading and the following vehicles data group within the main data set as reference points to ensure accurate data synchronisation was

done. Before the three vehicles synchronisation, the rear and the front observed target vehicles data sets were processed and analysed separately.

In all, 365 individual three consecutive vehicles movements were identified, processed and synchronised, representing 84,210 individual time series data points with a time step of 0.1 seconds. There were 13 buses, 259 cars, 33 trucks and 60 vans observed following the test vehicle as part of the three consecutive vehicles movements identified. As discussed in Chapter 4, the following distance headway threshold was set to 75 metres. Applying this threshold to the relative distances (i.e. between the second leader vehicle and the first leader (test vehicle) and, between the first leader and the following vehicles) for the three vehicles synchronised data set, a total of 82,939 individual time sequence data points were obtained. This resulted in 13 buses, 257 cars, 31 trucks and 58 vans individually following the test vehicle as part of the three consecutive vehicles movements, representing 359 individual following three vehicles movements' data as the main data set. The main data set or file then split into two sets of sub data files: Data file A and Data file B (see Figure 7-4), using the spreadsheet split data file program discussed in Chapter 6. One set of the data file (i.e. Data file B) was used for the model calibration and another set of the data file (i.e. Data file A) was used for the model validation.

7.4.2 The Two-Leader Car Following Model Formulation

In this section, a two-leader car following model capable of predicting the following distance in a two-leader car following process is proposed and developed. Considering the three consecutive vehicles movement shown in Figure 7-3, the same simple dynamic equations will result as earlier discussed in Section 7.2.1 of this chapter.

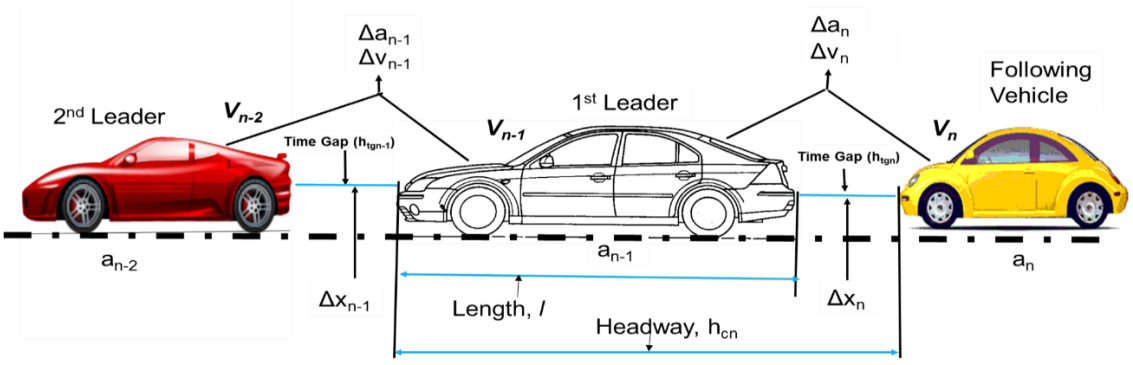

Figure 7-3: The three consecutive vehicles movement involving the test vehicle

The dynamic equations from the three vehicles movement (see Figure 7-3) are given by:

$$\Delta x_n = x_{n-1} - x_n \quad ; \quad \Delta x_{n-1} = x_{n-2} - x_{n-1} \tag{7-17}$$

$$\frac{dx}{dt} = \dot{x} = v \quad ; \quad \frac{dv}{dt} = \ddot{x} = a \tag{7-18}$$

$$\Delta v_n = v_{n-1} - v_n \quad ; \quad \Delta v_{n-1} = v_{n-2} - v_{n-1} \tag{7-19}$$

$$\Delta a_n = a_{n-1} - a_n \quad ; \quad \Delta a_{n-1} = a_{n-2} - a_{n-1} \tag{7-20}$$

$$h_{cd} = l + \Delta x_n \tag{7-21}$$

Where:

x_n, x_{n-1} and x_{n-2} – are the positions (m) of the following, first (1st) leader and second (2nd) leader vehicles respectively,

Δx_n – is the relative distance (m) between the first leader and the following vehicles,

Δx_{n-1} – is the relative distance (m) between the first leader and second leader vehicles,

v_n, v_{n-1} and v_{n-2} – are the speeds (km/h) of the following, first leader and second leader vehicles respectively,

Δv_n – is the relative speed (m/s) between the first leader and the following vehicle,

Δv_{n-1} – is the relative speed (m/s) between the second leader and the first leader vehicles,

a_n, a_{n-1} and a_{n-2} – are the accelerations (m/s^2) of the following, the first leader and the second leader vehicles respectively,

Δa_n – is the relative acceleration (m/s^2) between the first leader and the following vehicles,

Δa_{n-1} – is the relative acceleration (m/s^2) between the second leader and the first leader vehicles,

h_{cn} – is the distance headway (m) of the following vehicle,

h_{tgn} – is time gap (s) between the first leader and the following vehicles,

h_{tgn-1} –- is time gap (s) between the first leader and the second leader vehicles,

l – is the length (m) of the first leader vehicle (test vehicle).

In order to determine the two-leader model parameters, a preliminary model formulation was carried out using a sizable data set and later using the whole data set. In developing

the model, the model parameters were added to the model one at a time and at different stages of the modelling process, after which multiple linear regression analysis performed to ascertain the significance of each individual parameters included in the model. The parameters that were found not to be statistically significant at 95% confidence level with p-value > 0.05 were eliminated. The process continued until the final model parameters were determined with all the model parameters statistically significant at 0.05 confidence level (i.e. p-values < 0.05).

The final model describes the relative distance of following vehicle in a three consecutive vehicles following movement. The new model proposed is expressed as a function of the relative acceleration and relative distance between the first leader and second leader vehicles, the speed of the second leader vehicle, the relative speed between the first leader and the following vehicles, the speed of the following vehicle, the time gap (h_{tgn}) between the first leader and the following vehicles and the acceleration of the following vehicle. The model is expressed as:

$$\Delta x(t+\Delta t) = f\left(\Delta a_{n-1}, \Delta x_{n-1}, \Delta v_n, v_{n-1}, v_n, h_{tgn}, a_n\right) \tag{7-22}$$

Two different models, one model incorporates the following vehicle's acceleration and the other model is without the following vehicle's acceleration, emanated from the two-leader model formulation. The general formulation of the two-leader models are given by:

Model A2:

$$\begin{aligned}\Delta x(t+\Delta t) = {} & \beta_0 \Delta a_{n-1}(t+\Delta t) + \beta_1 \Delta x_{n-1}(t+\Delta t) + \beta_2 v_{n-2}(t) \\ & + \beta_3 \Delta v_n(t+\Delta t) + \beta_4 v_n(t) + \beta_5 h_{tgn}(t) + \beta_6 a_n(t+\Delta t) \\ & + \varepsilon\end{aligned} \tag{7-23}$$

Model B2:

$$\begin{aligned}\Delta x(t+\Delta t) = {} & \beta_0 \Delta a_{n-1}(t+\Delta t) + \beta_1 \Delta x_{n-1}(t+\Delta t) + \beta_2 v_{n-2}(t) + \\ & \beta_3 \Delta v(t+\Delta t) + \beta_4 v_n(t) + \beta_5 h_{tgn}(t) + \varepsilon\end{aligned} \tag{7-24}$$

where $\beta_0,\ \beta_1,\ \beta_2,\ \beta_3,\ \beta_4, \beta_5$ and β_6 are the calibration parameters to be determined; t is the time in seconds, Δt is the time step or increment in seconds and ε is the error term. The general model estimation (where b_0 = constant) are as follows:

Model A2:

$$\Delta x(t+\Delta t) = \beta_0 \Delta a_{n-1}(t+\Delta t) + \beta_1 \Delta x_{n-1}(t+\Delta t) + \beta_2 v_{n-2}(t) + \beta_3 \Delta v_n(t+\Delta t) + \beta_4 v_n(t) + \beta_5 h_{tgn}(t) + \beta_6 a_n(t+\Delta t) + b_0 \quad (7\text{-}25)$$

Model B2:

$$\Delta x(t+\Delta t) = \beta_0 \Delta a_{n-1}(t+\Delta t) + \beta_1 \Delta x_{n-1}(t+\Delta t) + \beta_2 v_{n-2}(t) + \beta_3 \Delta v(t+\Delta t) + \beta_4 v_n(t) + \beta_5 h_{tgn}(t) + b_0 \quad (7\text{-}26)$$

7.5 The Two-Leader Model Extension Formulation

As earlier discussed, the transport related variables or factors considered in the extension of the follow-the-leader distance-based car following model proposed in Section 7.3 are investigated further with the two-leader car following model proposed in this study to assess their influence on driving behaviour. The extension of the two-leader model formulated to incorporate the gender of the driver, the following vehicle occupancy and the corridor type characteristics. Model A2 was developed further to incorporate these variables or factors in order to investigate their effects on driving behaviour.

7.5.1 The Gender Two-Leader Model

To investigate the effect of gender on two-leader car following model, an extension of the general model (Model A2) to include the gender characteristic is proposed. The general equation of the model (i.e. Model A2-5) is given by:

$$\Delta x(t+\Delta t) = \beta_0 \Delta a_{n-1}(t+\Delta t) + \beta_1 \Delta x_{n-1}(t+\Delta t) + \beta_2 v_{n-2}(t) + \beta_3 \Delta v_n(t+\Delta t) + \beta_4 v_n(t) + \beta_5 h_{tgn}(t) + \beta_6 a_n(t+\Delta t) + \beta_7 g + \varepsilon \quad (7\text{-}27)$$

To calibrate Model A2-5 (i.e. eqn. 7-27), the gender (g) variable is assigned a binary value of 1 or 0 as discussed in Section 7.3.1. For this investigation, the male is assigned 1 and female is assigned 0. The model estimate equation is as follows:

Model A2-5:

$$\Delta x(t+\Delta t) = \beta_0 \Delta a_{n-1}(t+\Delta t) + \beta_1 \Delta x_{n-1}(t+\Delta t) + \beta_2 v_{n-2}(t) + \beta_3 \Delta v_n(t+\Delta t) + \beta_4 v_n(t) + \beta_5 h_{tgn}(t) + \beta_6 a_n(t+\Delta t) + \beta_7 g + b_0 \quad (7\text{-}28)$$

The sample size of the data set used for calibrating Model A2-5 (eqn. 7-28) is 74,999 individual time series data points with a time step of 0.1 seconds. The data set consists of 75 individual following vehicles with female drivers and 319 individual following vehicles with male drivers observed during the experiment and used for Model A2-5 (eqn. 7-28) calibration discussed in Chapter 9.

7.5.2 The Vehicle Occupancy Two-Leader Model

To investigate the effect of following vehicle occupancy on a three consecutive vehicles in motion, an extension of the general distance-based two-leader car following model (Model A2) to include vehicle occupancy is proposed to assess its effect on driving behaviour. The proposed model (Model A2-6) equation formulated as:

$$\Delta x(t+\Delta t) = \beta_0 \Delta a_{n-1}(t+\Delta t) + \beta_1 \Delta x_{n-1}(t+\Delta t) + \beta_2 v_{n-2}(t) + \beta_3 \Delta v_n(t+\Delta t) + \beta_4 v_n(t) + \beta_5 h_{tgn}(t) + \beta_6 a_n(t+\Delta t) + \beta_7 oc + \varepsilon \quad (7\text{-}29)$$

A binary value of 1 or 0 is assigned to the occupancy (oc) indicator variable in the general Model A2-6 for the calibration of the model. As earlier discussed in Section 7.3.2,

vehicles with occupancy of one (1) is assigned 1 and vehicles with two or more (2+) occupancy is assigned 0. The model estimate is given by:

Model A2-6:

$$\Delta x(t+\Delta t) = \beta_0 \Delta a_{n-1}(t+\Delta t) + \beta_1 \Delta x_{n-1}(t+\Delta t) + \beta_2 v_{n-2}(t) + \beta_3 \Delta v_n(t+\Delta t) + \beta_4 v_n(t) + \beta_5 h_{tgn}(t) + \beta_6 a_n(t+\Delta t) + \beta_7 oc + b_0 \quad (7\text{-}30)$$

The sample size of the data set used for calibrating Model A2-6 (eqn. 7-30) is 74,999 individual time series data points. The data set consists of 238 individual identified following vehicles with only the drivers as the occupant (i.e. occupancy = 1) and 111 individual following vehicles with two or more occupants including the drivers (i.e. occupancy = 2+) observed during the experiment. Model A2-6 calibration is further discussed in Chapter 9.

7.5.3 The Corridor Type Two-Leader Model

To ascertain the effect of corridor type characteristics on three consecutive vehicles in motion, an extension of the two-leader car following model that incorporates the corridor type is proposed. The model describes the influence of the type of corridor on driving behaviour of following vehicle in a two-leader car following movement. The model (Model A2-7) equation is given by:

$$\Delta x(t+\Delta t) = \beta_0 \Delta a_{n-1}(t+\Delta t) + \beta_1 \Delta x_{n-1}(t+\Delta t) + \beta_2 v_{n-2}(t) + \beta_3 \Delta v_n(t+\Delta t) + \beta_4 v_n(t) + \beta_5 h_{tgn}(t) + \beta_6 a_n(t+\Delta t) + \beta_7 cr1 + \beta_8 cr2 + \beta_9 cr3 + \varepsilon \quad (7\text{-}31)$$

The corridor type variables $cr1$, $cr2$ and $cr3$ introduced into the model as dummy variables. As earlier discussed in Section 7.3.3, binary value (1 or 0) is assigned to the dummy variables in order to calibrate the model and investigate the effects of the corridor type characteristics on driving behaviour. The model estimate is as follows:

Model A2-7:

$$\Delta x(t+\Delta t) = \beta_0 \Delta a_{n-1}(t+\Delta t) + \beta_1 \Delta x_{n-1}(t+\Delta t) + \beta_2 v_{n-2}(t) + \beta_3 \Delta v_n(t+\Delta t) + \beta_4 v_n(t) + \beta_5 h_{tgn}(t) + \beta_6 a_n(t+\Delta t) + \beta_7 cr1 + \beta_8 cr2 + \beta_9 cr3 + b_0 \quad (7\text{-}32)$$

The sample size of the data used for Model A2-7 (eqn. 7-32) calibration is 74,999 individual time series data points. The data set consists of 74, 102, 134 and 80 individual three consecutive vehicles movements identified for Corridor 1, Corridor 2, Corridor 3 and Corridor 4 used for Model A2-7 calibration respectively. Model A2-7 calibration is discussed in detail in Chapter 9.

7.6 The Two-Leader Model Parameters

The leading relative acceleration Δa_{n-1} (m/s^2) and leading relative distance Δx_{n-1} (m/s) between the first leading and the second leading vehicles are measured directly by the front sensor. The speed v_{n-2} (km/h) of the second leading vehicle was calculated using the leading relative speed Δv_{n-1} (between the first leading vehicle and the second leading vehicle) and the test vehicle's speed v_{n-1} (km/h) measured directly from the test vehicle's ground speed via the engine. These parameters obtained during the experiment, in addition to the model parameters discussed in Chapter 6 Section 6.2.1.1 and Section 7.2.2 were used in the modelling of the distance-based two-leader car following models. Table 7-2 shows a sample of the data set used to calibrate the two-leader distance-based car following models.

Table 7-2: Illustrate sample of the data set used to calibrate the two-leader distance-based car following model

Time [s]	Veh_ID	Δx [m]	Δa_{n-1} [m/s²]	Δx_{n-1} [m]	v_{n-1} [km/h]	Δv_n [m/s]	v_n [km/h]	h_{tgn} [s]	a_n [m/s²]	Occupancy	Gender	Corridor (Cdr) Type		
										Occ 1= 1	Male = 1	Cdr 1	Cdr 2	Cdr 3
2.1	1	11.1	-1	47.8	22.338	-1.25	40.788	0.9797	-1.1925	1	1	1	0	0
2.2	1	11	-0.9375	47.6	20.322	-1.3125	38.997	1.015463	-1.0675	1	1	1	0	0
2.3	1	10.8	0	47	19.872	-1.4375	39.447	0.985626	-1.0675	1	1	1	0	0
2.4	1	10.8	-0.625	46.8	19.422	-1.375	39.222	0.99128	-1.1925	1	1	1	0	0
2.5	1	10.7	-1.125	46.2	18.747	-1.4375	39.447	0.9765	-0.365	1	1	1	0	0
2.6	1	10.5	-1.3125	45.9	18.522	-1.375	39.222	0.963745	-0.615	1	1	1	0	0
2.7	1	10.3	-1.375	45.3	17.847	-1.4375	39.447	0.939995	-0.865	1	1	1	0	0
2.8	1	10.2	-1.4375	44.9	17.397	-1.4375	39.447	0.930869	-0.865	1	1	1	0	0
2.9	1	10.1	-1.4375	44.3	16.497	-1.4375	39.447	0.921743	-0.9275	1	1	1	0	0
3.0	1	10	-1.5	44	14.256	-1.375	37.206	0.967586	-1.115	1	1	1	0	0
3.1	1	9.8	-0.5	43.3	13.581	-1.4375	37.431	0.942534	-0.4275	1	1	1	0	0
3.2	1	9.5	-1.1875	43	13.356	-1.375	37.206	0.919207	-0.9275	1	1	1	0	0
3.3	1	9.4	-1.5625	42.2	12.906	-1.375	37.206	0.909531	-0.990	1	1	1	0	0
3.4	1	9.3	-1.6875	41.9	12.456	-1.4375	37.431	0.894446	-0.603	1	1	1	0	0
3.5	1	9.1	-1.6875	41.1	11.556	-1.5625	37.881	0.864813	-0.353	1	1	1	0	0
3.6	1	9	-1.75	40.7	11.106	-1.5625	37.881	0.85531	-0.353	1	1	1	0	0
3.7	1	8.9	-1.6875	39.9	10.431	-1.5	37.656	0.85086	-0.665	1	1	1	0	0

7.7 The Two-Leader Model Validation and Simulation

The whole data set (consisting of 82,939 individual data points) was split into two sets of data files as earlier discussed. One set of the data file was used for the validation of the two-leader car following models proposed in this chapter. The model validation is to ascertain the model's reliability and the magnitude of deviation from the predicted data set. T-test statistics method discussed in Chapter 6 was used to carry out the model validation analysis. Data file A was used for the model validation. Data file A was split into two halves, AA and AB sub data files. Sub data files AA and AB each consisting of 20,735 individual time series data points. Each set of sub data files were further divided into two halves (i.e. Sub data files AAA and AAB for data file AA; Sub data files ABA and ABB for data file AB) with each data file consisting of a minimum of 10,368 individual time series data points (see Figure 7-4). In all, four different sub data sets or files were used for the validation of the general models.

In order to assess the reliability of the models in describing real world scenarios of two-leader car following, a number of selected three vehicles movements were simulated against the observed data. The results of the simulation runs then compared with the selected vehicle's own observed data and analysed to assess the capabilities of the models developed. The model simulation process strengthens the reliability of the two-leader car following model in describing the driving behaviour of a three consecutive vehicles movement. The three vehicles movements used for the model simulation were selected based on the following vehicles (i.e. vehicles following the test vehicle). The following vehicles were identified by the vehicle's ID assigned during the data processing stage.

The four selected following vehicles were identified as Driver 413, Driver 414, Driver 453 and Driver 340. Driver 413 and Driver 414 following vehicle data sets were collected on Friday, 31 July 2015 with a following duration of 83 seconds and 192 seconds respectively. The data sample size for Driver 413 consists of 174 individual time series data points and for Driver 414 consists of 248 individual time series data points used for the respective simulation runs. Driver 453 following data set was obtained on Wednesday, 05 August 2015 with a following time duration of 40 seconds and data sample size consisting of 110 individual time series data points. Driver 340 following data set was

obtained on Wednesday, 16 September 2015 with a following duration of 132 seconds and data sample size consisting of 161 individual time series data points.

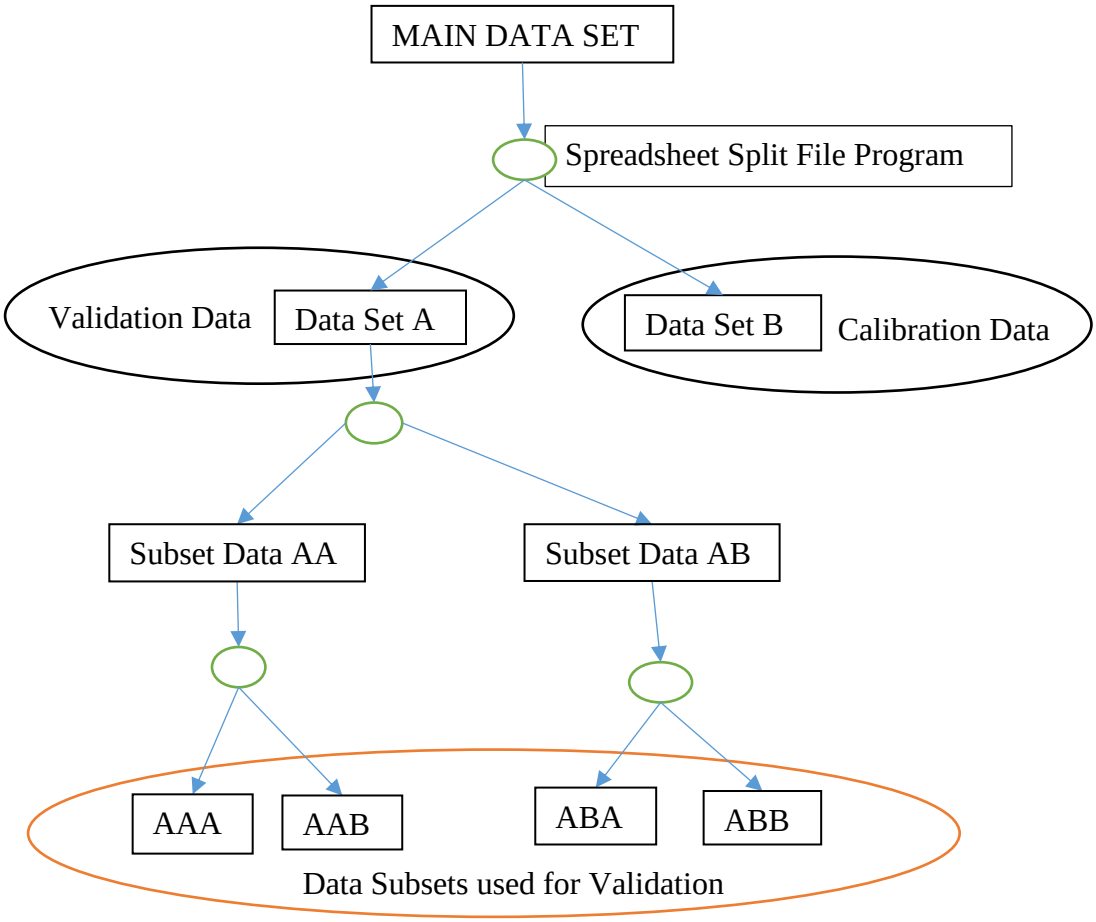

Data Set A and Data Set B	Subset data of Main Data Set that comprises the Out and Return runs for all the AM and the PM data sets
Data AA and AB	Subset data of Sub Data Set A
Data AAA and AAB	Subset data of Sub Data Set AA
Data ABA and ABB	Subset data of Sub Data Set AB

Figure 7-4*:* Flowchart of data sets used for the calibration and validation of distance-based two-leader car following models

7.8 The Bus Following Model Formulation

Vehicle following, in recent years, have gained much attention resulting in a number of different car following models being proposed or developed. Each of these models seeks to describe vehicle-to-vehicle interactions in a car following scenario. Large vehicle interactions with other vehicle types have not been given much attention in car following

situations. Studies have shown that car drivers interact differently following large vehicles to following vehicles of the same type or size (Sayer et al., 2003; Hoogendoorn and Ossen, 2006) in car following situations. For instance, in the urban areas, public commuter buses often share the same road space with other vehicle types within the network, and by so doing, the buses interact with the vehicles as they commute via the network. Little is known in the literature to support models that describe the interactions between cars following buses in a car following scenario.

Many studies have been conducted involving public buses but very few attention given to studies on bus following. Rothery et al. (1964) conducted a study involving one bus following another bus to determine the validity of existing car following model calibration parameters. The study focused on using the two buses following speed variability to determine the validity and parameters of the existing car following models. It also compared the steady-state stream properties of a single-lane bus flow involving several buses following each other with the car following model prediction of the two buses following situation. The study was only limited, supposedly, to bus following bus but not on other vehicle types following the buses considered in the study.

In attempt to evaluate the effect of a bus station on bus movement, Tang et al. (2012) developed a bus following model base on an online bus station. The model only considers the phenomena that result from the behaviour of a bus and that of a bus station, but did not consider the bus following effect on the traffic flow dynamics. Appiah et al. (2015) proposed a bus following model that describe the interaction between a car and a bus in a car following situation within an urban area. The study suggested that size of the bus and its associated slow movement within the city affects driver behaviour of the following car. The interactions between cars and buses required to be investigated further, as evidence suggests that not much attention have been given to this special kind of driving behaviour involving a car following a bus or a number of buses in a bus following situation within a congested urban networks. With the improvements in driver behaviour microscopic data acquisition, this study proposes and develop new bus following models that best describe the driver behaviour in keeping a safe or desired following distance directly behind a bus in a bus following situation within urban-rural driving conditions.

7.8.1 Bus Following Model Formulation

A new bus following model that describes the behaviour of a car following a bus is proposed and developed in this section. To develop the model, a number of traffic corridors were selected where there were no restrictions on road lane use (i.e. no-bus only lane restrictions) to follow a number of buses for the collection of bus following microscopic data for this study. Eight different double decker commuter buses were followed using the instrumented vehicle discussed in Chapter 3. The whole bus following data set consists of 30,948 individual time series data points with a time step of 0.1 seconds. The safe headway distance threshed of 75 metres was applied to the whole data set and obtained 30,766 individual time series data points. The data set was obtained from the front radar sensor of the instrumented vehicle when following the buses. This data set was used for the bus following models development. The whole data set was split into two equal halves: Data file A and Data file B. Data set B was used for the model calibration and Data set A was used for the model validation (see Figure 7-6).

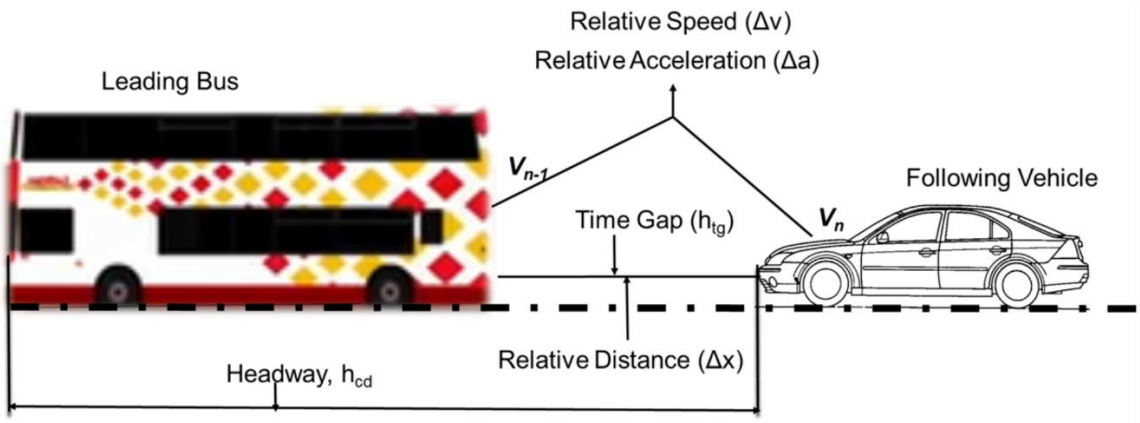

Figure 7-5: Simple bus following scenario

Consider the simple bus following scenario shown in Figure 7-5, the same dynamic equations discussed in Sections 7.2.1 and 7.4.2 can be observed for the bus following scenario. The whole data set was first used to carry out preliminary formulation of the models to determine the models parameters that were included in the final bus following models. The model parameters not statistically significant at 95% confidence level were eliminated until the final models parameters were determined. The final models parameters were all statistically significant at 95% confidence level (i.e. all p-values < 0.05). The proposed models describes the following behaviour of a car following a bus in

keeping a safe or desired following distance to the bus. The following distance expressed as a function of the following vehicle speed, the time gap between the bus and the following vehicle, the relative speed and relative acceleration between the bus and the following vehicle. The model is expressed as:

$$\Delta x(t+\Delta t) = f\left(\Delta a_n, \Delta v_n, v_n, h_{tg}\right) \text{ or } f\left(\Delta a_n, v_{n-1}, v_n, h_{tg}\right) \quad (7\text{-}33)$$

Three main bus following models are proposed for this study. The general formulation of the models are as follows:

Model B1-1:

$$\Delta x(t+\Delta t) = \lambda_0 v_n(t) + \lambda_1 \Delta v_n(t+\Delta t) + \lambda_2 \Delta a_n(t+\Delta t) + \lambda_3 h_{tg}(t) + \varepsilon \quad (7\text{-}34)$$

Model B1-2:

$$\Delta x(t+\Delta t) = \lambda_0 v_{n-1}(t) + \lambda_1 \Delta v_n(t) + \lambda_2 \Delta a_n(t+\Delta t) + \lambda_3 h_{tg}(t) + \varepsilon \quad (7\text{-}35)$$

Model B1-3:

$$\Delta x(t+\Delta t) = \lambda_0 v_n(t) + \lambda_1 v_{n-1}(t) + \lambda_2 \Delta a_n(t+\Delta t) + \lambda_3 h_{tg}(t) + \varepsilon \quad (7\text{-}36)$$

where λ_0, λ_1, λ_2 and λ_3 are the calibration parameters to be determined and ε is the error term of the model. All the model parameters produced estimates with p-values < 0.05. Data set B consisting of 15,379 time series data points was used for the models calibration. The models calibrations are further discussed in Chapter 10. Model B1-1 and Model B1-2 produced the same R^2 values during the models development. The general model estimation equations are as follows:

Model B1-1:

$$\Delta x(t+\Delta t) = \lambda_0 v_n(t) + \lambda_1 \Delta v_n(t+\Delta t) + \lambda_2 \Delta a_n(t+\Delta t) + \lambda_3 h_{tg}(t) + b_0 \quad (7\text{-}37)$$

Model B1-2:

$$\Delta x(t+\Delta t) = \lambda_0 v_{n-1}(t) + \lambda_1 \Delta v_n(t+\Delta t) + \lambda_2 \Delta a_n(t+\Delta t) + \lambda_3 h_{tg}(t) + b_0 \quad (7\text{-}38)$$

Model B1-3:

$$\Delta x(t+\Delta t) = \lambda_0 v_n(t) + \lambda_1 v_{n-1}(t) + \lambda_2 \Delta a_n(t+\Delta t) + \lambda_3 h_{tg}(t) + b_0 \quad (7\text{-}39)$$

7.8.2 The Bus Following Model Validation

As earlier discussed, the whole data set was split into two sets of sub data. Data file A was used for the model validation process. Data file A consists of 15,387 individual time series data points. Data file A was further split into two sets of sub data files: Sub Data file AA and Sub Data file AB. Sub Data file AA and Sub Data file AB consists of 7,694 and 7,695 individual time series data points respectively. Sub Data files AA and AB was further split into two equal halves, resulting in four separate new sub data files (i.e. Sub Data files AAA, AAB, ABA and ABB) (see Figure 7-6). These data files were used for the validation of the models discussed in Chapter 10. The four sub data files each consists of a minimum of 3,845 individual time series data points. The t-test statistical analysis method discussed in Chapter 6 was again used for the models validation to ascertain the significant differences between the predicted data and the observed data.

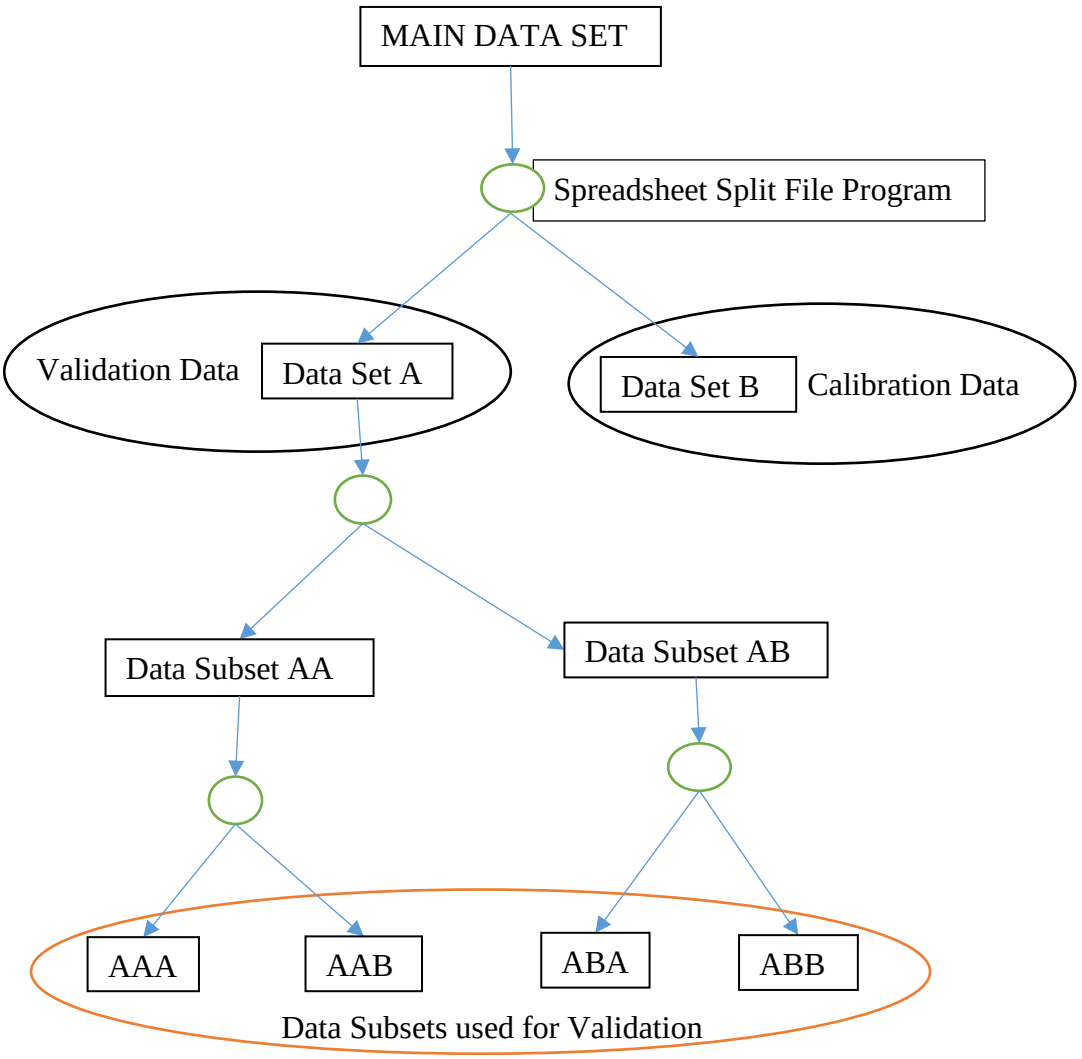

Data Set A and Data Set B	Subset data of Main Data Set that comprises the Out and Return runs for the PM data set
Data AA and AB	Subset data of Sub Data Set A
Data AAA, AAB and ABA, ABB	Subset data of Sub Data Set AA and AB respectively

Figure 7-6: Flowchart of data sets used for the calibration and validation of distance-based bus following model

7.9 Summary

In this chapter, the formulation of distance-based car following models, which include single leader car following model, two-leader car following model and bus following model as well as the extension of these models to include other socioeconomic variables were discussed. Car following models application in microscopic simulation models have helped transport researchers and policy makers to understand the complexity involved in driving behaviour studies to improve road safety and reduce traffic congestions. In this chapter, three main different types of car following models were proposed, formulated

and discussed. All the proposed models describes the driving behaviour of following vehicle in trying to keep a safe or desired following distance behind the vehicle(s) directly ahead in car following situations.

Firstly, a distance-based car following model that often refers to as follow-the-leader model that is capable of predicting the desired following distance between two vehicles in motion was developed. Secondly, the development of distance-based two-leader car following model that is capable of describing the following behaviour of a vehicle in a three consecutive vehicles motion was discussed in this chapter. Transport related factors such as the gender characteristics, the corridor type and vehicle characteristics considered as an influential factor that affects car following behaviour were investigated. These factors or variables inclusion in the models development were proposed. Thirdly, a bus following model considered as a special case of car following was proposed and developed in this chapter. The models calibration, validation and simulation processes were discussed to ascertain the models reliability in describing real world driving behaviour scenarios.

The next chapter discusses the distance-based car following model results and analysis. It discusses the calibration of follow-the-leader models proposed in this study. It also discusses the effects of socioeconomic factors on car following behaviour in both the urban and rural traffic conditions including the highways.

CHAPTER 8 DISTANCE-BASED CAR FOLLOWING MODELS: RESULTS AND ANALYSIS

8.1 Introduction

The formulation of car following models, including two-leader car following model and bus following model were discussed in Chapter 7. Also discussed were the extension of the car following models to include transport related variables. In this chapter, the distance-based car following model calibration results and analysis is discussed. There have been numerous car following models proposed and developed based on different assumptions, such as all drivers follows similar or same driving rules (Kim et al., 2003), and calibrated or validated using uncertain data sets (Kim, 2005) or any data sets that may be available to the researchers (Brockfeld et al., 2004) hindering the models ability to predict real world driving scenarios.

Enough evidence in the literature suggests that, the majority of the existing car following models were developed based on predicting the acceleration of the following vehicles and very little suggestion on the following distance (see Brackstone and McDonald, 1999). One of the early car following models developed to predict the safe following distance of vehicles was developed by Kometani and Sasaki (1959), which only utilizes the speed of the leading and the following vehicles in predicting the safe following distance in order to avoid a collision. The next major development of this model was by Gipps (1981) who developed a model that predicts the speed of the following vehicles. Since then not much work have been carried out that predicts the safe headway or following distance between two successive vehicles.

It is obvious that most of the microscopic simulation tools, which are based on the car following models, based their predictions on acceleration or speed of the following vehicles and as such may limit its application in predicting the safe following headway distance. Moreover, these microscopic models are often calibrated using data which do not include stop-start–and-go (Piao and McDonald, 2003) data that mimic urban driving behaviour, and sometimes actual driving behaviour data due to the lack of available and accurate microscopic data (Ossen and Hoogendoorn, 2005). Since keeping a safe following distance in a car following scenario may be a concern to many, especially traffic safety researchers and policy makers, it is important to develop a model that can accurately predict the safe following distance between two vehicles in motion.

Also, existing literature suggests that researchers have recognised that factors such as individual differences factors (i.e. gender) and situational factors (i.e. road and weather conditions) (Ranney, 1999; Panwai and Dia, 2005) influence the driver behaviour, but not enough evidence to suggests their inclusion in a car following model to ascertain their effects in a car following scenario. With very few car following models that take into account these factors such as gender (Mehmood and Easa, 2009), there is the need for car following models to be developed to include factors such as vehicle occupancy, road type which generally influence driving behaviour. However, there have been little or no attention given in this area to address the gap in the literature. Evidence in the literature also supports a demand for the development of better car following models (Brockfeld et al., 2004) that will closely replicates real world car following scenarios. Models developed with microscopic driver behaviour data can account for naturalistic driving behaviours and may closely replicate actual driving behaviours in real world car following scenarios.

This study has proposed car following models not only developed with naturalistic observed driver behaviour data, but best describes the safe or desired following distance between two successive vehicles in motion. The models proposed mimic real world car following scenarios. This study also proposed extended car following model to include other transport related variables which the existing models does not address in the relevant literature. This chapter discusses the calibration and analysis of the proposed distance-based car following models and presents the tables of calibration results of the models discussed in Chapter 7. It also discusses the models validation analysis, including simulation analysis of the basic car following models proposed.

8.1.1 Models Description

The distance-based car following models descriptions presented in Chapter 6 Section 6.1.1 and the formulation of the models discussed in Chapter 7 are calibrated and validated in this chapter. The models unique names and description of each calibrated models discussed in this chapter are presented in Table 8-1.

Table 8-1: Distance-based models names and descriptions

Model	Model Description
Model A	Distance model with Relative Acceleration and Time Gap
Model C	Distance model with Acceleration of Following Vehicle and Time Gap
Model A-1	Model with Gender
Model A-2	Model with Vehicle Occupancy
Model A-3	Model with Corridor Type
Model A-4	Model with Gender and Vehicle Occupancy
Model A-5	Model with Gender, Vehicle Occupancy and Corridor Type
Model A-6	Corridor 1 Model with Gender and Vehicle Occupancy
Model A-7	Corridor 2 Model with Gender and Vehicle Occupancy
Model A-8	Corridor 3 Model with Gender and Vehicle Occupancy

8.2 Model Analysis: The Calibration of the Basic Models

In this section, the calibration of car following models proposed in this study is discussed. The calibration of Model A and Model C developed in Chapter 7 to determine the models calibration parameters values is discussed. As discussed in Chapter 7, the whole data set (i.e. 96,054 individual time series data points) was equally divided into two separate halves (i.e. Data set 1 and Data set 2). Half of the data set was used for the models calibration process and the other half was used for the models validation process discussed in this chapter. Data set (file) 1 was used to calibrate basic Model A and Model C, which forms the basis of all other models discussed in this chapter. Data set 1 consists of 214 individual following vehicles, which represents 48,027 individual time series data points.

Using Data set 1 to calibrate Model A and Model C and applying multiple linear regression analysis method, the calibrated general models are as follows:

Model A:

$$\Delta x(t+\Delta t) = 0.996\Delta v_n(t+\Delta t) - 0.993\Delta a_n(t+\Delta t) + 0.277 v_n(t) + 3.618 h_{tg}(t) - 3.723 \quad (8\text{-}1)$$

Model C:

$$\Delta x(t+\Delta t) = 0.912\Delta v_n(t+\Delta t) + 0.580a_n(t+\Delta t) + 0.277v_n(t) + 3.627h_{tg}(t) - 3.781 \quad (8\text{-}2)$$

where:

Δx – is the desired following distance (m) of the following vehicle,

Δv_n – is the Relative speed (m/s) between the following vehicle and the leading vehicle,

Δa_n – is the relative acceleration (m/s^2) between the following vehicle and the leading vehicle,

a_n – is the acceleration (m/s^2) of the following vehicle,

v_n – is the speed (km/h) of the following vehicle,

h_{tg} – is the time gap (s) between the following vehicle and the leading vehicle,

t – is the time (s),

Δt – is the time step or increment (s),

Both Model A and Model C produced statistically significant calibration parameters estimates with p-values < 0.05 and R^2 value of 0.577 for Model A and 0.575 for Model C. The sample size used for the models calibration is 48,026 individual time series data points (see Table 8-2 and Table 8-3 for calibration output). The positive signs of the parameters estimates in the models shows an increase effects of the parameters on the following distance. The negative signs of the parameters estimates shows a decrease effects on the following distance between the two vehicles in motion.

For Model A, the following driver takes into consideration the acceleration of the lead vehicle in keeping a safe or desired following distance behind the lead vehicle. For instance, if the relative speed between the two vehicles is greater than zero, the overall distance between the vehicles will be increased by a factor of 0.996 and if it is less than zero, there will be a reduction in the distance by a factor of 0.996. The same principles apply to Model C that takes into consideration the acceleration of the following vehicle, that is, if the following vehicle accelerates by one (1) unit, the following distance will be increased by a factor of 0.580 and if it decelerates by the same unit, the following distance

will be reduced by a factor of 0.580. The same line of thought can be used to explain in line with the relative speed parameter in the models.

For the purpose of this study, Model A is developed further by introducing other variables into the model. Model A takes into consideration the acceleration of the lead vehicle (i.e. as in the relative acceleration which was measured directly by the radar sensors) to determine the desired following distance of a driver in car following scenario. Moreover, Model A produced a better calibration regression output results than Model C (see Table 8-2 and Table 8-3). It is important to note that Model C can equally be used where the relative acceleration between the leading and the following vehicles in the car following situation is not readily available for model calibration and simulation. As earlier mentioned, the basic or general model that is developed further or extended to include other transport related variables in the subsequent sections of this chapter is Model A.

8.3 The Extended Models Calibration

This section discusses the calibration of the extended basic Model A that incorporates the transport related variables. The extended models incorporates the gender characteristics, the vehicle characteristics and the corridor type characteristics. The whole data set was used to calibrate the extended distance-based car following models discussed in this chapter.

8.3.1 The Gender Model

As discussed in Chapter 7, a binary value of 1 or 0 was assigned to the gender dummy in the model as male = 1 and female = 0. Using the whole the data set (i.e. 96,051 individual data points) and applying multiple linear regression analysis method, the calibrated Gender model (A-1) is as follows:

Model A-1:

$$\Delta x(t+\Delta t) = 0.960\Delta v_n(t+\Delta t) - 0.830\Delta a_n(t+\Delta t) + 0.268 v_n(t) + 3.365 h_{tg}(t) - 0.203 g - 2.988 \quad (8\text{-}3)$$

The sample size of the data used was 96,051 individual time series data points (with 0.1 seconds time step). The model produced R^2 of 0.555 and regression standard error of

5.691. All the model parameters estimates including the gender parameter were statistically significant at 95% confidence level with p-values < 0.05 (see Table 8-4). The gender parameter represents the male category in the model and has a parameter estimate negative sign. This means that male drivers have a reduced effect on the following distance, and as such drive with shorter following distance when following other vehicles compared to the female drivers. As discussed in Chapter 5, male drivers were found to have shorter following distances than female drivers at high speed ranges.

Mehmood and Easa (2009) in their study found that female drivers were slower in brake-reaction time than male drivers at normal driving condition, which makes female drivers taking longer distance to come to a stop. McKenna et. al. (1998) found that female drivers travel less close to target lead vehicles than male drivers. They also revealed that young male drivers follow closer to the vehicle in front than their female counterparts. They reported this in a study where participant of different age groups were asked to press a button when they reach a normal following distance and again, when they begin to feel uncomfortably close to the target car as they watch a digitised footage of a camera car following a target car on a motorway. The McKenna et. al. (1998) study suggests that female drivers drive with longer following distance than the male counterpart in general.

8.3.2 Vehicle Occupancy Model

Again, as discussed in Chapter 7, a binary value of 1 was assigned to vehicle occupancy = 1 and a value of 0 assigned to vehicle occupancy = 2+. Using data sample size of 96,051 individual time series data points and applying multiple linear regression analysis method to the occupancy model, the calibrated Occupancy Model (A-2) is as follows:

Model A-2:

$$\Delta x(t+\Delta t) = 0.960\Delta v_n(t+\Delta t) - 0.836\Delta a_n(t+\Delta t) + 0.268 v_n(t) + 3.364 h_{tg}(t) - 0.448 oc - 2.822 \quad (8\text{-}4)$$

All the model parameters estimates were statistically significant at 95% confidence level with p-values < 0.05. The model produced R^2 value of 0.555 and regression standard error of 5.688 (see Table 8-5). The negative sign of the vehicle occupancy parameter indicates that vehicles with only the driver as the occupant follow closer to other vehicles than vehicles with occupancy of two or more (2+) passengers including the driver. The

explanation to this could be that drivers of vehicles with 2+ occupancy could be engaged in conversation with or be distracted by other occupants in the vehicle and as a result, may not fully concentrate on the driving, hence maintain longer distance to the vehicle in front. This could also be that, these drivers are more concerned about the safety when they have passengers on board, hence may tend to drive with a considerable following distance compared to the driver only occupancy vehicles. Vehicles with more occupancy may tend to travel with unsteady following distance as a result of distraction by other occupants compared to the driver only vehicle occupancy.

8.3.3 Corridor Type Model

A binary value of 1 or 0 was assigned to the corridor type categories in the Corridor type model equation discussed in Chapter 7 as follows:

Traffic corridor 1 (cr1) = 1, all other traffic corridors = 0

Traffic corridor 2 (cr2) = 1, all other traffic corridors = 0

Traffic corridor 3 (cr3) = 1, all other traffic corridors = 0

Using data sample size of 96,051 individual time series data points and applying multiple linear regression analysis method to the Model A-3, the calibrated generalised Corridor type model is as follows:

Model A-3:

$$\Delta x(t+\Delta t) = 0.934\Delta v_n(t+\Delta t) - 0.833\Delta a_n(t+\Delta t) + 0.275 v_n(t) + 3.470 h_{tg}(t) - 0.366 cr1 - 1.975 cr2 - 0.509 cr3 - 2.749 \quad (8\text{-}5)$$

All the model parameters estimates were statistically significant at 95% confidence level and p-values for all the model parameters estimates were less than 0.05. The model produced R^2 value of 0.562 and a standard error of 5.645 (see Table 8-6). Model A-3 best describes car following behaviour within an urban, highway and urban-rural traffic conditions. It is evident from the model that the type of road affects the following distance between two vehicles in car following situation.

It is interesting to note that all the three traffic corridors have reduced effects on the desired following distance between two vehicles. It shows that the highway (i.e. Corridor 2) have the largest effects on the following distance than the urban-rural (i.e. Corridor 3) and the urban (i.e. Corridor 1) roads. A possible explanation is that highways tend to have high vehicle speed, which encourages shorter following distances between vehicles. Urban roads seem to have low speed limits, which encourages longer following distances between vehicles as a result of low vehicles speed.

8.3.4 Gender - Vehicle Occupancy Model

In this section, a car following model is proposed that is an extension of the basic Model A to include two independent variables. The model incorporates both the gender and the vehicle occupancy to ascertain their combined influence on the following distance. It has been established that both the gender and vehicle occupancy characteristics, individually affects the following distance, hence it is appropriate to assess the significant effects of both on driving behaviour. Model A-4 equation is expressed as:

$$\Delta x(t+\Delta t) = \alpha_0 \Delta v_n(t+\Delta t) + \alpha_1 \Delta a_n(t+\Delta t) + \alpha_2 v_n(t) + \alpha_3 h_{tg}(t) + \alpha_4 oc + \alpha_5 g + b_o \quad (8\text{-}6)$$

Using the whole data set and assigning binary value of 1 or 0 to the categories of each independent dummy variable (i.e. vehicle occupancy of 1 = 1, vehicle occupancy of 2+ = 0 and male = 1, female = 0) in the model equation, the proposed calibrated Gender-Occupancy model (A-4) is as follows:

Model A-4:

$$\Delta x(t+\Delta t) = 0.961\Delta v_n(t+\Delta t) - 0.836\Delta a_n(t+\Delta t) + 0.268 v_n(t) + 3.366 h_{tg}(t) - 0.430 oc - 0.119 g - 2.741 \quad (8\text{-}7)$$

All the model parameters estimates were statistically significant at 95% confidence level with p-values < 0.05 and R^2 value of 0.556 (see Table 8-8). The data sample size used for the model calibration was 96,051 individual time series data points. Both the vehicle occupancy and the gender parameters in Model A-4 have negative parameters estimates signs. The negative sign indicates a reduction in the desired following distance between

two vehicles in motion. What this means is that, the vehicles with male drivers as the only occupant follows other vehicles at closer following distance than vehicles with either female drivers as the only occupant or female drivers having one or more passengers as the vehicle occupants. Also, male drivers as the only occupant will have shorter following distance than male drivers with occupants in the vehicle. Similarly, female drivers as only vehicle occupant will have shorter following distance than female drivers with passengers on board the vehicle. Model A-4 shows that, the combination of the gender and the vehicle occupancy characteristics have influence on the desired following distance between two vehicles in car following situation.

8.3.5 Gender, Vehicle Occupancy and Corridor Type Model

In Section 8.3.1 through to Section 8.3.4, the models that incorporates gender, vehicle occupancy and corridor type variables were discussed. All these variables considered in the models were found to have significant effects on the following distance between two vehicles in car following scenarios. In this section, a car following model is proposed that incorporates the combination of the gender, vehicle occupancy and corridor type considered in this chapter. This enables further investigation to be carried out to understand their combined effects on driving behaviour. As previous models were developed, dummy variables are introduced into the equation of the general Model A to represent the gender, vehicle occupancy and the corridor type characteristics. The proposed car following model (i.e. Model A-5) equation is expressed as:

$$\Delta x(t+\Delta t) = \alpha_0 \Delta v_n(t+\Delta t) + \alpha_1 \Delta a_n(t+\Delta t) + \alpha_2 v_n(t) + \alpha_3 h_{tg}(t) + \alpha_4 cr1 + \alpha_5 cr2 + \alpha_6 cr3 + \alpha_7 oc + \alpha_8 g + \varepsilon \quad (8\text{-}8)$$

The model estimate equation is given as:

$$\Delta x(t+\Delta t) = \alpha_0 \Delta v_n(t+\Delta t) + \alpha_1 \Delta a_n(t+\Delta t) + \alpha_2 v_n(t) + \alpha_3 h_{tg}(t) + \alpha_4 cr1 + \alpha_5 cr2 + \alpha_6 cr3 + \alpha_7 oc + \alpha_8 g + b_0 \quad (8\text{-}9)$$

The model parameters definitions remains the same as previously defined. As usual, a binary value of 1 or 0 was assigned to each independent dummy variable's categories in the model equation in order to calibrate Model A-5 (eqn.8-9). The binary values assigned to the dummy variables are as follows:

Traffic corridor 1 (cr1) = 1, all other traffic corridors = 0

Traffic corridor 2 (cr2) = 1, all other traffic corridors = 0

Traffic corridor 3 (cr3) = 1, all other traffic corridors = 0

For Vehicle occupancy: vehicle occupancy of 1 = 1, vehicle occupancy of 2+ = 0

For Gender: male = 1, female = 0

A total of 96,051 individual time series data points were used for Model A-5 calibration. Using multiple linear regression analysis method, the calibrated Model A-5 is given as:

Model A-5:

$$\begin{aligned}\Delta x(t+\Delta t) = {} & 0.934\Delta v_n(t+\Delta t) - 0.839\Delta a_n(t+\Delta t) + 0.274 v_n(t) \\ & + 3.466 h_{tg}(t) - 0.380 cr1 - 2.021 cr2 - 0.598 cr3 \\ & - 0.454 oc + 0.189 g - 2.503\end{aligned} \quad (8\text{-}10)$$

All the model parameters estimates were statistically significant at 95% confidence level with p-values < 0.05. The model R^2 value is 0.563 and the regression standard error is 5.641 (see Table 8-8). As expected, almost all the model parameters estimates signs remained unchanged as previous models discussed, except that of the gender parameter estimate sign. It can be seen that with the inclusion of the corridor type in Model A-5, the gender parameter estimate sign changed from negative to positive for the male drivers. Positive sign of the gender parameter estimate indicates an increase in male drivers following distance than female drivers with this model.

This trend was observed in the analysis of the data discussed in Chapter 5 when the following distances of male drivers and female drivers were compared with the following speed. As discussed in Chapter 5, visual comparisons of the difference in the following distance showed that female drivers tend to have closer following distances than male drivers at low speed ranges. Low speed encourages longer following distances and high speed encourages shorter following distances of the following vehicles as was seen in the distance comparisons chart (see Figure 5-13). At high speed, male drivers were seen to be following with shorter following distances than the female counterparts as discussed in Chapter 5.

Kim (2005) compared 44 individual vehicles with male drivers and 20 individual vehicles with female drivers with a chart, for a study conducted on I-295 and I-495 near the Washington D.C. area. Kim suggested that male drivers at all speed ranges kept considerable following distances than their female counterparts. However, he pointed out that with the exception of the speed range from 81 km/h to 85 km/h, the following distances between male and female drivers were not significant at 0.05 (i.e. 95% confidence level). He asserted that male drivers have more variability in driving and in keeping considerable following distance than female drivers. Model A-5 proposed in this chapter shows that the combination of these three transport related variables in the model affects the driver behaviour in keeping a safe or desired following distance behind leading vehicle.

8.3.6 Analysis of Corridor Type effects on Gender

The gender-occupancy model (i.e. Model A-4) (eqn. 8-7) have the gender variable estimates sign as negative indicating that male drivers follow closer than that of the female counterparts. But in Model A-5 (i.e. the corridor type, the gender and vehicle occupancy model) (eqn. 8-10), the gender parameter estimate have a positive sign indicating that female drivers follow closer than male drivers in this case. The gender variable sign change in Model A-5 indicates that the corridor type characteristics have effects on the gender characteristics when both variables are considered in the same model. To understand the gender behavioural change in Model A-5, further investigation was carried out to ascertain the effect of the corridor type on the gender characteristics.

To carry out the investigation, new models were proposed that incorporates each of the corridor type separately with the gender and the vehicle occupancy characteristics to ascertain the particular corridor type that influence the gender variable sign change in Model A-5. As earlier discussed, Corridor 1 is urban road, Corridor 2 is highway road and Corridor 3 is urban-rural road. Three different sets of models were proposed with each model incorporating one corridor type classification together with the gender and the vehicle occupancy characteristics to investigate the effect of the particular corridor type on the gender parameter in Model A-5. The whole data set (consisting of 96,051 individual data points) was used to calibrate each of the three models proposed. Using multiple regression analysis method, the models are given by:

Model A-6: Corridor 1 Model – (oc-1 = 1, oc-2+ = 0; male = 1, female = 0; cr1 = 1, cr2 = cr3 = 0);

$$\Delta x(t+\Delta t) = 0.965\Delta v_n(t+\Delta t) - 0.833\Delta a_n(t+\Delta t) + 0.267 v_n(t) + 3.373 h_{tg}(t) - 0.462 oc - 0.053 g + 0.519 cr1 - 2.918;$$

$R^2 = 0.56$ (8-11)

Model A-7: Corridor 2 Model – (oc-1 = 1, oc-2+ = 0; male = 1, female = 0; cr2 = 1, cr1 = cr3 = 0);

$$\Delta x(t+\Delta t) = 0.932\Delta v_n(t+\Delta t) - 0.840\Delta a_n(t+\Delta t) + 0.277 v_n(t) + 3.490 h_{tg}(t) - 0.388 oc + 0.145 g - 1.648 cr2 - 3.022;$$

$R^2 = 0.56$ (8-12)

Model A-8: Corridor 3 Model – (oc-1 = 1, oc-2+ = 0; male = 1, female = 0; cr3 = 1, cr1 = cr2 = 0);

$$\Delta x(t+\Delta t) = 0.954\Delta v_n(t+\Delta t) - 0.838\Delta a_n(t+\Delta t) + 0.270 v_n(t) + 3.393 h_{tg}(t) - 0.373 oc - 0.138 g + 0.346 cr3 - 3.004;$$

$R^2 = 0.56$ (8-13)

All the models parameters estimates were statistically significant at 0.05 (or 95%) significance level. It can be seen that Model A-7 (i.e. the Corridor 2 Model) which represents the highway with speed limits ranging from 50 to 70 miles per hour (mph) has the positive sign for the gender variable estimate. It can be observed from Models A-6, A-7 and A-8 that whenever the gender parameters estimate sign is negative, the corridor type variable estimates are positive as found in Model A-6 and Model A-8 and vice versa as in Model A-7.

This further explain why in Model A-5 all the corridor type variables estimates are negative with positive gender variable estimates which represents male drivers. The results from this investigation show that the positive sign in Model A-5 involving all the three corridor types is as a result of Corridor 2 having strong influence on the driving behaviours of both male and female drivers. The outputs of Models A-6, A-7 and A-8 results are presented in Table 8-10.

8.4 Tables of Models Calibration Results

This section presents the tables of results of the model calibrations discussed in this chapter. The tables define the models parameters and present the calibration parameters estimates (i.e. parameters coefficients) for each model, together with the individual calibration parameters standard errors and their corresponding p-values. The R^2 values, the overall standard errors and sample sizes or observations that was used in the models calibrations are presented in the tables of calibration results.

Table 8-2: Model A (eqn. 8-1) calibration parameters regression output

Model Parameters	Coefficient	Standard Error	P-value
Constant	-3.723211	0.07037198	0
Relative Speed [m/s]	0.9957133	0.02111049	0
Relative Acc. [m/s²]*	-0.9925316	0.03995312	2.2E-135
Following Vehicle Speed [km/h]	0.27705786	0.00115142	0
Time Gap [s]	3.6177402	0.0225954	0
R^2	0.57722286		
Standard Error	5.80121112		
Observation	48026		

* Acc. = Acceleration

Table 8-3: Model C (eqn. 8-2) calibration parameters regression output

Model Parameters	Coefficient	Standard Error	P-value
Constant	-3.78095	0.070463871	0
Relative Speed [m/s]	0.9117796	0.020427783	0
Acceleration [m/s²]	0.5796668	0.028970697	1.06E-88
Foll. Veh. Speed [km/h]*	0.2771891	0.001153975	0
Time Gap [s]	3.626628	0.022638178	0
R^2	0.57533		
Standard Error	5.8141834		
Observation	48026		

*Foll. Veh. = Following Vehicle

Table 8-4: Model A-1, Gender Model (eqn. 8-3) calibration parameters regression output

Model Parameters	Coefficient	Standard Error	P-value
Constant	-2.988275663	0.061871371	0
Relative Speed [m/s]	0.960638975	0.014441834	0
Relative Acc [m/s²]	-0.829709157	0.027485832	3E-199
Foll. Veh. Speed [km/h]	0.267795135	0.000834699	0
Time Gap [s]	3.364700349	0.015535265	0
Gender	-0.202772915	0.048287029	2.68E-05
R^2	0.555045289	Male	1
Standard Error	5.690569085	Female	0
Observations	96051		

Table 8-5 Model A-2, Occupancy Model (eqn. 8-4) calibration parameters regression output

Model Parameters	Coefficient	Standard Error	P-value
Constant	-2.8216634	0.057736367	0
Relative Speed [m/s]	0.9598834	0.014423919	0
Relative Acc. [m/s²]	-0.8359558	0.027478921	3E-202
Foll. Veh. Speed [km/h]	0.26782877	0.000834196	0
Time Gap [s]	3.36372841	0.015504635	0
Vehicle Occupancy	-0.4476956	0.042027986	1.8E-26
R^2	0.55548876	Occupancy 1	1
Standard Error	5.68773259	Occupancy 2+	0
Observations	96051		

*Acc. = Acceleration, Foll. Veh. = Following Vehicle

Table 8-6: Model A-3, Corridor Type Model (eqn. 8-5) calibration parameters regression output

Model Parameters	Coefficient	Standard Error	P-value
Constant	-2.748804738	0.069559333	0
Relative Speed [m/s]	0.93376572	0.0143444	0
Relative Acc. [m/s²]	-0.833240033	0.027266416	4.1E-204
Foll. Veh. Speed [km/h]	0.274554619	0.000887197	0
Time Gap [s]	3.470165096	0.015896641	0
Traffic Corridor (Cr)1*	-0.365883257	0.062207558	4.08E-09
Traffic Corridor (Cr) 2*	-1.974944787	0.056594325	3.9E-265
Traffic Corridor (Cr) 3*	-0.508817358	0.055445119	4.52E-20
R^2	0.5622081	Standard Error	5.644639
Observations	96051		

* Cr1 = 1, Cr2 = Cr3 = 0; Cr2 = 1, Cr1 = Cr3 = 0 and Cr3 =1, Cr1 = Cr2 = 0

Table 8-7: Model A-4, Gender-Vehicle Occupancy Model (eqn. 8-7) calibration regression output

Model Parameters	Coefficient	Standard Error	P-value
Constant	-2.741332313	0.06650871	0
Relative Acc. [m/s²]	-0.835878586	0.027478235	2.8E-202
Relative Velocity [m/s]	0.96124426	0.014434391	0
Foll. Veh. Speed [km/h]	0.267862186	0.000834288	0
Time Gap [s]	3.365795739	0.015527503	0
Vehicle Occupancy[1]	-0.430129355	0.042642551	6.49E-24
Gender[2]	-0.11914361	0.048968697	0.01497
R^2	0.555516155		
Standard Error	5.68758692		
Observations	96051		

[1] Vehicle Occupancy: OC 1 = 1, OC 2+ = 0
[2] Gender: Male = 1, Female = 0

Table 8-8: Model A-5, Gender-Vehicle Occupancy-Corridor Type Model (eqn. 8-10) calibration regression output

Model Parameters	Coefficient	Standard Error	P-value
Constant	-2.503267604	0.084049802	5E-194
Relative Velocity [m/s]	0.934116572	0.014350227	0
Relative Acc. [m/s²]	-0.839062758	0.027256218	4.4E-207
Foll. Veh. Speed [km/h]	0.274290293	0.000887127	0
Time Gap [s]	3.465862935	0.015898964	0
Traffic Corridor (Cr) 1[1]	-0.379626981	0.062211569	1.05E-09
Traffic Corridor (Cr) 2[1]	-2.020676788	0.057108209	1.8E-272
Traffic Corridor (Cr) 3[1]	-0.597826192	0.056046259	1.51E-26
Veh. Occupancy (OC)[2]	-0.454234588	0.04285665	3.12E-26
Gender[3]	0.18904324	0.049399687	0.00013
R^2	0.562737173		
Standard Error	5.641286001		
Observations	96051		

[1] Cr1 = 1, Cr2 = Cr3 = 0; Cr2 = 1, Cr1 = Cr3 = 0 and Cr3 =1, Cr1 = Cr2 = 0
[2] OC 1 = 1, OC 2+ = 0
[3] Male = 1, Female = 0

Table 8-9: The regression outputs for the individual Corridor Type Model, Model A-6 (eqn. 8-11), Model A-7 (eqn. 8-12) and Model A-8 (eqn. 8-13)

Model Parameters	Model A-6		Model A-7		Model A-8	
	Standard Error	P-value	Standard Error	P-value	Standard Error	P-value
Constant	0.0684	0	0.06641	0	0.07	0
Rel. Acc. [m/s²]	0.02746	2.8E-201	0.02727	3E-207	0.03	2E-203
Rel. Speed [m/s]	0.01443	0	0.01435	0	0.01	0
Foll. Veh. Speed [km/h]	0.00084	0	0.00086	0	0	0
Time Gap [s]	0.01553	0	0.01575	0	0.02	0
Veh. Occupancy[1]	0.04271	3.29E-27	0.04233	4.6E-20	0.04	5.1E-18
Gender[2]	0.04932	0.02859	0.04908	0.00312	0.05	0.00482
Corridor (Cr)1*	0.04755	9.03E-28	-	-	-	-
Corridor (Cr) 2*	-	-	0.04298	0	-	-
Corridor (Cr) 3*	-	-	-	-	0.04	6.8E-18
R^2	0.55607		0.56222		0.55585	
Standard Error	5.68409		5.64458		5.68541	
Observations	96051					

*Model A-6: Cr1 = 1, Cr2 = Cr3 = 0; Model A-7: Cr2 = 1, Cr1 = Cr3 = 0 and Model A-8: Cr3 =1, Cr1 = Cr2 = 0
[1]Veh. Occupancy: OC 1 = 1, OC 2+ = 0
[2]Gender: Male = 1, Female = 0

8.5 Model Validation

In this section, the validation and simulation of the general model is discussed. Data set 2, designated as Data set A, which is half of the main data set was used for the model validation. A number of following vehicles were randomly selected from the whole data set and used to simulate Model A only. Though Model C was not developed further by extending with the transport related variables in this study, it is equally important to validate the model to ascertain its reliability in predicting the desired following distance between two successive vehicles in a car following situation. Therefore, Model A and Model C were modelled against the observed data in this study.

8.5.1 Modelled Against Observed Data

To ascertain the reliability of the general models, validation of the models were carried out by modelling against the observed data. As discussed in Chapter 7, the Data set or file A was split further into four equal sets of sub data files (i.e. AAA, AAB, ABA and ABB data files). Using the basic models (i.e. Model A and Model C), the desired following

distance at each time step for each sub data sets was estimated and the average desired following distance calculated. The average following distances for both the observed and the predicted data sets were used in the t-test statistical significant test. To begin the models validation, two hypothetical questions were set:

H_0: There is no significant difference between the observed and the model predicted data sets (i.e., $H_0: \mu_d = 0$).

Ha: There is significant difference between the observed and the model predicted data sets (i.e., $H_a: \mu_d \neq 0$).

where H_0 and H_a are the null and the alternative hypotheses respectively, μ_d is the population mean of the differences in the means between the two groups of data.

As discussed in Chapter 6, the t-test statistics was computed using Microsoft Excel data analysis tool and obtained the p-values and t-values for Model A and Model C. The paired two-sample for means two-tail t-test statistics was used for this analysis. Table 8-10 shows the t-test statistics results for both Model A and Model C. For degree of freedom (df) of 3 (i.e. 4 - 1), the two-tailed t-test statistics p-value of 0.72 and t-stat value of -0.390 for Model A were obtained. For Model C, the t-test statistics p-value of 0.74, t-stat value of -0.363 were obtained. It can be seen that the p-values for Model A and Model C are all greater than the p-value of 0.05 (95%) confidence level. Similarly, the t-stat values for Model A and Model C are also less than the two-tail t-critical value of 3.182 (for df = 3, at 95% cl). The t-test statistics results showed that there was no enough evidence in the mean differences between the observed and predicted data to suggest the rejection of the null hypothesis and therefore, the alternative hypothesis was rejected since no significant differences were observed in the two groups of data sets for both Model A and Model C.

The t-test statistics was used to test the significant differences between the observed and the predicted data sets for the new distance-based car following models developed in this study and discussed in this chapter. The analysis found that at p-value of 0.05 (i.e. 95%) confidence level, there was no statistical significant differences observed between the observed (or measured) and the models predicted data sets to suggest the rejection of the null hypothesis (H_0). Therefore, we conclude that, there was no statistical significant difference between the observed and the predicted data sets for Model A [t(3) = -0.390, p-value > 0.05, 2-tail] and Model C [t(3) = -0.363, p-value > 0.05, 2-tail]. The basic Model A and Model C proposed and developed in this study have been shown to predict

accurately the desired following distance between two successive vehicles in a car following situation in a real world driving scenario. The models developed and calibrated in this chapter best describe a car following behaviour within urban, highway and urban-rural driving conditions.

Table 8-10: The paired two sample means t-test results of Model A and Model C (the basic or general models)

MODEL A					
Data Set	Observed	Predicted	T-Test Result		
				Observed	Predicted
Data AAA	10.21	9.73	Mean	10.551982	10.87
Data AAB	11.02	13.77	Variance	1.93331032	5.116067
Data ABA	8.84	8.56	Observations	4	4
Data ABB	12.14	11.42	Pearson Correlation	0.69759229	
			Hypothesized Mean Difference	0	
			df	3	
			t Stat	-0.3898659	
			P(T<=t) one-tail	0.3613333	
			t Critical one-tail	2.35336343	
			P(T<=t) two-tail	0.7226666	
			t Critical two-tail	3.18244631	
MODEL C					
Data Set	Observed	Predicted	T-Test Result		
				Observed	Predicted
Data AAA	10.21	9.67	Mean	10.5526038	10.845
Data AAB	11.02	13.72	Variance	1.93490733	5.1279
Data ABA	8.84	8.53	Observations	4	4
Data ABB	12.14	11.46	Pearson Correlation	0.70975811	
			Hypothesized Mean Difference	0	
			df	3	
			t Stat	-0.3632713	
			P(T<=t) one-tail	0.37024553	
			t Critical one-tail	2.35336343	
			P(T<=t) two-tail	0.74049105	
			t Critical two-tail	3.18244631	

8.5.2 Model Simulation

After the validation of the basic models and found no statistical differences in the data sets at 95% (0.05) confidence level, it is necessary to simulate the basic model with some selected vehicle data sets and compare with the observed data. As discussed in Chapter 7, four randomly selected vehicles following data sets were used to carry out the basic model simulation. The following vehicles were identified as Driver 117, Driver 102, Driver 129 and Driver 8 with a minimum following duration of 35 seconds. The time series data points for Driver 117, Driver 102, Driver 129 and Driver 8 used for the simulation were 120, 524, 601 and 128 respectively. The individual vehicle's desired following distances were simulated using the basic Model A. The results from Model A simulation for each selected vehicle were compared with the individual vehicle's corresponding field observed following distances. The speed of the individual selected following vehicles plotted against the observed and the simulation following distances. The average following (relative) distance values at each speed range were plotted using charts. Figure 8-1, Figure 8-2, Figure 8-3 and Figure 8-4 shows the model simulation relative distance and the field observed relative distance for Driver 117, Driver 8, Driver 129 and Driver 102 respectively.

It can be observed from the Figures that all the individual drivers following distances from the simulation model closely replicate their corresponding observed following distances. The average following relative distance observed for Driver 117 is 8.11 metres and for the simulation run is 7.80 metres. This represents a difference of 0.31 metres between the observed and the simulation relative distances (see Figure 8-1). The observed average relative distance of 15.81 metres for Driver 8 was less than that of the simulation average relative distance by 0.32 metres for the same driver (see Figure 8-2). Similarly, the simulation average relative distance of 7.52 metres for Driver 102 was less than that of the observed relative distance by 0.32 metres for the same driver (see Figure 8-4). In the case of Driver 129, the average observed relative distance of 7.37 metres was less than the average simulation relative distance of 7.65 metres by 0.28 metres for the same driver (se Figure 8-3).

The differences in the average relative distances between the observed and the simulation runs for all the four drivers analysed range between 0.28 metres to 0.32 metres. It was found that the differences in the relative distances between the observed and simulation runs for all the drivers selected for the model simulation analysis were less than 0.4

metres. This shows that the simulation of the car following models developed in this study numerically perform better and closely relates to the real world car following driving behaviour observed during the experiment.

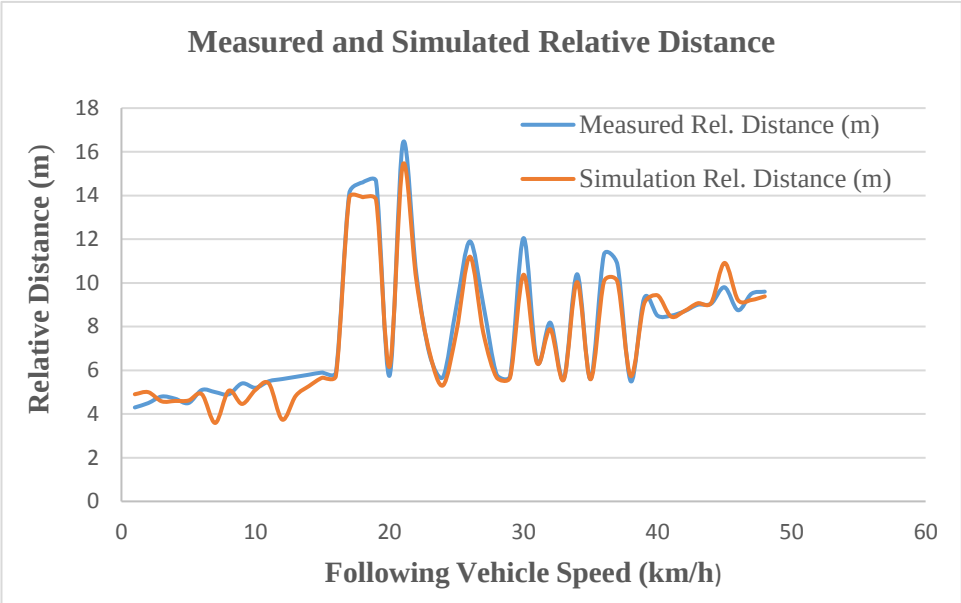

Figure 8-1: Driver 117 field measured and simulation relative distance comparison

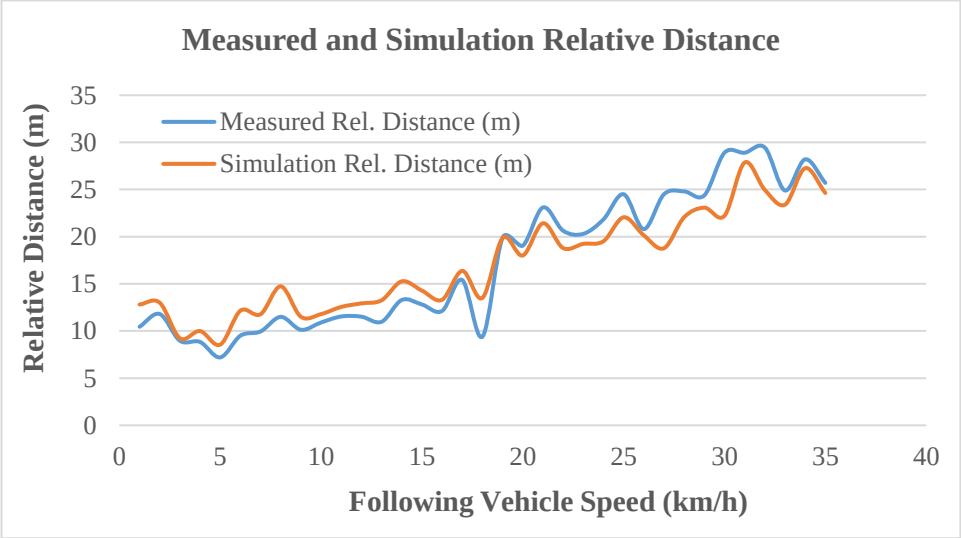

Figure 8-2: Driver 8 field measured and simulation relative distance comparison

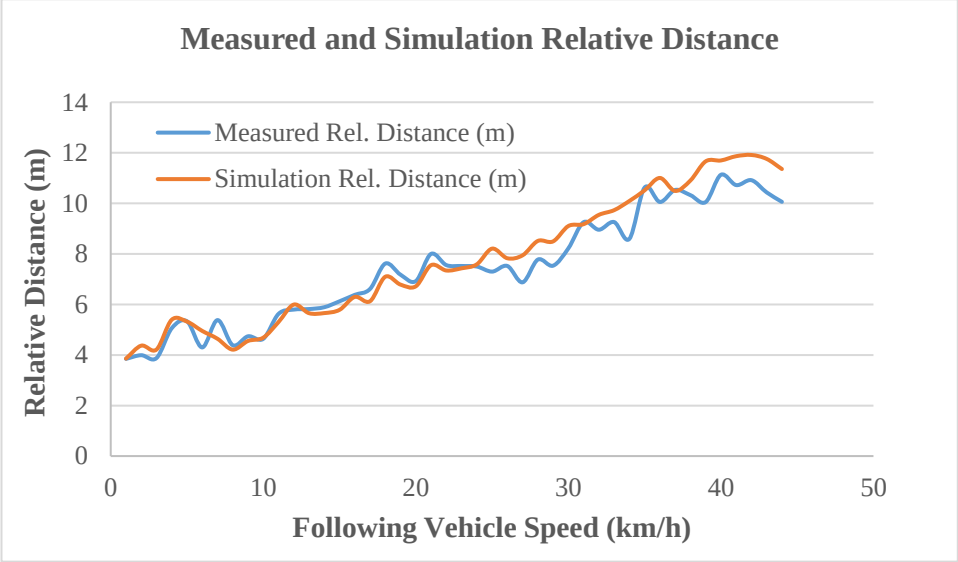

Figure 8-3: Driver 129 field measured and simulation relative distance

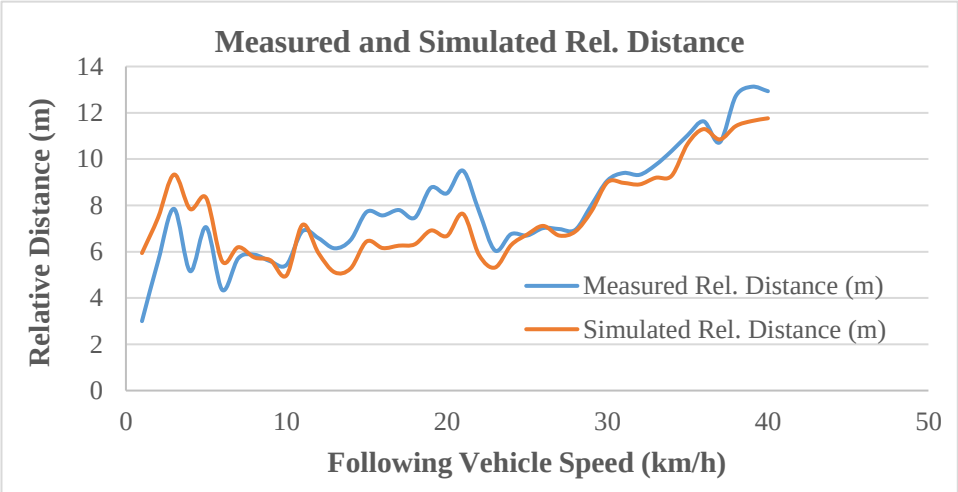

Figure 8-4: Driver 102 field measured and simulation relative distance

8.6 Summary

A general car following models that serve as the basic models from which other extension models were developed were discussed. Two general or basic models (i.e. Model A and Model C) were proposed and developed. The models calibration parameters estimates or values were all found to be statistically significant at 0.05 (95% confidence level). To ascertain the reliability of these models, validation of the models were carried out using one half of the whole data set. T-test statistics analysis was carried out for Model A [t(3) = -0.390, p>0.05, 2-tail] and Model C [t(3) = -0.363, p>0.05, 2-tail] and found that there was no statistical significant differences between the observed and the predicted data at 0.05 (95%) confidence level. As already discussed, Model A produced the best statistical

regression output results than Model C, hence Model A was used as the basic model and developed further in this chapter.

Transport related variables such as gender characteristics, corridor type (road) characteristics and vehicle occupancy characteristics were introduced into the basic Model A as an extended models to ascertain their effects on the safe or desired following distance between two vehicles in car following situation. Each transport related variables in the extended models including the model that incorporates all the three variables (i.e. gender, vehicle occupancy and corridor type) combined and considered in this chapter were found to be statistically significant at 0.05 (or 95%) confidence level. These factors were found to have significant effect on the desired following distance between two vehicles in motion in car following scenario. The tables of the models' calibration results for the statistical regression outputs were presented in this chapter.

Further validation of the basic model was carried out by simulating some selected vehicles observed in the field. Four different following vehicles with a minimum following duration of 35 seconds were randomly selected and simulated. The analysis of the simulation results was discussed. It is interesting to note that the differences between the average simulation following distance and the average observed following distance for all the four selected following vehicles were found to be in the range of 0.28 metres to 0.32 metres and less than 0.4 metres. The simulation results showed that the basic model perform better in predicting the following distance between two successive vehicles in car following situation in a real world driving scenario.

Two-leader car following models have recently gained more attention by various transport researchers, but very few models exist to explain this phenomena of one car following two leading vehicles in a car following scenario. The next chapter discusses the calibration of the new two-leader car following model proposed that best describe urban, highway and urban-rural driving conditions. It also discusses the validation and simulation of the two-leader car following model proposed in this study.

CHAPTER 9 DISTANCE-BASED TWO-LEADER MODEL: RESULTS AND ANALYSIS

9.1 Introduction

A general distance-based car following models calibration and validation were discussed in Chapter 8. The extension of the basic distance-based car following model that incoraperates transport related variables were discussed in Chapter 8. In this chapter, a distance-based two-leader car following model results and analysis are discussed. Driving behaviour involving two or three vehicles movements have been gaining the attention of a number of researchers in recent years. Studies have shown that drivers foresee the traffic downstream and process the information, thereby responding not only to the vehicle directly ahead but the second vehicle (i.e. ahead of first leader) in a car following scenario (Hoogendoorn and Ossen, 2006).

The growing interest in multiple cars following behaviour has led to a number of multiple vehicles leader car following models been proposed. For instance, Bexelius (1968) proposed a car following model by extending the GHR car-following model (Chandler et al., 1958) on the assumption that every individual driver response to many of the preceding vehicles. Bando et al. (1995) optimal velocity model was extended by Lenz et al. (1999) by including multi-vehicles interactions in the model. By extending the model, they showed that following vehicle responding to several vehicles ahead contributes to the stabilization of the dynamic behaviour of the model. The extension of one-car leader model into multiple-vehicles leader model continued over the years. For instance, Zhou and Li (2012) extended the basic optimal velocity car following model proposed by Bando et al. (1995) by including the vehicle immediately preceding the lead vehicle. Farhi et al. (2012) also extended the piecewise-linear car following model proposed by Bando et al. (1995). Extending the existing car following models does not necessarily make these extended models accurate in describing the driving behaviour of a three vehicles movement in a multiple-leader car following scenario.

It has been reported that these models were developed with studies that were based on non-scientific arguments (Hoogendoorn and Ossen, 2006) but on the assumption that drivers response to multiple vehicles ahead downstream and as such might not effectively replicate real world driving situation. Because these models are extensions of the existing models, it can be argued that they were developed first before calibration using uncertain

empirical data (Kim, 2005) or video data such as helicopter mounted with cameras (Treiterer and Myers, 1974: Hoogendoorn and Ossen, 2006), Next Generation Simulation (NGSIM) database (Mehmood and Easa, 2010). Calibrating these models might not necessarily make the models better and replicate the actual driving behaviour that the models were develop to predict. In addition, the multiple-leader models mostly tend to predict the acceleration of the following vehicle rather than the following distance.

Studies have shown that the empirical evidence that these multiple-leader models required to give better description of triple vehicles car following is lacking in the relevant literature (Hoogendoorn and Ossen, 2006). Evidence in literature (Hoogendoorn and Ossen, 2006) suggests that there is a requirement for better two-leader car following models not develop as extension of existing single-leader models whose reliability may be uncertain but a two-leader model capable of predicting safe or desired following distance that provide better description of triple vehicles movement.

This study proposed and developed two-leader car following models capable of predicting a safe or desired following distance in a three consecutive vehicles movement in a car following situation that best describes urban, rural and highway driving conditions. In this chapter, distance-based two-leader car following models development is discussed. The extension of the two-leader model to include transport related variables such as gender characteristics, corridor type characterstics and vehicle characheristics are dicsussed. It further discusses the calibration and validation of the distance-based two-leader car following models. Finally, the summary of this chapter is presented.

9.1.1 Models Description

The distance-based two-leader car following models descriptions presented in Chapter 6 and the models formulation discussed in Chapter 7 are calibrated and validated in this chapter. The unique names and descriptions of the two-leader models, including the extended models calibrated and discussed in this chapter are presented in Table 9-1.

Table 9-1: Distance-based two-leader models and their descriptions

Model	Model Description
Model A2	Basic Distance-based Two-Leader Model with the Acceleration of the Following Vehicle
Model B2	Basic Distance-based Two-Leader Model without the Acceleration of the Following Vehicle
A2-1	Distance-based two-leader Car-Car-Car Model
A2-2	Distance-based two-leader Large Vehicle-Car-Car Model
A2-3	Distance-based two-leader Car-Car-Large Vehicle Model
A2-4	Distance-based two-leader Large Vehicle-Car-Large Vehicle Model
A2-5	Two-Leader Model with Gender characteristics
A2-6	Two-Leader Model with Vehicle Occupancy characteristics
A2-7	Two-Leader Model with Corridor Type characteristics
A2-8	Two-Leader Model with Gender and Vehicle Occupancy characteristics
A2-9	Two-Leader Model with Corridor Type, Gender and Vehicle Occupancy characteristics

9.2 Model Calibration Analysis: The Basic Two-Leader Models Calibration

The calibration of the two-leader car following models proposed in this study is discussed. The calibration of Model A2 and Model B2 proposed in Chapter 7 to determine the models calibration parameters values is discussed in this section. Data set B consisting of 41,469 individual time series data points discussed in Chapter 7 was used to calibrate the models. Using multilinear regression analysis and applying Data set B (with time step of 0.1 seconds), the calibration of the basic models (i.e. Model A2 and Model B2) are as follows:

Model A2:

$$\begin{aligned}\Delta x(t+\Delta t) = {} & 0.137\Delta a_{n-1}(t+\Delta t) + 0.075\Delta x_{n-1}(t+\Delta t) - \\ & 0.051 v_{n-2}(t) + 1.417\Delta v(t+\Delta t) + 0.273 v_n(t) + \\ & 1.223 h_{tgn}(t) + 0.670 a_n(t+\Delta t) + 1.112 \end{aligned} \quad (9\text{-}1)$$

Model B2:

$$\begin{aligned}\Delta x(t+\Delta t) = {} & 0.155\Delta a_{n-1}(t+\Delta t) + 0.075\Delta x_{n-1}(t+\Delta t) - \\ & 0.060 v_{n-2}(t) + 1.326\Delta v(t+\Delta t) + 0.283 v_n(t) + \\ & 1.227 h_{tgn}(t) + 1.089 \end{aligned} \quad (9\text{-}2)$$

Where:

Δx – is the desired or safe following distance of the following vehicle to the first leading vehicle [m],

Δa_{n-1} – is the relative acceleration between the second (2^{nd}) and the first (1^{st}) leading vehicles [m/s²],

Δx_{n-1} – is the relative distance between the second and the first leading vehicles [m],

v_{n-2} – is the speed of the second leading vehicle [km/h],

Δv_n – is the relative speed between the first leading vehicle and the following vehicle [m/s],

v_n – is the speed of the following vehicle [km/h],

h_{tgn} – is the time gap between the first leading vehicle and the following vehicle [s],

a_n –is the acceleration of the following vehicle [m/s²],

t – is the time [s],

Δt – is the time step [s],

Both Model A2 and Model B2 calibration parameters estimates were statistically significant at 0.05 (i.e. 95%) confidence level (see Table 9-2 and Table 9-3). The models produced R^2 values of 0.526 and 0.523 for Model A2 and Model B2 respectively. It can be observed that the speed variable parameter estimate sign of the second leader vehicle is negative in both models, which indicates some form of anticipation occurring by the following driver in keeping safe or desired following distance in a triple consecutive vehicles movement. The relative acceleration and the relative distance between the second leader and the first leader significantly influence the choice of a driver in keeping a safe or desired following distance in avoiding a collision should the second leader suddenly applies the brakes to stop. To extend the model to include the gender, vehicle occupancy and vehicle type characteristics discussed in Chapter 7, Model A2 (eqn. 9-1) is extended further since it produced the best statistical regression output.

9.3 The Type of Vehicle Two-Leader Models Development

The type of vehicle following and/or leading in a two-leader three consecutive vehicles movement models are proposed. Literature suggests that the type of lead vehicle affect a

car following process (Kumar et al., 2014; Hoogendoorn and Ossen, 2006) and normal everyday driving observations also shows that drivers observe more than one vehicles ahead (Lenz et al., 1999), hence the type of vehicle leading and/or following in a three vehicles movement influence the following process. It is important to investigate this phenomenon by proposing distance-based two-leader car following models that incorporates the type of vehicles in the following process. For this study, two types of vehicles are considered for the models development: cars and large vehicles (include vans, buses and trucks).

Here, two scenarios based on the position of the following vehicle and the second leading vehicle type in three vehicles movement are considered. The first scenario is when the following vehicle is either a car or a large vehicle and the two leading vehicles are cars (i.e. including the test vehicle as the first leader). The second scenario is when the following vehicle is either a car or a large vehicle and the second leading vehicle is a large vehicle directly ahead of the test vehicle as the first leader. It is assumed that the following vehicles can see around and beyond the first leading vehicle (i.e. the test vehicle) directly ahead. Figure 9-1 presents the data sorting process of the data sets used to calibrate the models for the two scenarios discussed in this section.

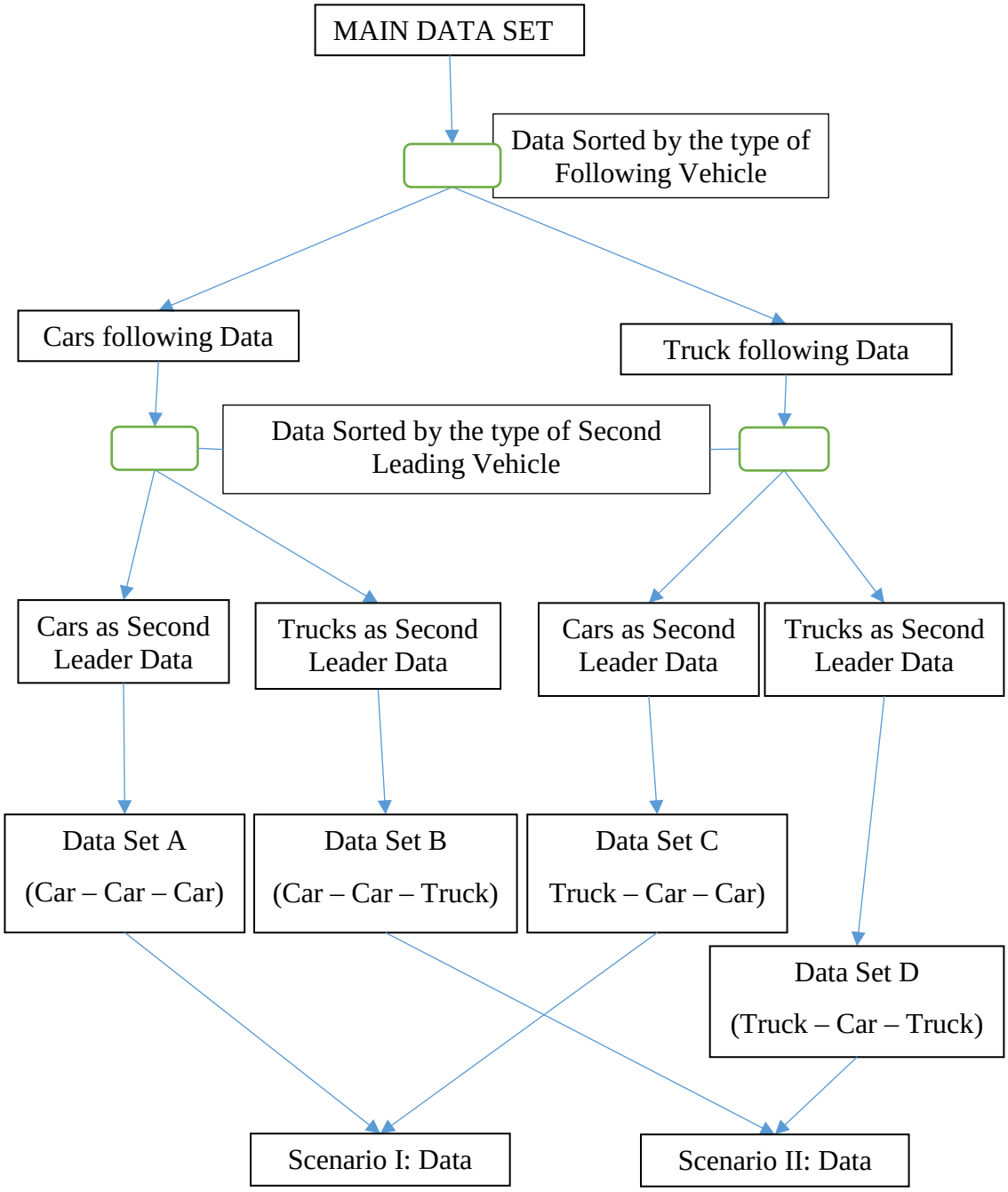

Figure 9-1: Flowchart of data sorting process for data used for the calibration of the type of vehicle distance-based two-leader models

9.3.1 Scenario I: The Car or Large Vehicle Following – and – Car as Second Leader Model

The data set was sorted into vehicle type category based on the following vehicle in the triple vehicles movement. Cars following the test vehicle (i.e. first leader) were sorted first from the whole data set, then followed by sorting the second leading cars (i.e. second leader to the following car) to produce new data set containing only cars data (i.e. follower

car – test vehicle – leading car). This resulted in obtaining a data sample size of 17,000 individual time series data points for the three cars movement data set (designated as Data set A). Similarly, large vehicles following the test vehicle was sorted first from the main data set, followed by sorting the second leading cars resulting in 7,895 individual time series data points for a three vehicles movement data set (designated as Data set C) involving large vehicle and two leading cars (i.e. large vehicle following – test vehicle – leading car) (see Figure 9-1).

In all these cases, the second leading vehicle was maintained as a car (i.e. test vehicle) and the following vehicle changing as either a car or a large vehicle following in a three consecutive vehicles movement. This will enable the development of a model to describe the type of vehicle following behaviour in a distance-based two-leader car following scenarios. Model A2 was used as the basic model for the vehicle type model development. Calibrating Model A2 (i.e. the general or basic model) with the vehicle type following data sets, the models proposed are as follows:

(I). **Model A2-1**: The Following vehicle: Car - and - The Second leader vehicle: Car (i.e. all cars three vehicles model);

Using multilinear regression analysis and applying Data set A with 17,000 individual time series data points, the calibrated model is given by:

Model A2-1:

$$\begin{aligned}\Delta x(t+\Delta t) = {} & 0.130\Delta a_{n-1}(t+\Delta t) + 0.018\Delta x_{n-1}(t+\Delta t) - \\ & 0.032 v_{n-2}(t) + 1.665\Delta v(t+\Delta t) + 0.216 v_n(t) + \\ & 0.330 h_{tg}(t) + 0.638 a_n(t+\Delta t) + 3.803 \end{aligned} \quad (9\text{-}3)$$

The model calibration parameters estimates were all statistically significant with p-values < 0.05 (i.e. 95%) confidence level and R^2 value of 0.563 (see Table 9-4). The three cars model, Model A2-1 (eqn. 9-3), shows the same behaviour as the basic Model A2, indicating that all the model calibration parameters estimates signs are the same as the basic Model A2 calibration parameters estimates.

(II). **Model A2-2**: The Following vehicle: large vehicle – and - The Second leader: car (i.e. large vehicle – car - car model)

Using Data set C with 7,895 individual time series data points for the model calibration, the generalised Model A2-2 equation is given by:

Model A2-2:

$$\Delta x(t+\Delta t) = 0.611\Delta a_{n-1}(t+\Delta t) + 0.086\Delta x_{n-1}(t+\Delta t) - 0.196 v_{n-2}(t) + 1.018\Delta v(t+\Delta t) + 0.441 v_n(t) + 4.923 h_{tgn}(t) + 0.627 a_n(t+\Delta t) - 5.835 \quad (9\text{-}4)$$

All the model calibration parameters estimates were statistically significant at 95% confidence level with p-values < 0.05 and R^2 value of 0.602 (see Table 9-5). The model has the same model calibration parameters estimates signs with Model A2-1 (i.e. when car is following) except the constant term. Different following behaviour was observed for Model A2-1 and Model A2-2. With all conditions the same and in comparison, Model A2-1 will have a longer following distance than Model A2-2 at low speed of the leading vehicles due to the high vantage point of large vehicle drivers (Model A2-2) to see beyond the second leading car or small vehicle. However, in a high speed range of the leading vehicles, Model A2-1 will tend to have shorter following distance than Model A2-2. This is because at high speed, large vehicles may be required to leave longer following distance behind the vehicle directly ahead to compensate for the slow deceleration rate in order to bring the vehicle to a safe stop.

9.3.2 Scenario II: The Car or Large Vehicle Following – and – Large Vehicle as Second Leader Model

Similar data sorting and processes earlier described in Section 9.3.1 was used in this section to sort the whole data set into different type of triple vehicles movement data sets. In this scenario, the second leading vehicle (i.e. ahead of the test vehicle) is a large vehicle and the following vehicle remains as either a car or a large vehicle in the three consecutive vehicles movements. The first case is when car is following and the second leader is large vehicle with the test vehicle as the first leader. The second case is when large vehicle is following and second leader is large vehicle and the test vehicle remained as the first leader. For the first case, the whole data set was sorted first as car following and later second leader as large vehicle. In all, 6,368 individual time series data points (designated as Data set B) was obtained for the first case.

For the second case, the data set was first sorted as large vehicle following and later sorted as second leader vehicle as large vehicle. A total of 3,982 individual time series data points (designated as Data set D) was obtained for the second case (see Figure 9-1). In all these cases, the second leading vehicle was maintained as large vehicle and the following vehicle as either a car or a large vehicle following in the three consecutive vehicles movements with the test vehicle as first leader. This enabled the development of a model to describe the type of vehicle leading (i.e. second leader vehicle) behaviour in a distance-based two-leader car following situation. Calibrating Model A2 with the vehicle type data sets, the models proposed are as follows:

(I). **Model A2-3** (case I): - The Following vehicle: Car – and – The Second leader vehicle: Large vehicle (i.e. car-car-large vehicle model);

Using Data set B with 6,368 individual time sequence data points and applying multilinear regression analysis method, the generalised calibrated model is given by:

Model A2-3:

$$\begin{aligned}\Delta x(t+\Delta t) = {} & -0.223\Delta a_{n-1}(t+\Delta t) - 0.021\Delta x_{n-1}(t+\Delta t) - \\ & 0.058v_{n-2}(t) + 0.688\Delta v(t+\Delta t) + 0.399v_n(t) + \\ & 4.766h_{tg}(t) + 0.248a_n(t+\Delta t) - 6.690 \end{aligned} \quad (9\text{-}5)$$

The calibration parameters estimates were all statistically significant at 95% confidence level with p-values < 0.05. The R^2 value is 0.638 (see Table 9-6). The model have the relative acceleration and the relative distance calibration parameters estimates as negative, which is different from the corresponding basic Model A2 (eqn. 9-1) calibration parameters estimates signs, and that of Scenario I where car was the second leader models. This indicates a stronger response of car following drivers to the second leading large vehicle with this model in a three vehicles following scenario. The model shows that there is a much stronger effect on the following distance of cars when the second leader is a large vehicle than when the second leader is a car as seen in Model A2-1.

This is because the field of view of the driver of the following car downstream will be limited or obstructed by (i.e. could not see beyond) the second leading large vehicle due to its large size and this will affects the car's following behaviour much more than when the following car can see beyond the second leading car of the same size.

(II). **Model A2-4** (case 2): The Following vehicle: Large vehicle - and – The Second leader vehicle: Large vehicle (i.e. large vehicle-car-large vehicle model);

Using Data set D with 3,982 individual time series data points for Model A2-4 calibration, the generalised model is given by:

Model A2-4:

$$\begin{aligned}\Delta x(t+\Delta t) = {} & 0.324\Delta a_{n-1}(t+\Delta t) - 0.055\Delta x_{n-1}(t+\Delta t) - \\ & 0.066 v_{n-2}(t) + 1.487\Delta v(t+\Delta t) + 0.328 v_n(t) + \\ & 3.764 h_{tg}(t) + 0.851 a_n(t+\Delta t) - 1.691 \end{aligned} \quad (9\text{-}6)$$

All the model calibration parameters estimates obtained have p-values < 0.05 that were statistically significant at 95% confidence level and R^2 value of 0.474 (see Table 9-7). For this model, it can be observed that the calibration parameter estimate sign of the relative acceleration between the second and the first leader vehicles is positive compared to Model A2-3 (eqn. 9-5). It shows that there is a behavioural change from when a car is following (Model A2-3) to when a large vehicle is following (Model A2-4) with large vehicle as the second leading vehicle in a three consecutive vehicles movement.

In comparison with the same driving conditions, Model A2-4 will generally have shorter following distance than Model A2-3. This may be explained by the high vantage point of large vehicle drivers and ability to see clearly around and beyond the vehicle directly ahead, coupled with their experience in the low deceleration capabilities of large vehicles (i.e. second leader in this case).

9.4 The Extended Models: Two-Leader Model Extension Calibration

In this section, the calibration of the extended basic distance-based two-leader car following models are discussed. As discussed in Chapter 7, the general or basic two-leader car following model was extended to include the transport related variables to assess their effects on driving behaviour in a three consecutive vehicles movement. The transport related variables such gender characteristics, vehicle occupancy characteristics and corridor type characteristics considered in this study were obtained during the field experiment. The whole data set consisting of 74,998 individual time series data points was used for all the extended models calibration.

9.4.1 The Two-Leader Gender Model

As discussed in Chapter 7, a binary value of 1 or 0 was assigned to the gender variable in the model as Male = 1 and Female = 0. Using the whole data set with 74,998 individual data points with a time step (Δt) of 0.1 seconds and applying multiple linear regression analysis method, the calibrated gender model is as follows:

Model A2-5:

$$\Delta x(t+\Delta t) = 0.110\Delta a_{n-1}(t+\Delta t) + 0.038\Delta x_{n-1}(t+\Delta t) - 0.015v_{n-2}(t) + 1.371\Delta v_n(t+\Delta t) + 0.188v_n(t) + 0.512h_{tgn}(t) + 0.505a_n(t+\Delta t) - 0.249g + 4.054 \quad (9\text{-}7)$$

The model calibration parameters estimates were all statistically significant at 95% confidence level, with p-values < 0.05 and R^2 value of 0.517 (see Table 9-8). There were 75 vehicles with female drivers and 319 vehicles with male drivers identified following in the three vehicles movement data set used for the model calibration. It can be observed that the gender of the driver influence the following distance in a triple vehicles movement. The negative sign of the gender variable estimate suggests that male drivers travel with shorter following distance than their female counterpart does in a two-leader car following situation. Even though Model A2-5 shows that, in general, male drivers follow with shorter following distances than female drivers, male drivers tend to have more driving variability than their female counterparts (see Kim, 2005).

9.4.2 The Two-Leader Vehicle Occupancy Model

Again, a binary value of 1 was assigned to vehicle with occupancy of 1 (oc 1=1) and a value of 0 was assigned to the vehicle with occupancy of 2+ (i.e. two or more occupancy, oc 2+ = 0) dummy variable in Model A2-6 (see Chapter 7). Applying multiple linear regression analysis method using the whole data set, the calibrated vehicle occupancy model is given as follows:

Model A2-6:

$$\Delta x(t+\Delta t) = 0.11\Delta a_{n-1}(t+\Delta t) + 0.039\Delta x_{n-1}(t+\Delta t) - 0.015v_{n-2}(t) + 1.366\Delta v_n(t+\Delta t) + 0.188v_n(t) + 0.513h_{tgn}(t) + 0.507a_n(t+\Delta t) - 0.3746oc + 4.132 \quad (9\text{-}8)$$

The sample size used for the model calibration is 74,998 individual time series data points with time step of 0.1 seconds. There were 283 individual vehicles following in the triple vehicles movements identified with the vehicle driver as the only occupant and 111 individual vehicles with two or more (2+) vehicle occupancy including the vehicle driver in the data set used for Model A2-6 calibration. The model calibration parameters estimates were all statistically significant at 95% confidence level with all p-values < 0.05 and R^2 value of 0.517 (see Table 9-9). The vehicle occupancy model shows that the number of persons in a vehicle significantly affects the following behaviour of vehicles in a two-leader vehicle following situations.

The negative sign of the vehicle occupancy variable estimate shows that vehicles with more than one person occupancy (i.e. 2+ persons) tend to travel with longer following distances than that of vehicles with the driver as the sole vehicle occupant. In everyday driving experiences, it is common to observe drivers that engage in conversation with other passenger(s) in the vehicle. These drivers tend to be distracted and at times lose concentration driving. As a result leaves longer following distance behind the vehicle directly ahead of them. This enable the drivers to prepare to stop safely to avoid a collision in case of emergency. The model has shown that vehicle occupancy adversely affects driving behaviour in keeping a safe or desired following distance in a two-leader car following movement.

9.4.3 The Two-Leader Corridor Type Model

As discussed in Chapter 7, a binary value of 1 or 0 was assigned to the corridor type variables or dummies in Model A2-7 as follows:

Corridor (cr) 1 = 1, All other corridors (i.e. cr2 and cr3) = 0

Corridor (cr) 2 = 1, All other corridors (i.e. cr1 and cr3) = 0

Corridor (cr) 3 = 1, All other corridors (i.e. cr1 and cr2) = 0

Applying the above criteria and using multilinear regression analysis, the general corridor type calibrated model is given as:

Model A2-7:

$$\begin{aligned}\Delta x(t+\Delta t) = {} & 0.117\Delta a_{n-1}(t+\Delta t) + 0.026\Delta x_{n-1}(t+\Delta t) - \\ & 0.015v_{n-2}(t) + 1.376\Delta v_n(t+\Delta t) + 0.190v_n(t) + \\ & 0.504h_{tgn}(t) + 0.498a_n(t+\Delta t) - 1.352cr1 - \\ & 1.486cr2 - 2.065cr3 + 5.546 \end{aligned} \quad (9\text{-}9)$$

The data sample size used for Model A2-7 calibration is 74,998 individual time series data points with a time step of 0.1 seconds. All the model calibration parameters estimates were statistically significant at 95% confidence level and all p-values < 0.05 and R^2 value of 0.517 (see Table 9-10). Model A2-7 shows that the type of traffic corridor affects the following behaviour of a vehicle in a two-leader car following situation. The negative sign of the corridor type variables estimates indicates a reduction in the following distance in all the corridors under investigation. The magnitude of the corridor effect on the following behaviour in a three vehicles movement depends on the type of corridor the driver chooses to use in a journey since all the corridors under investigation negatively affect the driving behaviour.

9.4.4 The Two-Leader Gender - Vehicle Occupancy Model

As earlier discussed in Sections 9.4.1 and 9.4.2, the gender and the vehicle occupancy variables individually were shown to significantly influence the following behaviour of a driver in keeping a desired or safe following distance in a two-leader car following scenario. To investigate further the effect of the gender and vehicle occupancy combination on driver behaviour, a distance-based two-leader model is proposed that incorporates both the gender and the vehicle occupancy characteristics. Model A2-8 general equation is expressed as:

$$\Delta x(t+\Delta t) = \beta_0 \Delta a_{n-1}(t+\Delta t) + \beta_1 \Delta x_{n-1}(t+\Delta t) + \beta_2 v_{n-2}(t) + \beta_3 \Delta v_n(t+\Delta t) + \beta_4 v_n(t) + \beta_5 h_{tgn}(t) + \beta_6 a_n(t+\Delta t) + \beta_7 g + \beta_8 oc + b_0 \quad (9\text{-}10)$$

In calibrating the model, a binary value of 1 or 0 was assigned to the gender and the vehicle occupancy categories as follows:

Gender: Male = 1, Female = 0

Vehicle Occupancy: oc 1 = 1, oc 2+ = 0

Using Model A2-8 (equation 9-10) and apply multiple linear regression analysis method, the model calibration is given by:

Model A2-8:

$$\Delta x(t+\Delta t) = 0.110 \Delta a_{n-1}(t+\Delta t) + 0.039 \Delta x_{n-1}(t+\Delta t) - 0.015 v_{n-2}(t) + 1.369 \Delta v_n(t+\Delta t) + 0.188 v_n(t) + 0.513 h_{tgn}(t) + 0.507 a_n(t+\Delta t) - 0.210 g - 0.358 oc + 4.299 \quad (9\text{-}11)$$

The sample size used for Model A2-8 calibration is 74,998 individual data points with a time step of 0.1 seconds. All the model calibration parameters estimates produced p-values < 0.05 that means all the calibration parameters estimates were statistically significant at 95% confidence level. The model produced R^2 value of 0.517 (see Table 9-11). Again, the model showed that the gender and the vehicle occupancy variables together have significant effects on the following distance of a vehicle in a two-leader vehicle following movement. The negative calibration variables estimates signs for the gender and occupancy variables indicates shorter following distances for male drivers as the only vehicle occupant. It also shows longer following distances for male drivers with two or more vehicle occupant than male drivers as the sole vehicle occupant.

9.4.5 The Two-Leader Corridor Type - Gender - Vehicle Occupancy Model

To investigate the effects of corridor type, the gender of a driver and the vehicle occupancy combination on the following distance of a vehicle in a two-leader car

following scenario, a distance-based two-leader model is proposed that takes into account the corridor type characteristics, the driver gender and the vehicle occupancy characteristics. The proposed Model A2-9 is formulated as follows:

$$\begin{aligned}\Delta x(t+\Delta t) = {} & \beta_0 \Delta a_{n-1}(t+\Delta t) + \beta_1 \Delta x_{n-1}(t+\Delta t) + \beta_2 v_{n-2}(t) + \\ & \beta_3 \Delta v_n(t+\Delta t) + \beta_4 v_n(t) + \beta_5 h_{tgn}(t) + \beta_6 a_n(t+\Delta t) + \\ & \beta_7 cr1 + \beta_8 cr2 + \beta_9 cr3 + \beta_{10} g + \beta_{11} oc + b_0 \end{aligned} \quad (9\text{-}12)$$

In order to calibrate Model A2-9 to ascertain the significance of the variables combination in the model, a binary value of 1 or 0 was assigned to each indicator variable categories. The binary value was assigned to each category as follows:

Corridor (cr) 1 = 1, All other corridors (i.e. cr2 and cr3) = 0

Corridor (cr) 2 = 1, All other corridors (i.e. cr1 and cr3) = 0

Corridor (cr) 3 = 1, All other corridors (i.e. cr1 and cr2) = 0

Gender: Male = 1, Female = 0

Vehicle Occupancy: oc 1 = 1, oc 2+ = 0

Using Model A2-9 (equation 9-12) and applying the above indicator variables criteria to the data set, the model calibration is given by:

Model A2-9:

$$\begin{aligned}\Delta x(t+\Delta t) = {} & 0.126 \Delta a_{n-1}(t+\Delta t) + 0.031 \Delta x_{n-1}(t+\Delta t) - \\ & 0.013 v_{n-2}(t) + 1.382 \Delta v_n(t+\Delta t) + 0.178 v_n(t) + \\ & 0.441 h_{tgn}(t) + 0.542 a_n(t+\Delta t) - 1.393 cr1 - \\ & 2.269 cr2 - 2.418 cr3 - 0.344 g - 0.867 oc + 6.838 \end{aligned}$$

(9-13)

All the model calibration parameters estimates were statistically significant at 95% confidence level with all parameters estimates having p-values < 0.05 and R^2 value of 0.519 (see Table 9-12). The sample size used for the model calibration is 54,998 individual data points with 0.1 seconds time step. There were 74, 102, 134 and 80 individual triple vehicle movements in a car following situations identified for Corridor 1, Corridor 2, Corridor 3 and Corridor 4 respectively, making up the data set used for Model A2-9

calibration. The negative signs of the corridor type variables estimates indicates a reduction in the following distance and the positive sign of the calibration parameters estimates indicates an increase in the distance of following.

The model shows that there is a significant effect on driver behaviour in keeping a desired following distance when taking into consideration the gender of the driver, the vehicle occupancy and the corridor type characteristics all together in a three consecutive vehicles movement. It also indicates that single vehicle occupancy male drivers will have shorter following distance than male drivers with more than one occupancy vehicle on any of the corridors considered. Female drivers will have longer following distance than male drivers on all the corridors in a three vehicles following movements.

9.5 The Distance-Based Two-Leader Car Following Model Validation

To assess the reliability of the basic or the general two-leader car following models developed in this study, it is important to validate the models to ascertain the level of magnitude of variation between the observed data sets and the models predicted data sets. It is, also, important to simulate the models against real world driving scenarios in order to assess its reliability in accurately describing real driver behaviour in a two-leader car following situation. In this section, validation and simulation of the distance-based two-leader car following models is discussed. The two basic models, Model A2 (eqn. 9-1) and Model B2 (eqn. 9-2) are validated since both models are recommended for use in vehicle following distance predictions.

9.5.1 Two-Leader Car Following Modelled Against Observed Data

The whole data set (consisting of 82,939 individual data points) divided into two sets of data: Data set A and Data set B. Data set B file was used for the model calibration process discussed in Section 9.2. Data set A file was used for the validation of the model to ascertain its reliability in real world driving behaviour predictions in a two-leader car following scenario. Data set A file consists of 41,470 individual data points with a time step of 0.1 seconds. Data set A file was split into two halves: Data files AA and AB with each consisting 20,435 individual time series data points. Each sets of data files were further split into two separate data set files, resulting in four different sets of data files (i.e. Data files AAA, AAB, ABA and ABB) with each consisting of a minimum of 10,368

individual data points discussed in Chapter 7. These data sets were used for the model validation.

The t-test statistical analysis method discussed in Chapter 6 was used for the validation of the basic models. The two basic models, Model A2 (eqn. 9-1) and Model B2 (eqn. 9-2) are validated, since both models are recommended for use in vehicle following distance predictions. Each basic model was modelled separately against the observed data. Applying the data sets to Model A2 and Model B2, the basic two-leader models, the predicted following distances for all the four separate data sets were obtained for every data point. The average of the predicted following distances for each of the four sets of data were calculated. The average of the observed following distances for each of the four data sets were also calculated.

The averages of the following distances for both the observed and predicted data sets for the four data sets were used in the t-test statistical significant test. To begin the models validation, two hypothetical questions were set for the t-test as follows:

H_0: There is no significant difference between the observed and the models predicted data sets (i.e., $H_0: \mu_d = 0$).

Ha: There is significant difference between the observed and the models predicted data sets (i.e., $H_a: \mu_d \neq 0$).

where H_0 and H_a are the null and the alternative hypotheses respectively, μ_d is the population mean of the differences in the means between the two groups of data.

As discussed in Chapter 6, the t-test statistics was computed using Microsoft Excel data analysis tool and obtained the p-values and t-values for Model A2 and Model B2. The paired two-sample for means two-tail t-test statistics was used for this analysis. Table 9-13 shows the t-test statistics results for both Model A2 and Model B2. The two-tailed t-test statistics results produced p-value of 0.17 and t-stat value of -1.774 for Model A2. The t-test statistics for Model B2 resulted in the p-value of 0.17 and t-stat value of -1.827 for degree of freedom (df) of 3 (i.e. 4 - 1). It can be seen that the p-values for Model A2 and Model B are all greater than the p-value of 0.05 (95% confidence level). Similarly, the t-stat values for Model A2 and Model B2 are also less than the two-tail t-critical value of 3.182 (for df = 3, at 95% cl). The t-test statistics results shows that there is no enough evidence in the mean differences between the observed and predicted two-leader car

following data sets to suggests the rejection of the null hypothesis. Therefore, the alternative hypothesis was rejected since no significant differences were observed in the two groups of the two-leader car following data sets for both Model A2 and Model B2.

The t-test statistics was used to test the significant differences between the observed and the predicted data sets for the new distance-based two-leader car following models developed in this study. The t-test statistical analysis found that at p-value ≤ 0.05 (i.e. 95% confidence level), there was no statistical significant differences observed between the observed or measured and the models predicted data sets for the two-leader car following models developed to suggests the rejection of the null hypothesis (H_0). Therefore, we conclude that, there is no statistical significant differences between the observed and the predicted data sets for Model A2 [t(3) = -1.774, p-value > 0.05, 2-tail] and Model B2 [t(3) = -1.827, p-value > 0.05, 2-tail]. The basic Model A2 and Model B2 proposed and developed in this study has been shown to predict accurately the safe or desired following distance of a vehicle in a three successive vehicles movement in a car following situation in a real world driving scenario. The models developed in this study best describe a two-leader car following behaviour within urban, urban-rural and highway driving conditions.

9.5.2 Two-Leader Model Simulation

Four randomly selected individual triple vehicle movements observed from the field were selected for model simulation using Model A2 (eqn. 9-1), the basic two-leader car following model developed in this study. The selected individual three vehicles movements were identified by the following vehicles as Driver 340, Driver 413, Driver 414 and Driver 453. All the three consecutive vehicles movements selected have a minimum following time duration of 40 seconds and maximum following time duration of 192 seconds in a two-leader car following scenario without stopping throughout the following process. The data sample sizes used for the model simulation was 161, 175, 249 and 100 individual time series data points for Drivers 340, 413, 414 and 453 respectively. Model A2, the basic model, was used for simulating the four selected triple vehicles movements considered for this research and discussed in Chapter 7. Each individual selected triple vehicles movements data sets was applied to the base model separately and the relative following distances at each time step simulated for all the identified drivers.

The simulation outputs and the observed data sets for each selected following drivers were plotted on charts for comparative analysis. The speed of the following vehicles plotted against the simulated and the observed relative distances for each selected vehicle. The average of the relative distances at each speed range were plotted for the individual identified vehicles (or drivers) (see Figure 9-2, Figure 9-3, Figure 9-4 and Figure 9-5). It can be seen from all the figures that the simulation results replicates closely to the measured/observed following distances of each identified vehicle in the two-leader vehicle following movement. For Driver 340, the average simulation relative distance is 7.99 metres and that of the observed is 7.40 metres representing a difference of 0.26 metres (see Figure 9-2). In the case of Driver 413 (see Figure 9-4), the observed and the simulated average relative distance were 8.42 metres and 7.86 metres respectively. This represents an average distance difference of 0.56 metres between the observed and the simulation results. The simulation average relative distance of Driver 414 was less than the observed relative distance by 0.07 metres. The average observed relative distance of Driver 414 is 7.21 metres and that of the simulation average relative distance is 7.14 metres (see Figure 9-3).

In the case of Driver 453, the average observed relative distance was less than the average simulation relative distance by 0.26 metres (see Figure 9-5). The simulation model produced an average relative distance of 9.14 metres compared with that of the observed relative distance of 8.88 metres for Driver 453. In all, the difference in the average relative distances between the observed and the simulation results for all the four selected following vehicles were less than 0.6 metres. The low values of the average following distance differences between the observed and the simulated results shows that the model developed in this study closely replicates real world driving scenarios of two-leader car following behaviour. The simulation results suggests that the model performs better in describing the following behaviour of a vehicle following in a three consecutive vehicles movement in a car following scenario.

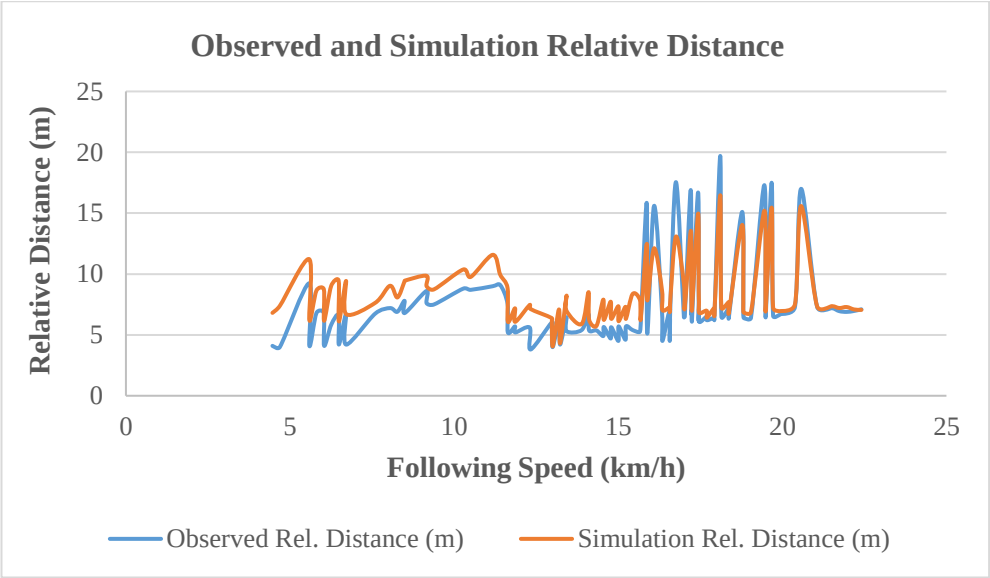

Figure 9-2: The simulated and the observed triple vehicles movement comparison for following Driver 340

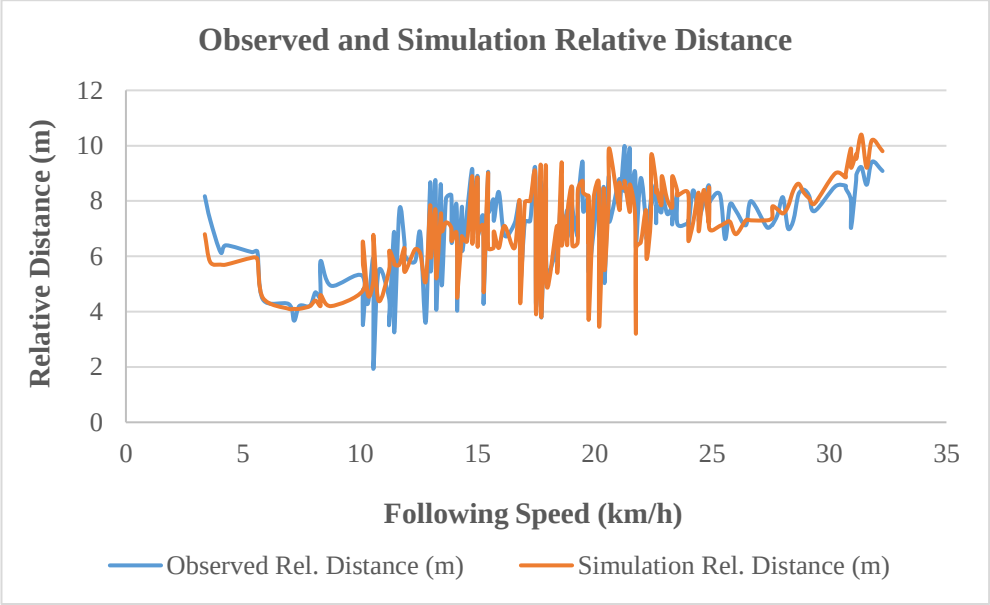

Figure 9-3: The simulated and the observed triple vehicles movement comparison for following Driver 414

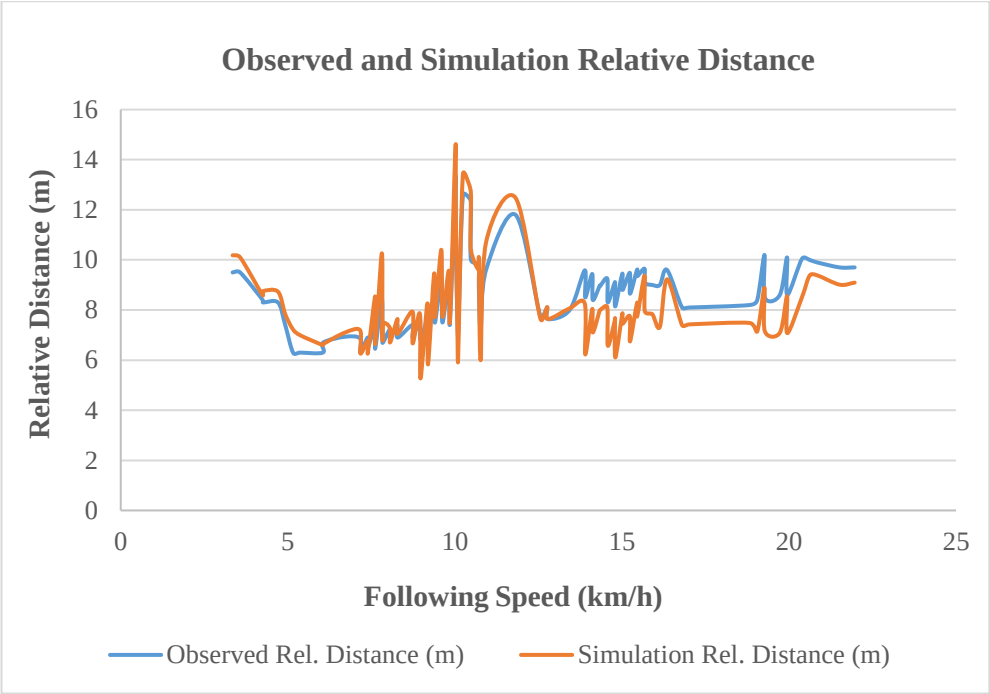

Figure 9-4: The simulated and the observed triple vehicles movement comparison for following Driver 413

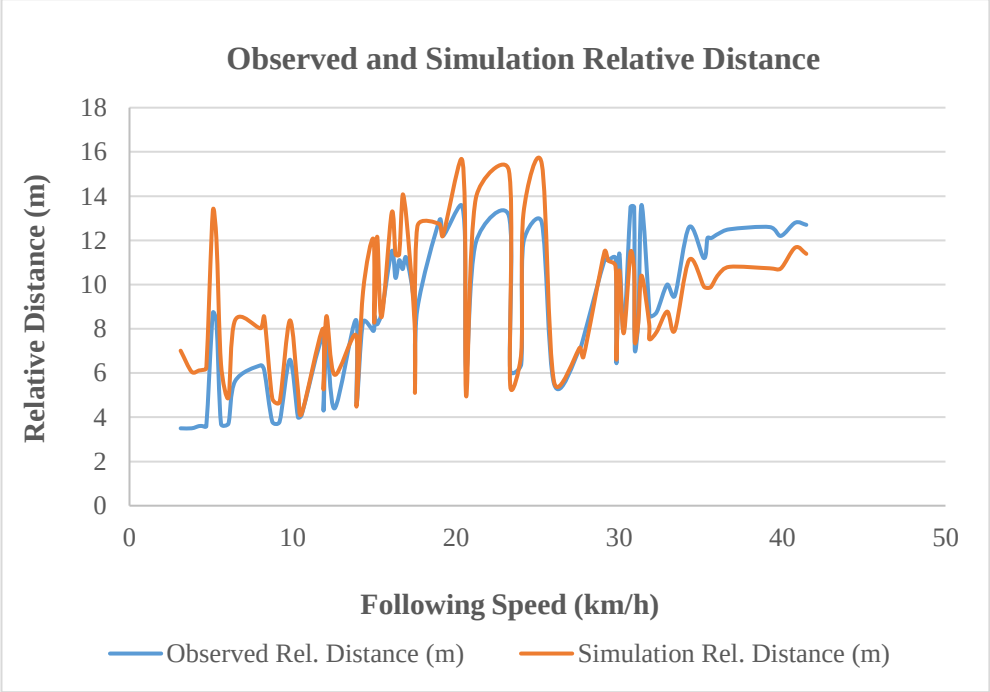

Figure 9-5: The simulated and the observed triple vehicles movement comparison for following Driver 453

9.6 Tables of Models Calibration Results

The regression analysis outputs of the models calibrations discussed in this chapter are presented in tables in this section. The tables of results presented in this section include the basic or general models, the vehicle type following models and all the extended models as well as the validation of the models computation results. The models calibration tables present and define the models parameters, the parameters coefficients with the corresponding standard errors and p-values. The sample sizes, the R^2 values and regression analysis overall standard errors are presented in the models results tables. The models parameters in the tables are defined as follows:

b_o – is the constant term of the model,

Δa_{n-1} – the relative acceleration between the second (2^{nd}) vehicle and the first (1^{st}) leading vehicle (test vehicle) [m/s²],

Δx_{n-1} – the relative distance between the second and the first leading vehicles [m],

v_{n-2} – is the speed of the second leading vehicle [km/h],

Δv_n – is the relative speed between the first leading vehicle and the following vehicle [m/s],

v_n – is the speed of the following vehicle [km/h],

h_{tgn} – is the time gap between the first leading vehicle and the following vehicle [s],

a_n – is the acceleration of the following vehicle [m/s²].

Table 9-2: Model A2 - the basic distance-based two-leader model regression output

Model A2: Basic Model			
Model Parameters	Coefficient	Standard Error	P-value
b_0	1.112384747	0.076262501	4.56E-48
Δa_{n-1} [m/s²]	0.137451351	0.046084347	0.00286
Δx_{n-1} [m]	0.07489847	0.003384522	7E-108
v_{n-2} [km/h]	-0.05084632	0.006536731	7.5E-15
Δv_n [m/s]	1.416587911	0.036484223	0
v_n [km/h]	0.273459392	0.006686921	0
h_{tgn} [s]	1.222806742	0.017468292	0
a_n [m/s²]	0.670083178	0.038899378	2.9E-66
R^2	0.526564423		
Standard Error	7.198665351		
Observations	40176		

Table 9-3: Model B2 – the basic distance-based two-leader model regression output results

Model B2: Basic Model			
Model Parameters	Coefficient	Standard Error	P-value
b_0	1.08891965	0.076530509	7.8746E-46
Δa_{n-1} [m/s²]	0.15505163	0.046242310	0.000800073
Δx_{n-1} [m]	0.075445562	0.003396809	1.2229E-108
v_{n-2} [km/h]	-0.06047401	0.006536724	2.32084E-20
Δv_n [m/s]	1.326043454	0.036236266	1.9728E-288
v_n [km/h]	0.283139464	0.006687751	0
h_{tgn} [s]	1.226839796	0.017530903	0
R^2	0.523121476		
Standard Error	7.225116217		
Observations	40176		

Table 9-4: Model A2-1 (i.e. all Car Model) regression analysis output results*

Model A2-1: Car-Car-Car Model			
Model Parameters	Coefficient	Standard Error	P-value
b_0	3.803735876	0.094089384	0
Δa_{n-1} [m/s²]	0.129515636	0.060757695	0.03305
Δx_{n-1} [m]	0.018454994	0.005580766	0.00095
v_{n-2} [km/h]	-0.03203889	0.005845101	4.3E-08
Δv_n [m/s]	1.665048535	0.039851591	0
v_n [km/h]	0.216261378	0.005791443	2E-293
h_{tgn} [s]	0.330254641	0.012136687	1E-159
a_n [m/s²]	0.638123324	0.049328908	4.3E-38
R^2	0.582200647		
Standard Error	6.038375867		
Observations	17000		

*Car - Car - Car Model = Car following first leading Car (Test Vehicle) and second leading Car

Table 9-5: Model A2-2 (Large vehicle - Car - Car Model) regression output results*

Model A2-2: Large vehicle - Car - Car Model			
Model Parameters	Coefficient	Standard Error	P-value
b_0	-5.83546392	0.216418650	2.9659E-153
Δa_{n-1} [m/s²]	0.611341339	0.098454694	5.58913E-10
Δx_{n-1} [m]	0.085980399	0.006700887	2.58552E-37
v_{n-2} [km/h]	-0.19586632	0.011874438	4.03269E-60
Δv_n [m/s]	1.017633348	0.068501984	2.95634E-49
v_n [km/h]	0.441188767	0.012123711	3.5602E-268
h_{tgn} [s]	4.923458974	0.073594821	0
a_n [m/s²]	0.627317794	0.078838838	2.00861E-15
R^2	0.60237489		
Standard Error	6.346880504		
Observations	7895		

*Large Vehicle - Car - Car Model = Large Vehicle following first leading Car and second leading Car

Table 9-6: Model A2-3 (Car - Car - Large vehicle Model) regression output results*

Model A2-3: Car - Car - Large vehicle Model			
Model Parameters	Coefficient	Standard Error	P-value
b_0	-6.69046026	0.203686829	1E-218
Δa_{n-1} [m/s²]	-0.22308234	0.093434399	0.01699
Δx_{n-1} [m]	-0.02065379	0.006884683	0.00271
v_{n-2} [km/h]	-0.05759951	0.014273201	5.5E-05
Δv_n [m/s]	0.688284007	0.076419187	2.8E-19
v_n [km/h]	0.39945202	0.015397569	4E-141
h_{tgn} [s]	4.765529153	0.074605050	0
a_n [m/s²]	0.248476357	0.077325001	0.00132
R^2	0.637949058		
Standard Error	5.703570722		
Observations	6368		

*Car - Car - Large Vehicle Model = Car following first Leading Car and second leading Large Vehicle

Table 9-7: Model A2-4 (Large vehicle - Car - Large vehicle Model) regression output results*

Model A2-4: Large vehicle - Car - Large vehicle Model			
Model Parameters	Coefficient	Standard Error	P-value
b_0	-1.69122109	0.303088458	2.5661E-08
Δa_{n-1} [m/s²]	0.324089145	0.142332970	0.022840419
Δx_{n-1} [m]	-0.05455154	0.008529964	1.78809E-10
v_{n-2} [km/h]	-0.06611964	0.018610272	0.000385498
Δv_n [m/s]	1.487271659	0.098426552	3.34549E-50
v_n [km/h]	0.328177632	0.019363657	2.91352E-62
h_{tgn} [s]	3.763793872	0.087647349	0
a_n [m/s²]	0.851180436	0.111527529	2.87566E-14
R^2	0.4739137		
Standard Error	6.00078331		
Observations	3982		

*Large Vehicle - Car - Large Vehicle Model = Large Vehicle following first leading Car and second leading Large Vehicle

Table 9-8: Model A2-5 (Gender Model) regression analysis output results

Model A2-5: Gender Model			
Model Parameters	Coefficient	Standard Error	P-value
b_0	4.053585640	0.074285917	0
Δa_{n-1} [m/s²]	0.109677452	0.032591509	0.00077
Δx_{n-1} [m]	0.038276521	0.002578411	8.8E-50
v_{n-2} [km/h]	-0.01496745	0.003695654	5.1E-05
Δv_n [m/s]	1.370647201	0.022679992	0
v_n [km/h]	0.188438152	0.003728546	0
h_{tgn} [s]	0.512477127	0.007571935	0
a_n [m/s²]	0.504687658	0.026459871	6.5E-81
Gender[a]	-0.24856418	0.066385273	0.00018
R^2	0.517012586		
Standard Error	6.543712855		
Observations	74999		

[a] Gender: Male = 1; Female = 0

Table 9-9: Model A2-6 (Vehicle Occupancy Model) regression analysis output results

Model A2-6: Vehicle Occupancy Model			
Model Parameters	Coefficient	Standard Error	P-value
b_0	4.132487491	0.064891709	0
Δa_{n-1} [m/s²]	0.110095066	0.032584999	0.000728654
Δx_{n-1} [m]	0.038610988	0.002578444	1.27535E-50
v_{n-2} [km/h]	-0.01486125	0.003694439	5.76157E-05
Δv_n [m/s]	1.366376637	0.022660490	0
v_n [km/h]	0.187999125	0.003727950	0
h_{tgn} [s]	0.512567063	0.007569388	0
a_n [m/s²]	0.507066381	0.026457760	1.13595E-81
Occupancy[b]	-0.37457686	0.056222750	2.71298E-11
R^2	0.516574243		
Standard Error	6.542388546		
Observations	74999		

[b] Occupancy: oc 1 = 1; oc 2+ = 0

Table 9-10: Model A2-7 (Corridor Type Model) regression analysis output results

Model A2-7: Corridor Type Model			
Model Parameters	Coefficient	Standard Error	P-value
b_0	5.545592077	0.089637050	0
Δa_{n-1} [m/s²]	0.116945329	0.032498350	0.00032
Δx_{n-1} [m]	0.02636627	0.002636160	1.5E-23
v_{n-2} [km/h]	-0.01529739	0.003681452	3.3E-05
Δv_n [m/s]	1.37633473	0.022602665	0
v_n [km/h]	0.189632208	0.003715536	0
h_{tgn} [s]	0.503622777	0.007582991	0
a_n [m/s²]	0.497790184	0.026359432	2.3E-79
Corridor (Cr) 1*	-1.35179467	0.089566974	2.2E-51
Corridor (Cr) 2*	-1.48638547	0.084194758	1.3E-69
Corridor (Cr) 3*	-2.06536489	0.084357841	7E-132
R^2	0.517494624		
Standard Error	6.51768512		
Observations	74999		

*Corridor Type: Cr1 = 1, Cr2 = Cr3 = 0; Cr2 = 1, Cr1 = Cr3 = 0; Cr3 = 1, Cr1 = Cr2 = 0

Table 9-11: Model A2-8 (Gender - Vehicle Occupancy Model) regression analysis output results

Model A2-8: Gender – Vehicle Occupancy Model			
Model Parameters	Coefficient	Standard Error	P-value
b_0	4.298985804	0.083732829	0
Δa_{n-1} [m/s²]	0.110187385	0.032583079	0.00072066
Δx_{n-1} [m]	0.038615962	0.002578292	1.22264E-50
v_{n-2} [km/h]	-0.01505044	0.003694710	4.63571E-05
Δv_n [m/s]	1.369077820	0.022675406	0
v_n [km/h]	0.188116227	0.003727915	0
h_{tgn} [s]	0.513049286	0.007570491	0
a_n [m/s²]	0.507402286	0.026456406	8.74433E-82
Gender[a]	-0.20968785	0.066650095	0.001655282
Occupancy[b]	-0.35824897	0.056458458	2.23174E-10
R^2	0.517204415		
Standard Error	6.542000437		
Observations	74999		

[a] Gender: Male = 1; Female = 0
[b] Occupancy: oc 1 = 1; oc 2+ = 0

Table 9-12: Model A2-9 (Corridor – Gender-Vehicle Occupancy Model) regression analysis output results

Model A2-9: Corridor type – Gender – Vehicle Occupancy Model			
Model Parameters	Coefficient	Standard Error	P-value
b_0	6.838365745	0.130607132	0
Δa_{n-1} [m/s²]	0.125872542	0.038092469	0.00095
Δx_{n-1} [m]	0.031451242	0.003472847	1.4E-19
v_{n-2} [km/h]	-0.01274464	0.004165913	0.00222
Δv_n [m/s]	1.382461131	0.026212388	0
v_n [km/h]	0.178012936	0.004230188	0
h_{tgn} [s]	0.441284271	0.007903246	0
a_n [m/s²]	0.542231787	0.030908481	1E-68
Corridor (Cr) 1*	-1.39309109	0.092497245	3.7E-51
Corridor (Cr) 2*	-2.26870641	0.095598937	7E-124
Corridor (Cr) 3*	-2.41842229	0.091577745	1E-152
Gender[a]	-0.34392587	0.079449326	1.5E-05
Occupancy[b]	-0.86732926	0.069056972	3.9E-36
R^2	0.518838751		
Standard Error	6.628186435		
Observations	54999		

*Corridor Type: Cr1 = 1, Cr2 = Cr3 = 0; Cr2 = 1, Cr1 = Cr3 = 0; Cr3 = 1, Cr1 = Cr2 = 0
[a] Gender: Male = 1; Female = 0
[b] Vehicle. Occupancy: oc 1 = 1; oc 2+ = 0

Table 9-13: The paired two sample means t-test results for Model A2 and Model B2 (the basic or general models)

MODEL A2					
Data Set	Observed	Predicted	T-Test Result		
				Observed	Predicted
Data AAA	10.54	11.13	Mean	10.3575	11.14
Data AAB	10.15	12.23	Variance	0.281825	0.8897333
Data ABA	9.75	9.93	Observations	4	4
Data ABB	10.99	11.27	Pearson Correlation	0.3922794	
			Hypothesized Mean Difference	0	
			df	3	
			t Stat	-1.7735016	
			P(T<=t) one-tail	0.08712593	
			t Critical one-tail	2.35336343	
			P(T<=t) two-tail	0.17425187	
			t Critical two-tail	3.18244631	
MODEL B2					
Data Set	Observed	Predicted	T-Test Result		
				Observed	Predicted
Data AAA	10.54	11.15	Mean	10.3575	11.1475
Data AAB	10.15	12.21	Variance	0.281825	0.8601583
Data ABA	9.75	9.95	Observations	4	4
Data ABB	10.99	11.28	Pearson Correlation	0.40030342	
			Hypothesized Mean Difference	0	
			df	3	
			t Stat	-1.8271086	
			P(T<=t) one-tail	0.08257257	
			t Critical one-tail	2.35336343	
			P(T<=t) two-tail	0.16514515	
			t Critical two-tail	3.18244631	

9.7 Summary

A triple vehicles (i.e. three consecutive vehicles) movement in a car following situation was modelled and calibrated in this chapter. A distance-based two-leader car following models that best describes the desired or safe following distance of a vehicle following in a triple vehicles movement were developed and discussed. In addition to the model extensions that takes into account other transport related variables that influence driving

behaviour, the models that takes into consideration the type of following vehicles and/or type of second leading vehicles were proposed and calibrated.

Factors or variables such as the vehicle occupancy characteristics, the type of traffic corridors characteristics and the gender characteristics introduced in the basic model were found to be statistically significant at 95% (i.e. p-values $\leq$ 0.05) confidence level. Combination of two or more of these variables introduced in the basic model were found to be statistically significant at 95% significance level. The study showed that these factors considered in this study does influence the driving behaviour of a vehicle following in a triple vehicles movement in a two-leader car following situation, since they were all found to be statistically significant at p-value of 0.05 (i.e. 95% confidence level).

To determine the magnitude of variation between the predicted and the observed data sets, models validation process was carried out to ascertain the models reliability against real world two-leader car following scenario. The t-test statistical analysis results (i.e., for Model A2 [t(3) = -1.774, p-value > 0.05, 2-tail] and for Model B2 [t(3) = -1.827, p-value > 0.05, 2-tail]) were found to have no statistical differences between the observed and the predicted data sets. Four randomly selected triple vehicles following movements observed in the field were identified, simulated and compared with the corresponding field data. The differences in the average relative distance between the simulation and the observed following distances for all the four selected triple vehicles movements ranges from 0.07 metres to 0.56 metres. The analysis showed that the simulation results closely mimic the real world two-leader car following scenario of three vehicles in consecutive motion observed in the field experiment. It showed that the distance-based two-leader car following model developed in this study performs better in real world car following situations.

The next chapter discusses the bus following model proposed in this study. It also discusses the variability of bus drivers' driving behaviour within urban-rural traffic conditions. It discusses the calibration and validation of the bus following model.

CHAPTER 10 BUS FOLLOWING MODEL: RESULTS AND ANALYSIS

10.1 Introduction

The calibration, validation and simulation of the distance-based two-leader car following models including the extension of the model to include the gender, vehicle occupancy and corridor type (road) characteristics were discussed in Chapter 9. In this chapter, bus speed variability and bus following models calibration and validation are discussed. A number of research on vehicle following behaviour have been studied. These studies are often focused on car following car driving behaviour. However, there has been very limited attention and understanding on the following behaviour of car following bus within urban-rural areas.

There are also insufficient data to describe the variability of driving behaviours of bus drivers and the effect on other vehicles in a bus-following scenario. For instance, in a situation where a car follows a bus on busy traffic corridor, in the absence of dedicated bus lanes (i.e. unrestricted lane use), the bus driving behaviour would certainly affect the driving behaviour of the vehicle directly behind the bus and the effect trickling on to the other following vehicles upstream. Moreover, mathematical models describing the bus following behaviour has not been given the needed attention it is required, when in fact, bus following behaviour and effect on the traffic flow in everyday driving experiences within the cities are frequently observed. For instance, in the urban areas, public commuter buses often share the same road space with other vehicle types within the network and by so doing, interact with these vehicles as they commutes, which affects their driving behaviour.

Studies have shown that car drivers interact differently following large vehicles to following vehicles of the same type or size (Sayer et al., 2003; Hoogendoorn and Ossen, 2006) in a car following situation. Little is known in literature to support models that describe the interactions between cars following buses in bus following scenario. A bus following study conducted by Rothery et al. (1964) focused on bus following bus behaviour to determine the validity and parameters of the existing car following models. The study did not consider the interactions between other vehicle types and buses in a bus following behaviour. Using an online platform to investigate the bus station effect on bus movements, Tang et al. (2012) developed a bus following model that describe the phenomena resulting from bus station effect on the bus behaviour. The study did not

investigate the effect of the bus movement on the traffic flow dynamics. A recent study by Appiah et al. (2015) developed a mathematical model that describes the interactions between a car and a bus in a bus following situation. The interactions between cars and buses required to be investigated further as evidence suggests that not much attention has been given to this special kind of driving behaviour in which a car follow a bus within urban road networks.

This study investigate bus driving speed variability and effect on the time gap choice of the following vehicles. This study proposes and develops bus following models that describes the interactions between a car and a bus in a bus following scenario within urban-rural driving conditions. The analysis of individual bus driver's driving speed variability is discussed in this chapter. The effect of individual bus driving speed variability on the time gap of the following vehicles (i.e. the immediate two following vehicles) are discussed in Section 10.4. The calibration and validation of bus following models are discussed in Section 10.4. Section 10.5 summarise the analysis of this chapter. In this chapter, the bus following models were developed with data sets obtained using the test vehicle (different driver) as the following vehicle following a number of different double decker buses.

10.1.1 Bus Network and Services in Edinburgh

Lothian Bus Company is the dominant public bus service operator in Edinburgh, owned and operated by The City of Edinburgh Council, the majority shareholder. Other bus companies operates in Edinburgh, such as First Buses, which provides services for passengers mostly between the city and the surrounding towns or counties unlike the Lothian Buses, which provide services for the local communities in and around Edinburgh. Lothian Buses in 2013 carried over 2.2 million passengers per week with 711 operational buses on 70 routes across Edinburgh, Midlothian and East Lothian. The bus company operates with 2,550 active bus stops in Edinburgh, Midlothian and East Lothian, with 4 travelshops and bus depots, and serving 5 park and rides sites around the city (Lothian Buses, 2013).

The passenger numbers increased with 6 million extra passengers over 2014 reporting period. The company's fleet of buses increased to over 721 vehicles, all fully accessible and fitted with Wi-Fi, attracting over 350,000 passenger journeys per day. Passenger numbers increased to 2.3 million passengers per week with increase in active bus stops

to 2,788 from 2,550 in 2013. The bus services were supported with 27 trams operating on a 14 kilometres tram route with 15 stops between Edinburgh Airport and the city centre with 3 million passenger journeys. In addition, there are 46 tour buses operated by Lothian buses operating within the city on 5 routes with 10,000 passengers per week (TfE, 2015).

Lothian Buses offer two main services (i.e. day and night services) for the residence of Edinburgh and the Lothians, including residence outside the Lothian area using the Lothian Country buses. During the day service, more than 50 bus routes across the City of Edinburgh and the Lothians are served. The day service buses are considered the normal and express service for Lothian Buses, which runs from approximately 0400 hours to just after midnight. Lothian Buses have installed GPS (Global Positioning System) position equipment on all the service buses which send the position of all the service buses to a central server at approximately every 30 seconds, which then estimate the arrival times at various bus stops across the city using predictive model (Vissat et al., 2015). Live bus departures can be tracked using the journey planner on the company's website or through smart phone apps. The estimated real time arrivals of service buses are relayed back to waiting passengers from the central servers through real time bus tracker digital display signage installed at various bus stops along the service routes.

10.2 Bus Following Behaviour Analysis

As discussed in Chapter 3, eight double decker buses were followed on a number of urban-rural corridors in two consecutive days during the PM peak hours. During the experiment, a number of vehicles were observed following the test vehicle at the same time when the test vehicle was following the buses in a three consecutive vehicles movement (see Figure 10-4). A total of 42 vehicles followed the test vehicle in three vehicles movement with the buses leading. For every bus followed, the number of vehicles following the test vehicle were identified and analysed. Each bus followed by the test vehicle was assigned an identification number, such as BD (i.e. Bus Driver), for instance, bus 1 denoted as BD1. Table 10-1 shows the following duration of each bus followed and the corresponding number of vehicles that were captured following the test vehicle in a three vehicles bus following movement. On average, the bus waiting time at the bus stop is 16.9 seconds and waiting time stationary or queuing in traffic is 18.9 seconds for every average travel time of 699.4 seconds during the PM rush hours. The buses heading towards Edinburgh city centre, on average, spend about 3 seconds more at

the bus stops and 13 seconds more in traffic queues than buses heading towards the outskirt of Edinburgh city centre on corridors without dedicated bus lanes.

Table 10-1: Bus following duration of individual bus observed

Bus ID	Overall Time Bus leading (including stops) (seconds)	Average Time Bus stopped at Bus Stops (seconds)	Average Time Bus stopped at Traffic (seconds)	Actual Total Time Bus leading (without stopping) (seconds)	Total vehicle following the test vehicle for each bus followed
BD1	1130	17	13	832	7
BD2	346	11	5	298	1
BD3	148	19	0	110	1
BD4-r*	1220	27	14	882	7
BD5-r*	132	11	21	100	3
BD6	584	14	31	281	5
BD7	891	18	9	666	11
BD8-r*	1144	18	39	588	6

*r = returning bus to Edinburgh city centre

10.3 Bus Driving Speed Variability and Effect on Following Time Gap

In this section, the speed variability of bus driving behaviour and the effect on the time gap (i.e. time headway) of the vehicle (test vehicle) following directly behind the bus are discussed.

10.3.1 Speed Variability in Bus Driving Behaviour

The time - speed profile relationship of all the buses followed throughout the experiment without stopping are presented in Figure 10-1 and Figure 10-2. The speed of the buses were observed to be varying per driver on the same corridor. It can be seen from Figure 10-1 and Figure 10-2 that, there are driving speed variations among the individual bus drivers on the corridor during the evening peak period. The buses that were found to have high variability in driving speed were buses BD2, BD4 for day 1 (see Figure 10-1) and buses BD7, BD8 for day 2 (see Figure 10-2) during the bus following process. These buses were observed travelling on corridors at the outskirts of the city. On average, bus BD4 (i.e. BD4-r) and BD8 (i.e. BD8-r) observed to have the highest average speed of 37.48 km/h and 36.43 km/h respectively. Both buses were observed travelling towards Edinburgh city centre where vehicular traffic tend to be less congested than that of the

traffic leaving the city to the outskirt towns during the PM peak hours. This is because most people commutes from and beyond the study area to Edinburgh on daily basis to work, as a result the traffic on the corridor are expected to be heavy during the PM rush hours. The buses heading outskirt of the city where traffic are heavy during the PM rush hours recorded average speed of 33.14 km/h (see Table 10-2). The lowest average speed of the buses followed was 25.45 km/h.

It can be seen that from speed up to 40 km/h, the buses showed similar driving speed profile in all direction of travel regardless of the traffic flow conditions on the corridors or roads. The results clearly showed that the speed varies per bus driver and that the speed variations are influenced by the general traffic conditions on the corridor. The bus drivers tend to adjust their driving behaviour according to the general traffic flow conditions on all the corridors considered. This type of bus driving behaviours were observed across all areas where there were congestion on both direction of travel.

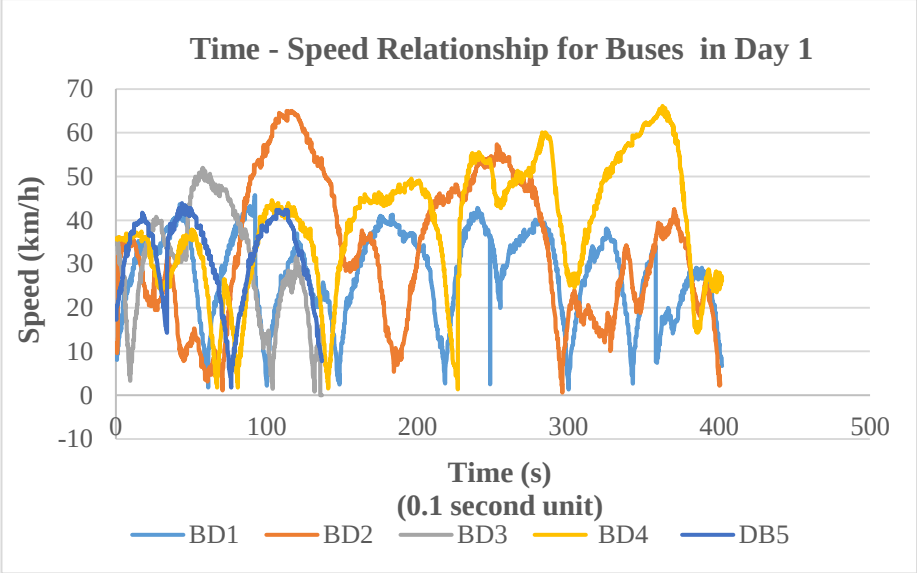

Figure 10-1: Time – speed relationship of buses followed without stopping in Day 1

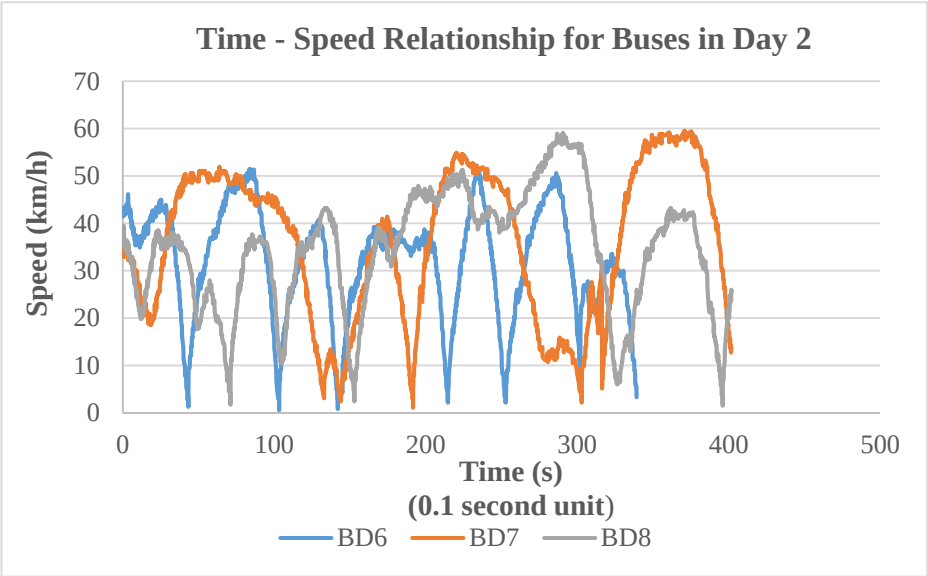

Figure 10-2: Time – speed relationship of buses followed without stopping in Day 2

10.3.2 Speed Variability Effect on Following Time Gap

The effect of bus driving speed variability on the time gap choice of the following vehicle was analysed. Since the test vehicle followed all the buses, it is important to combine all the individual bus data sets as one complete data set in order to assess the overall effect of the bus speed variability on the following test vehicle in a bus following scenario. Figure 10-3 presents the bus speed and the following vehicle time gap relationship. The average time gap at each speed range were used to plot the charts. It can be seen that, as the bus speed increase, the time gap of the following vehicle (i.e. test vehicle) decreases. It can also be seen from Figure 10-3 that, the time gap varies as the spend increase. For bus speed of up to 35 km/h, there was steady decrease of the time gap of the following vehicle. The time gap of the following vehicle fluctuates as the bus speed increase beyond 35 km/h.

The time gap of the following vehicle varies from 5.3 seconds to 1.7 seconds as the bus speed increase from 10 km/h. The size of the bus (i.e. angular size) which could obscure the field of view of the vehicle directly following behind affects the time gap of the following vehicle. This is because, the following driver unable to see the traffic beyond the bus will have to leave enough gap in order to react safely to any sudden change to the traffic condition downstream especially at low speed ranges. Because the following driver's view of traffic ahead may be obstructed, the large time gap choice of the following driver observed at lower speed ranges was reasonable, this will enable the

following vehicle to come to a safe stop in case there is any sudden change to the traffic condition ahead of the bus.

High driving speed encourages shorter following distance hence shorter following time gap, therefore, the lower time gap choice of the test vehicle at higher speed range was expected. Moreover, because large vehicles are normally presumed to have longer deceleration rate and less likely, to misjudge any traffic condition including the ability to see far and beyond the traffic ahead more accurately than that of other small vehicles (Brackstone et al., 2009), following drivers will tend to follow closer to large vehicles at high speed. In a free flow high speed traffic, drivers in general, are likely to follow closely behind bus or large vehicles knowing large vehicles' slow deceleration rates and their ability not to misjudge the traffic condition downstream, but still be able to stop safely without collision in case of any sudden change to the traffic flow downstream.

Table 10-2 shows the general statistics of the test car following the buses. The average relative acceleration, relative speed and relative following distance between the bus and test vehicle are -0.048 m/s^2, 0.272 m/s and 20.97 metres respectively for an average test vehicle following speed of 30.8 km/h. It can be seen from Table 10-2 that the test vehicle following bus BD6, BD1 and BD3 had time gap greater than 3 seconds. These buses were all travelling to the outskirt of Edinburgh where the traffic were expected to be congested during the PM peak hours. Congested traffic encourages lower driving speed which encourages longer time gap between the bus and the test vehicle. The overall average time gap of the following vehicle (test vehicle) following the buses on all corridors is 2.9 seconds

It is worth to note that, even though several buses were followed, using a single independent driver restricts the observation of the effect of different bus driving behaviours on the time headway of the immediate following vehicle. It is recommended that more subject drivers of different age groups and gender with different driving experience be use for further experiment on the headway choice of the vehicle following bus in a bus following situation.

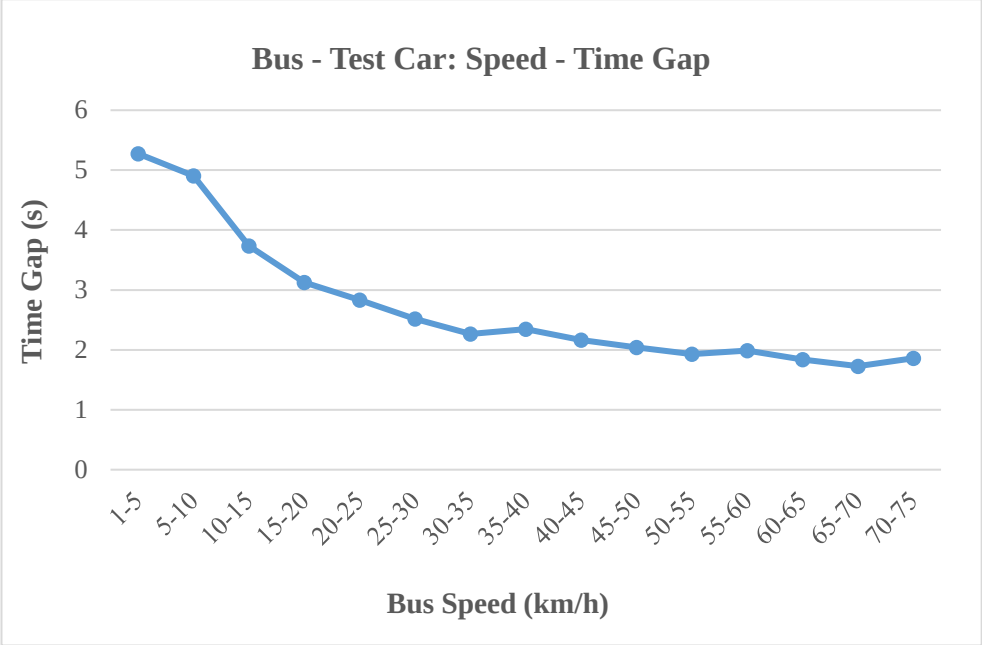

Figure 10-3: The bus speed and following time gap relationship (Bus - Test Car)

Table 10-2: General statistics of test vehicle following buses*

Bus Leading ID	Average Rel. Acc. (m/s^2)	Average Rel. Vel. (m/s)	Average Rev. Distance [m]	Average Time Gap (s)	Average Bus Speed (km/h)	Average Following (Test) Vehicle Speed (km/h)
BD1	-0.030	0.037	21.58	3.42	27.31	27.18
BD2	-0.016	0.083	21.41	2.87	33.14	32.84
BD3	-0.098	-0.028	22.81	3.40	30.30	30.40
BD4-r	-0.038	0.011	21.36	2.42	36.43	36.39
BD5-r	-0.110	-0.325	18.71	2.09	31.33	32.50
BD6	-0.019	2.516	20.49	4.37	25.45	16.39
BD7	-0.028	0.103	16.54	2.23	32.78	32.40
BD8-r	-0.047	-0.221	24.83	2.69	37.48	38.28

*ID = Identification; Rel. Acc. = Relative Acceleration; Rel. Vel. = Relative Velocity

10.4 Bus Following Behaviour and Effect on Car Following Car

In this section, a time gap analysis of a car following a car in a bus following scenario is discussed. The effect of bus following behaviour on a car following behaviour in a three vehicles movement is discussed (see Figure 10-4).

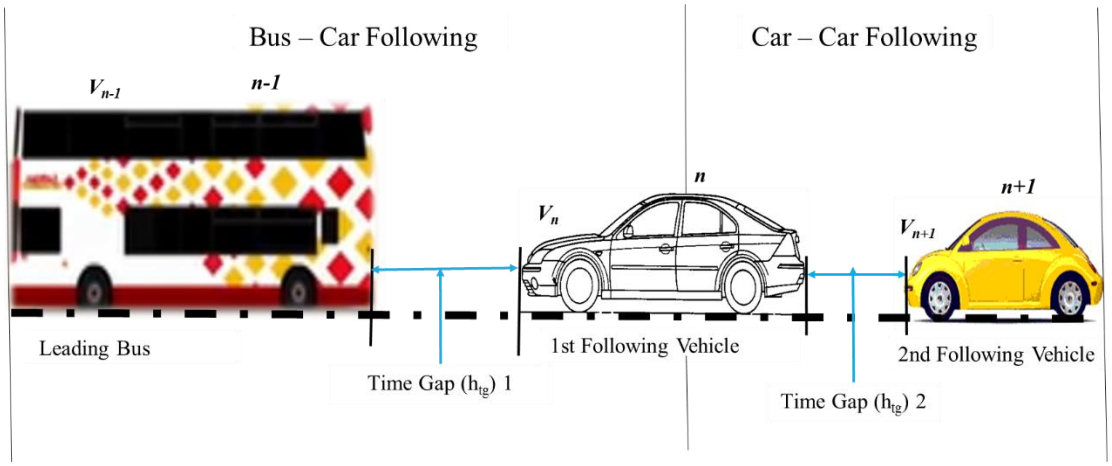

Figure 10-4: A prototype of a bus following scenario in a three vehicles bus following movement.

10.4.1 Analysis of Car following Test Car in a Bus Following Scenario

The time gap of vehicle following the test vehicle in a bus following scenario as seen in Figure 10-4 is discussed. It can be seen from Figure 10-5 that the time gap of the following vehicles significantly vary with increase in the test vehicle speed during the bus following process. The time gap of the following vehicles, on average, vary from 1.2 seconds to 3.8 seconds. It can be seen that there is steady decrease in the time gap as the test vehicle speed increase and vary at higher speed range. The variation in the higher speed range may due to the fact that fewer vehicles followed the test vehicle as compared to vehicles that followed in the low speed range. Large time gaps were observed at low speed range from 1 km/h to 10 km/h. Table 10-3 shows the general statistics of the vehicles following the test vehicle for each of the bus followed.

The average relative acceleration, relative speed, relative distance and time gap of the vehicles following the test vehicle are 0.026 m/s^2, -0.199 m/s, 10.20 metres and 2.4 seconds respectively for an average test vehicle speed of 18.71 km/h. Large time gaps of more than 3 seconds of the following vehicles following the test vehicle were observed when bus BD2, BD5-r and BD6 were leading in the three consecutive vehicles movement as it can be seen in Table 10-3. The results showed that the test vehicle following behaviour while following the buses influence the time gap of the vehicles following the test vehicle in a bus following three vehicles movement.

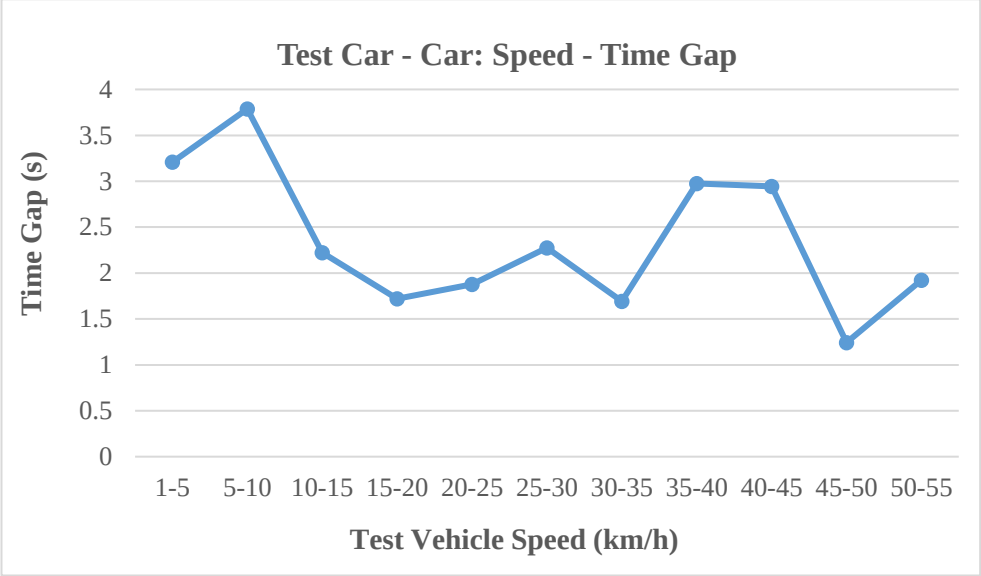

Figure 10-5: The test vehicle speed and following vehicles time gap relationship (i.e. Test Car – Car)

Table 10-3: General statistics of cars following the test vehicle in a three vehicles movement with bus leading

Leading Bus ID (second leader)*	Average Relative Acceleration (m/s^2)	Average Relative Distance (m)	Average Relative Speed (m/s)	Average Time Gap (s)	Average Following Vehicles Speed (km/h)
BD1	0.001	9.884	-0.271	2.65	16.35
BD2	-0.025	6.757	-0.145	3.65	7.68
BD3	0.342	7.875	-0.111	2.72	11.82
BD4-r	0.142	7.426	-0.132	2.36	14.31
BD5-r	0.159	29.991	0.122	4.06	25.08
BD6	0.041	11.226	-0.086	3.16	19.80
BD7	-0.038	7.406	-0.334	1.75	18.88
BD8-r	0.026	9.792	-0.082	1.82	24.10

*The bus used as reference in the three vehicles bus following movement

10.4.2 Comparisons of Car Following Bus and Car following Car Behaviour

It is expected that the leading bus driving behaviour may affect the vehicle directly following behind and two or three vehicles following upstream. A study by Sayer et al. (2003) suggested that following vehicle driver knowing the conditions of the traffic beyond the vehicle directly ahead affect the choice of the following distance gap of the following driver. From Figure 10-4, it can be seen that there are two scenarios of vehicle following process that can be observed in the triple vehicles movement in a bus following

scenario. The two scenarios include the test car following bus (i.e. Bus – Test Car) scenario and car following test car (i.e. Test Car - Car) scenario in a triple vehicles movement in a bus following situation. Considering the two following scenarios, the time gaps choice of the bus following scenario are compared to that of the car following scenario in a three consecutive vehicles movement. In the case of the Test Car – Car following behaviour, the assumption is that the following driver can see beyond and around the test vehicle. Table 10-4 shows the time gaps and the following distances of Bus – Test Car and Test Car – Car following scenarios.

From Table 10-4, it can be seen that the following distances of the Test Car – Car scenario are shorter than the following distances of the Bus – Test Car scenario for all the speed ranges. The overall average following distance of the test car following the bus is 21.20 metres and that of the car following the test car scenario is 10.20 metres. Also, the time gaps, in general, were smaller for the Test Car – Car following scenario than the Bus – Test Car following scenario for all the speed ranges except at the speed range of 35-40 km/h. The average overall time gap of the Test Car – Car scenario is 2.4 seconds and that of the Bus – Test Car scenario is 2.6 seconds. The results show that, on average, the second vehicle (i.e. n+1 vehicle) follow closer to the test vehicle (n) than the test vehicle following the bus (i.e. n-1 vehicle) in a continuous three consecutive vehicles bus following movement (see Figure 10-4). The vehicles following close with shorter time gap in the case of the Test Car – Car scenario may be attributed to the possibility of the following drivers' ability to see beyond and around the test vehicle directly ahead and their possible knowledge of the deceleration rate of large vehicles.

From Figure 10-6, it can be seen that in both cases of the Bus – Test Car and the Test Car – Car following scenarios, the time gap decreases with increase in the test vehicle speed across all the speed ranges except at 35-40 km/h where the Test Car – Car following has slight increase in the time gap than the Bus – Test Car scenario. Now, for the case of individual bus leading in the triple vehicles movement, the time gap of vehicles observed following the test vehicle (i.e. Test Car – Car) were found be larger than the time gap of the test vehicle following bus BD4-r, BD5-r and BD8-r (i.e. Bus – Test Car following) as shown in Table 10-5. All these buses were heading towards Edinburgh city centre where the traffic was less congested. The time gap of vehicles following the test vehicle averaged 3.02 seconds and that of the test vehicle following the buses (i.e. BD4-r, BD5-r and BD8-r) averaged 2.28 seconds.

For the test vehicle following buses BD1, BD2, BD3, BD6 and BD7 (i.e. Bus – Test Car scenario) heading towards the towns outskirt of Edinburgh where the traffic was heaviest during the PM peak hours, the time gap of the Test Car – Car following were shorter than that of the Bus – Test Car following scenario. The time gap of the vehicles following the test vehicle averaged 1.9 seconds and that of the test vehicle following the buses (i.e. BD1, BD2, BD3, BD6 and BD7) averaged 2.86 seconds. The analysis showed that vehicles follow closer to the test vehicle with shorter time gap than the test vehicle follow the buses in the heavy traffic flow phase. In the light traffic flow phase, the test vehicle follow the buses with shorter time gap than the following vehicles (n+1) follow the test vehicle in a three consecutive vehicles movement in a bus following situation.

Table 10-4: Average time gaps and following distances for the test car following bus (Bus – Test Car) and car following the test car (Test Car - Car)

Speed (km/h)	Bus - Test Car		Test Car - Car	
	Average Time Gap (s)	Average Following Distance (m)	Average Time Gap (s)	Average Following Distance (m)
1-5	10.78	11.43	6.46	7.33
5-10	5.27	10.52	3.76	7.45
10-15	3.61	11.92	2.13	7.18
15-20	3.07	14.61	1.83	8.84
20-25	2.77	17.05	1.65	10.36
25-30	2.39	18.03	1.55	11.91
30-35	2.31	20.73	1.50	13.41
35-40	2.25	23.24	2.65	27.99
40-45	2.18	25.57	1.77	20.56
45-50	1.94	25.43	1.30	16.95
50-55	1.90	27.59	1.20	17.14

Table 10-5: Bus – Test Car and Test Car – Car time gaps comparisons for individual bus leading in a three consecutive vehicles movement.

Bus ID	Bus – Test Car	Test Car-Car
	Average Time Gap (s)	Average Time Gap (s)
DB1	3.1	2.86
DB2	2.63	1.91
DB3	3.25	1.15
DB4-r	2.29	2.76
DB5-r	2.06	3.28
DB6	2.95	1.64
DB7	2.36	1.91
DB8-r	2.49	3.01

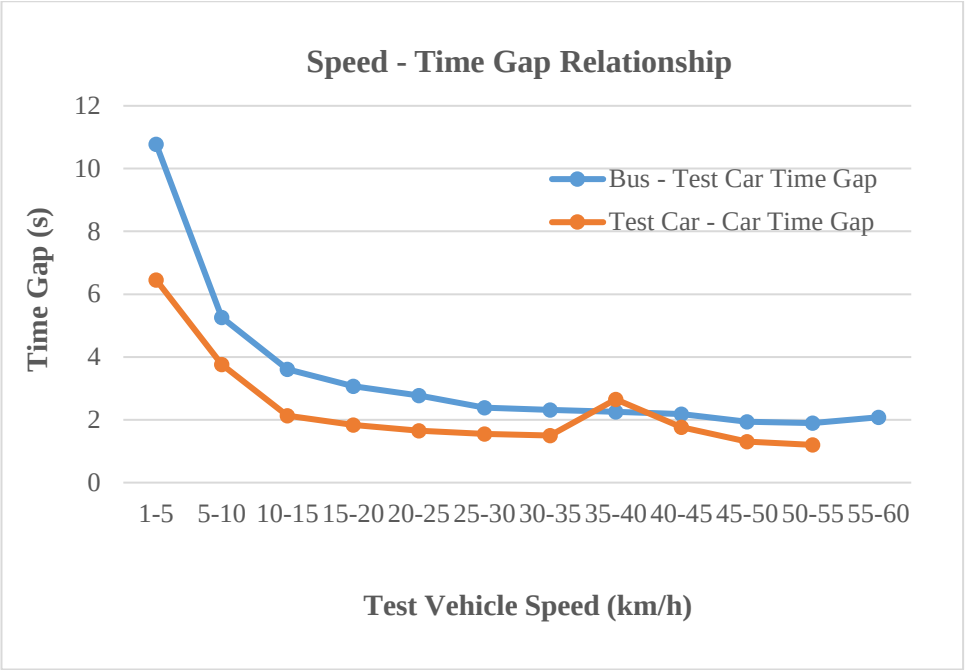

Figure 10-6: Speed and time gap relationship for Bus – Test Car and Test Car – Car following in a three vehicles bus following movement

10.5 Bus Following Model Calibration and Validation

As discussed in Chapter 7, bus following models that describes the interaction between a car and a bus in a bus following scenario within urban-rural area are proposed for this study. The bus following Model B1-1, Model B1-2 and Model B1-3 developed and discussed in Chapter 7 are calibrated and validated in this chapter. The whole data set consisting of 30,948 individual time series data points was split into two set of data files A and B. One set of the data file (i.e. Data file B) was used for the model calibration discussed in Section 10.5.1 and the other set of the data file (i.e. Data file A) was used for the bus following model validation discussed in Section 10.5.2.

10.5.1 Bus Following Model Calibration

Data set B (i.e. half the whole data set) consisting of 15,379 individual time series data points (Δt of 0.1 seconds) was used for the bus following models calibration. Model B1-1 incorporates the speed of the following car (vehicle), Model B1-2 incorporates the speed of the leading bus and Model B1-3 incorporates the speed of both the leading bus and the following car in predicting the desired or safe following distance of the following car.

Using Data set B to calibrate Model B1-1, Model B1-2 and Model B1-3 and applying multiple linear regression analysis method, the calibrated models are as follows:

Model B1-1:

$$\Delta x(t+\Delta t) = 0.550 v_n(t) + 0.088 \Delta v_n(t+\Delta t) - 0.889 \Delta a_n(t+\Delta t) + 2.255 h_{tgn}(t) - 3.74 \quad (10\text{-}1)$$

Model B1-2:

$$\Delta x(t+\Delta t) = 0.550 v_{n-1}(t) - 1.893 \Delta v_n(t+\Delta t) - 0.889 \Delta a_n(t+\Delta t) + 2.255 h_{tgn}(t) - 3.743 \quad 10\text{-}2)$$

Model B1-3:

$$\Delta x(t+\Delta t) = 0.526 v_n(t) + 0.024 v_{n-1}(t) - 0.889 \Delta a_n(t+\Delta t) + 2.256 h_{tgn}(t) - 3.743 \quad (10\text{-}3)$$

Where Δx is the desired or safe following distance of the following car to the leading bus [m], Δv_n is the relative speed between the leading bus and the following car [m/s], Δa_n is the relative acceleration between the leading bus and the following car [m/s²], v_n is the speed of the following car [km/h], v_{n-1} is the speed of the leading bus [km/h], h_{tgn} is the time gap between the leading bus and the following car [s], t is the time [s] and Δt is the time step [s]. The calibration parameters estimates for Model B1-1, Model B1-2 and Model B1-3 were all statistically significant at 95% confidence level with p-values < 0.05 (see Table 10-6, Table 10-7 and Table 10-8). All the models produced the same R^2 value of 0.624. The sample size used to calibrate the models consists of 15,379 individual data points. For all the models (i.e. Model B1-1, Model B1-2 and Model B1-3), the calibration parameter estimate sign of the relative acceleration is negative.

The calibration parameter estimate sign of the relative speed is positive for Model B1-1 and negative for Model B1-2. In case of Model B1-2, it showed that the following driver takes into consideration the speed of the bus in keeping a safe or desired following distance as compared to Model B1-1 where the driver's own speed is key in keeping a safe distance following the bus. The negative sign of relative speed calibration parameter estimate for Model B1-2 also indicates a strong response to the bus speed in keeping a desired following distance to the bus. For Model B1-1, the following driver tend to

depend more on their own speed profile during the following process. The calibration parameters estimates signs of the following vehicle speed and the leading bus speed for Model B1-1, Model B1-2 and Model B1-3 are positive. The speed of the leading bus and the following vehicle has a positive effect on the desired following distance of the following vehicle. The time gap of all the models, also positively contributes to the desired following distance of the following vehicle. All the bus following models developed in this study are all equally recommended for use in describing the interactions between a car and a bus in a bus following scenario.

10.5.2 Bus Following Model Validation

To ascertain the reliability of the bus following models discussed in Section 10.5.1, validation of the models was carried out by modelling the bus following data sets against the observed data sets obtained from the field. Data set A consisting of 15,387 individual time series data points with a time step of 0.1 seconds was used for the models validation. Data set A was split into two sets of equal sub data files (i.e. Sub Data files AA and AB). Each sub data files was further randomly and equally divided into two sub sets of data files, resulting in four different sub data files (i.e. Sub Data files AAA, AAB, ABA and ABB) with each consisting of a minimum of 3,845 individual time series data points as discussed in Chapter 7. Model B1-1, Model B1-2 and Model B1-3 are all validated separately since all the models are equally recommended for bus following analysis. The t-test statistical test analysis discussed in Chapter 6 was used to validate the models. To begin with the validation, Model B1-1 (eqn. 10-1), Model B1-2 (eqn. 10-2) and Model B1-3 (eqn. 10-3) applied to the four sets of sub data files and separately estimated the relative distances at each time step. The average relative distances of both the observed and the predicted relative distances of all the four sub data sets for each of the models were calculated and used in the t-test statistical significant test. Before the t-test analysis was performed, two hypothetical questions to test the models were set:

H_0: There is no significant difference between the observed bus following data sets and bus following model predicted data sets (i.e., $H_0: \mu_d = 0;\ \mu_d = \mu_o - \mu_d$).

H_a: There is significant difference between the observed bus following data sets and bus following model predicted data sets (i.e., $H_a: \mu_d \neq 0$).

where H_0 and H_a are the null and alternative hypotheses respectively, μ_d is the population mean of the differences in the means between the two groups of bus following data. μ_o is the observed true bus following population mean and μ_p is the predicted true bus following population mean.

As discussed in Chapter 6, the t-test statistics was computed using Microsoft Excel data analysis tool and obtained the p-values and t-values for Model B1-1, Model B1-2 and Model B1-3. The paired two-sample for means two-tail t-test statistics was used for this analysis. The t-test statistics results for Model B1-1 is presented in Table 10-9 and that for Model B1-2 and Model B1-3 are presented in Table 10-10. Given the degree of freedom (df) of 3 (i.e. 4 - 1), the two-tailed paired sample t-test statistics p-value of 0.73 and t-stat value of -0.375 for Model B1-1 were obtained. For Model B1-2, the t-test statistics p-value of 0.78 and t-stat value of 0.306 were obtained. Finally, Model B1-3 t-test statistics produced p-value of 0.78 and t-stat value of 0.304. It can be seen that the p-values for Model B1-1, Model B1-2 and Model B1-3 are all greater than the p-value of 0.05 (95% confidence level). Similarly, the t-stat values for Model B1-1, Model B1-2 and Model B1-3 are also less than the two-tail t-critical value of 3.182 (for df = 3, at 95% cl). The t-test statistics results show that there are no enough evidence in the mean differences between the observed and predicted bus following data sets to suggest the rejection of the null hypothesis. Therefore, the alternative hypothesis was rejected since no significant differences were observed in the two groups of bus following data sets for Model B1-1, Model B1-2 and Model B1-3.

A t-test statistical test analysis was used to test the significant differences between the observed and the predicted bus following data sets using the distance-based bus-following models developed in this study. The t-test analysis found that at p-value of 0.05 (i.e. 95% confidence level), there was no statistical significant differences observed between the observed or measured and the models predicted data sets to suggests the rejection of the null hypothesis (H_0). Therefore, we conclude that, there are no statistical significant differences between the observed and the predicted data sets for bus following Model B1-1 [t(3) = 0.374, p-value > 0.05, 2-tail], Model B1-2 [t(3) = 0.306, p-value > 0.05, 2-tail] and Model B1-3 [t(3) = 0.304, p-value > 0.05, 2-tail]. Model B1-1, Model B1-2 and Model B1-3 proposed and developed in this study has been shown to predict accurately the safe or desired following distance of a car following a bus in a real world driving scenario in a bus following situation. The bus following models developed in this study

best describes a car following a bus within urban-rural driving conditions and closely replicates real world bus following situation.

Table 10-6: Model B1-1 - bus following model calibration parameters estimates regression output results

Model B1-1			
Model Parameters	Coefficient	Standard Error	P-value
b_0	-3.74343285	0.172593074	8.9296E-103
Δa_n [m/s²]	-0.8893397	0.073130698	7.1769E-34
Δv_n [m/s]	0.088131883	0.029609532	0.002920416
v_n [km/h]	0.550185933	0.003551093	0
h_{tgn} [s]	2.255248318	0.028629775	0
R^2	0.623847388		
Standard Error	6.263842884		
Observations	15379		

Table 10-7: Model B1-2 - bus following model calibration parameters estimates regression output results

Model B1-2			
Model Parameters	Coefficient	Standard Error	P-value
b_0	-3.743432849	0.172593074	8.93E-103
Δa_n [m/s²]	-0.889339704	0.073130698	7.1769E-34
Δv_n [m/s]	-1.892537476	0.030627477	0
v_{n-1} [km/h]	0.550185933	0.003551093	0
h_{tgn} [s]	2.255248318	0.028629775	0
R^2	0.623847388		
Standard Error	6.263842884		
Observations	15379		

Table 10-8: Model B1-3 - bus following model calibration parameters estimates regression output results

Model B1-3			
Model Parameters	Coefficient	Standard Error	P-value
b_0	-3.74343285	0.172593074	8.93E-103
Δa_n [m/s²]	-0.8893397	0.073130698	7.177E-34
v_n [m/s]	0.525704854	0.008507633	0
v_{n-1} [km/h]	0.024481079	0.00822487	0.0029204
h_{tgn} [s]	2.255248318	0.028629775	0
R^2	0.623847388		
Standard Error	6.263842884		
Observations	15379		

Table 10-9: The paired two sample means t-test results for Model B1-1

MODEL B1-1					
Data Set	Observed	Predicted	T-Test Result		
				Observed	Predicted
Data AAA	21.25	20.03	Mean	20.6125	20.1345
Data AAB	16.54	17.20	Variance	9.57329	5.49762
Data ABA	24.03	20.39	Observations	4	4
Data ABB	20.63	22.92	Pearson Correlation	0.58967	
			Hypothesized Mean Difference	0	
			df	3	
			t Stat	0.37454	
			P(T<=t) one-tail	0.36646	
			t Critical one-tail	2.35336	
			P(T<=t) two-tail	0.73291	
			t Critical two-tail	3.18245	

Table 10-10: The paired two sample means t-test results for Model B1-2 and Model B1-3

MODEL B1-2					
Data Set	Observed	Predicted	T-Test Result		
				Observed	Predicted
Data AAA	21.25	20.12	Mean	20.6125	20.2226
Data AAB	16.54	17.30	Variance	9.57329	5.43145
Data ABA	24.03	20.48	Observations	4	4
Data ABB	20.63	22.99	Pearson Correlation	0.59075	
			Hypothesized Mean Difference	0	
			df	3	
			t Stat	0.30623	
			P(T<=t) one-tail	0.38973	
			t Critical one-tail	2.35336	
			P(T<=t) two-tail	0.77945	
			t Critical two-tail	3.18245	
MODEL B1-3					
Data Set	Observed	Predicted	T-Test Result		
				Observed	Predicted
Data AAA	21.25	20.13	Mean	20.6125	20.2255
Data AAB	16.54	17.30	Variance	9.57329	5.42928
Data ABA	24.03	20.48	Observations	4	4
Data ABB	20.63	22.99	Pearson Correlation	0.59081	
			Hypothesized Mean Difference	0	
			df	3	
			t Stat	0.30398	
			P(T<=t) one-tail	0.3905	
			t Critical one-tail	2.35336	
			P(T<=t) two-tail	0.78101	
			t Critical two-tail	3.18245	

10.6 Summary

In this chapter, a number of buses were followed using an instrumented vehicle to investigate bus following behaviour and to develop bus following models. Bus driving speed variability and bus following effect on the time gap choice of the following vehicle in a bus following scenario were discussed in this chapter. The bus following effect on

the time gaps of the vehicles following directly behind the test vehicle while the test vehicle follows the commuter buses in a three consecutive vehicles movement were discussed in this chapter. The analysis of the results found that the time gap choice of the test vehicle was affected by the leading buses. Also, the analysis found that the time gap choice of the vehicles following the test vehicle were affected by the driving behaviour of the test vehicle in a three vehicles bus following scenario.

The following vehicle drivers were found to be inconsistent with the time gap choice in both the Bus – Test Car and the Test Car – Car following scenarios in bus following three vehicles movement. It was found that car following the bus behave differently to car following car in a bus following three vehicles movement scenario. This was as a result of the limited visibility of the following vehicle driver beyond the bus, the size of the bus and the driving characteristics of the bus compared to the scenario of a vehicle following the test vehicle where the following vehicle driver could see around and beyond the test vehicle.

The calibration and validation of the bus following models developed in this study were discussed. The bus following models that describes the behaviour of car following bus were calibrated using data sets obtained using an instrumented vehicle that followed a number of double decker commuter buses. The models calibration parameters estimates were all found to be statistically significant at 95% (p-values < 0.05) confidence level. Also, to ascertain the bus following models reliability in describing the actual scenarios of car following bus, the proposed models were validated using half the whole data set. The t-test statistical analysis results found that there were no statistical significant differences between the observed data sets and the predicted data sets. The analysis found that the bus following models proposed and calibrated in this chapter were all able to predict accurately the safe or desired following distance of a vehicle following a bus in a real world driving scenario in a bus following situation.

The next chapter presents the discussions and conclusions of this study. It discusses the aim and objectives of this study in relation to the study findings and presents recommendations for further studies.

CHAPTER 11 DISCUSSIONS AND CONCLUSIONS

11.1 Study Background

The main aim of this study was to investigate driving behaviour and car following models and techniques as well as enhancing the collection of microscopic traffic flow and driver behaviour data. Car following research enables better understanding of driver behaviour and driver-vehicle interactions so as to improve road safety and better management of traffic networks. It also enables better integration of driver-vehicle interactions with Intelligent Transport Systems (ITS) for the improvement of road infrastructure to help reduce traffic delays. In attempt to improve car following and driver behaviour models, different techniques have been employed to collect driving behaviour car following data, especially microscopic data, which until recent years was not possible, to calibrate or develop better car following models that best describe the driver-vehicle interactions. Technological advancement has made it possible to acquire more realistic microscopic traffic flow data to calibrate or develop better and more realistic car following models that tends to replicate real world traffic scenarios.

Car following and driving behaviour models have been used for various traffic and transportation management systems for safety impact studies, traffic network analysis and network capacity analysis. These models forms the basis of all microscopic traffic simulation tools. These models application in microscopic traffic simulation tools, such as PARAMICS and VISSIM, that simulates real world traffic and driver behaviour situations, provides the platform for transportation researchers and policy makers in their decision making process in providing real working solutions to real world traffic problems. These models have been used extensively in transportation research into driving behaviours, traffic management and road safety improvement schemes, and evaluation of traffic engineering applications such as ITS.

Moreover, advancement in technology including in-vehicle control systems, such as Advanced Vehicle Control and Safety Systems (AVCSS), and the improvement in microscopic data collection techniques has led to the extensive use of car following models application in the area of vehicle design and the evaluation of the human factor in Advanced Driver Assistance Systems (ADAS), such as Adaptive Cruise Control

(ACC). The ACC enables vehicle's speed to adapt to the traffic environment in keeping safe following distance to the vehicle directly ahead of the ACC vehicle. Detailed investigations carried out for meeting the aim and objectives of this study are discussed in this chapter.

11.2 Meeting the Research Objectives

To carry out the investigation into driving behaviour and car following models and ways to enhance the collection of microscopic traffic flow data, a number of objectives were set to address the shortfalls and limitations that were identified in the previous studies and to answer the research questions. Car following models often describe the interactions between two successive vehicles travelling in the same direction on the same single lane of traffic without the possibility of passing or overtaking. Car following models literature stretching from the 1950s to present day have been reviewed. Different car following models exist with each attempting to mimic the driving behaviour in a real world driving scenario. In attempt to improve these models to replicate actual driving behaviours, different data sets were used to calibrate these models. In fact, most of these models were modelled first before calibration with simple empirical or limited data sets rendering the models less reliable.

In recent years, there has been improvement in driving behaviour data collection techniques with technological advancement, such as video recordings, the use of inductive loop detectors and the use of instruments on-board vehicles. Even though with the technological advancement in the area of driving behaviour data collection, there are still limitations to the level of efficiency, the quality and quantity, and the type of data that can be obtained during experiment. Further investigation was needed to identify some of these shortfalls in the data collection techniques and address them to improve driving behaviour modelling.

The first objective of this research has been to review the relevant literature and identify the gaps in the literature

The work carried out here showed that numerous car following models have been proposed since the inception of the first experiment on traffic flow studies leading to the

development of the Gazis-Herman-Rothery (GHR) car following model. Subsequent to the GHR model development, different versions of the GHR model have been proposed by different researchers in their attempt to calibrate the model parameters. The calibration of the same model produced different versions of the model, yet only few models were deemed to be reliable when they were modelled against observed data by other researchers. This was because, most of the data sets used to calibrate the model were obtained from simple experimental data sets or limited data sets available to the researchers at the time. Even though considerable number of different versions of the GHR models have been proposed, it was established that there has not been an agreement on the correct set of calibration parameters as a result of lack of reliable and modern data sets to calibrate the model.

Since the establishment of the GHR model, different forms of car following models have been proposed, for example linear model and safety distance model, with each describing different driving behaviours in car following scenarios. Again, the use of limited data sets or simple experimental data sets result in obtaining different calibration parameters of the same model. The growing interest in car following studies have led to further research into multiple-leader car following models. In fact, these models have been proposed as a result of extending the already existing one-leader car following models and that seems to be the trend among researchers. In fact, models which are developed first before calibration with simple empirical data sets have doubts on their reliability to replicates real world driving scenarios of car following.

The experimental methods used in collecting traffic data has been improving over the years, from simple experiments to a more advanced use of experimental techniques. All these improvements are with the goal of improving the quality and the range of car following models calibration, and to enhance the understanding of driving behaviour. For instance, the use of inductive loop data collection method enabled researchers to determine the volume of traffic, occupancy and the speed of passing vehicles in a specific location. Although, large data sets could be collected using this advanced method which will require additional software to process the data set, which might not be readily available. This data collection techniques' inability to account for the following behaviour of vehicle pairs over long period of time at different locations on the same stretch of road hinder its use in car following experiments.

However, to overcome the limitations of the loop system techniques, more advanced data collection techniques, such as video camera recording of driving behaviour, have been used in considerable number of experiments. The video camera use have certainly improved traffic data collection and the study of driving behaviour, however, there are some drawbacks identified with the use of this techniques. For instance, mounting of the video cameras high on the road side or on tall buildings overlooking the highway or on helicopter can only observe the vehicles trajectories for specific lengths or stretch of the road. The vehicles interactions beyond the cameras' field of view or beyond the lengths of the cameras coverage area or the entire stretch of the road where the video cameras are installed cannot be observed.

Moreover, bad weather, high wind that could cause the video camera's instability, and poor image quality may result in some inconsistency and errors in creating driving behaviour database, which could render some data sets unusable. However, further advancement in the data collection techniques have led to the use of vehicles equipped with instruments to observe and collect data on driving behaviour and vehicles movements. Over the years, the measuring equipment on-board vehicles have been improving, thereby enabling data to be collected for longer period of time. Notwithstanding the usefulness of this techniques, more improvement is required to enhance the collection of quality traffic follow data sets with the latest advanced technology. In view of these shortfalls, the gaps in the literature were identified and investigated in this study to address the shortfalls.

For this research, the gaps identified include:

1. Little recent research on car following model have been studied on multiple-leader car following models. The very few available multiple-leader models are extension of the existing car following models that does not necessarily describe the actual driving behaviour of multiple-leader car following scenarios. Literature suggests the need for a better, more reliable and robust distance-based two-leader car following model.

2. Most of the previous work on car following models were mostly using the acceleration to describe driving behaviour, and very little work on models using the safe or desired following distance to describe driving behaviour. Therefore, there is a requirement for new and better car following models capable of describing the safe or desired distance

following behaviour of a driver, which at the moment has not been given much attention in the literature.

3. The driving behaviour data normally used for car following models calibrations are mainly obtained using observers stationed at temporal locations/points or by measurements and video recording cameras situated at fixed locations/points or on moving objects as well as data from simple experiments. These data collection methods, in most cases, will not give adequate and quality data that will warrant proper study of microscopic driving behaviour activities that requires continuous longitudinal measurements over a longer period of travel distance within the traffic network. Therefore, there was a need for a more novel data collection systems to be developed using floating vehicle equipped with a more advanced data measuring devices such as radar sensors and video cameras. This vehicle can be driven within the traffic stream to observe the driving behaviour in the driving lanes as well as the neighbouring adjacent and opposing lane traffic behaviour and measure accurately the inter-vehicle variables, such as relative acceleration, speed and distance, in a three vehicles movement to gain quality and quantitative microscopic driving behaviour data.

4. Very little or no work on socioeconomic or driving/transport-related factors or variables have been investigated in the previous car following models. Though, extensive research have been carried out to understand the microscopic driving behaviour activities including other factors that could affect the behaviour of drivers, but very little or no attention have been given to the socioeconomic or driving/transport-related factors or variables effect in car following studies. Empirical evidence showing that the existing car following models certainly provide a better description of the effect of socioeconomic or driving/transport-related variables on car following was, however, missing in the current models.

5. Different versions of GHR car following model have been proposed with each intended to describe driving behaviour, but very few of these models are found to be most reliable. Moreover, the different versions of the GHR model were calibrated using data obtained from a car following a car, but no attention have been given to the calibration of the GHR model using data obtained from a truck following a car or a car following a truck. Evidence in the relevant literature suggests the need for more reliable and accurate driver behaviour data to calibrate the GHR model to produce a more reliable and acceptable

model calibration parameters that best describe individual driving behaviour within urban-rural driving conditions.

Major cities in the United Kingdom (UK) have seen increase in car usage over the past decades causing traffic delays, which inadvertently affecting driving behaviour as the vehicles follow each other. For instance, the rapid economic growth in Scotland and UK as a whole saw cities like Edinburgh car usage doubled over the past three decades. During the recent population census, the City of Edinburgh recorded households without access to own car or do not have a car or van less than that of Glasgow and Dundee and above the Scottish national average. In view of this, the City of Edinburgh stands out to be more appropriate for driving behaviour research since the households with car usage are more than the rest of the Scottish major cities. The selection of the case study was essential for this research and that leads to the next research objective.

The second objective has been to select a case study and to identify the research study area

For this study, the City of Edinburgh was chosen as the case study area. The City of Edinburgh is the capital of Scotland in the United Kingdom, with current population close to half a million inhabitants. The City of Edinburgh is the financial hub of Scotland and its economy is mostly centred on banking and finance, hospitality, services and education. The city host four universities. From the 2011 population census, Edinburgh recorded nearly 60% of the households with access to car or van or own a car or van. This made the city to record an increase in car usage to about 48% in the last thirty years to 2011. Although, there was a significant increase in household car ownership in the last decades, few residents drove to work within Edinburgh. However, car journeys into Edinburgh significantly increased due to more car travel from the neighbouring local authority areas resulting in, at times, heavy traffic congestion in some part of the city.

The study area has a mixed traffic flow. The roads in the inner city or urban areas, in most cases, has public bus only restricted lane use. Different road types were identified and selected within the study area that formed the corridors used for this study. After a series of drive around surveys, four main traffic corridors each with different road characteristics were finally identified and selected for this study. These traffic corridors

has a combined speed limit ranging from 30 mph to 70 mph (miles per hour) maximum. Corridor 1 was described as urban traffic condition with speed below 40 mph. This corridor runs from the northwest to southwest of the city with a distance of about 19.4 kilometres (12 miles) for both direction of travel. Corridor 2 was described as highway traffic condition with speed above 50 mph and running from northeast to southwest outskirts of the city with a distance of about 42.2 kilometres (26.2 miles) for both direction of travel. Corridor 3 was described as urban-rural traffic condition with speed up to 50 mph and running from the northwest (inner city) to southeast outside of the city with a distance of about 50.4 kilometres (31.4 miles) for both direction of travel. Corridor 4 was described as highway-urban traffic condition with speed up to 40 mph and above 50 mph and running from the northeast through southwest (outside the city) to northwest of the city with a distance of about 64.4 kilometres (40 miles) for both direction of travel.

All the individual identified traffic corridor's total distances were measured from the start point to the finish point (i.e. start point) of the corridor covering both direction of travel. The traffic corridors used for this study utilise the traffic conditions within and outside of the City of Edinburgh where traffic are considered to be heavy. Data collection method for this study was identified, finalised and the necessary arrangements were made to purchase the equipment across the UK and Germany in central Europe. Pre-testing of individual data collection devices were carried out to ensure any defective equipment was repaired before the final use for the experiment.

Good and reliable data collection techniques are essential to every research. The driving behaviour data collection techniques have seen improvement with the use of modern equipment, but these techniques have their shortcomings. For instance, the use of video camera techniques have improved the observation of inter-vehicle interactions, but this technique could not capture the inter-vehicle interactions beyond the field of view of the video cameras. Moreover, high winds (in case of helicopter with video cameras), bad weather conditions and poor image quality affects the data processing. Driving behaviour data collection techniques continue to improve with the use of vehicles equipped with instruments to observe driving behaviour within traffic streams. The vehicles with instruments data collection techniques has some drawbacks since most of the existing techniques uses lidar or sensors with short ranges, which do not observe vehicles beyond the detection zone of the sensors. Moreover, most of these techniques observe vehicles

only following directly behind the instrumented vehicle and leaving other adjacent vehicles not observed, hence could not be used for three vehicles movement driving behaviour observation.

A more robust data collection techniques to collect microscopic driver behaviour data using vehicle equipped with more advanced instruments that can observe vehicles in a three consecutive vehicles movement and the traffic in the neighbouring or opposing driving lane was required. Obtaining realistic, sufficient quality and quantity of driving behaviour data was central to this study. A novel data collection techniques that enables the acquisition of more accurate and realistic data on driving behaviour was developed and utilised to enhance the collection of microscopic traffic data to improve driving behaviour models. The development of new data collection technique leads to the next objective of this research.

The third objective has been to instrument a vehicle with advanced measuring equipment for microscopic traffic data collection

For this study, an instrumented vehicle (a hatchback Ford Mondeo 2002 LX model with a 1.8 litre engine capacity running on unleaded petrol) equipped with both forward and rear facing video-audio camera recorders connected to GPS based time series speed and distance measuring Video Velocity BOX (VBOX), GPS based PerformanceBox, both front and rear facing Radar Sensors, in-vehicle Laptop computer logging vehicle speed and Controller Area Network (CAN) monitoring interface user program to provide real time monitoring and display of data was utilised to collect microscopic traffic flow and driving behaviour data. The novel data collection techniques developed for this research have the capacity to observe both the immediate front leading vehicle and the immediate rear following vehicle in a three consecutive vehicles movements and able to distinguished the observed vehicle types. The instrumented vehicle also has the capability to observe several vehicles both front and rear of the test vehicle. The developed instrumented test vehicle has the capacity to also track and observe the traffic flow and driving behaviour of oncoming vehicles in the opposing driving lane. Vehicles both front and rear in the adjacent driving lane (i.e. double lane) as well as opposing driving lane can be tracked up to 200 metres from the test vehicle.

A special controller area network monitoring and communication software, i.e. Peak CAN Explorer 5, was utilised to monitor and display live status of each CAN messages from the radar sensors and the instrumented vehicle's engine on in-vehicle laptop computer as the messages were being transmitted and received. The robustness of the data collection system was such that changing any settings of the radar sensors' default configuration, such as changes to the radar beam or plate elevation angle, the radar tracking distance or fixing any malfunctioning of the radar sensors, during the experiment were done via the PCAN Explorer 5 without physically touching the radar sensors during the experiment. With this and other features, interruption to the experiment was rare. The instrumented vehicle measured accurately the inter-vehicle variables such as the relative acceleration, the relative speed and the relative distance as well as the measurement of the instrumented vehicle's own speed via CAN connection to the vehicle's engine through the OBD-II port.

Live stream of video recordings from both the forward and the rear facing video cameras were displayed with the test vehicle's speed information via a preview display screen attached to the front windscreen. The video camera recordings were linked to the speed information of the test vehicle measured by the GPS based Video VBOX. This enabled easy synchronisation of the video data with other devices measured data during the data processing stage. The two rear facing video cameras helped to identify the in-vehicle activities of the following vehicles such as gender or vehicle occupancy. Prior to the setting up of the vehicle with the measuring devices, laboratory testing was carried out to ensure that the radar sensors, the CAN-bus, the transmission cables and CAN monitoring software (i.e. PCAN-Explorer 5) installed on the laptop computer all established better communication links and work as expected. The successful laboratory testing helped with the familiarisation of the system and the operations of the essential elements of the data collection system. This research objective was achieved with the successful setting up of the advanced instrumented vehicle data collection technique to collect microscopic driving behaviour data for this study.

As mentioned earlier, a more reliable, realistic and sufficient quality driving behaviour data was central to this study. The instrumented vehicle developed and utilised for the data collection provides more realistic and sufficient quality data for this study. The

acquisition of the data was from different measuring devices that make up the setup of the test vehicle.

The data collected from the radar sensors include the default radar sensors' information that were not relevant to this study but important for the radar devices operation. The raw data from the radar sensors and other measuring devices required to be cleaned before it could be used for further data analysis. The data from the video recordings also required to be processed and the required data extracted for further analysis. The acquisition of accurate and realistic data and the processing of the data leads to the next objective of this study.

The fourth objective has been to collect driving behaviour data and carry out data extraction, management and data preparation for driving behaviour analysis

For this study, an instrumented vehicle equipped with radar sensors, video-audio recording cameras, speed and distance measuring devices and laptop computer was utilised to collect time series driving behaviour data. Prior to the start of the data acquisition, a series of testing and experimental trials were carried out to ensure the collection of quality data. For instance, tests were carried out to determine the appropriate elevation angles of the radar radiation plate suitable for the mounted heights of the radar sensors (i.e., 24 centimetres for the front and 20 centimetres for the back) on the instrumented vehicle for efficient data collection. To determine the appropriate radiation plate angle, six different radar elevation angles were chosen ranging from 14.5 degrees to 16.0 degrees with incremental intervals of 0.25 degrees. The distances of four selected parked vehicles were measured from 10 metres to 50 metres with incremental interval of 10 metres to both the front and the rear radar sensors for each selected elevation angles. The RMSE method was used to determine the appropriate radar elevation angle suitable for the experiment. The minimum RMSE of the measured distances corresponding to the elevation angles for both the front and the rear radar sensors was selected for the experiment. Elevation plate angle of 15.75 degrees produced the minimum RMSE of the measured distances corresponding to the mounted heights of both the front and the rear radar sensors that was used throughout the experiment.

The radar sensors required the test vehicle's own speed information (including the yaw rate) as input signals to determine the course of the test vehicle which was not readily available. The instrumented test vehicle speed information was reverse-engineered through a series of field experiments to determine the speed information. The test vehicle speed information (including the yaw rate) was automated to transmit to the radar sensors to determine the course of the instrumented test vehicle for effective tracking of the target vehicles using visual basic macros developed for the purpose of the signal automation. Pilot data collection was carried out, firstly, to test the performance and the resilience of the data collection system in withstanding long period of working operations. Secondly, to have general understanding of the driving behaviour within the study area and help with the effective planning of the final data collection.

The findings from the pilot data collection provided a better understanding of the driving manoeuvres and the car following behaviours under different driving conditions within the study area. It provided an insight into the type of driving related variables to observe that affect driving behaviour in addition to the inter-vehicle variables, which helped with the effective design of the final data acquisition. The data for this study was collected on four main traffic corridors together with an additional traffic corridors for the collection of bus following data. Traffic Corridor 1 was mainly urban driving conditions through the city centre and Corridor 2 was mainly highway driving conditions mainly outskirt of the city. Corridor 3 was urban-rural driving conditions through the principal streets of the city to the rural roads outskirt of the city and Corridor 4 was mainly the combination of Corridor 1 and Corridor 2 driving conditions.

The data acquisition was done mainly on weekdays excluding weekends on each traffic corridors identified. Two data acquisition test runs were carried out during the morning peak hours and two test runs during the afternoon off-peak hours from July 2015 to October 2015. Data from the leading vehicles and the following vehicles in a three consecutive vehicles movement were collected for this study. Extra data was collected on bus corridors different from the four main selected study traffic corridors. The bus corridors were mainly single lane roads with no-bus only lane restrictions in place. The test vehicle followed eight (8) different double decker public buses during the evening peak hours to collect bus following data in two consecutive days.

For this study, radar sensors collected inter-vehicle variables data of vehicles (both front and rear of the test vehicle), host test vehicle's acceleration, speed and distance data, and video recordings (both forward and rear of the test vehicle) for all the data collection runs. The video data from the three video cameras (one forward facing and two rear facing) were processed and each identified captured vehicle data extracted for further analysis. The captured vehicles total durations in the car following process were determined using the time differences between the time when the vehicles were first seen (i.e. start of car following) in the video recording and the time when the vehicles were last seen (i.e. termination of car following) in the video recording. The actual car following (without stopping) durations of each vehicle observed were determined by excluding all the stopping durations from the total duration during the car following process. Data parameters such as vehicle characteristics, corridor type (road) characteristics, gender characteristics and in-vehicle activities (following vehicles only), weather conditions, traffic and road characteristics, and all other relevant data parameters were obtained from the video recording data. The Video VBOX and the PerformanceBox data were processed to extract the test vehicle speed, acceleration and distance information.

The relevant information from the sensors' raw data were extracted and exported as comma separated values (csv) file. Due to the large data file sizes, a spreadsheet file split computer program was developed to split the csv files into smaller file sizes for data analysis tools, such as Microsoft Excel, to handle the data for processing and analysis. Each sensor data contains time series data points obtained at a rate of 600 messages for every 15 cycles per second. Each cycle contains 40 objects assigned with a unique numeric identification (ID), numbering from 1 to 40. Not all detected objects in a cycle were valid, hence the repeated cycle processes confirm and measure the valid objects it detects the third time as it tracks the objects and stores them. A valid object (i.e. vehicle) was assigned object measurement status value of three (3) in the data set, indicating the presence of a tracked valid object in a cycle. The front leading vehicles tracked were assigned object dynamic property value of 3 and the valid rear following vehicles tracked were assigned object dynamic property value of four (4) due to the initial settings of the rear radar sensor. The object dynamic property indicates the motion state of the valid objects in relation to the test vehicle's movement. The object dynamic property values of 3 and 4 for the front and the rear tracked vehicles respectively indicates the movements

of the vehicles in the same direction of the test vehicle. The front and the rear radar sensors data were extracted and processed separately from the data file.

Extensive preliminary data cleaning and filtering of the non-essential data from the exported raw data sets was carried out. In order to make the data cleaning process less complicated, even though time consuming, a four stage approach in cleaning the data sets was adapted using a series of computer software and visual basic macro programs developed for the data processing. At each stage of the data processing, manual inspections were carried out to ensure that the appropriate data was processed and the expected output results obtained. Further and more intensive data preparations were carried out by extracting the final individual vehicle's data as captured by the sensors and seen or observed in the video data. The data preparation was completed by matching and joining the Video VBOX data with the rest of the radar sensors data.

An overview of the general statistics of the whole data set was carried out. In all, a total of 1,387 vehicles were observed and captured for both the leading and following vehicles throughout the experiment**.** From the total vehicles captured, a total of 1,302 vehicles comprising 621 vehicles and 582 vehicles were successful for data analysis for the AM and the PM study respectively. In all, 274 following vehicles and 347 leading vehicles were analysed out of the total vehicles observed following and leading the test vehicle during the morning data acquisition. Similarly, 251 following vehicles and 331 leading vehicles were analysed for the vehicles observed following and leading the test vehicle during the afternoon data acquisition. Cars were found to be more than all the other vehicle types observed and analysed for both the leading and the following vehicles.

The average overall following durations of the vehicles following the test vehicle for Traffic Corridor 1, Corridor 2, Corridor 3 and Corridor 4 were 97 seconds, 68 seconds, 129 seconds and 71 seconds for AM test runs respectively. Similarly, during the PM test runs, the average overall following durations of the vehicles following the test vehicle for Traffic Corridor 1, Corridor 2, Corridor 3 and Corridor 4 were 83 seconds, 118 seconds, 113 seconds and 77 seconds respectively. Vehicles observed leading the test vehicle during the test runs on Traffic Corridor 1, Corridor 2, Corridor 3 and Corridor 4 recorded an average overall leading durations of 249 seconds, 40 seconds, 124 seconds and 53 seconds respectively for the AM test runs. During the PM test runs, the average overall leading durations of 55 seconds, 90 seconds, 114 seconds and 74 seconds were observed

for Traffic Corridor 1, Corridor 2, Corridor 3 and Corridor 4 respectively. The overall average time gap of the following vehicles for all the corridors combined was found to range from 1.89 seconds to 1.92 seconds, which was less than the recommended UK (including other EU countries) guidelines of 2 seconds minimum following time gap.

In order to prepare the data for modelling car following, a safe following distance headway threshold was set for this study at which the following distances of vehicles observed will have significant effect on driving behaviour. Using existing formula in the relevant literature, the safe distance headway threshold was calculated. The threshold was set to 75 metres based on the radar sensors' detection range, which was 200 metres long. All the vehicles (both following and leading) captured and analysed with the following distance of less than 75 metres were included in the data used for the modelling of the car following models developed in this study.

Different factors such as traffic and road characteristics, human characteristics, environmental characteristics affects the driving behaviour in keeping a safe or desired following distance and time gap during vehicle or car following process. Better understanding of these factors effects on driving behaviour enables better management of the traffic and the road infrastructure to improve traffic flow. Understanding driving behaviour better under some of these factors enables the improvement of driver safety measures.

Most of the existing car following models are calibrated using simple experimental data that makes the models less reliable to describe the interactions between vehicles. The models that are calibrated with complex experimental data are, sometimes, first developed (i.e. theoretical models) before the models calibration, which may not necessarily reflect the actual driving behaviour in the real world driving scenarios. Most of the developed existing car following models use acceleration to describe driving behaviour and few use the distance following. In fact, very few models use the following distance to describe driving behaviour in keeping a safe or desired following distance in order to avoid collision in a car following situation. Most of the existing two-leader car following models are developed with studies based on non-scientific arguments by extending, mostly, existing one-leader car following models on the assumption that drivers response to multiple vehicles ahead of them. Moreover, since these models are developed based on existing one-leader car following models, it can be argued that these

models were developed first before calibration, which may not necessarily mimic real world two-leader car following scenarios. There are little or no socioeconomic data available as many of the car following models do not address the effects of socioeconomic or driving/transport-related variables on driving behaviour in car following scenario. To understand driving behaviour better under different factors and develop car following models with a more realistic microscopic data leads to the next objective of this research.

The fifth and final objective has been to analyse the data collected and model distance-based car following models including calibrating existing GHR car following model

For this study, microscopic driving behaviour data were collected for vehicles leading the test vehicle and vehicles following from the rear of the test vehicle in a three consecutive vehicles movement. The inter-vehicle variables data were used together with the video data which captured information such as gender, weather condition, road type and other factors to investigate driving behaviour in a car following scenario. The analysis of the overall data was discussed in terms of the following behaviour of vehicles following the test vehicle. To analyse the driving behaviour, the data was grouped and discussed under different factors that affects driving behaviour in general.

The work, which has been done here showed that drivers were inconsistent with their driving behaviour in keeping a safe or desired following distance and time gap following other vehicles. It also showed that there were variability in driving behaviour across the drivers observed and that each driver does not follow a set of deterministic driving behaviour. For a three consecutive vehicles movement, it was found that the following vehicle follows closer to the first leading vehicle (test vehicle) than the first leading vehicle follows the second leading vehicle. The average time gap of the vehicle following the first leading vehicle was 0.96 seconds and that of the first leading vehicle following the second leading vehicle was averaged 2.0 seconds. The average overall time gap measured for all the following vehicles observed and analysed following the test vehicle was found to be 1.86 seconds. The average vehicle following time gap obtained for this study was less than the UK (including other EU countries) guidelines for minimum following time gap of 2 seconds.

Factors such as human characteristics, vehicle characteristics, traffic flow and road characteristics which affects driving behaviour were analysed. Considering vehicles following the test vehicle, it was observed that factors such as gender characteristics and vehicle characteristics including the type of vehicle affects the driving behaviour in keeping the safe or desired following distance and time gap to the lead vehicle. The analysis found that female drivers follow other vehicles with shorter following distances than male drivers at low speed ranges and longer following distances than male drivers at high speed ranges. It was found, in general, that male drivers tend to have more driving variability than the female drivers. For the vehicle occupancy effect, it was found that the following distance of one occupancy vehicles was shorter than that of the two or more occupancy vehicles at the low speed ranges. At higher speed above 60 km/h, the following distance of two or more occupancy vehicles was, on average, shorter than that of one occupancy vehicles. In general, it was found that one occupancy vehicle drivers have shorter following distances than that of the two or more occupancy vehicle drivers. It was also found that the two or more occupancy vehicle drivers tend to have, on average, shorter following time gaps that makes these drivers to have less driving variability in following other vehicles.

The type of vehicle following had different effect on the following distance in a car following situation. The analysis revealed that vans and buses tend to follow closer to other vehicles directly in front than cars and trucks do. It was found that truck drivers travel with longer following distances than all the other vehicle types drivers at speed above 40 km/h. Slow deceleration rate and longer braking distance of trucks may be some of the reasons why truck drivers decides to keep a longer following distance in order to bring the trucks to a safe stop when traffic comes to a halt. On average, buses were found to have larger following time gap than the other vehicle types, followed by trucks with vans having the least following time gap.

For factors such as weather condition, day of the week, time of day and direction of travel (i.e. data collection run) have different effects on the driving behaviour in keeping a desired following distance. For the weather condition, it was found that at speed below 35 km/h the following vehicles kept shorter following distances in both the dry and the wet conditions. At speed above 35 km/h, it was found, on average, that the following vehicles kept longer following distances in the wet conditions than in the dry conditions.

This kind of driving behaviour was expected since drivers are more cautious driving in the wet conditions, which might affect their braking distance hence tend to leave more space in between vehicles. For the day of the week effect on driving behaviour, it was revealed, on average, that drivers driving on Tuesday and Friday tend to have longer following distance than the rest of days of the week. Also, drivers driving on Wednesday and Thursday tend to have shorter following distance than drivers driving on other days of the week. It was found that midweek tend to have vehicles travelling with shorter following distances. The average time gaps of drivers driving on Tuesday, Wednesday and Friday were found to be shorter than that of Monday and Thursday.

For the time of day analysis, it was shown that drivers driving during the AM peak hours, relatively had shorter following distances compared to the PM off-peak hours. This is because as the traffic volumes increase, drivers are forced to follow at closer distances and shorter time gaps to maximise the use of the available road spaces. The results indicate that drivers feel more comfortable driving during the off-peak hours when there are less traffic volume. The analysis of the data collection run (i.e. direction of travel of the test vehicle during data collection) showed that vehicles travelling towards the city, on average, has longer following distances and time gaps than vehicles travelling in the opposite direction towards the outskirts of the city.

Different traffic and road characteristics such as corridor type, number of lanes, availability of bus lanes and traffic flow have different effects on driving behaviour of the following vehicles. The analysis of the traffic flow found that vehicles follow closer in the congested phase than in the uncongested phase in car following situation. The standard deviation of the time gaps of the following vehicles during the uncongested traffic phase was found, in general, to be larger than the congested traffic phase across all the speed ranges. The findings suggests that drivers generally tend to be more aware of the traffic condition and in control of the vehicle during the congested phase than in the uncongested phase due to the possibility of sudden disturbance in the traffic flow that could affect their driving behaviour. Analysis of the corridor type shown that the type of corridor does affect the driving behaviour in car following situation. Among the four different corridors analysed, Corridor 3, classified as urban-rural traffic condition, tend to have vehicles with shorter following distances and time gaps than all the other corridor

types considered in this study. The results indicate that road characteristics affect the driving behaviour of following vehicles in a car following situation.

The analysis of the corridors driving lanes found that, the following distance of vehicles travelling on single lane roads was less than that of the double (i.e. two) lane roads. Because of limited or no availability of enough road space to do certain driving manoeuvres on single lane roads, drivers tend to follow with, relatively, stable following distances thereby restricting their driving variability as compared to double lane roads. Also, the availability of bus only lane on the study corridors were found to influence the driving behaviour of the following vehicles in a car following situation. Roads with bus only lane enforcement in place were found to have vehicles following with shorter following distances than roads where there is no-bus only lane restrictions. The average standard deviation of the following distances of vehicles on roads with no-bus lane was found to be higher than roads with bus only lane available. Also the average standard deviation of the time gaps of the roads with bus only lane was less than roads with no-bus lane.

For this study, distance-based car following model, distance-based two-leader car following models and bus following models were developed, calibrated and validated. We extended the distance-based car following model and the distance-based two-leader car following model to include transport-related variables such as vehicle characteristics, traffic corridor type characteristics and driver characteristics. In addition, new versions of the GHR car following model were proposed with new sets of calibration parameters for a car following a car, a truck following a car and a car following a truck.

The microscopic driving behaviour data obtained using the instrumented vehicle was used to calibrate the GHR car following model and determined new sets of the model calibration parameters estimates or values. In calibrating the GHR model, two main scenarios involving the test vehicle driving position in the car following situation was proposed. The first scenario was when the test vehicle was following either large or small vehicles and the second scenario was when the test vehicle was leading either large or small vehicles in a car following situation. This resulted in three main car following scenarios that were described as a passenger-car following the test vehicle, a truck following the test vehicle and the test vehicle following a truck in a single lane of traffic. The three different vehicle following scenarios were calibrated to determine the

calibration parameters of the GHR model for each scenario. The work done in this study produced the GHR model calibration parameters estimates for car following car as m = -0.12, l = 0.19, c = 1.62 and m = 0.07, l = 0.75, c = 3.45 for the acceleration and deceleration phases respectively. For truck following car as m = -0.16, l = 0.07, c = 1.24 and m = 0.15, l = 0.43, c = 1.24 for the acceleration and the deceleration phases respectively. Finally, for car following truck as m = 0.29, l = 0.60, c = 2.02 and m = 0.29, l = 0.34, c = 0.66 for the acceleration and the deceleration phases respectively.

The work done here showed that modelling the observed data of the new sets of the GHR car following model calibration parameters estimates of the three vehicle following scenarios against the models predicted data using t-test statistics found no statistical significant differences in the data sets at 95% (i.e. p value $\leq$ 0.05) confidence level. In comparison with the GHR model calibration parameters estimates reviewed in the relevant literature for car following car, the new sets of the GHR model calibration parameters estimates obtained in this study were found to closely relate to the most reliable calibration parameters estimates of the GHR model reviewed in the relevant literature. Further investigations were carried out involving driver-vehicle interactions mainly when the test vehicle was leading and when the test vehicle was following different vehicle types (i.e. cars and trucks).

The investigations showed that, in both the acceleration phase and the deceleration phase when the test vehicle was leading, the response of the passenger-car driver in terms of the following behaviour was much stronger than the response of the truck driver. It also revealed that, the response of the test vehicle as a follower was much stronger with high sensitivity to the leading trucks than that of the leading passenger-car in the acceleration phase. In the deceleration phase, the findings revealed that the response of the test vehicle following behaviour when following the trucks was less than that of the passenger-cars. This could be explained in line with the driver's awareness of the longer braking distance of large vehicles and the reduced speed during deceleration. This might have prompted the driver to begin to anticipate that the traffic downstream was slowly coming to a stop, hence decides to react earlier than expected to the large vehicle in front.

Distance-based car following model that predict the following distance between two successive vehicles in motion was developed. Two different versions of the same model were proposed. One version of the model uses the following vehicle's acceleration and

the other model uses the relative acceleration between the two vehicles to predict the safe or desired following distance of following vehicles. We extended the basic model with the relative acceleration to include other driving/transport-related variables such as gender characteristics, vehicle characteristics and the corridor type characteristics to investigate their effects on the following behaviour of vehicle drivers which the existing models lack. The work done here showed that, the models including the extended models calibration parameters estimates were all statistically significant at 95% (i.e. p-value $\leq$ 0.05) confidence level. It showed that these variables considered in this study were individually or as a combination of two or more in the model significantly influence driving behaviour in car following situations.

The basic models validation showed that, there were no statistical significant differences between the observed data and the models predicted data. The t-test statistics results for Model A [t(3) = -0.390, p-value > 0.05, 2-tail] and Model C [t(3) = -0.363, p-value > 0.05, 2-tail] further indicates the models reliability in a real world car following scenario. Further validation of the basic model was carried out by simulating four selected following vehicles with minimum following duration of 35 seconds observed on the field. The analysis of the simulation results showed that the differences between the average simulation following distances and the observed following distances for all the four selected vehicles were found to be in the range of 0.28 metres to 0.32 metres. The simulation results showed that the basic models perform better in predicting closely the driving behaviour in real world car following scenarios.

A distance-based two-leader car following model that is not extension of existing car following model was developed that predict the following distance of a vehicle following in a three consecutive vehicles movement in a single lane of traffic stream. Two different versions of the distance-based two-leader car following models were developed with each model describing the driving behaviour of following vehicle in a three vehicles movement. One version of the model incorporates the acceleration of the following vehicle and the other model does not include the following vehicle's acceleration in predicting the safe or desired following distance of a vehicle following in a three consecutive vehicles following movement. We extended the basic two–leader model (i.e. model with the following vehicle's acceleration) to include gender characteristics, vehicle

characteristics and corridor type characteristics to investigate further their effects on the following behaviour in a two-leader car following scenario.

Further investigations were carried out to ascertain the effect of vehicle type either following or leading on the following distance behaviour in the two-leader car following scenario. The vehicle types considered were classified into two groups, such as cars and large vehicles (i.e. vans, buses and trucks). Two scenarios of the vehicle type either following or leading in the two-leader model investigation were considered. The first scenario was where the second leader vehicle was a passenger-car and the following vehicle was either passenger-car or large vehicle and the second scenario was where the second leader vehicle was a large vehicle and the following vehicle was either passenger-car or large vehicle. To investigate these scenarios of two-leader car following behaviour, the data set was sorted into the vehicle type following and leading sub data sets. The basic two-leader model was calibrated using these different sets of sub data under each scenario of vehicle type following or leading considered.

The work done here showed that the basic two-leader models including the extended models that incorporates the transport-related variables and the vehicle type either following or leading scenarios models calibration parameters estimates were all statistically significant at 95% (i.e. p-value ≤ 0.05) confidence level. The study found that the inclusion of these variables into the distance-based two-leader car following model significantly affect the driving behaviour of a driver following in a three consecutive vehicles movement. The results showed that the vehicle type either following or leading in a two-leader car following situation significantly affects the driving behaviour of the following vehicle driver in a three consecutive vehicles following movement.

The basic distance-based two-leader car following models validation showed that there were no statistical significant differences between the observed data and the models predicted data. The t-test statistical analysis results for Model A2 [$t(3) = -1.774$, p-value > 0.05, 2-tail] and Model B2 [$t(3) = -1.827$, p-value > 0.05, 2-tail] were found to be statistically non-significant as the p-values were greater than 0.05 and the t-stat values less than the t-critical two tail value.

To further assess the validity of the basic two-leader car following models, four different three consecutive vehicles following movements with minimum following time duration

of 40 seconds were randomly selected from the field data. The selected three vehicles movements were based on four (4) individual following drivers with different identifications. These four selected triple vehicles movements were simulated and the results compared with the observed field data of each selected three consecutive vehicles following behaviour. The simulation results analysis showed that the basic two-leader models closely replicates the real world driving scenarios of three vehicles in consecutive motion observed on the field. It was found that the differences between the simulated following distances and the observed following distances for all the four selected triple vehicles movements, on average, range from 0.07 metres to 0.56 metres. The analysis showed that the basic distance-based two-leader car following models developed in this study performs better to the real world two-leader three consecutive cars following scenarios.

A bus following behaviour involving the test vehicle following a number of public commuter buses was investigated as a special case in this study. Bus driving speed variability and bus following effect on the time gap of the following test vehicle in a bus following scenario was investigated. The leading vehicle effect on the time gap of the following vehicles in a bus following three consecutive vehicles movement was further investigated in this study. Two scenarios was considered investigating the effect of the leading vehicle driving behaviour on the time gap of the following vehicle in a bus following scenario. The first scenario considered the test vehicle following directly behind the leading bus (i.e. Bus – Test Car) and the second scenario considered other vehicles following directly behind the test vehicle (Test Car – Car) in a bus following three consecutive vehicles movement scenario.

A bus following model that describe the interactions between a car and a bus was developed in this study. Three different versions of bus following model was developed. The first version of the bus following model (Model B1-1) incorporates the following vehicle speed, the second version (Model B1-2) incorporates the bus speed and the third version (Model B1-3) incorporates both the bus speed (leading vehicle) and the following vehicle speed in predicting the desired or safe following distance of the following vehicle. The bus following models were calibrated and validated using data obtained from the test vehicle following eight (8) different double decker buses on different bus corridors.

The work done here showed that, the traffic conditions of the bus corridor affects the bus driving behaviour which varies per bus driver. It was found that the bus driving behaviour affected the time gap of the following vehicle directly behind the bus. Also the test vehicle driving behaviour was found to affects the time gap of the vehicles following directly behind the test vehicle. The results showed that, the following vehicle drivers were inconsistent with the time gap choice in both cases of car following bus (Bus – Test Car) scenario and car following car (Test Car – Car) scenario in a bus following three consecutive vehicles movement. It was found that vehicle (car) following bus behaves differently to car following car in a bus following three vehicles movement scenario. It was found that drivers ability to see around and beyond the lead vehicles in a three vehicles movement affects their following behaviour in terms of the time gaps choice to the vehicle directly ahead.

The bus following models calibration showed that the models calibration parameters estimates were all found to be statistically significant at 95% (i.e. p-values ≤ 0.05) confidence level. In order to ascertain the bus following models reliability in describing the actual scenarios of car following bus, the models were validated using t-test statistical analysis method. The t-test statistical analysis results for the bus following models (i.e., Model B1-1 [$t(3) = 0.374$, p-value > 0.05, 2-tail], Model B1-2 [$t(3) = 0.306$, p-value > 0.05, 2-tail] and Model B1-3 [$t(3) = 0.304$, p-value > 0.05, 2-tail]) were found to have no statistical significant differences between the observed bus data and bus model predicted data. This indicates that the bus following models developed in this study are capable of predicting accurately the desired or safe following distance of a vehicle following a bus in real world bus following scenario.

11.3 Limitations of the Study

There are a number of limitations that were identified with this study and these limitations are as follows.

1. The number of traffic corridors considered in this study was limited to four corridors due to time constraints and budget. The data collection was also limited to a two-man team.

2. Data collection was done mainly on week days excluding weekends and therefore, there was no available data on weekends to investigate the weekend driving behaviour in a car following situation.

3. Data collection test runs were limited to four test runs (i.e. two pairs of out and return runs) per day. Also, the time for data collection test runs were limited to AM peak and PM off-peak hours due to limitations of time and budget for data collection.

4. The bus following data collection was limited to corridors without lane restrictions and therefore, there was no available data on corridors with bus only lane restrictions enforced for investigation. The bus data collection was limited to PM peak hours due to time constraints.

11.4 Study Conclusions

This study investigates the driving behaviour and car following models and techniques to provide better understanding of driver-vehicle interactions in a car following situation. This study also investigates driving behaviour and traffic flow data collection techniques to provide better way to develop novel data collection system to improve the collection of microscopic driving behaviour and traffic flow data. To carry out the investigations, a number of objectives were outlined to address and answer the research questions outlined for this study. To achieve the research aim, literature review on car following models, data collection techniques and analytical approach used in data analysis were carried out and gaps in the literature identified.

The City of Edinburgh was chosen as the study area to carry out the investigations. The study traffic corridors within the case study area were identified and selected for the investigations. A novel data collection system was developed by equipping a private vehicle with advanced measuring devices, such as radar sensors and video recording cameras, to enhance the collection of driving behaviour and traffic flow data. With the use of the novel instrumented vehicle developed, driving behaviour and traffic flow data were collected on a number of traffic corridors identified within the study area over several days and months. The data collected was processed and prepared for data analysis. Using the improved, accurate and sufficient quality driving behaviour data collected and analysed, different distance-based car following models including bus following models

were developed that best describes driving behaviour and driver-vehicle interactions in car following scenarios. The car following models developed in this study provided better understanding of driving behaviour in keeping a safe or desired following distance between vehicles for different traffic conditions in car following situations.

In answering the research questions set for this study, each objective set for this study was addressed. Addressing the research questions, a summary of the answers to the research questions have been provided as follows. In addressing the first research question:

Can the available vehicle monitoring devices be used to improve the understanding of driving behaviour and data collection techniques related to the car following models?

Advanced radar sensors with range length of 200 metres, advanced CAN-buses with faster transmission and receiving rate of 66 microseconds, modern GPS based devices for distance and speed measurement linked to video-audio camera recorders, advanced CAN signals or messages monitoring software and in-vehicle laptop computer logging vehicle speed were used to equipped the test vehicle. The systems allow changes to be effected in the configuration of the measuring devices without interference of the experiment. The front and the rear mounted radar sensors, the forward and the rear facing video-audio cameras enabled the accurate measurement of inter-vehicle variables and the recording of factors relating to driving behaviour of three consecutive vehicles movement in a car following situation at the same time for the entire selected traffic corridors or road network. The data collection system also allows a range of vehicles and traffic parameters downstream and upstream of the traffic to be monitored without interference of the traffic streams. The data collection system allows sufficient, accurate and quality of traffic data to be collected. Analysis of the data collected using the instrumented vehicle developed showed a considerable improvement in the quality and accuracy of driving behaviour and traffic flow data collection that enhance car following and other traffic related studies.

Many of the existing car following models use driver's acceleration behaviour in predicting driving behaviour. Most of the existing two-leader car following models were proposed based on the extension of existing car following models, and these models often

predict the driver's acceleration behaviour in describing driving behaviour. In addressing the second research question:

Can we improve the existing car following models formulations using the newly data collected?

The driving behaviour data collected were processed and all the following vehicles observed data were used to develop new distance-based car following models. The distance-based car following models developed predicts the safe following distance between two successive vehicles in motion in a car following situation. Two different versions of the distance-based car following models were developed, one version of the model incorporates the following vehicle's acceleration and the other version of the model incorporates the relative acceleration between the leading and the following vehicles to predict the safe or desired following distance of a following vehicle. The models calibration parameters estimates were all statistically significant at 95% confidence level having all p-values < 0.05.

Three consecutive vehicles movement data involving the front leading vehicles and the following vehicles to the test vehicle observed were processed. All the instances of three consecutive vehicles movements observed data were grouped together. Linear distance-based two-leader car following models that predict the safe or desired following distance of a vehicle following in a three consecutive vehicles movement in car following situation were developed using multiple linear regression analysis method. All the two-leader models developed calibration parameters estimates were statistically significant at 95% confidence level (i.e. all p-values < 0.05). The two-leader models were not developed based on extending existing car following model and not using the driver's acceleration behaviour predictions but the driver's desired or safe following distance behaviour in describing driving behaviour. The validation and simulation of the models developed in this study showed significant improvements in the formulations of car following models in replicating real world driving behaviour car following scenarios.

The inclusion of driving/transported-related variables or parameters in car following models are lacking in most of the existing car following models. In addressing the third research question:

What is the impact of further parameters such as gender, vehicle occupancy, corridor (road) type and other parameters on the accuracy of existing car following models?

For this study, distance-based car following models and distance-based two-leader car following models were developed. To assess the effects of gender, vehicle occupancy and corridor type on driving behaviour in a car following situation, a number of variables or parameters such as gender characteristics, vehicle characteristics and study traffic corridor characteristics were introduced in the car following models developed in this study. Firstly, each of the three variables (i.e. gender, vehicle occupancy and corridor type) identified were individually introduced in the car following models developed. Secondly, two combination of the variables were introduced in the models. Finally, all the three variables considered were introduced in the models. The models with gender, vehicle occupancy and corridor type variables included were calibrated using the data collected for this study.

Statistical analysis of the distance-based car following model and distance-based two-leader car following model with the gender, vehicle occupancy and corridor type variables included were all found to have calibration parameters estimates statistically significant at 95% (i.e. all p-values < 0.05) confidence level. The results showed that these variables considered and included in the car following models have significant effects on driving behaviour in car following situations. The analysis of the results showed significant improvements in the formulations of car following models that includes further driving related parameters such as gender, vehicle occupancy and corridor type in replicating the effect on driving behaviour in real world car following scenarios.

11.4.1 Research Contributions

A number of contributions were made in this research, but the main contributions of this research has been the development of distance-based car following models. Distance-based single-leader car following models and distance-based two-leader car following models were developed. These models predict the following vehicle driver's safe or desired following distance behaviour in car following situations. The models improve the car following models predictions and improve the understanding of driving behaviour in

relation to car following. Another contribution has been the extension of the car following model and the two-leader car following model to include other variables such as gender, vehicle occupancy and corridor type to provide better understanding of their effect on driving behaviour in car following situations. Another contribution of this research has been the development of the bus following models that describes the interactions between car and bus in a bus following situation. The bus following models predicts the safe or desired following distance of a vehicle following a bus in a bus following scenario. The bus following behaviour models provide better understanding of driving behaviour in terms of the distance following interactions between car and bus within urban-rural traffic conditions in real world driving scenarios.

Another contribution of this research has been the development of novel and advanced, reliable, accurate and realistic microscopic driving behaviour and traffic flow data collection system or technique. The instrumented vehicle data collection system developed in this study can produce sufficient and quality microscopic driving behaviour and traffic flow data within an entire stretch of traffic corridor or road network without any disturbances in the traffic stream. The instrumented vehicle data collection technique developed for this research is aimed to enhance and improve driving behaviour data collection. The instrumented vehicle data collection system can:

- Observe or measure and collect real time series driving behaviour data of the front leading vehicle and the rear following vehicle simultaneously in a three consecutive vehicles movements over a long distance and time. Several vehicles following and leading the instrumented vehicle both upstream and downstream can be tracked and measured by the advanced radar sensors up to 200 metres range.
- Observe and track vehicles in the adjacent driving lanes moving in the same direction of travel as the instrumented vehicle.
- Observe and track the oncoming vehicles and, the vehicles passing and moving away from the rear of the test vehicle in the opposite driving lanes.
- Display and monitor real time series data on an in-vehicle laptop computer, which helps to know the status of the radar sensors, host vehicle speed information and the data collected at every point in time. It also provides the platform to make changes to the basic settings of the radar sensors without any interruption to the operations of the systems during the experiment.

- Identify and differentiate individual targets such as pedestrian, bike, car and truck that is tracked and measured during the experiment.
- Observe in-vehicle activities of the vehicles following from the rear of the instrumented vehicle.
- Measure the instrumented vehicle's own speed information and travel distance during the experiment and permanently record the experiment for further analysis.

11.5 Further Research

The data collection system developed for this study provides a number of benefits and opportunities for immediate applications to aid future research. The instrumented vehicle data collection system provides the opportunity to monitor a range of variables and factors that relates to driving behaviour. It also provides the benefits of observing and monitoring a range of vehicles and traffic parameters to help in the integration with ITS systems and road infrastructures for effective traffic management. It provides better accuracy measurements of driving behaviour data. More accurate data acquisition can be used in studies such as traffic performance studies, speed measurement studies, studies on driving cycle and traffic flow studies such as delay and queue length.

The following are recommended for further research:

1. It is suggested that the technique of using the instrumented vehicle data collection system could be used to improve the representation of driving behaviour parameters, including socioeconomic and environmental scenarios. For instance, driving behaviour and its impacts on vehicle emissions could be investigated using this technique.

2. Further research is recommended to use realistic and reliable car following data obtained using the instrumented vehicle to calibrate the existing theoretical car following models in literature, and carryout comparative study of these models to ascertain the models reliability in predicting driver behaviour in real world car following scenarios.

3. The driving behaviour of following vehicle can be affected by other vehicles in the vicinity of the following vehicle in car following scenario, especially, the oncoming vehicles in the opposite driving lane traffic on single lane roads. The effect of the

oncoming vehicles in the opposite driving lane traffic on car following behaviour can be investigated using data obtain from the instrumented vehicle.

4. The instrumented vehicle could be deployed to collect driving behaviour data in different cities to investigate and compare the driving cycle patterns, and driving behaviour within the cities to develop a benchmark model to describe city driving behaviour. The instrumented vehicle could also be used to investigate lane changing behaviour as well as merging and diverging of vehicles on to highways or motorways.

5. Driving behaviour varies among individual drivers depending on the age, gender and driving experience. Studies involving these groups of drivers are often done using laboratory simulated vehicles. A group of subjects with different age group, driving experience and gender could be recruited to drive the instrumented vehicle with extra video cameras installed inside the test vehicle to monitor the subjects' in-vehicle driving behaviours or activities to investigate the subjects driving behaviours and effects on the following vehicles in car following scenarios.

6. Further research is recommended to simulate a traffic corridor using traffic microsimulation tool, such as PARAMICS or VISSIM, using driving behaviour data obtain using the instrumented vehicle, and compare the simulation output results with the observed data and suggest improvements for the performance of the traffic microsimulation tools.

7. Are the behaviour of the following vehicle influenced by only one lead vehicle? Or more lead vehicles? The effect of other vehicles in the vicinity of the following vehicle in the same direction of travel required to be investigated.

8. The data provides opportunities for further analysis including reaction time analysis and investigation.

9. The data collected using the instrumented vehicle is recommended for further research to analyse the time-to-collision (TTC) of the following vehicles for driver safety improvement studies.

10. UK Highway Code sets a standard typical stopping distances as a guide for different vehicle types on UK roads. It is recommended for further research to use the instrumented

vehicle data collection technique to undertake studies into stopping or sight distances of different vehicle types and recommend a more realistic stopping distances for all vehicle types.

The huge advances in radar sensor technology and data collection have enabled a big improvement in traffic data collection recently. The data availability will have inputs to improve the quality and the range of models calibrated and to further enhance the understanding of traffic and driving behaviour including car following models

REFERENCES

Ahmed, K.I., 1999. Modeling Drivers' Acceleration and Lane Changing Behavior. PhD Thesis Submitted to the Department of Civil and Envirnmental Engineering, Massachusetts Institute of Technology, USA, pp.1–189.

Al-Jameel, H.H.E., 2010. Evaluation of car-following models using field data. In SPARC (Salford Postgraduate Annual Research Conference), 11-10 June, University of Salford, UK, pp.1–10.

Anderson, D.R., Sweeney, D.J., and Williams, T.A., 2010. Statistics for Business and Economics. Statistics for Business and Economics, Eleventh Edition, Solution Manuel to Acompany, pp.1–41.

Appiah, J., 2008. Investigation of Queues, Delays and Amber Dilemma at Signalised Junctions using Micro-simulation model (VISSIM). MSc in Transport Planning and Engineering Dissertation, Edinburgh Napier University, pp.1–139.

Appiah, J., Galevko, A., Saleh, W., and Kumar, R., 2015. Bus Following Model : A Case Study in Edinburgh. International Journal of Transportation, [online] Vol. 3(2), pp.1–16. Available at: <http://dx.doi.org/10.14257/ijt.2015.3.2.01>.

Appiah, J., Saleh, W., and Stewart, K., 2015. Evaluation of Existing Car-Following Models and Calibration Parameters Using Real Time Series Data. UTSG 47th Annual Conference, City University London, (January), pp.1–12.

Aron, M., 1988. Car-following in an urban network: simulation and experiments. Proceedings of Seminar D, 16th PTRC (Planning and Transport, Research and Computation) Meeting, Barth, U.K., pp.29–39.

Ayres, T.J., Li, L., Schleuning, D., and Young, D., 2001. Preferred Time-Headway of Highway Drivers. IEEE Transportation Systems Conference Proceedings - Oakland (CA), USA, pp.827–830.

Baldi, P., and Long, A.D., 2001. A Bayesian framework for the analysis of microarray expression data: regularized t-test and statistical inferences of gene changes. Bioinformatics, 17(6), pp.509–519.

Bando, M., Hasebe, K., Nakayama, A., Shibata, A., and Sugiyama, Y., 1995. Dynamical

model of traffic congestion and numerical simulation. Physical review. E, Statistical physics, plasmas, fluids, and related interdisciplinary topics, 51(2), pp.1035–1042.

Barceló, J., and Casas, J., 2005. Dynamic Network Simulation with AIMSUN. In Simulation Approaches in Transportation Analysis, Springer US, pp.57–98.

Bekey, G.A., Burnham, G.O., and Seo, J., 1977. Control theoretic models of human drivers in car-following. Human Factors, Vol. 19(4), pp.399–413.

Bevrani, K., and Chung, E., 2011. Car following model improvement for traffic safety metrics reproduction. Proceedings of the Australasian Transport Research Forum 2011, (September), pp.1–14.

Bevrani, K., Chung, E., and Miska, M., 2012. Evaluation of the GHR car following model for traffic safety studies. 25th ARRB Conference - Shaping the future: Linking policy, research and outcomes, Perth, Australia, pp.1–11.

Bexelius, S., 1968. An extended model for car-following. Transportation Research Board, Vol. 2, pp.13–21.

Blaauw, G.J., 1982. Driving Experience and Task Demands in Simulator and Instrumented Car: A Validation Study. Human Factors: The Journal of the Human Factors and Ergonomics Society, 24(4), pp.473–486.

Brackstone, M., 2003. Driver psychological types and car following: is there a correlation? results of a pilot study. In Proceedings of the Second International Driving Symposium on Human Factors in Driver Assessment, Training and Vehicle Design, pp.245–250.

Brackstone, M., and McDonald, M., 1999. Car-following : a historical review. Transportation Research Part F, Vol. 2(4), pp.181–196.

Brackstone, M., and McDonald, M., 2003. Driver behaviour and traffic modelling. Are we looking at the right issues? In Proceedings of the IEEE Intelligent Vehicles Symposium 2003, Piscataway, USA., pp.517–521.

Brackstone, M., McDonald, M., Sultan, B., and Mould, B., 1999. Five years of the instrumented vehicle: What have we learned? Traffic Engineering and Control (TEC), Vol. 40(11), pp.537–540.

Brackstone, M., Sultan, B., and McDonald, M., 2002. Motorway driver behaviour: studies on car following. Transportation Research Part F: Traffic Psychology and Behaviour, Vol. 5(1), pp.31–46.

Brackstone, M., Waterson, B., and McDonald, M., 2009. Determinants of following headway in congested traffic. Transportation Research Part F: Traffic Psychology and Behaviour, Vol. 12(2), pp.131–142.

Brackstone, M.A., Sultan, B., and McDonald, M., 2000. Finding on the Approach Process Between Vehicles Implications for Collision Warning. Transport Research Record: Safety and Human Performance, No. 1724, pp.21–28.

Brockfeld, E., Kühne, R., Skabardonis, A., and Wagner, P., 2003. Toward Benchmarking of Microscopic Traffic Flow Models. Transportation Research Record: Journal of the Transportation Research Board, 1852(250), pp.124–129.

Brockfeld, E., Kühne, R.D., and Wagner, P., 2004. Calibration and validation of microscopic traffic flow models. Transportation Research Record: Journal of the Transportation Research Board, No. 1876(1), pp.62–70.

Chakroborty, P., and Kikuchi, S., 1999. Evaluation of the General Motors based car-following models and a proposed fuzzy inference model. Transportation Research Part C: Emerging Technologies, Vol. 7, pp.209–235.

Chandler, R.E., Herman, R., and Montroll, E.W., 1958. Traffic Dynamics: Studies in Car Following. Operations Research, Vol. 6(2), pp.165–184.

Chang, K., and Chong, K., 2005. A car following model applied reaction times distribution and perceptual threshold. Journal of the Eastern Asia Society for Transportation Studies, Vol. 6, pp.1888–1903.

Christidis, P., and Rivas, J.N.I., 2012. Measuring road congestion. Joint Research Centre Scientic and Policy Reports, Institute for Prospective Technological studies, European Commission, pp.1–32.

Continental, 2012. Continental Industrial Sensors Datasheet. Continental Engineering Services GmBH, pp.9–10.

Continental, 2013. Continental Standardized ARS Interface Technical Documentation. Continental Engineering Services GmBH, pp.1–33.

Continental, 2014. Sensorcable ARS 308-2X (terminated). Continental Engineering Services GmBH, Germany.

Corrigan, S., 2008. Controller Area Network Physical Layer Requirements. Texas Instruments Application Report , SLLA270-January, pp.1–15.

Daly, L.E., Bourke, G.J., and McGilvray, J., 1991. Interpretation and Uses of Medical Statistics. Blackwell Scientic Publication, pp.54–137.

Edie, L.C., 1961. Car-following and steady-state theory for noncongested traffic. Operations Research, Vol. 9(1), pp.66–76.

Edinburgh Census, 2013. Census 2011: Transport and travel. Planning information, Planning and Building Standards, Services for Communities, The City of Edinburgh Council, December 2013.

ELTS, 2014. Edinburgh Local Transport Stategy 2014 - 2019. The City of Edinburgh Council, pp.1–86.

ENU (Edinburgh Napier University), 2017. Test for two-sample problem. Research skills (BE71009) - Statistics coursenotes, Edinburgh Napier University, Edinburgh, pp.1–14.

Ervin, R., MacAdam, C., Walker, J., Bogard, S., Hagan, M., Vayda, A., and Anderson, E., 2000. System for Assessment of the Vehicle Motion Environment (SAVME). The University of Michigan Transportation Research Institute (UMTRI), USA., Volume 1,2, pp.1–110, 1–124.

Farhi, N., Haj-Salem, H., and Lebacque, J.P., 2012. Multianticipative Piecewise-Linear Car-Following Model. Transportation Research Record: Journal of the Transportation Research Board, No. 2315, pp.100–109.

Fritzsche, H., 1994. A model for traffic simulation. Traffic Engineering & Control, 35(5), pp.317–321.

Gajdos, M., 2008. CAN bus communication protocol support and monitoring. Diploma Theses, Czech Technical University In Prague, Faculty Of Electrical Engineering, pp.1–90.

Gates, T.J., Noyce, D.A., Laracuente, L., and Nordheim, E. V., 2007. Analysis of Driver Behavior in Dilemma Zones at Signalized Intersections. Transportation Research Record:

Journal of the Transportation Research Board, No. 2030, pp.29–39.

Gazis, D.C., 2002. The Origins of the Traffic Theory. Operations Research. 50th Anniversary Issue, Vol. 50(1), pp.69–77.

Gazis, D.C., Herman, R., and Potts, R.B., 1959. Car-Following Theory of Steady-State Traffic Flow. Operations Research, Vol. 7(4), pp.499–505.

Gazis, D.C., Herman, R., and Rothery, R.W., 1961. Nonliner follow-the-leader models of traffic flow. Operations Research, Vol. 9(4), pp.545–567.

Gipps, P.G., 1981. A behavioural car-following model for computer simulation. Transportation Research Part B, 15B, pp.105–111.

Greenberg, H., 1959. An Analysis of Traffic Flow. Operations Research, Vol. 7(1), pp.79–85.

Greenberg, H., and Daou, A., 1960. The Control of Traffic Flow to Increase the Flow. Operations Research, Vol. 8(4), pp.524–532.

Greenshields, B.D., 1935. A Study of Traffic Capacity. Proceedings of the 14th Annual Meeting, Highway Research Board, pp.448–477.

Gunay, B., 2004. An investigation of lane utilisation on Turkish highways. Proceedings of the Institute of Civil Engineers -Transport, Vol. 157(1), pp.43–49.

Gunay, B., 2007. Car following theory with lateral discomfort. Transportation Research Part B, Vol. 41, pp.722–735.

Gunay, B., 2012. Using automatic number plate recognition technology to observe drivers' headway preferences. Journal of Advanced Transportation, Vol. 46(4), pp.305–317.

Gunay, B., and Erdemir, G., 2011. Lateral analysis of longitudinal headways in traffic flow. International Journal of Engineering and Applied Sciences (IJEAS), Vol. 3(2), pp.90–100.

Gunay, B., and Woodward, D., 2007. Lateral position of traffic negotiating horizontal bends. Proceedings of the Institute of Civil Engineers, Transport 160 Issue TRI, (February), pp.1–11.

Halkias, J., and Colyar, J., 2006. NGSIM - Next Generation Simulation FACTsheet. Federal Highway Administration - U.S. Department of Transportation, FHWA-HRT-06-135, HRDO-03/12-06(IM)E, USA.

Hamdar, S.H., and Mahmassani, H.S., 2008. From Existing Accident-Free Car-Following Models to Colliding Vehicles: Exploration and Assessment. Transportation Research Record: Journal of the Transportation Research Board, No. 2088, pp.45–56.

Hanken, A., and Rockwell, T.H., 1967. A model of car-following derived empirically by piece-wise regression analysis. In Proceedings of the 3rd International Symposium on the Teory of Traffic Flow, New York: Elsevier, pp.40–41.

Helly, W., 1959. Simulation of bottlenecks in single lane traffic flow. Proceedings of the Symposium on Theory of Traffic Flow, Research Laboratories, General Motors, Elsevier, New York.

Herman, R., and Potts, R.B., 1959. Single lane trafic theory and experiment. In Proceedings of the Symposium on Theory of Traffic Flow, Research Labs, General Motors, New York: Elsevier, pp.147–157.

Herman, R., and Rothery, R.W., 1962. Microscopic and Macrospic Aspects of the Single Lane Traffic Flow. The Operations Research Society of Japan, pp.74–93.

Heyes, M.P., and Ashworth, R., 1972. Further research on car-following models. Transportation Research Board, Vol. 6, pp.287–291.

Higgs, B., Abbas, M.M., and Medina, A., 2011. Analysis of the Wiedemann Car Following Model over Different Speeds using Naturalistic Data. In 3rd International Conference on Road Safety and Simulation, pp.1–22.

Hoberock, L.L., 1976. A Survey Of Longitudinal Acceleration Comfort Studies Department Of Transportation. Research Reports Published by the Council for Advanced Transportation Studies. The University of Texas at Austin, No. 40, pp.1–54.

Hoefs, D.H., 1972. Entwicklung einer Messmethode uber den Bewegungsablauf des Kolonnenverrkehrs. Universitat (TH) Karlsruhe, Germany.

Hoogendoorn, S., Van Zuylen, H., Schreuder, M., Gorte, B., and Vosselman, G., 2003. Microscopic Traffic Data Collection by Remote Sensing. Transportation Research Record, Vol. 1855(1), pp.121–128.

Hoogendoorn, S.P., and Ossen, S., 2006. Empirical Analysis of Two-Leader Car-Following Behavior. European Journal of Transport and Infrastucture Reseach (EJTIR), Vol. 6(3), pp.229–246.

Horst, R. Van Der, and Hogema, J., 1993. Time-To-Collision and Collision Advoidance Systems. 6th ICTCT Workshop Proceedings, Salzburg, pp.1–12.

Jin, S., Huang, Z., Tao, P., and Wang, D., 2011. Car-following theory of steady-state traffic flow using time-to-collision. Journal of Zhejiang University SCIENCE A (Applied Physics & Engineering), Vol. 12(8), pp.645–654.

Kanhere, N.K., and Birchfield, S.T., 2008. Real-Time Increamental Segmentation and Tracking of Vehicles at Low Camera Angles Using Stable Features. IEEE Transaction on Intelligent Transportation Systems, Vol. 9(1), pp.148–160.

Kesting, A., and Treiber, M., 2008a. Calibrating Car-Following Models using Trajectory Data: Methodological Study. Transportation Research Record: Journal of the Transportation Research Board 2088, pp.148–156.

Kesting, A., and Treiber, M., 2008b. How Reaction Time, Update Time, and Adaptation Time Influence the Stability of Traffic Flow. Computer-Aided Civil and Infrastructure Engineering, Vol. 23, pp.125–137.

Kikuchi, S., and Chakroborty, P., 1992. Car-following model based on fuzzy inference system. Transortation Research Board, No. 1365, pp.82–91.

Kim, T., 2005. Analysis of variability in car-following behavior over long-term driving maneuvers. PhD Dissertation submitted to the Faculty of the Graduate School of the University of Maryland, College Park, pp.1–175.

Kim, T., Lovell, D.J., and Yongjin, P., 2003. Limitations of Previous Models on Car-Following Behavior and Research Needs. Proceedings of the 82th TRB Annual Meeting, Washington D.C., No. 03-3721.

Kim, T., Park, Y., and Lovell, D.J., 2003. A new methodology to overcome memoryless property of car-following models. Journal of the Eastern Asia Society for Transportation Studies, 5, pp.1194–1210.

Kitamura, R., 1988. An evaluation of activity-based travel analysis. Transportation, 15(1), pp.9–34.

Kometani, E., and Sasaki, T., 1958. On the stability of traffic flow. Journal of Operations Research, Japan, Vol. 2, pp.11–26.

Kometani, E., and Sasaki, T., 1959. Dynamic behaviour of traffic with a nonlinear spacing-speed relationship. In Proceedings of the Symposium on Theory of Traffic Flow, Research Laboratories, General Motors, New York., pp.105–119.

Kumar, R., 2009. Modelling Motorcycles Driving Cycles and Emissions in Edinburgh. PhD Thesis - Transport Resarch Institute, School of Edinburgh and the Built Environment, Edinburgh Napier University, UK.

Kumar, R., Parida, P., and Saleh, W., 2014. Effect of type of lead vehicle on following headway behaviour in mixed traffic. World Journal of Science, Technology and Sustainable Development, 11(1), pp.28–43.

Laerd, S., 2017. Paired t-test uing Stata. https://statistics.laerd.com/stata-tutorials/paired-t-test-using-stata.php (Date Accessed: 11/12/2017).

Lee-Gosselin, M.E.H., 1995. Scope and Potential of Interactive Stated Response Data Collection Methods. Conference on Household Travel Surveys: New Concepts and Research Needs, pp.115–133.

Lenz, H., Wagner, C.K., and Sollacher, R., 1999. Multi-anticipative car-following model. The European Physical Journal B, Vol. 7, pp.331–335.

Li, Y., and Sun, D., 2012. Microscopic car-following model for the traffic flow: the state of the art. Journal of Control Theory and Applications, Vol. 10(2), pp.133–143.

Lighthill, P.I., and Whitham, G.B., 1955. On Kinematic Waves II. A Theory of Flow on Long Crowded Roads. Proceedings of the Royal Society of London. Series A. Mathematical and Physical Sciences, Vol. 229(1178), pp.317–345.

Lothian Buses, 2013. Annual Report and Accounts. Lothian Buses Ltd, Transport for Edinburgh, Edinburgh, Scotland, UK, pp.1–33.

Ma, X., 2007. Behavior Measurement, Analysis, and Regime Classification in Car Following. IEEE Transactions on Intelligent Transportation Systems, Vol. 8(1), pp.144–156.

Ma, X., and Andreasson, I., 2005. Dynamic car following data collection and noise

cancellation based on the Kalman smoothing. IEEE International Conference on Vehicular Electronics and Safety, pp.35–41.

Ma, X., and Andréasson, I., 2006. Driver reaction time estimation from real car following data and application in GM-type model evaluation. In Proceedings of the 85th Transport Research Board Annual Meeting, pp.1–19.

Ma, X., and Andréasson, I., 2007. Statistical Analysis of Driver Behavior Data in Different Regimes of the Car-Following Stage. Transportation Research Board, No. 2018, pp.87–96.

Markowski, C.A., and Markowski, E.P., 1990. Conditions for the Effectiveness of a Preliminary Test of Variance. The American Statistician, Vol. 44(4), pp.322–326.

May, Jr., A.D., and Keller, H.E.M., 1967. Non integer car following models. Highway Research Record, No. 199, pp.19–32.

May, A.D., 1990. Traffic Flow Fundamentals. Prentice Hall, Eaglewood Cliffs, New Jersey.

May, A.D., Roberts, M., and Mason, P.J., 1992. The Development of Transport Strategies for Edinburgh. Proceedings of the ICE - Transport, 95(1), pp.51–59.

McClave, J.T., Benon, P.G., and Sincich, T., 2008. Stataistics for Business and Economics. Tenth Edit ed. New Jersey: Pearson International Edition, Pearson Educational, Inc.

McDonald, M., Brackstone, M.A., Sultan, B., and Roach, C., 1999. Close following on the motorway: initial findings of an instrumented vehicle study. Presented at the 7th Vision in Vehicles Conf., Marseille, France, September 1997, 7, pp.381–389.

McKenna, F.P., Waylen, A.E., and Burkes, M.E., 1998. Male and Female drivers: how different are they? AA Foundation for Road Safety Reseach, The University of Reading, pp.1–66.

Mehmood, A., and Easa, S.M., 2009. Modeling Reaction Time in Car-Following Behaviour Based on Human Factors. International Journal of Engineering and Applied Sciences, Vol. 5(2), pp.93–101.

Mehmood, A., and Easa, S.M., 2010. Development of a New and Improved Driver-

sensitive Car-following Model. Canadian Journal of Transportation, Vol. 4(Part 1), pp.11–26.

Mehmood, A., Saccomanno, F., and Hellinga, B., 2003. Application of System Dynamics in Car-following Models. Journal of Transportation Engineering, Vol. 129(6), pp.625–635.

Michaels, R.M., 1963. Perceptual factors in car-following. Proceedings of the 2th International Symposium on Thory of Traffic Flow, OECD, Paris, pp.44–59.

Newell, G.F., 1961. Nonlinear Effects in the Dynamics of Car Following. Operations Research, Vol. 9(2), pp.209–229.

Olstam, J.J., and Tapani, A., 2004. Comparison of Car-following models. Swedish National Road and Transport Research Institute, 1–45.

Orosz, G, Moehlis, J., Bullo, F. and Stépán, G., 2011. Dynamics of delayed car-following models: human vs. robotic drivers. ENOC, Rome, Italy., pp.24–29.

Ossen, S., and Hoogendoorn, S., 2005. Car-Following Behavior Analysis from Microscopic Trajectory Data. Transportation Research Record, Vol. 1934(1), pp.13–21.

Ossen, S., and Hoogendoorn, S.P., 2011. Heterogeneity in car-following behavior: Theory and empirics. Transportation Research Part C: Emerging Technologies, Vol.19(2), pp.182–195.

Ozaki, H., 1993. Reaction and anticipation in the car-following behaviour. Proceedings of the 13th International Symposium on Traffic and Transportation Theory, pp.349–366.

Panwai, S., and Dia, H., 2005. Comparative Evaluation of Microscopic Car-Following Behavior. IEEE Transactions on Intelligent Transportation Systems, Vol. 6(3), pp.314–325.

Papageorgiou, G., and Maimaris, A., 2012. Modelling, Simulation Methods for Intelligent Transportation Systems. Intelligent Transportion Systems, pp.101–123.

Peak-System, 2013. PCAN-USB Pro CAN / LIN Interface for High-Speed usb 2.0 User Manual. PEAK-System Technik GmbH, Germany., pp.1–45.

Peak-System, 2014a. PEAK-System Product Overview. PEAK-System Technik GmbH, Germany, pp.1–107.

Peak-System, 2014b. Peak PCAN-Explorer Software - Information leaflet. (further information can be found in www.peak-system.com and COSMOL - Computer Solution website www.computer-solutions.co.uk), PEAK-System Technik Gmbh, Germany.

Peak-System, 2015. Peak-System Product Overview. PEAK-System Technik GmbH, Germany, pp.1–117.

Piao, J., and McDonald, M., 2003. Low Speed Car Following Behaviour from Floating Vehicle Data. Proceedings of the Intelligent Vehicles Symposium, IEEE, pp.462–467.

Racelogic, 2003. VBOXTools SOFTWARE Manual. Racelogic Ltd, Buckingham, United, (Version 1.11), pp.1–102.

Racelogic, 2009. Video VBOX Pro hardware and software manual. Racelogic Ltd, Buckingham, United Kingdom, (1), pp.1–87.

Racelogic, 2012. Video VBOX Hardware Manual. Racelogic Ltd, Buckingham, United Kingdom, (10).

Racelogic, 2014. PerformanceBox RLPB Manual. Racelogic Ltd, Buckingham, United Kingdom, pp.1–74.

Ranjitkar, P., Kawamua, A. and Nakatsui, T., 2005. Car-Following Models: An Experiment Based Benchmarking. Journal of the Eastern Asia Society for Transpotation Studies, Vol. 6, pp.1582–1596.

Ranjitkar, P., Nakatsuji, T., Azuta, Y., Asano, M., and Kawamura, A., 2005. A contemporary reassesment of GM car-following model using RTK GPS data. J. Infrastructure Plan. and Man., JSCE, No. 793/IV, pp.121–132.

Ranjitkar, P., Nakatsuji, T., and Kawamura, A., 2005. Experimental Analysis of Car-Following Dynamics and Traffic Stability. Transportation Research Record, 1934(1), pp.22–32.

Ranney, T.A., 1999. Psychological factors that influence car-following and car-following model development. Transport Research, Part F, Vol. 2, pp.213–219.

Rockwell, T.H., Ernst, R.L., and Hanken, A., 1968. A sensitivity analysis of empirically derived car following models. Transportation Research, Vol. 2, pp.363–373.

Rothery, R., Silver, R., and Herman, R., 1964. Analysis of Experiments on Single-Lane

Bus Flow. Operations Research - Special Transportation Science Issue, 12(6), pp.913–933.

Saleh, W., and Lawson, A., 2013. Investigations of impacts of junction design on emissions: are our junctions sustainable? World Journal of Science, Technology and Sustainable Development, Vol. 10(2), pp.143–151.

Sayer, J., Mefford, M., and Huang, R., 2003. The effects of lead-vehicle size on driver following behavior: is ignorance truly bliss? Proceedings of the Second International Driving Symposium on Human Factors in Driver Assessment, Training and Vehicle Design, pp.221–225.

Sayer, J.R., Mefford, M.L., and Huang, R., 2000. The effect of lead-vehicle size on driver following behavior. Umtri-2000-15, (June), pp.221–225.

Seddon, P.A., 1972. A program for simulating the dispersion of platoons of road traffic. Simulation, Vol. 18(3), pp.81–90.

Soria, I., Elefteriadou, L., and Kondyli, A., 2014. Simulation Modelling Practice and Theory. Simulation Modelling Practice and Theory, Vol. 40, pp.208–220.

Sultan, B., and Mcdonald, M., 2003. Assessing The Safety Benefit of Automatic Collision Avoidance Systems (During Emergency Braking Situations). Proceedings of the 18th International Technical Conference on the Enhanced Safety of Vehicles (ESV), 44(0), pp.1–13.

SWOV, 2012. Headway times and road safety. SWOV Fact sheet, Instittute for Road Safety Research, The Hague, the Netherlands, (December), pp.1–5.

Tang, T., Shi, Y., Wang, Y., and Yu, G., 2012. A bus-following model with an on-line bus station. Nonlinear Dynamics, 70(1), pp.209–215.

TfE, 2015. Transport for Edinburgh Annual Report and Accounts. Transport for Edinburgh, Edinburgh, Scotland, UK, pp.1–68.

Toledo, T., Koutsopoulos, H.N., Davol, A., Ben-akiva, M.E., Burghout, W., Andréasson, I., Johansson, T., and Lundin, C., 2003. Calibration and Validation of Microscopic Traffic Simulation Tools - Stockholm Case Study. Transportation Research Record: Journal of the Transportation Research Board, No. 1831(1), pp.65–75.

Transportscotland.gov.uk, 2014. The A720 - Edinburgh City Bypass. http://www.transportscotland.gov.uk/a720-edinburgh-city-bypass-trunk-road. Accessed on 24/06/2014.

Treiber, M., and Kesting, A., 2013. Microscopic Calibration and Validation of Car-Following Models - A Systematic Approach. Pocedia - Social and Behavioral Sciences, 80, pp.922–939.

Treiterer, J., and Myers, J., 1974. The hysteresis phenomenon in traffic flow. D. Buckley (ed), In Proceedings of the 6th Symposium on Transportation and Traffic Flow Theory, Sydney, pp.13–38.

Vissat, L.L., Clark, A., and Gilmore, S., 2015. Finding Optimal Timetables for Edinburgh Bus Routes. Electronic Notes in Theoretical Computer Science, 301, pp.179–199.

Vogel, K., 2003. A comparison of headway and time to collision as safety indicators. Accident Analysis & Prevention, 35, pp.427–433.

Wang, J., Liu, R., and Montgomery, F., 2005. Car-Following Model for Motorway Traffic. Transportation Research Board, No. 1934, pp.33–42.

Wiedemann, R., 1994. Simulation of road traffic flow. Reports of the Institute for Transport and Communication, University of Karlsruhe.

Wilson, R.E., 2001. An analysis of Gipps' car-following model of highway traffic. TMA Journal on Applied Mathematics, pp.1–26.

Van Winsum, W., 1999. The human element in car following models. Transportation Research Part F: Traffic Psychology and Behaviour, Vol. 2, pp.207–211.

Van Winsum, W., and Heino, A., 1996. Choice of time-headway in car-following and the role of time-to-collision information in braking. Ergonomics, Vol. 39(4), pp.579–592.

Wolf, D.E., 1999. Cellular automata for traffic simulations. Physics A, Vol. 263, pp.438–451.

Wright, C., 1973. A Theoretical Analysis Of The Moving Observer Method. Transportation Research, 7, pp.293–311.

Wu, J., Brackstone, M., and McDonald, M., 2000. Fuzzy sets and systems for a motorway microscopic simulation model. Fuzzy Sets and Systems, Vol. 116, pp.65–76.

Xing, J., 1995. A parameter idenfication of a car following model. In Steps Forward, Intelligent Transport Systems World Congress on ATT., Vol. 4, pp.1739–1754.

Yang, Q., and Koutsopoulos, H.N., 1996. A Microscopic Traffic Simulator for Evaluation of Dynamic Traffic Management Systems. Transport Research, .

Zhang, H.M., and Kim, T., 2002. Understanding and Modeling Driver Behavior in Dense Traffic Flow. University of California Transportation Center, Davis, California, pp.1–20.

Zhang, H.M., and Kim, T., 2005. A car-following theory for multiphase vehicular traffic flow. Transportation Research Part B, Vol. 39(5), pp.385–399.

Zhao, X., and Gao, Z., 2005. A new car-following model: full velocity and acceleration difference model. The European Physical Journal B, Vol. 47, pp.145–150.

Zhou, Y., and Li, Z., 2012. An extended car-following model with the dynamical collaborative between two consecutive vehicles. IEEE Fifth International Conference on Advanced Computational Intelligence (ICACI), Nanjng, Jiangsu, China, pp.914–918.

APPENDIX

APPENDICES

APPENDIX 3.3.2 Hardware and Software Used for the Study

The description and the functions of each hardware used to equip the test vehicle and software used to process the data are discussed in this section. The hardware used for the development of the instrumented test vehicle includes the ARS 308-2 radar sensors, PCAN–USB Buses, Video VBOX and Performance box, Sony camcorder video camera, advanced HP laptop computer and Ford Mondeo hatchback vehicle. The software application used in combination with the system hardware include PCAN Explorer 5, VBOX SETUP, VBOXTools and PerformanceBoxTools.

3.3.2.1 The ARS 308-2 Long Range Radar Sensor

The ARS 308-2 Long Range Radar Sensor with a self-monitoring software was developed by Continental Engineering Services GmbH in Germany. The ARS radar sensor is the type of sensor deployed in adaptive cruise control (ACC) equipped vehicles for their protection against collision, especially autonomous vehicles. The ARS radar (radio detection and ranging) sensor has operating frequency range between 76 - 77 GHz. The sensor has one CAN interface referred to as CAN1 and its network communication is a CAN bus (ISO 11898-2 specified). The sensor is physically robust, impervious to rain, mud, fog and even material built-up on its surface. The radar sensor has an operational distance range of 0.25 metres to 200 metres far field and 0.25 metres to 60 metres close-up range with distance measurement accuracy of 0.25 metres, 1.5% at greater than 1 metres (see Figure A3-1).

Overall the sensor is capable of measuring distances up to a maximum of 200 metres. The radar sensor is able to distinguished targets from object with distance measuring resolution of 2 metres or greater than 5.5 km/h. It has a speed range of -88 km/h to +265 km/h (“-” leaving objects to “+” approximation) with speed accuracy of 0.5 km/h far field and 1.0 km/h close-up range. It has speed resolution of 2.76 km/h and 5.52 km/h for far field and close-up respectively, with a cycle time of approximately 66 microseconds close and far measurement. The ARS 308-2 long range has azimuth angle augmentation (i.e. field of view, FoV) of -8.5^{o} to +8.5^{o} far field and -28.0^{o} to +28.0^{o} close-up range with

angle measurement accuracy of 0.1^{o} far field and 1^{o} to 2^{o} close-up. The sensor operates with resolution angle of 1^{o} far field, 4^{o} close-up with angle of elevation augmentation of 4.3^{o} at 6 dBm (Continental, 2012).

The ARS 308-2 long range radar sensor uses radar emission to analyse its environments. When signals are sent by the sensor, the signals are reflected, processed and after a series of multiple steps, the signals become available in the form of targets and objects. Targets and Objects are the two speed output types that the radar sensor send to detect obstacles. A single target comprises multiple reflections, which have similar position and movement. Targets are a moment view which are newly evaluated for each cycle, whereas objects are tracked target groups that keeps a history of detected obstacle in every cycle. Because the object output type tracks and contains the history of tracked targets, it produces a more reliable and less cycle information about the detected object than the targets output type information. The ARS radar sensor continuously assesses new targets or objects it detects for every cycle. The detail information about a target or object such as the position, relative speed, size and angle is transmitted and received through a Control-Area-Network (CAN) bus at a rate of 500 kbit/s. The ARS radar sensor calculates the position of object using angular coordinates system (i.e. distance and angle) relative to the movement and direction of the host vehicle. The host vehicle course is determined by the yaw rate (i.e. the angular velocity) and the speed information that is transmitted to the radar sensor.

The radar sensor is programmed in such a way that when the speed or yaw rate information is missing during operation, the sensor reset to default (i.e. speed = 0 m/s, yaw rate = 0 degree/second) and standstill (i.e. with no sensor speed direction). One advantage of the ARS radar sensor is that, the elevation of the radar radiation can be changed to different range through the radar sensor configuration parameters. The sensor configuration parameters can be change individually or in combinations using the validity bit contained in the CAN message. Setting the validity bit of the sensor configuration to valid or true subsequently update the corresponding parameter of the sensor and stored in a non-volatile memory of the sensor, which set it at start-up automatically on any subsequent power up. The settings will be ignored if the configuration parameter is set to invalid (Continental, 2013). These features makes the ARS sensor more suitable and

adaptable for any specific application. The main function of the ARS 308-2 radar sensor is to detect targets or objects and measure their velocity, acceleration and distance in real time relative to the movement and the driving speed of the host vehicle equipped with the radar sensor. Two ARS 308-2 long range radar sensors were used for this study (see Figure A3-2a) and mounted at the front (behind the bumper inside the engine compartment) and the rear (below the back bumper) of the host vehicle (see Figure A3-2b) to measure the relative speed, following distance and relative acceleration of both the leading and the rear following vehicles simultaneously. Figure A3-2 shows the ARS 308-2 long range 77 GHz radar sensor used to equip the test vehicle.

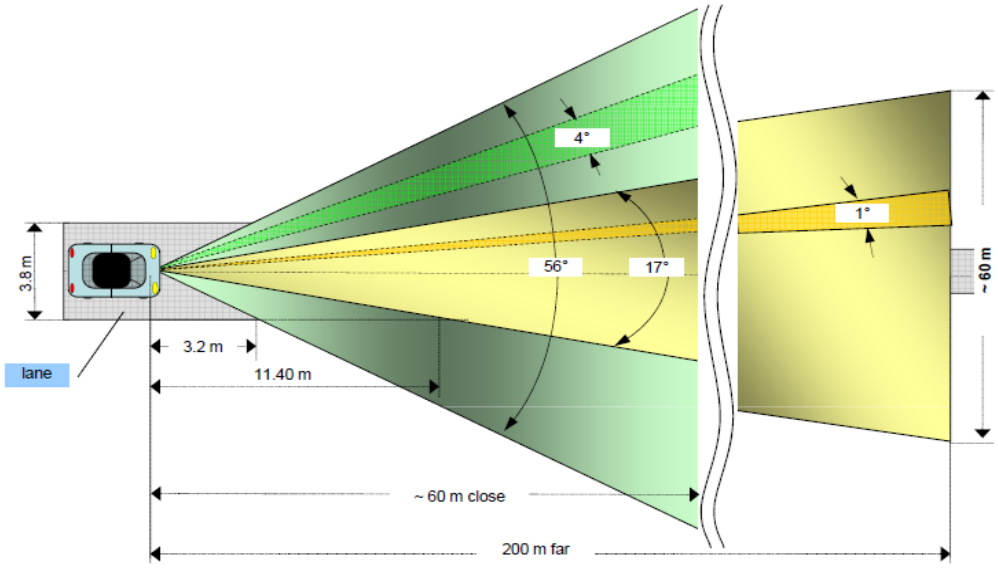

Figure A3-1: ARS 308-2 operational scanning area (Field of View) for Close-up and Far range (Continental, 2012)

(a) ARS 308-2 long range radar sensor

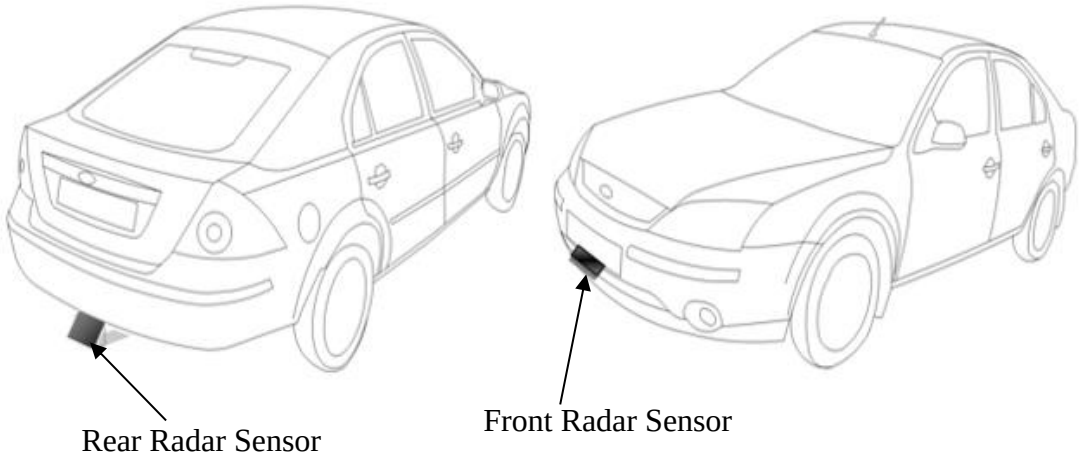

(b) ARS 308-2 radar sensors mounted on the car

Figure A3-2: ARS 308-2 long range radar sensors used for the study (a) and the radar sensors mounted on the car (b)

3.3.2.2 The PCAN-USB Pro and PCAN-USB Buses (Adapters)

The PCAN (PEAK Controller Area Network) adapters and tools that include software are developed by PEAK System Technik GmbH, a company based in Germany. The PCAN-USB Pro CAN-Bus and PCAN-USB CAN-Bus (ISO 11898-2 specified) serves as a communication channels for the ARS 308-2 long range radar sensors and the host vehicle on-board diagnostic (ODB) interface to a computer. The PCAN-USB Pro adapter has a two D-Sub connections that allows two field buses to be connected at the same time and simultaneously transmit and receive radar signals of CAN and LIN (Local Interconnect Network) messages. Using an appropriate adapter cables, the PCAN-USB Pro adapter can connect up to four connections (i.e. 2 x CAN and 2 x LIN) simultaneously and transmit and receive CAN and LIN messages at a full bit rates of 1Mbit/s and 2Kbit/s respectively. The PCAN-USB adapter uses a single D-Sub (9-pin) connection that allows CAN-Bus connection to transmit and receive a CAN messages. The PCAN interface provides the PC with a time stamp for each CAN message with a resolution of approximately 1 microseconds and 40 microseconds (μs) for PCAN-USB Pro and PCAN-USB CAN messages respectively.

The PCAN-USB Pro and PCAN-USB adapters have a high-speed USB plug to make a simple connection to a computer to CAN networks which eliminates the use of a PC card. The adapters are compatible with USB (universal serial bus) 1.1, USB 2.0 and USB 3.0 ports for simple connections. The adapters which operate on a 5-Volts (V) power supply is powered via the USB connection to the computer. The adapters with it aluminium casings make it robust and suitable for mobile applications which were suitable for this study. They have an extended operating temperature range of -40 degrees to 85 degrees Celsius (i.e. -40^{o}F to 185^{o}F) (Peak-System, 2013).

They operates at a rate of up to 1Mbit/s and compliant with CAN specifications of 2.0A (11-bit ID (Identifier)) and 2.0B (29-bit ID). The adapters operates in such a way that each CAN channel is separately opto-decoupled against USB and LIN up to 500V. The use of the PCAN adapters as a test and developmental tool is enhanced by their ability to measure bus loads, including the introduction of error frames and overloads frames when required. Error generations are also induced for incoming and outgoing CAN messages. The CAN message from the PCAN adapters connection to a PC can be easily accessed by software interface programs that is compatible with different operating systems such as PEAK Explorer 5.

The adapters can operate on computers running Windows 10. 8.1, 7, Vista and Linux (32/64-bit) programs. The PCAN adapters are supplied with a basic PC interface software PCAN-View for Windows, which allows for a simple CAN monitor for viewing, sending, and recording CAN data traffic. The communication for the radar sensors and the host vehicle's OBD-II interface to the PC is through the high speed PCAN Buses that receive and transmit messages from each radar sensor and the host vehicle OBD-II at 500kbit/s (Peak-System, 2013). The PCAN adapters was suitable for this study since two radar sensors were used and the host vehicle OBD-II interface. The two radar sensors were connected to the PCAN-USB Pro adapter and the host vehicle's OBD-II interface connected to the PCAN-USB for this study. The PCAN adapters served as signals communication channels between the radar sensors, the test vehicle's OBD-II and the on-board computer for the experiment. Figure A3-3 shows the PCAN adapters used as a

communication CAN-Bus channel for the radar sensors and the host vehicle's OBD-II to the PC with CAN software monitor.

Figure A3-3: PCAN-USB Pro adapter (left) and PCAN-USB (right) from PEAK-System

3.3.2.3 The Video Velocity BOX (Video VBOX)

The Video Velocity BOX (Video VBOX, VB) used for this study is a powerful Global Position System (GPS) based data logger with a high quality solid-state video-audio recorder developed by Racelogic Ltd, based in Buckingham in the United Kingdom. Its robust aluminum casing makes it suitable for outdoor and mobile use. The Video VBOX takes multiple cameras inputs simultaneously and combines the cameras output with a graphical overlay. The type of Video VBOX used for this study is the 2-camera input Video VBOX Pro with a preview screen (see Figure A3-4) as this suits the study more than the four camera version of this type. The logging data and the resulting video-audio stream direct onto a removable Secure Digital (SD) High Capacity (HC) card of up to 32GB during operation. The 32GB SDHC card can take about 640 minutes of video-audio (DVD quality MPEG4 PAL/NTSC file format) recordings enough to carry out continuous testing/experiment for all day without changing the SDHC card. The Video VBOX can log data at a rate of 10 Hz or 20 Hz during operation. For this study, the Video VBOX

was set to the default data logging rate of 10 samples per second and 25 display frames per second (Racelogic, 2009).

The Video VBOX can be powered by the mains power supply or the car cigarette lighter plug (the primary input power source) with an input voltage of 9V – 15V with a maximum power of 11.6 Watts (~4.5 Watts with no camera and ~8 Watts with 2 cameras). It has an operating and storage temperature of -10^{o}C to +60^{o}C and -40^{o}C to +85^{o}C respectively. The Video VBOX operates with a speed accuracy of ±0.1 km/h (kilometre per hour), lateral and longitudinal acceleration accuracy of ±0.5% and radius of turn accuracy of ±5 centimetres. It operates at a distance accuracy of 0.5% (<50 centimetres per kilometre) and a velocity accuracy of 0.2 km/h (averaged over 4 samples, unit: km/h or mph) with a resolution of 0.01 km/h. It operates at a maximum velocity of 1600 km/h and a minimum velocity of 0.1 km/h with time accuracy and resolution of 0.01 second. The Video VBOX logs one CAN channel in addition to the 10 standard data logging channels along with the MPEG4 video. The logging of Video VBOX CAN parameter data is done by loading CAN database into the software. The output of Video VBOX CAN channel logging is a Motorola data format on a 5-way connector output at a baud rate of 500kb/s. The Video VBOX logs the time, velocity, acceleration and distance travel as part of the standard data logging along with the video file.

It has a USB connection that allows changes to the default settings on a computer and uploads data, such as VBOX Scene and CAN database, into the Video VBOX. The Scene can be set to user preference to show the overlay elements (i.e. the graphical representations of the channel data such as speedometer) for all the logging channels during operation using Video VBOX Set-up Tools software. The data logged and the video data are time synchronized to allow linked analysis of the data using the VBOX Tools software. By default, the Video VBOX starts to log data when the host vehicle speed exceeds 0.5 km/h and set to record or log ‘Only when moving’, which can be change to “Continuously” to log all enabled data continuously even when the vehicle is stationary (Racelogic, 2009). For this study, the Video VBOX default settings was set to continuous logging. The Video VBOX main function is to provide visual and permanent recordings of driver and vehicle characteristics, and the environment in addition to the test

Vehicle's speed, acceleration, distance travel and UTC time. Figure A3-5 shows the cable connections of the Video VBOX with the SD Card during operation. Figure A3-6 shows the input and output of the overview of Video VBOX interface.

Figure A3-4: Video VBOX with two cameras, GPS anatenna and the preview screen (right)

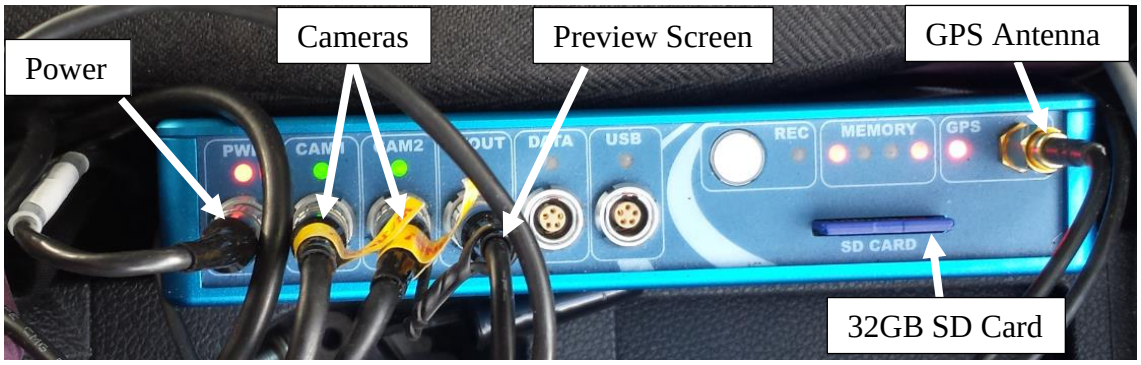

Figure A3-5: The cable connections of the Video VBOX with the 32GB SD card for data storage

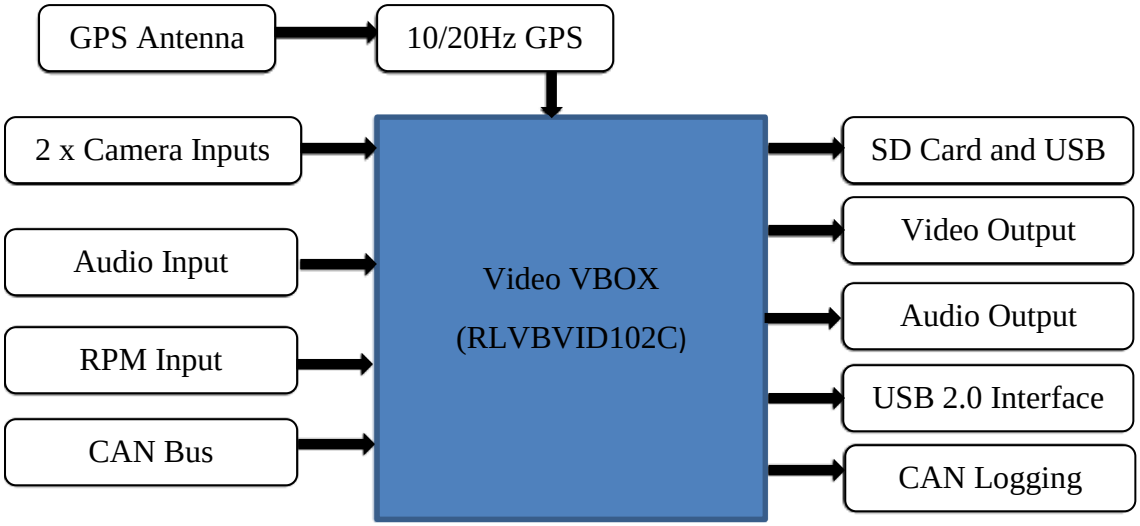

Figure A3-6: The overview of the inputs and the resulting outputs of the Video VBOX (reproduced from Video VBOX Manual, 2009)

3.3.2.4 The PerformanceBox

The Racelogic PerformanceBox Performance Meter (see PerformanceBox, PB) is a high performance GPS based data logger and performance meter easy to measure the acceleration, speed, time and distance travelled by the test vehicle (Figure A3-7). It has data logging frequency of 10Hz coupled with fully calibrated GPS engine used to provide accuracy and precision. The data logged is stored on a removable 2GB (maximum) SD card. It has a USB connection port that allows data to be downloaded to a computer for in-depth data analysis using data-logging analysis software, such as Performance Tools, Circuit Tools and VBOX Tools. It has a real time back-lit LCD display screen that displays a large digital speed value and the performance compass (Racelogic, 2014).

The PerformanceBox in open conditions has a velocity accuracy of 0.1 km/h and a resolution of 0.01 km/h, which becomes useful when checking the accuracy of own vehicle's speedometer, and distance accuracy 0.05% (<50 centimetres per kilometre). It has an operating and storage temperature of -20ºC to +50ºC and -30ºC to +80ºC respectively. The Odometer and Height can also be displayed on the screen in the speed display mode. It can continuously log data for a maximum of 50 hours if used with 64mb SD card during operation. The PerformanceBox when used in combination with a Micro

Input Module can record the data of the vehicle (such as RPM and throttle angle) alongside the GPS logging parameters. The data starts to log when the velocity is above 0.5 km/h. It has both internal and external GPS antenna and can be powered by the mains power supply, a battery pack or the host vehicle cigarette plug with voltage input of between 6V – 28V (Racelogic, 2014). The main use of the PerformanceBox is to measure the acceleration and deceleration (i.e. the G-force), travel distance, speed, the UTC time of the instrumented test vehicle and as a backup of test vehicle information. The test vehicle's speed generated by the PerformanceBox was used to compare and validate the test vehicle's speed during the reverse-engineering experiment to determine the test vehicle's ground speed directly from the vehicle's engine.

Figure A3-7: PerformanceBox and GPS antenna (right) used for the study (manufactured by Racelogic Ltd)

3.3.2.5 The Video Camera

A high resolution Sony digital video camera was used for this study. The video camera has an optical zoom of 40x with a maximum internal storage capacity of 30GB (see Figure A3-8). It can record continuously for up 20 hours of video images at a rate of 3Mbps. The video camera is powered by using the mains power cable or a battery pack. For this study, a Sony battery pack that continuously power the video camera for 240 minutes when fully charged without stopping was used. A car battery was on standby (as a backup) to supply power to the video camera (in case of complete battery drain) through an in-vehicle cigarette lighter plug mains power converter.

The camera was mounted facing the rear of the test vehicle in conjunction with the Video VBOX camera (see Figure A3-15d). The primary function of the video camera apart from providing high resolution video records of the experiment at the rear of the test vehicle, it records additional information such as the rear following vehicle drivers characteristics and in-vehicle driver behaviour activities, which could not be captured by the Video VBOX rear camera for vehicles not following closely due its lack of zoom functions.

Figure A3-8: The Sony digital video camera used for the study

3.3.2.6 The On-Board Computer (Laptop)

Hewlett-Packard (HP) Pavilion 15.6" touchscreen laptop computer was used as on-board computer for this study (see Figure A3-9). The laptop runs on Windows 8.1 with Intel Core i5-4210u processor. It has 8GB RAM (16GB maximum on upgrade) and 1TB hard drive storage capacity enough to store and process the experimental data. It has two high speed USB 3.0 port and one USB 2.0 enough to allow three USB devices to be connected during the experiment. The battery capacity last for up to 6 hours when fully charge. Additional power supplied to the laptop was provided using the in-vehicle cigarette lighter plug mains power converter. The laptop was installed with PCAN Explorer 5 software tool to monitor the live signal feed from the radar sensors and the speed information from the test vehicle's OBD-II. The on-board computer serves as the central data monitoring, processing, storing of traffic signal data from the radar sensors and the test vehicle's speed information received via the on-board diagnostic port.

Figure A3-9: HP Laptop used as the on-board PC for the instrumented vehicle

3.3.2.7 The Vehicle

A hatchback Ford Mondeo 2002 LX model with a 1.8 litre engine capacity running on unleaded petrol was used as the test vehicle for the study (see Figure A3-10). The car has a standard dimensions of 4731 millimetres, 1812 millimetres and 1429 millimetres as the length, width and height respectively. The car has enough room inside to accommodate all the elements of measuring devices, including the installation cables, and still provides enough space for more than one observers to monitor the equipment without interference. A private vehicle which was readily available and owned by the researcher was used for the study. The vehicle was used to house all the experimental measuring instruments and used to conduct the experiment on the identified traffic corridors to collect traffic data.

Figure A3-10: The Ford Mondeo 2002 model used as the test vehicle for the study

3.3.2.8 The PCAN-Explorer 5

PCAN-Explorer 5 (PE5) is a PCAN software tool developed by PEAK-System Technik, a German based company, used as an interface to monitor CAN messages. It is advanced software and a universal tool for traffic data monitoring on a CAN network. The PE5 is available in two types of user licenses. The single computer license which comes with installation CD including PCAN line writer Add-in and license file, allows the user to install, unlock, and use the software on a single computer (PC) only. The portable license with USB copy protection dongle which comes with installation CD, allows the user to install the PE5 on several computers but only allows for use on one PC at a time by plugging the copy protection dongle into a free USB port to unlock the software for use.

The PE5 used for this study is PCAN-Explorer 5 Version 5.3.4.823 with a USB copy protection dongle ID 520420 (see Figure A3-11) released on 10/03/2014. This version of PE5 allows for further improvement with the latest J1939 database 2013-11 as an Add-in and other Add-in applications purchase separately if required, which were not use for this study. The PE5 operates on computers running Windows 10, 8.1, 7, Vista (32/64-bit) programs with at least 512MB RAM and 1GHz CPU and complies with CAN specifications 2.0 A/B the type used by PCAN Bus adaptors (Peak-System, 2014b). The PE5 interface has a number of display windows including Receive/Transmit, Line Writer (chart plotting), Tracer, Project Browser and Properties, and Connections windows that the user can resize to monitor all CAN activities on the PE5 (see Figure A3-12).

The Connections window provides an overview of all the CAN connections, complete with various CAN networks status, error counters, bus load, bus heavy (when there is a problem with a connection) and bit rates. The Receive/Transmit window provides an overview of all the live CAN messages that is being received from or transmitted to the connected CAN networks, complete with bus, CAN-O, DLC, symbols, time-out and circle-time. The PE5 allows all files and elements to be managed and saved in the projects. The project browser displays clear and laid out features of the project components such

as the CAN connections, symbols files, macros and signals for easy navigation of active files and for possible editing if required.

The Explorer provides some unique features that allow message identifiers to be assigned names in order to avoid having to keep note of each data (HEX) value. It also permits the display of message data in different formats such as text, hex, signed, unsigned and floating point. The PE5 is user friendly that allows the user to define the display columns and arrange the messages in the receive/transmit window to their preference. It can monitor in real time several CAN traffic data or signals through the integrated watch window. The in-built features allow for the simultaneous connection of up 16 CAN networks/CAN interfaces of the same hardware type to be monitored. It provides complicated graphing of data and a visual Graphic User Interface to control and display CAN messages.

The display CAN messages shows the message variables such as the ID, length, data bytes, number of messages received and the receiving interval. CAN messages for transmission to connected networks can be set to manual or as a reply to remote request or frames at a fixed time intervals during operation. The PE5 periodically transmit CAN messages with up to 1 microsecond precision, making the PE5 more accurate in sending CAN messages to the networks. The message transmission cycle time can be set to suit the user preference. The user can create messages as transmit list and stored them, which can later be loaded in order to, for example, emulate CAN nodes when desired.

The explorer enables the creation of macros to automate complex tasks through the support of the integrated VBScript and text editor. The VBS scripts are able to run in the background even without PE5 interface. The integrated VB Script can be coded to perform unique functions, such as sending of e-mails when a temperature of a network is exceeded, excel sheet opening when an event occurs, initiating a test tool when certain messages are received and data saving in individual cells. PE5 software tool as reported by the developers, is perfect for use as a test tool to develop or implement CAN systems (Peak-System, 2014b; 2015).

Appendix 3.3.2

The PCAN-Explorer 5 has unique integrated and configurable data logging properties that enables the operations of multiple tracers of messages to be received and monitored at the same time. The data logger with data logging time-out properties enables all CAN data traffic to be monitored, recorded, analysed and stored in multiple tracers (i.e., TRC file format) for future use. The saving of the tracers could be done automatic during the operations by codes in the integrated VB script and text editor. The PE5 has some useful data logging properties that is important for the operations of CAN networks. These properties include the filtering of messages or signals for logging through symbols definitions, logging of errors occurring during message transmission/receiving. The data logging properties also includes varying the buffer size with the optional line buffer (i.e. logging curtailed immediately the buffer is completely filled) or circular buffer (i.e. incoming new messages overwritten the oldest messages when the buffer is filled) and, the logging of the representative messages with time stamp, type, ID, Length and data bytes.

The flexible data storage capabilities of the PE5 enables CAN data to be logged in a text form for subsequent import into comma separated values file or similar text file supported programs. The most important properties of the PE5 data logger is the ability to export the trace files (i.e. the recorded CAN messages) to a Comma Separated Values (CSV) file format for subsequent analysis and examination of the CAN data. This feature was very useful for this study as all saved tracers of the experiment were able to be converted in readable CSV file format for further analysis.

Efficient and important feature of PE5 is the ability to display in a symbolic form the message objects from a CAN bus, and permitting the symbolic input of data which brings the CAN messages into an easily understandable form for the program user. The PE5 is integrated with text editor (with syntax highlighting), and with standalone Symbol Editor that allows the creation of symbols files (also known as Database Container, DBC) for defining the CAN messages. The PE5 applies the definition of the symbolic interpretation of the CAN messages from the symbols files (called text files or DBC) for the user to understand each assigned messages. The Peak Explorer 5 support the integrations of external tools (Peak-System, 2014b; 2015). The PE5 is a user friendly tool, which took consideration time to learn and understand the basic functions of this advanced software

for CAN monitoring. The PE5 software primary function is to monitor live signal feed from the radar sensors and the speed information from the test vehicle's OBD-II. It provides the platform that enable the radar sensor default configuration settings to be changed. It also serves a means of communication between the radar sensors, the test vehicle and the on-board computer. Figure A3-12 shows the screen shot of Peak Explorer 5 interface displaying some active windows during the experiment.

Figure A3-11: The PEAK Explorer 5 USB copy protection dongle (ID 520420)

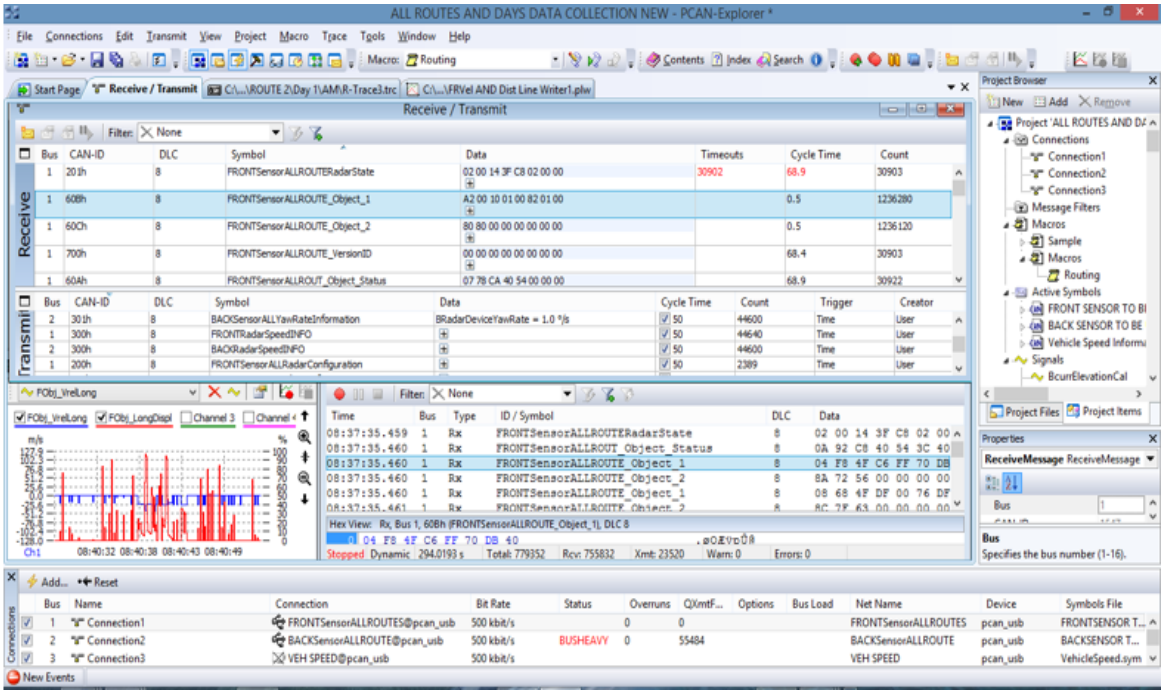

Figure A3-12: Screenshot of the main screen of the PCAN-Explorer 5 interface display during the experiment

3.3.2.9 The Video VBOX Setup Software

The Video VBOX Setup is a software tool that allows the user to prepare the Video VBOX to suit their own preferences on the graphical overlay before the start of experiment. The software enables the user to freely and completely define the data looks and feel that is displayed in the available graphical overlay superimposed over the Video VBOX recorded video. It provides options for the user to choose from a number of predefined Scenes (i.e. the look of the video overlay during the recording of the video file by the Video VBOX), which contains scene properties such as gauges, picture-in-picture windows, map tracking, all of which are completely customizable to suit the user preference.

It allows the user to import already created scenes and download it into the software for use and also allows the use to create from scratch their own scene with own gauges and upload into the Video VBOX either through SD card or USB cable connection. The Video VBOX setup software allows the settings to the video recordings to be set in PAL or NTSC format. The default video recording quality of the software is set to high, which can be changed to either median or low depending on the user preference (Racelogic, 2009).

The Scene has a number of properties (such as grid set-up, system info, smooth level settings, GPS settings, serial application, log settings, video settings, audio settings, camera settings, lap timing, CAN and module configuration, performance tests and maths channels) that allows the user to change the default settings of the Video VBOX if the user so desire. The Video VBOX Setup software is not restricted to one user or computer but can be used on multiple computers or work stations at the same time. For this study, a Scene to display the video overlay during the experiment was created. The Scene was created to display the two camera (same size) overlay, the speed of the test vehicle in mph (miles per hour), the speedometer or gauge with G (gravity acceleration) loading, UK summer time with satellite tracking numbers, the coordinated universal time (UTC) and the date of the experiment (see Figure A3-13). With the available preview OLED (organic light-emitting diode) display screen, the Video VBOX Scene was displayed with live

feeds of data during the experiment.

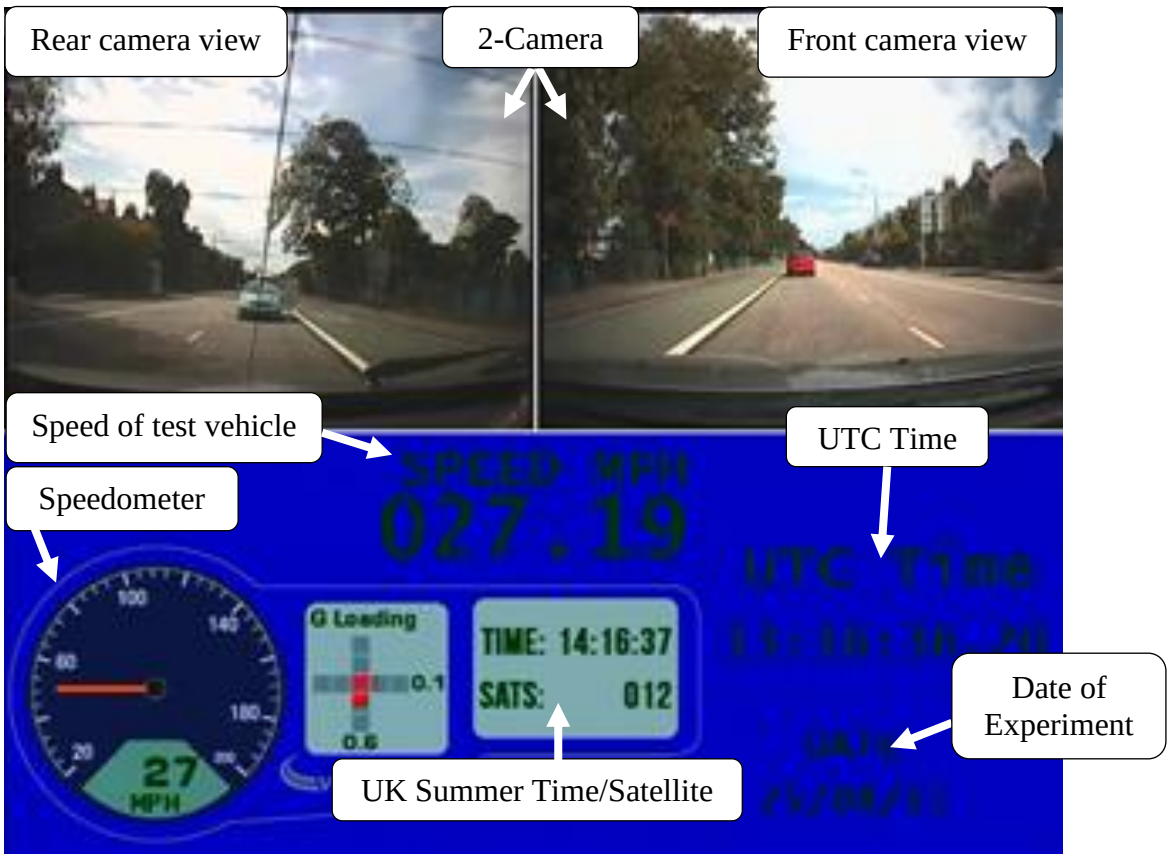

Figure A3-13: The Scene created for the Video VBOX video overlay display

3.3.2.10 The VBOX Tools Software

The VBOX Tools is a software tool developed by Racelogic Ltd that allows the setting up and the configuration of Video VBOX. The VBOX Tools is a multi-computer user program that can be installed on a number of computers and used at the same time by different users. The version of the software used for this research is firmware version V2.15b369. The software provides the user with the ability to monitor live log data from the Video VBOX in many formats. The user has the ability to view or process the VBOX data through the software in real time or offline during experiment.

When the Video VBOX is connected to a computer, the software allows the live streaming of the Serial Video VBOX data to a VBOX file recorded directly to the computer's hard drive. These features enables the quick view of the log data in the graph screen at the end

of each test without the need to remove the SD card from the Video VBOX and load the logged file from the SD card (Racelogic, 2003), however, these features were outside the scope of this study as the VBOX was not connected to a computer during the experiment.

The software enables the user to generate complex testing scenarios with the VBOX log data without any difficulties when use in combination with the software features and the existing default profiles. One of the main features of the VBOX Tools is the Report Generator Data processing engine, which the software is mainly based around. There are other features of the software such as the graphing tools, mapping tools, live data windows and VBOX setup tools that is available for data processing. The Report Generator data processing feature has been designed to provide accurate and fast method of generating text-based data.

The data processing facility allows the user to set the test profiles to their preference and select to add or remove the column titles before scanning the loaded file containing the log data to show the results from all the occurrences of the test profile. It has five pre-defined test setup profile on the interface easily to access with a button that allows the user not only with a quick way of extracting the data from the test runs in a file, but also allows the graphical viewing of the data on the screen which can also come in the form of results table (Racelogic, 2003). The Report Generator was mainly used for the purpose of this study for the extraction and processing of the Video VBOX and the PerformanceBox data offline for further analysis.

3.3.2.11 The Performance Tools Software

The PerformanceTools software version that was used in this instrumentation is firmware version 1.8.2 (Build 012). The software is used to carry out detail investigations of vehicle and driver performance during test runs. It also allows the user to view all the driving data logs by the PerformanceBox in an experiment. The software contains a number of windows with each capable of showing a variety of data in different format, such as graphical and textual form. The software has features that allows different

PerformanceBox channels of up to four to be plotted (either against time or distance) and overlaid on the graph for further comparison of driving performances and analysis.

The software also shows the path of the host vehicle during test runs, which is calculated from the latitude and the longitude data. It allows vehicle paths created in Google Earth to be imported into the software, and also allows the location data stored by the PerformanceBox to be exported to Google Earth for the data to be viewed on satellite images. The features also allows the user to see the position of the host vehicle in relation to the boundaries of the roadway. The software enables graphs to be exported to other programs as a picture file and also enables data to be exported as CSV file format to be analysed further in Microsoft Excel (Racelogic, 2014).

APPENDIX 3.3.4 Laboratory Testing and Mounted Devices on the Test Vehicle

3.3.4.1 Laboratory Testing Of Devices

To ensure that the radar sensors, the PCAN-USB adapters and the PCAN-Explorer 5 all establish communication links and function well as expected after the termination of the CAN-Bus cables, a laboratory test was carried out. A series of trial tests in the laboratory was performed testing these vital instruments and software to ensure they communicate with each other without any difficulties. The PCAN-Explorer 5 (PE5) was installed on the laptop computer. New projects and symbols files were created for each radar sensors in the PE5. The systems were set up with the laptop connected to the PCAN-USB-Pro, which has been connected to one radar sensor using one 5-metre sensor terminated cable. The radar sensor was powered up using Thurlby PL154 15V/4A low voltage DC (direct current) variable power supply via the 12V DC power plug at the ends of the 5-metre CAN bus – sensor cable (see Figure A3-14). The supply voltage from the DC variable power was set to 12V to meet the required input voltage of the sensors. The PCAN-USB Pro draws its power from the connected laptop computer.

Initially, the test was conducted without any of the symbols files assigned to the individual CAN IDs and monitored the signals as they were being received and transmitted at the rate of 66 microseconds. The symbols files was loaded, applied and assigned to the individual CAN IDs and monitored all the signal traces that were being received and saved. This process were repeated with the other sensor and the other 5-metre terminated cable. The trace files were exported as a CSV (comma separated values) file format and analysed. The analysis enabled recoding of some of the variables in the symbols data files. Necessary changes were made to the sensor's default configurations that ensured that the correct targets or objects were tracked, which was essential for the study. The trial testing was also conducted in order to become accustom to the use of the PCAN-Explorer 5, which was the first time such an advanced CAN signal traffic data monitoring software was being used for this type of study. The laboratory testing ensured that the PCAN-Explorer 5, the PCAN-USB Pro CAN bus and the sensors together with the 5-metre terminated cables were all working and functioning as expected before all the equipment were transferred to the car permanently for further field pilot testing.

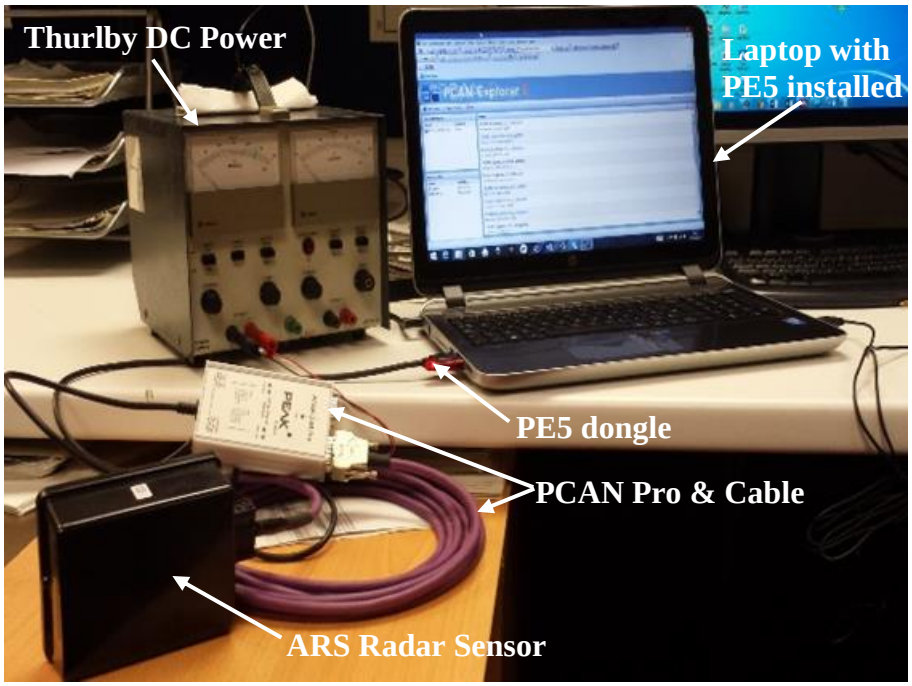

Figure A3-14: The initial laboratory testing of equipment and software

3.3.4.2 Equipment Mounted on the Test Vehicle

The pictorial view of both the external and the internal of the instrumented vehicle showing the individual components used in the instrumented vehicle setup described in Chapter 3 Section 3.3.4.

a: ARS 308-2 radar sensors mounted at back (LEFT) and front (RIGHT) of Test Vehicle

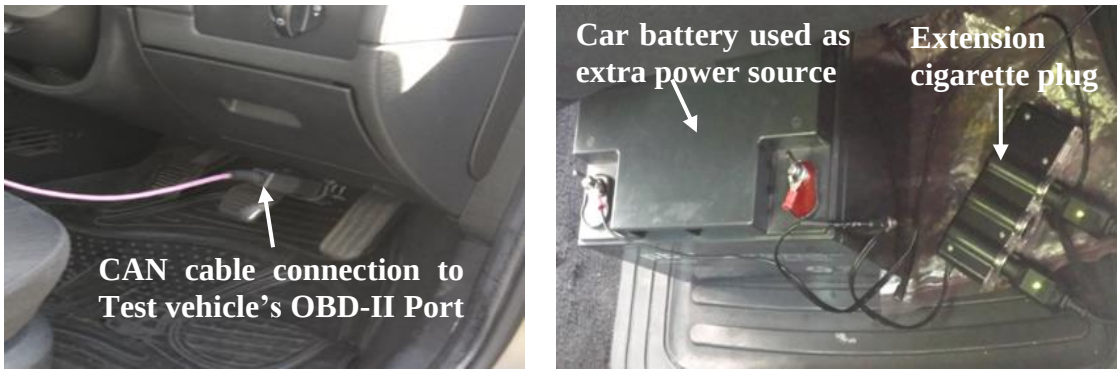

b: The Test Vehicle's OBD-II – CAN-USB connection (LEFT) and Stand-alone car battery supplying power to PB and VB (RIGHT)

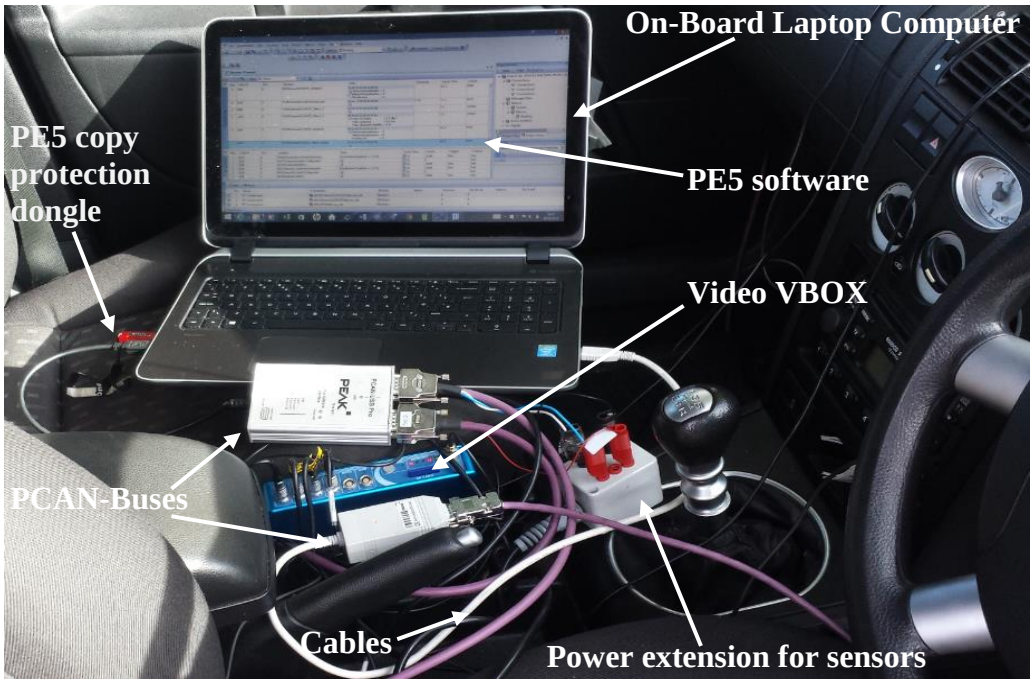

c: Inside setup of the instrumentation in the Test Vehicle

d: The Front (LEFT) and Rear (RIGHT) view setup of instrumentation in the Test Vehicle

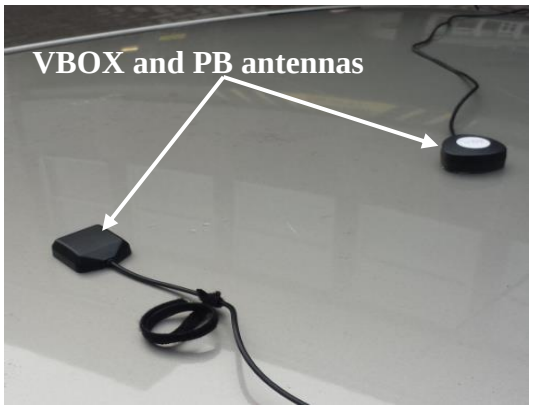

e: The PB and VBOX antennas on the Test Vehicle roof (LEFT) and rear facing Sony digital camera (RIGHT)

Figure A3-15: Individual instrumentation components

APPENDIX 3.3.5.2 Symbols File (Database Container (DBC))

The symbol file codes presented here was used for the rear mounted radar sensor operation. The same codes was used for the front mounted sensor. The prefix “B” for the variable (“Var”) referred to Back. The prefixed “F” for the variable referred to Front was used for the front mounted radar sensor. The prefix was assigned for easy identification of the leading and following vehicles data within the data file or set. The database container (symbols file) used for the radar sensor operation from Continental (2013) is shown below.

FormatVersion=5.0 // Do not edit this line!

Title="BACK SENSOR TO BE USED FOR ALL ROUTES AND DAYS DATA COLLECTION"

{ENUMS}
enum Enum_radar_enablePowerReductionV(0="False", 1="True")
enum Enum_radar_elevationV(0="Invalid", 1="Valid")
enum Enum_radar_enablePowerReduction(0="False", 1="True")
enum Enum_radar_output_type(0="reserved1", 1="SendObjects", 2="SendTargets", 3="reserved2")
enum Enum_radar_output_typeV(0="Invalid", 1="Valid")
enum Enum_radar_range_lengthV(0="Invalid", 1="Valid")
enum Enum_radar_start_service_align(0="False", 1="True")
enum Enum_radar_start_service_alignV(0="Invalid", 1="Valid")
enum Enum_radar_align_mode(0="useManualAlignmentValues", 1="UseServiceAlignmentValues")
enum Enum_RxInvalid(0="noneMissing", 1="speedMissing", 2="yawRateMissing", 3="speedAndYawRateMissing")
enum Enum_CurrentRadarPower(0="radarLowPower", 1="radarHighPower")
enum Enum_RadarPowerReduction(0="disabled", 1="enabled")enum Enum_NVMreadStatus(0="pending", 1="successful")
enum Enum_NVMwriteStatus(0="failed", 1="successful")
enum Enum_service_align_in_progress(0="False", 1="True")
enum Enum_radar_align_mode_output(0="useManualAlignmentValues", 1="useServiceAlignmentValues")
enum Enum_radarDeviceSpeed(8191="invalid")
enum Enum_radarDeviceSpeedDirection(0="Standstill", 1="forward", 2="reverse", 3="reserved")
enum Enum_radarDeviceYawRate(65535="invalid")

{SENDRECEIVE}

[BACKSensorALLRadarConfiguration]
ID=200h
DLC=8

Var=Bradar_elevation unsigned 16,8 -m /u:deg /f:0.25 /p:2 // elevation alignment of the radar sensor
Var=Bradar_enablePowerReduction unsigned 31,1 -m //
/e:Enum_radar_enablePowerReduction // Controls whether low power mode is allowed
Var=Bradar_elevationV unsigned 6,1 -m /e:Enum_radar_elevationV // elevation alignment of the radar sensor validity
Var=Bradar_enablePowerReductionV unsigned 5,1 -m
/e:Enum_radar_enablePowerReductionV // Controls whether low power mode is allowed validity
Var=Bradar_output_type unsigned 29,2 -m /e:Enum_radar_output_type /d:2 // The type of information that the radar will send on CAN channel 1
Var=Bradar_output_typeV unsigned 4,1 -m /e:Enum_radar_output_typeV // The type of information that the radar will send on CAN channel 1 validity
Var=Bradar_range_lengthV unsigned 0,1 /e:Enum_radar_range_lengthV // Range of radar validityVar=Bradar_start_service_align unsigned 27,1
/e:Enum_radar_start_service_align
Var=Bradar_start_service_alignV unsigned 4,1 /e:Enum_radar_start_service_alignV
Var=Bradar_align_mode unsigned 28,1 /e:Enum_radar_align_mode
Var=Bradar_range_length unsigned 8,8 -m /u:m

[BACKSensorALLROUTERadarState]
ID=201h
DLC=8
CycleTime=50
Timeout=20
Var=BSensTempErr unsigned 3,1 -b // Sensor: switched off; temperature too high
Var=BSensDef unsigned 5,1 // Sensor: defective
Var=BSupVolt_L unsigned 6,1 // Supply voltage low
Var=BCurrentRadarPower unsigned 6,1 -m /e:Enum_CurrentRadarPower // The radar output level
Var=BRadarPowerReduction unsigned 0,1 -m /e:Enum_RadarPowerReduction // The radar output level
Var=BRxInvalid unsigned 22,2 -m /e:Enum_RxInvalid // RX invalid (Timeout, Parity, MC)
Var=BcurrElevationCal unsigned 24,8 -m /f:0.25
Var=BNVMreadStatus unsigned 20,2 -m /u:N/A /e:Enum_NVMreadStatus //
Gives the status of reading the radar configuration from eeprom: 1) pending - in the process of reading 2) failed - reading failed 3) successful - reading completed successfully
Var=BNVMwriteStatus unsigned 19,1 -m /p:0 /e:Enum_NVMwriteStatus // Gives the status of writing the radar configuration from eeprom: - failed - the last configuration that was sent in via the RadarConfiguration message was NOT written to eeprom - successful - configuration was written to eeprom
Var=BswBuildVersion unsigned 56,8 -m
Var=BswMajorVersion unsigned 40,8 -m
Var=BswMinorVersion unsigned 48,8 –m
Var=Bservice_align_in_progress unsigned 3,1 -m /e:Enum_service_align_in_progress

```
Var=Bradar_align_mode_output unsigned 5, 1 -m /e:Enum_radar_align_mode_output
Var=BcurrRangeLengthCal unsigned 32,8 -m

[BACKSensorALLROUTE_Ch1_Target_1]
ID=701h        // Target informations part 1
DLC=8
Var=BTar_Dist unsigned 45,11 -m /u:m /f:0.1          // Target range
Var=BTar_Dist_rms unsigned 8,8 -m /u:m /f:0.1 /o:-10 /max:15.5  // Target range
standard deviation
Var=BTar_Vrel unsigned 32,12 -m /u:m/s /f:0.03 /o:-25      // Target relative velocity
Var=BTar_Vrel_rms unsigned 23,9 -m /u:m/s /f:0.03 /o:-5  // Target relative velocity
standard deviation
Var=BNoOfTarget_1 unsigned 0,8 -m -s /u:1          // Target number
Var=BTar_Ang_rms unsigned 16,7 -m /u:deg /f:0.1 // Target angle standard deviation

[BACKSensorALLROUTE_Ch1_Target_2]
ID=702h        // Target informations part 2
DLC=8
Var=BTar_RCSValue unsigned 54,10 -m /u:dBm² /f:0.1 /o:-50       // Radar cross
section
Var=BTar_Length unsigned 15,9 -m /u:m /f:0.1       // Target length
Var=BTar_Width unsigned 31,9 -m /u:m /f:0.1        // Target width
Var=BTar_PdH0 unsigned 8,7 -m /u:%        // Target false alarm probability
Var=BNoOfTarget_2 unsigned 0,8 -m -s /u:1          // Target number
Var=BTar_Type unsigned 45,2 -m /u:1        // Target type:: 0= No Target ; 1 =
Oncoming; 2 = Stationary; 3 = Traced (Tragets moving in the same direction)
Var=BTar_Ang unsigned 44,10 -m /u:deg /f:0.1 /o:-30        // Target angle
Var=BTar_Ang_stat unsigned 42,2 -m /u:1   // Target angle status:: 0 = Expanded
Target; 1 = Point Target; 2 = Digital; 3 = Invalid Data

[BACKSensorALLROUTE_Target_Status]
ID=600h        // Common status informations about the targets
DLC=8
Var=BNoOfTargetsNear unsigned 0,8 -m -t /u:1       // Number of valid targets in near
range scan
Var=BNoOfTargetsFar unsigned 8,8 -m -t /u:1        // Number of valid targets in far
range scan
Var=BTCIV unsigned 16,8 -m /f:0.1 // Target Can Interface Version: represents the
version number of the Target-CAN interface.

[BACKSensorALLROUTE_VersionID]
ID=700h        // Object List Interface Version ID
DLC=8
Var=BMajorReleaseNumber unsigned 0,8 -m          // Binary Coded number of MCU
major release Number
Var=BMinorReleaseNumber unsigned 8,8 -m          // Binary coded number of MCU
minor release number
```

Var=BPatchLevel unsigned 16,8 -m // Binary coded number of MCU patch level number

[BACKRadarSpeedINFO]
ID=300h
DLC=8
Var=BRadarDeviceSpeed unsigned 3, 13 -m -t /u:m/s /f:0.02 /max:122.82 // Speed of the radar unit
Var=BRadarDeviceSpeedDirection unsigned 22,2 -m -t /e:Enum_radarDeviceSpeedDirection// Speed direction of the radar unit: 0 = Standstill; 1 = forward; 2 = Reverse; 3 = Reserved

[BACKSensorALLXCP_Broadcast_TP]
ID=602h
DLC=8
Var=BXCP_Broadcast_TP unsigned 0,64

[BACKSensorALLROUTEXCP_CRO_RDP]
ID=603h
DLC=8

Var=BXCP_CRO_RDP unsigned 0,64

[BACKSensorALLROUTEXCP_DTO_RDP]
ID=604h
DLC=8
Var=BXCP_DTO_RDP unsigned 0,64 –m

[BACKSensorALLROUTEXCP_DTO_TP]
ID=601h
DLC=8
Var=BXCP_DTO_TP unsigned 0,64 –m

[BACKSensorALLYawRateInformation]
ID=301h // Yaw rate of the radar unit
DLC=8
Var=BRadarDeviceYawRate unsigned 0, 16 -h -m -t /u:°/s /f:0.01 /o:-327.68 /e:Enum_radarDeviceYawRate // Yaw rate of the radar unit

[BACKSensorALLROUTE_Object_1]
ID=60Bh
DLC=8
Var=BObj_AccelLong unsigned 31,9 -m /u:m/s² /f:0.0625 /o:-16 // Relative longitudinal acceleration (Base)
Var=BObj_DynProp unsigned 50,3 -m // Dynamic property (Base) 0- unclassified . 1 - standing . 2 - stopped . 3 - moving . 4 - oncoming
Var=BObj_ID unsigned 0, 6 -m // Object ID (Base)

Var=BObj_LatDispl unsigned 40, 10 -m /u:m /f:0.1 /o:-52 // Lateral displacement (Base)
Var=BObj_Length unsigned 61,3 -m // Object length: 0 - unknown. 1 - < 0.5m. 2 - < 2m. 3 - < 4m. 4 - < 6m. 5 - < 10m. 6 - < 20m. 7 - exceeds
Var=BObj_LongDispl unsigned 8, 11 -m /u:m /f:0.1// Longitudinal displacement (BaseVar=BObj_MeasStat unsigned 56,2 -m// Object measurement status: 0 - no object. 1 - new object. 2 - object not measured. 3 - object measured
Var=BObj_ProbOfExist unsigned 53,3 -m // Object propabiltiy of existence: 0 - invalid. 1 - < 25%. 2 - < 50%. 3 - < 75%. 4 - < 90%. 5 - < 99%. 6 - < 99,9%. 7 - < 99,99%
Var=BObj_RollCount unsigned 6,2 -m // Rolling Counter
Var=BObj_VrelLong unsigned 19,12 -m /u:m/s /f:0.0625 /o:-128 // Relative longitudinal speed (Base)
Var=BObj_Width unsigned 58, 3 -m // Object Width :: 0 = unknown; 1: < 0.5 m (pedestrian); 2: < 1 m (bike). 3: < 2 m (car); 4: < 3 m (truck); 5: < 4 m; 6: < 6 m; 7: exceeds

[BACKSensorALLROUTE_Object_2]
ID=60Ch // Object informations part 2
DLC=8
Var=BObj_RCSValue unsigned 0,8 -m /u:dBm² /f:0.5 /o:-64 // RCS value (radar cross section)
Var=BObj_LatSpeed unsigned 8,8 -m /u:m/s /f:0.25 /o:-32 // Object lateral velocity. Value negative = obj moves left to right. Value positive = obj moves right to left.
Var=BObj_ObstacleProbability unsigned 17,7 -m /u:%

[BACKSensorALLROUTE_Object_Status]
ID=60Ah // Common status informations about sensor and objects
DLC=8
Var=BLatDistToBorderLeft unsigned 40,8 -m /u:m /f:0.1 // Lateral distance to road border (left)
Var=BLatDistToBorderRight unsigned 48,8 -m /u:m /f:0.1 // Lateral Distance to road Border (right)
Var=BMeasCounter unsigned 8,16 -m // Meas Counter
Var=BNumOfLanesLeft unsigned 32,2 -m // Number of adjacent lanes to the left
Var=BNumOfLanesRight unsigned 34,2 -m // Number of lanes to the right
Var=BNumOfObjects unsigned 0,8 -m // Number of Objects sent (Base)Var=BInterfaceVersionNumber unsigned 36,4 -m // Unique number that identifies the version of the CAN interface
Var=BReserved unsigned 24,1 -m // Reserved (Sensor Status): 0 - NO . 1 - YES
Var=BSensorDefective unsigned 27,1 -m // Sensor defective: 0 - NO . 1 - YES
Var=BSensorExternalDisturbed unsigned 30,1 -m // SensorExternalDisturbed : 0 - NO . 1 - YES
Var=BSensorMisaligned unsigned 28,1 -m // Sensor Misaligned: 0 - NO . 1 - YES
Var=BSensorOutputReduced unsigned 31,1 -m // SensorOutputReduced : 0 - NO . 1 - YES
Var=BSensorRxInvalid unsigned 25,1 -m // SensorRxInvalid : 0 - NO . 1 - YES

```
Var=BSensorSupplyVoltageLow unsigned 26,1 -m  // SensorSupplyVoltageLow:   0 -
NO  .  1 - YES
Var=BSensorSwitchedOff unsigned 29,1 -m // Sensor Switched Off (temperature):   0 -
NO  .  1 – YES

[For Vehicle Speed]
FormatVersion=5.0 // Do not edit this line!

Title="Vehicle Speed Information"

{SENDRECEIVE}
["Vehicle Speed"]
ID=201h         // Vehicle Speed
DLC=8
Var=VehicleSpeed unsigned 32,8 -m -t /u:m/s /f:0.56          // Vehicle Speed in m/s
```

APPENDIX 3.4.1 Radar Beam Elevation Calibration Experiment and Results

3.4.1.1 Radar Sensor and Vehicles used for the Experiment

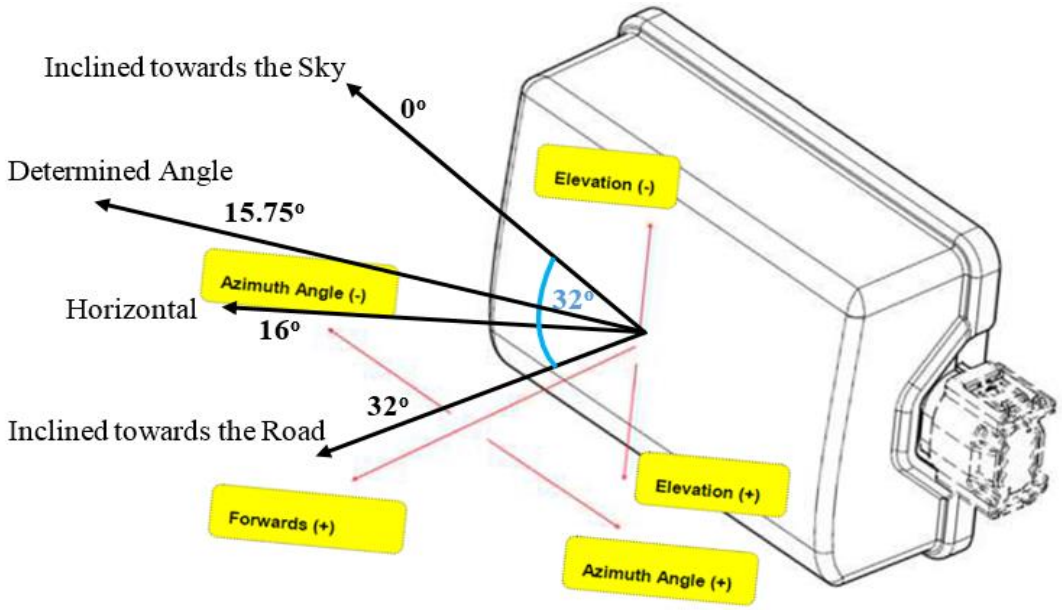

Figure A3-16: The elevation plate angle description (reproduced and modified from Continental, 2013)

Figure A3-17: The mounted heights of the radar sensors on the instrumented vehicle (Left: Front and Right: Rear)

The four different vehicles used for the radar beam elevation angle calibration experiment are shown in Figure A3-18.

a) Vehicle No. 1

b) Vehicle No. 2

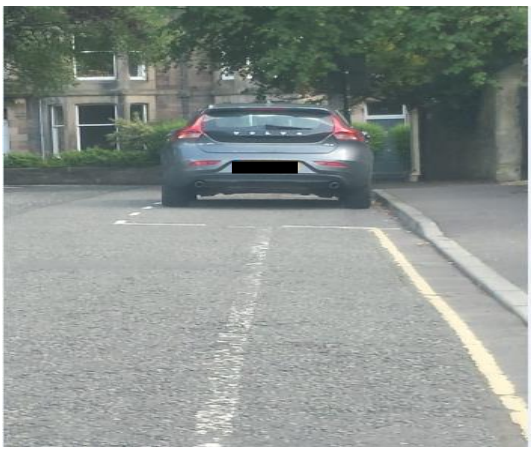

c) Vehicle No. 3

d) Vehicle No. 4

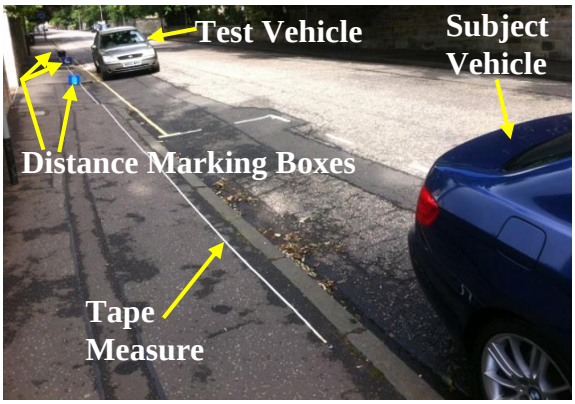

e) Coloured tool boxes marking the measured distances

Figure A3-18: The four stationary vehicles used for the sensor calibration field experiment and the boxes used for marking the measured distances

3.4.1.2 Table of Results of the Calibration Experiment

Table A3-1: The front sensor distance measurement for stationary subject vehicle No. 1

Marked distance (metres)	Measured distance from the radar sensor at different elevation angle (m)					
	14.50°	14.75°	15.25°	15.50°	15.75°	16.00°
10	10.1	10.2	10.1	9.9	10.0	9.8
20	20.8	20.8	20.6	20.5	20.5	20.6
30	30.3	30.3	30.3	30.1	30.1	30.2
40	38.7	38.9	39.5	39.5	39.9	39.8
50	51.1	50.9	50.9	50.6	50.6	50.6
RMSE	0.85	0.75	0.55	0.42	0.35	0.41

Table A3-2: The front sensor distance measurement for stationary subject vehicle No. 2

Marked distance (metres)	Measured distance from the radar sensor at different elevation angle (m)					
	14.50°	14.75°	15.25°	15.50°	15.75°	16.00°
10	9.8	9.8	9.9	9.9	9.9	9.9
20	20.0	20.0	20.0	20.0	20.0	20.1
30	29.7	29.7	29.8	29.8	29.9	29.8
40	40.8	40.8	40.6	40.6	40.4	40.4
50	50.7	50.7	50.6	50.5	50.2	50.5
RMSE	0.50	0.50	0.39	0.36	0.21	0.31

Table A3-3: The front sensor distance measurement for stationary subject vehicle No. 3

Marked distance (metres)	Measured distance from the radar sensor at different elevation angle (m)					
	14.50°	14.75°	15.25°	15.50°	15.75°	16.00°
10	9.7	9.7	9.8	9.9	9.9	9.8
20	19.9	20.0	20.0	20.4	20.0	19.9
30	30.0	30.0	30.0	30.0	30.0	30.0
40	38.9	38.9	39.5	39.5	39.9	39.5
50	51.0	51.0	50.5	50.5	50.3	49.7
RMSE	0.68	0.68	0.33	0.37	0.15	0.28

Table A3-4: The front sensor distance measurement for stationary subject vehicle No. 4

Marked distance (metres)	Measured distance from the radar sensor at different elevation angle (m)					
	14.50°	14.75°	15.25°	15.50°	15.75°	16.00°
10	10.1	10.1	10.1	10.1	10.1	10.1
20	20.4	20.4	20.4	20.3	20.1	19.9
30	29.7	29.8	29.8	29.7	29.9	29.7
40	41.4	41.0	40.7	40.5	40.5	39.5
50	51.0	51.0	49.7	49.7	50.0	48.7
RMSE	0.80	0.66	0.40	0.33	0.24	0.64

Table A3-5: The back sensor distance measurement for stationary subject vehicle No. 1

Marked distance (metres)	Measured distance from the radar sensor at different elevation angle (m)					
	14.50°	14.75°	15.25°	15.50°	15.75°	16.00°
10	10.4	10.3	10.3	10.1	10.1	10.1
20	21.0	21.0	21.0	20.8	20.7	20.7
30	30.6	30.5	30.4	30.4	30.1	30.4
40	41.5	41.0	41.0	40.8	40.6	40.7
50	51.6	51.0	49.5	49.6	49.8	49.5
RMSE	1.13	0.82	0.71	0.57	0.43	0.53

Table A3-6: The back sensor distance measurement for stationary subject vehicle No. 2

Marked distance (metres)	Measured distance from the radar sensor at different elevation angle (m)					
	14.50°	14.75°	15.25°	15.50°	15.75°	16.00°
10	9.8	9.8	9.9	9.9	9.9	9.9
20	20.6	20.6	20.6	20.6	20.6	20.6
30	30.3	30.3	30.3	30.2	30.1	30.1
40	39.8	39.8	39.8	39.8	39.9	39.8
50	50.4	50.3	50.3	50.2	50.0	49.7
RMSE	0.37	0.35	0.34	0.31	0.28	0.32

Table A3-7: The back sensor distance measurement for stationary subject vehicle No. 3

Marked distance (metres)	Measured distance from the radar sensor at different elevation angle (m)					
	14.50^o	14.75^o	15.25^o	15.50^o	15.75^o	16.00^o
10	10.0	10.0	10.0	10.0	10.0	10.0
20	21.0	20.7	20.7	20.5	20.2	20.5
30	29.7	29.7	29.8	29.8	29.9	29.9
40	38.7	38.7	39.5	39.5	40.1	39.7
50	51.5	51.5	50.9	50.9	50.4	50.5
RMSE	1.00	0.95	0.56	0.52	0.21	0.35

Table A3-8: The back sensor distance measurement for stationary subject vehicle No. 4

Marked distance (metres)	Measured distance from the radar sensor at different elevation angle (m)					
	14.50^o	14.75^o	15.25^o	15.50^o	15.75^o	16.00^o
10	9.9	9.9	9.9	9.9	9.9	9.9
20	20.9	20.9	20.8	20.5	20.0	20.8
30	31.5	31.4	30.8	29.9	30.0	30.6
40	38.8	39.5	39.5	39.9	40.0	38.8
50	52.0	51.8	51.0	50.8	50.2	51.1
RMSE	1.3	1.12	0.71	0.43	0.10	0.86

APENDIX 3.4.2 Test Vehicle Speed Re-Engineering Steps using the Video VBOX

The RACELOGIC Step by Step Experimental Instruction for Test Vehicle Speed Reverse (Re)-Engineering Process Using the Video Velocity Box (Video VBOX)

The test vehicle speed reverse engineering step by step experimental instruction was put together for this study by the Support Technical Team of RACELOGIC Ltd and send via email. Below is the experimental advice notes and the step by step experimental instruction (Racelogic Ltd).

Racelogic Advice Notes Explaining the Process

To enable Racelogic to reverse engineer the CAN data you will need to carry out a CAN log following the steps below. Carrying out the log in this way enables our engineers to match the change in data with the action in the video, if the log is not done like this it is very difficult for our engineer to find the correct CAN data.

I have attached a CAN logging scene which can be loaded into your Video VBOX unit. Please note this should ***not*** be loaded into the software, or the full CAN logging capability will be lost when re-exported or saved.

When this scene has been uploaded to a Video VBOX unit, if you connect this unit to your vehicle and log some data, we will be able to reverse engineer the CAN data from this. Note, your vehicle must have a CAN baud rate of 500Kbit (this is the most common baud rate for light vehicles so this should not be a problem).

You must make sure you tell us in an email what you have done in the vehicle while logging the data, otherwise we will be left with a mass of CAN data and no way to decrypt it.

You **must** tell us in the same way, **step by step** (in the correct order) what you did while logging your data to enable us to decrypt the information properly. E.g. :-

START OF TEST

1. I turned the ignition ON – the engine remained OFF.
2. I pressed on the throttle pedal, so that it reached 100% travel and held for 10 seconds.

3. I pressed on the throttle pedal, so that it reached 50% travel and held for 10 seconds.
4. I turned the steering wheel to full Left hand lock and held for 5 seconds.
5. I turned the steering wheel to full Right hand lock and held for 5 seconds.
6. I pressed on the brake pedal so that it went as close down to 100% travel as possible and held for 10 seconds.
7. I started the engine and allowed it to idle for around 30 seconds.
8. I held the vehicle engine speed at 2,000 RPM for 15 seconds.
9. I held the vehicle engine speed at 4,000 RPM for 15 seconds.
10. I went for a **short** drive using all gears incrementing in the correct order (missing no gears) - Note – high speed/revs ***not*** required.
11. I finished the drive making sure I dropped down all gears, again without missing any.
12. I stopped and allowed the vehicle to idle for another 15 seconds.

END OF TEST

Racelogic Advice Notes

It is most helpful if we have both **audio** and **visual** representatives of these steps. This enables us to work through the CAN data. Ideally, a passenger should read aloud each instuction before the driver carries it out.

You should also set a picture in picture camera up to record the RPM gauge in the car, so that we can match this to the data, for example Figure A3-19 (Racelogic Ltd).

Figure A3-19: Video VBOX Picture in Picture camera view of RPM gauge in car (Source: Racelogic Ltd)

APPENDIX 3.4.4 Vehicle Instrumentation Testing and Pilot Data Collection Routes

3.4.4.1 Testing of Test Vehicle's Instrumentation

In order to ensure that all the instruments on-board the test vehicle were functioning as expected and could withstand long periods of operation, a series of instrumentation testing was carried out all day after the completion of the setup of the instrumented vehicle. A drive around of the selected traffic corridors within the City of Edinburgh for long periods of time was done during the day, monitoring the performance of all the individual instruments on-board the instrumented vehicle. When a specific problem is identified with a specific instrument, the trial test is stopped and the problem investigated and rectified before the testing experiment is resumed. All the instrumentation of the instrumented vehicle were operating well and were able to cope with long period of continuous use during the testing experiment.

Because the natural driving behaviour of the following vehicles were needed to be captured and not to cause any distraction to the drivers due to the existence of the rear cameras, the following drivers were observed to ascertain if the presence of the cameras, especially the rear cameras, were attracting their attention and by way, distracting them while driving during the instrumentation testing experiment. First, an empty equipment boxes and other materials, such as cloths, were placed at the rear windscreen of the test vehicle to disguise the rear view cameras from the following vehicles (see Figure A3-20).

The observed following drivers captured on the rear view cameras with the cameras disguised were compared with the drivers captured without disguising the rear view cameras. Analysis of the video footage found that there was no effects on the drivers captured in both cases as the drivers were seen not to have noticed the cameras. Though both scenarios did not have any effects on the following drivers observed in the trial experiment, a decision was made to place the empty boxes and other materials at the rear windscreen to disguise the rear facing cameras throughout the subsequent experiments.

Figure A3-20: Rear view of the test vehicle with materials to disguise the rear view cameras

APENDIX 3.4.5 Observed Vehicle Manoeuvres and Car Following Termination Process

3.4.5.1 Different manoeuvres and behaviours observed during the experiment

(a) Occupants in a vehicle

(b) Driver performing other activities other than driving (e.g. drinking or eating)

(c) Truck following

(e) Driver and passenger chatting

(f) Car-following termination process for leading (left) and following (right) vehicles

(g) Front (right) and rear (left) cameras side by side showing a truck leading.

Figure A3-21: Different following behaviours and distractions captured by the video cameras in car following situations

3.4.5.2 Termination of Car Following Process

Throughout the data acquisition period, it was observed that different vehicles were leading or following the instrumented vehicle at different periods as a result of the termination of the car following process. Whilst the previously tracked vehicles were lost in the car-following process, new vehicles were encountered by the instrumented vehicle and tracked throughout their encounter with the instrumented vehicle until termination of the car following process. This encounter with the instrumented vehicle repeat itself throughout the experiment.

The scenarios (or instances) where the car following process were terminated by either the leading or the following vehicles in direct view of the instrumented vehicle identified throughout the experiment are as follows:

- Leading or Following vehicle moving to the next adjacent lane out of direct view of the test vehicle.
- The Instrumented vehicle moving to the next adjacent lane, i.e. lane changing.
- Leading or Following vehicle changing direction of travel, i.e. either turning left or right at road intersections, i.e. lane changing.
- Instrumented vehicle changing direction of travel at traffic junctions or intersections.
- Other vehicles cutting in either between the Leading or Following vehicles and the Instrumented vehicle, and staying in lane after cut in to become either the new Leading or Following vehicles.
- Following vehicles allowing other vehicles the permission to cut in to join the traffic stream from adjacent lane or adjacent junction.

- Following vehicles overtaking the instrumented vehicle and joining in front of the instrumented vehicle to become the new leading vehicle in the traffic stream.
- The Leading vehicles overtaking the second lead vehicles in front and losing the former leading vehicle in the traffic flow.
- The Leading vehicle speeding off and driving away with speed beyond the normal traffic flow speed in which the instrumented vehicle couldn't keep up with.
- Following vehicle driving slowly and couldn't keep up with the instrumented vehicle's speed and the general traffic flow, thereby losing the following vehicle in the process.
- Losing the Leading vehicles as a result of the traffic signal turning red before the instrumented vehicle crosses the intersection, while the lead vehicle driving off.
- Losing the Following vehicles as a result of the traffic signals turning red before the Following vehicles could cross the intersection, while the instrumented vehicle driving off.
- Following vehicles being overtaken by other neighbouring vehicles in the traffic stream to cut in and stay in lane.
- Leading / Following vehicles pulling to the side of the road to stop and park discontinuing the driving.
- Losing both Leading and Following vehicles at roundabouts as a result of vehicles circulation.

APPENDIX 3.4.7 Data Collection Time Plan

Table A3-9: Data collection time plan 1*

Date		Data Collection			
July 2015		Run	Peak Period	Time	Traffic Corridor
Wednesday	22nd	All Day			Final Testing and Validation of Test Vehicle
Thursday	23rd	2	AM	08:00 - 09:30	Traffic Corridor 1 - Day 1
		2	PM-Off	14:00 – 16:00	
Monday	27th	2	AM	08:00 – 10:00	Traffic Corridor 3 - Day 1
		2	PM-Off	14:00 – 16:00	
Friday	31st	2	AM	08:00 – 10:00	Traffic Corridor 3 - Day 2
		2	PM-Off	14:00 – 16:00	
August 2015					
Tuesday	4th	2	AM	08:00 – 10:00	Traffic Corridor 3 - Day 3
		2	PM-Off	14:00 – 16:00	
Wednesday	5th	2	AM	08:00 – 10:00	Traffic Corridor 3 - Day 4
		2	PM-Off	14:00 – 16:00	
Thursday	6th	2	AM	08:00 – 09:30	Traffic Corridor 1 - Day 2
		2	PM-Off	14:00 – 16:00	
Friday	7th	2	AM	08:00 – 09:30	Traffic Corridor 1 - Day 3
		2	PM-Off	14:00 – 16:00	
Tuesday	18th	2	PM	17:00 – 18:30	Corridor - Bus Following – Day 1
Wednesday	19th	2	AM	08:00 – 10:00	Traffic Corridor 3 - Day 5
		2	PM-Off	14:00 – 16:00	
		2	PM	17:00 – 18:30	Corridor - Bus Following – Day 2
Thursday	20th	2	AM	08:00 – 09:30	Traffic Corridor 1 - Day 4
		2	PM-Off	14:00 – 16:00	
Monday	24th	2	AM	08:00 – 09:30	Traffic Corridor 1 - Day 5
		2	PM-Off	14:00 – 16:00	
Tuesday	25th	2	AM	08:00 – 09:30	Traffic Corridor 1 - Day 6
		2	PM-Off	14:00 – 16:00	
Friday	28th	2	AM	08:00 – 09:30	Traffic Corridor 2 - Day 1
		2	PM-Off	14:00-16:00	

*2 = Out and Return for the traffic corridor the test was conducted

Table A3-10: Data collection time plan 2*

Date		Data Collection			
September 2015		Run	Peak Period	Time	Traffic Corridor
Friday	4th	2	AM	08:00 – 09:30	Traffic Corridor 2 - Day 2
		2	PM-Off	14:00 – 16:00	
Monday	7th	2	AM	08:00 – 09:30	Traffic Corridor 2 - Day 3
		2	PM-Off	14:00 – 16:00	
Tuesday	8th	2	AM	08:00 – 10:00	Traffic Corridor 4 – Day 1
		2	PM-Off	14:00 – 16:00	
Wednesday	9th	2	AM	08:00 – 10:00	Traffic Corridor 4 – Day 2
		2	PM-Off	14:00 – 16:00	
Thursday	10th	2	AM	08:00 – 10:00	Traffic Corridor 2 - Day 4
		2	PM-Off	14:00 – 16:00	
Wednesday	16th	2	AM	08:00 – 10:00	Traffic Corridor 2 - Day 5
		2	PM-Off	14:00 – 16:00	
Thursday	17th	2	AM	08:00 – 10:00	Traffic Corridor 1 - Day 7
		2	PM-Off	14:00 – 16:00	
Monday	21st	2	PM-Off	12:00 – 16:00	Other Corridors – Edinburgh Town
October 2015					
Thursday	24th	2	PM-Off	12:00 – 18:00	M8 - (Edinburgh – Glasgow)
			PM		M8 - (Glasgow – Edinburgh)
					Glasgow Township

*2 = Out and Return for the traffic corridor the test was conducted

APPENDIX 4.2.2 Video Data Analysis Sample Template Sheet

The video data was manually recorded on a designed working template sheet and the records transferred onto electronic version of the working template sheet for further analysis. The tables below illustrate the data entry on the working template sheet.

Table A4-1: Illustrate Sample template for video extraction records showing Corridor 1 day 3 video data entry record for following vehicles

Position of the monitored vehicle: FOLLOWING			**Route & Day:** 1 / 3				**Page:** 1
			Date & Time: 24 August 2015 / 08:12				AM
Weather Condition: Dry/Sunny			**Type Of Analysis:** VBOX / Video Camera				
Veh. ID	Time Veh. On Scene	Time Veh. Off Scene	Time Veh. Stopped	Time Veh. Moved Off	Type Of Vehicle	Gender	Occupants / Inside Activity
1	08:12:51	08:13:39			Car	Female	1
2	08:13:40	08:14:27			Car	Female	1
3	08:14:23	08:36:39	08:14:45	08:15:16	Car	Female	1
			08:16:08	08:16:37			
			08:17:17	08:17:20			
			08:20:57	08:22:17			
			08:22:25	08:24:11			
			08:24:29	08:24:53			
			08:25:14	08:27:13			
			08:27:27	08:29:20			
			08:29:39	08:31:34			
			08:31:46	08:32:00			
			08:32:08	08:33:42			
			08:35:13	08:35:40			
4	08:37:14	08:37:26			Car	Female	2
5	08:40:21	08:40:23			Truck	Male	1
6	08:40:24	08:41:36	RETURN RUN BEGIN		Car	Male	2
7*	08:42:40	08:56:01	08:44:51	08:44:59	Van	Male	1
			08:45:05	08:45:26			
			08:45:38	08:45:52			
			08:45:58	08:46:04			
			08:46:27	08:46:44			
			08:47:06	08:47:50			
8*	08:55:03	08:56:11			Car	Male	1
7*	08:56:12	08:56:35			Van	Male	1
8*	08:56:36	08:57:22	08:57:06	08:57:01	Car	Male	1
7*	08:57:23	08:58:00			Van	Male	1
9	08:58:01	09:01:30	08:58:26	08:58:32	Car	Male	1
			08:58:49	08:59:35			
			08:59:48	08:59:52			

*Same vehicle observed following at different times during the car following process

Table A4-2: Illustrate sample template for video extraction records showing Corridor 1 day 4 video data entry record for leading vehicles

Position Of The Monitored Vehicle: LEADING			**Route & Day:** 1 / 3				Page: 1
			Date & Time: 24 August 2015 / 08:12				AM
Weather Condition: Dry/Sunny			**Type Of Analysis:** VBOX / Video Camera				
Veh. ID	Time Veh. On Scene	Time Veh. Off Scene	Time Veh. Stopped	Time Veh. Moved Off	Type Of Vehicle	Time Test Veh. Stopped	Time Test Veh. Moved Off
1	08:13:18	08:14:38	08:13:35	08:13:43	Car	08:14:38	08:15:14
2	08:15:19	08:24:13	08:15:57	08:16:35	Car	08:16:06	08:16:36
			08:17:10	08:17:17		08:17:16	08:17:18
			08:17:51	08:17:53			
			08:20:47	08:22:12			
			08:22:18	08:24:08		08:22:22	08:24:10
3	08:24:15	08:36:00	08:24:17	08:24:20	Van	08:24:19	08:24:22
			08:24:24	08:24:50		08:24:28	08:24:51
			08:24:59	08:27:10		08:25:07	08:27:12
4	08:36:01	08:37:01			Car		
5	08:37:03	08:37:21					
6	08:37:30	08:38:44			Car		
7	08:39:57	08:40:33	RETURN RUN BEGIN		Car		
8	08:40:33	08:41:35			Car		
9	08:41:36	08:51:09	08:42:17	08:42:44	Car	08:42:23	08:42:46
			08:44:20	08:44:23			
			08:44:43	08:44:54		08:44:50	08:44:56
			08:45:00	08:45:21		08:45:04	08:45:21
			08:45:33	08:45:48		08:45:36	08:45:50
			08:45:54	08:46:00		08:45:58	08:46:02
			08:46:22	08:46:39		08:46:27	08:46:41
			08:46:58	08:47:46		08:47:03	08:47:48
			08:48:03	08:48:11		08:48:10	08:48:15
			08:48:30	08:49:07		08:48:36	08:49:09
			08:49:46	08:50:48		08:49:50	08:50:49
						08:51:09	08:52:34
						08:53:11	08:53:23
10	08:53:39	08:54:07			Car		
11*	08:54:16	08:56:44	08:34:16	08:54:57	Car	08:54:30	08:34:58
11*	08:56:45	09:01:30	08:56:58	08:57:07		08:57:02	08:57:10
			08:58:19	08:58:23		08:58:26	08:58:29
			08:58:28	08:58:30			

*Same vehicle observed leading the test vehicle at different times during the car following process

Appendix 4.2.2

Table A4-3: Illustrate sample template showing final following total duration calculation for Corridor 1 day 3 for following vehicles*

Position of the monitored vehicle: FOLLOWING			**Route & Day:** 1 / 3			**Page:** 1
			Date & Time: 24 August 2015 / 08:12			AM
Weather Condition: Dry/Sunny			**Type Of Analysis:** VBOX / Video Camera			
Veh. ID	Time Veh. On Scene	Time Veh. Off Scene	Actual Duration Vehicle Following (sec)	Type Of Vehicle	Gender	Occupants / Inside Activity
1	08:12:51	08:13:39	48	Car	Female	1
2	08:13:40	08:14:27	47	Car	Female	1
3	08:14:23	08:36:39	581	Car	Female	1
4	08:37:14	08:37:26	12	Car	Female	2
5	08:40:21	08:40:23	2	Truck	Male	1
6	08:40:24	08:41:36	72	Car	Male	2
7	08:42:40	08:58:00	525	Small Van	Male	1
8	08:55:03	08:57:22	114	Car	Male	1
9	08:58:01	09:01:30	153	Car	Male	1

*Highlight is the beginning of the Return test run